

Lectures on the quantum phase transitions of metals

Subir Sachdev

*Department of Physics, Harvard University,
Cambridge, Massachusetts, 02138, USA*

(Dated: August 20, 2024)

Abstract

Quantum phase transitions of metals involve changes in the Fermi surface, and can be divided into three categories. The first two categories involve symmetry breaking, and lead to a deformation or reconstruction of the Fermi surface. The third category involves a change in the volume enclosed by the Fermi surface without any symmetry breaking: one phase is a Fermi liquid (FL) with the conventional Luttinger volume, while the other phase is a ‘fractionalized Fermi liquid’ (FL^{*}), which has a non-Luttinger volume Fermi surface accompanied by a spin liquid with fractionalized excitations. It is a relatively simple matter to obtain a FL^{*}-FL transition in Kondo lattice models. However, the FL^{*}-FL transition can also be present in single-band Hubbard-like models: this is efficiently described by the ‘ancilla’ method, which shows that the transition is a ‘flipped’ Kondo lattice transition. This single-band FL^{*}-FL transition is argued to apply to the metallic states of the hole-doped cuprates. In the clean limit, the critical properties of the quantum transitions in the three categories are distinct, but all lead to perfect metal transport in the quantum-critical regime. Impurity-induced ‘Harris disorder’, with spatial fluctuations in the local position of the quantum critical point, is a relevant perturbation to the clean critical points. In the presence of Harris disorder, all three categories exhibit strange metal behavior, which can be described by a universal two-dimensional Yukawa-Sachdev-Ye-Kitaev model.

Lecture notes and slides for

‘Prospects in Theoretical Physics 2024’, Quantum Matter Summer School,
Institute for Advanced Study, Princeton, July 8–19, 2024.

Lecture Videos on [YouTube](#).

Contains extracts from:

- *Quantum Phases of Matter*, by S. S., Cambridge University Press (2023).
- *Strange Metals and Black Holes: Insights From the Sachdev-Ye-Kitaev Model*, S. S., Oxford Research Encyclopedia in Physics, December 2023; [arXiv:2305.01001](#)

CONTENTS

I. Fermi liquid theory	3
A. Free electron gas	3
B. Interacting electron gas	4
C. Green's functions and quasiparticle lifetime	7
D. The Luttinger relation	12
II. Quantum phase transition of Ising qubits	15
III. Ising ferromagnetism in a metal	27
IV. Spin density wave order in a metal	27
A. Fermi surface reconstruction	29
V. Fermi volume change in a metal	32
VI. The SYK model	32
A. The Yukawa-SYK model	37
VII. Quantum criticality of clean metals	39
A. Luttinger relation	43
B. Transport	44
VIII. Universal theory of strange metals: the 2d-YSYK model	45
References	48
A. Hertz-Millis transitions in metals	53
B. Transitions from a Fermi liquid to a fractionalized Fermi liquid (FL*)	95
C. The SYK model	170
D. Quantum criticality of metals	190

I. FERMI LIQUID THEORY

The conventional theory of metals starts from a theory of the free electron gas, and then perturbatively accounts for the Coulomb interactions between the electrons. Already at leading order, we find a rather strong effect of the Coulomb interactions: a logarithmic divergence in the effective mass of the single-particle excitations near the Fermi surface. Further examination of the perturbation theory shows that this divergence is an artifact of failing to account for the screening of the long-range Coulomb interactions. Formally, screening can be accounted for by a simple modification of the perturbative series: introduce a dielectric constant in the interaction propagator, and sum only graphs which are irreducible with respect to the interaction line. Once screening is accounted for by this method, the effective mass of the single-particle excitations becomes finite.

In this initial section we ask: is it possible to give a description of the interacting electron gas which is valid to all orders in the Coulomb interactions? By “all orders in perturbation theory” we are assuming the validity of perturbation theory, and cannot rule out non-perturbative effects which could lead to the appearance of new phases of matter. Indeed the study of such new phases of matter is the focus of a major part of this book. But in this chapter, we present an all-orders description of the electron gas. This starts by formalizing the definition of a “quasiparticle” excitation, as a central ingredient in the theory of many-particle quantum systems.

A. Free electron gas

Let us start by recalling the basic properties of the free electron gas. We work in a second quantized formalism with electron annihilation operators $c_{\mathbf{p}\alpha}$ where \mathbf{p} is momentum and $\alpha = \uparrow, \downarrow$ is the electron spin. The electron operator obeys the anti-commutation relation

$$[c_{\mathbf{k}\alpha}, c_{\mathbf{k}'\beta}^\dagger]_+ = \delta_{\mathbf{k},\mathbf{k}'} \delta_{\alpha\beta} \quad (1)$$

We assume the dispersion of a single electron is $\varepsilon_{\mathbf{p}}$. The chemical potential is assumed to be included in $\varepsilon_{\mathbf{p}}$; so for the jellium model $\varepsilon_{\mathbf{p}} = \hbar^2 \mathbf{p}^2 / (2m) - \mu$. Then the Hamiltonian is

$$H = \sum_{\mathbf{p},\alpha} \varepsilon_{\mathbf{p}} c_{\mathbf{p}\alpha}^\dagger c_{\mathbf{p}\alpha}. \quad (2)$$

The $T = 0$ ground state of this Hamiltonian is

$$|G\rangle = \prod_{\varepsilon_{\mathbf{p}} < 0, \alpha} c_{\mathbf{p}\alpha}^\dagger |0\rangle \quad (3)$$

The equation $\varepsilon_{\mathbf{p}} = 0$ defines the *Fermi surface* in momentum space, separating the occupied and unoccupied states.

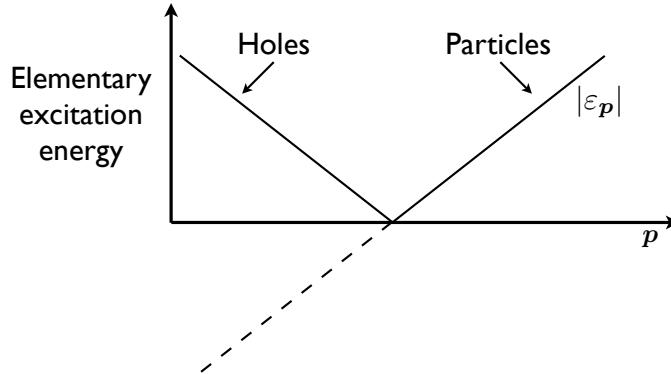


FIG. 1. Fermionic excitation spectrum of a Fermi liquid as a function of momentum \mathbf{p} along a fixed direction from the origin.

The elementary excitations of this state are of two types. Outside the Fermi surface we have particle-like excitations

$$\text{Particles: } c_{\mathbf{p},\alpha}^\dagger |G\rangle, \quad \mathbf{p} \text{ outside Fermi surface,} \quad (4)$$

while inside the Fermi surface we have hole-like excitations

$$\text{Holes: } c_{\mathbf{p},\alpha} |G\rangle, \quad \mathbf{p} \text{ inside Fermi surface.} \quad (5)$$

The energy of these excitations must be positive (by definition), and is easily seen to equal $|\varepsilon_{\mathbf{p}}|$, as illustrated in Fig. 1.

From these elementary excitations, we can now build an exponentially large number of multi-particle and multi-particle excitations. In the free electron theory, their energies are simple the sum of the energies of the elementary excitations $\sum_{\mathbf{p},\alpha} |\varepsilon_{\mathbf{p}}|$.

B. Interacting electron gas

Our basic assumption is one of adiabatic continuity from the free electron gas. We imagine we can tune the strength of the Coulomb interactions, and slowly turn them on from the free electron theory. Alternatively, we can assert that there is no quantum phase transition as the strength of the interactions is increased: note this is an assumption, we will meet situations where this is not the case later. In this adiabatic process, we assume that there is a correspondence between the ground states and the elementary excitations of the free and interacting electron gas. So the state $|G\rangle$ in (3) evolves smoothly to the unknown ground state of the interacting electron gas. And importantly, there is also a correspondence in the excitations. In the ‘jellium’ model, with continuous translational symmetry and a uniform background neutralizing charge, this correspondence is simply one-to-one: a particle excitation with energy $\varepsilon_{\mathbf{p}}$ evolves into a ‘quasiparticle excitation’ with

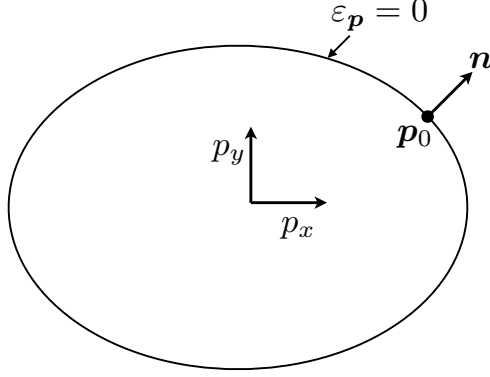


FIG. 2. A point \mathbf{p}_0 on the Fermi surface, and its unit normal \mathbf{n} .

a modified value of $\varepsilon_{\mathbf{p}}$. And similarly, for a ‘quasihole’ with modified energy $-\varepsilon_{\mathbf{p}}$. An important assumption will be that $\varepsilon_{\mathbf{p}}$ remains a smooth function through the Fermi surface, and the energies of both particles and holes is given by $|\varepsilon_{\mathbf{p}}|$.

In the presence of a lattice, the process of adiabatic evolution is more subtle, because we cannot assume that $\varepsilon_{\mathbf{p}}$ is only a function of $|\mathbf{p}|$. Consequently the *shape* of the Fermi surface can change in the adiabatic evolution, and a particle with momentum \mathbf{p} can be inside the Fermi surface for the free electron gas, and outside the Fermi surface for the interacting electron gas. The crucial Luttinger theorem states that even though the shape of the Fermi surface can evolve, the volume enclosed by the Fermi surface is an adiabatic invariant; we discuss this theorem in Section ID. In the presence of a lattice, our basic assumption is that there is a smooth function $\varepsilon_{\mathbf{p}}$ so that the Fermi surface is defined by $\varepsilon_{\mathbf{p}} = 0$, and the excitation energies of the quasiparticles and quasiholes is $|\varepsilon_{\mathbf{p}}|$. Near, the Fermi surface, we assume a linear dependence in momentum orthogonal to the Fermi surface: at a point \mathbf{p}_0 on the Fermi surface, let the normal to the Fermi surface be the direction \mathbf{n} (the value of p_F can depend upon \mathbf{p}_0 , see Fig. 2), and so we can write for \mathbf{p} close to \mathbf{p}_0

$$\varepsilon_{\mathbf{p}} = v_F(\mathbf{p} - \mathbf{p}_0) \cdot \mathbf{n}, \quad v_F = |\nabla_{\mathbf{p}}\varepsilon_{\mathbf{p}}| \equiv p_F/m^*, \quad (6)$$

where $p_F = |\mathbf{p}_0|$. This equation defines the Fermi momentum p_F , the Fermi velocity v_F , and the effective mass m^* , all of which can depend upon the direction $\hat{\mathbf{p}}_0$ in the presence of a lattice. Note that $\nabla_{\mathbf{p}}\varepsilon_{\mathbf{p}} = |\nabla_{\mathbf{p}}\varepsilon_{\mathbf{p}}|\mathbf{n}$ is a vector normal to the Fermi surface.

A further *assumption* in the theory of the interacting electron gas is that we can build up the exponentially large number of other excitations also be composing the elementary excitations. (In a finite system of size N , the number of elementary excitations is of order N , while the number of composite excitations is exponentially large in N .) As we are interested in the thermodynamic limit, we can characterize these excitations by the densities of quasiholes and quasiparticles. In practice, it is quite tedious to keep track of two separate densities, along with a non-analytic dependence of their excitation energy, $|\varepsilon_{\mathbf{p}}|$ on \mathbf{p} . Both these problems can be overcome by a clever

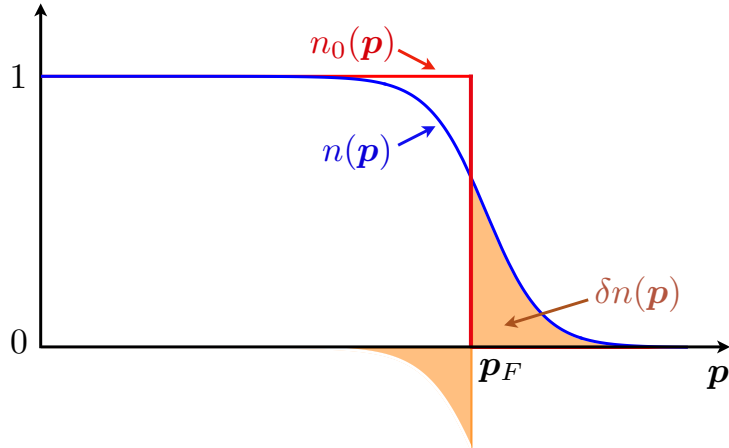


FIG. 3. Plot of the quasiparticle distribution functions $n(\mathbf{p})$ and $\delta n(\mathbf{p})$ of an excited state of the Fermi liquid. Note that $\delta n(\mathbf{p})$ has a discontinuity of unity at the Fermi surface.

mathematical trick; we emphasize that there is no physics assumption involved in this trick—it is merely a bookkeeping device. We *postulate* that the interacting ground state has the same form as the free electron ground state in (3). So the ground state has a density of quasiparticles $n_0(\mathbf{p})$ given by

$$\begin{aligned} n_0(\mathbf{p}) &= 1, & \mathbf{p} \text{ inside the Fermi surface} \\ n_0(\mathbf{p}) &= 0, & \mathbf{p} \text{ outside the Fermi surface} \end{aligned} \quad (7)$$

as shown in Fig. 3. Then, an excited state is characterized by density of quasiparticles $n(\mathbf{p})$, but the excitation energy will depend only upon

$$\delta n(\mathbf{p}) = n(\mathbf{p}) - n_0(\mathbf{p}), \quad (8)$$

where $\delta n(\mathbf{p})$ has a discontinuity of unity at the Fermi surface. So for \mathbf{p} outside the Fermi surface $\delta n(\mathbf{p})$ measures the density of quasiparticle excitations, while for \mathbf{p} inside the Fermi surface $-\delta n(\mathbf{p})$ measures the density of quasihole excitations. (All of these densities can also depend upon the spin of the quasiparticles or quasiholes, a complication we shall ignore in the following discussion.) So the actual density of excitations with energy $|\varepsilon_{\mathbf{p}}|$ is $|\delta n(\mathbf{p})|$. For the total excitation energy, which depends on their product, we can drop the absolute value: this is one of the advantages of this mathematical trick.

We assume we are at temperature $T \ll E_F$, so that the density of quasiparticles and quasiholes is small. Our first thought would be that because of the low density, we can ignore the interactions between the quasiparticles and quasiholes, and compute the total energy of the multiparticle/hole excitations simply by adding their individual energies. An important observation by Landau was

that this is not correct. If we wish to work consistently to order $(T/E_F)^2$ in the total energy, one (and only one) additional term is necessary; ignoring spin-dependence, we present the Landau energy functional

$$E[\delta n(\mathbf{p})] = \sum_{\mathbf{p}} \varepsilon_{\mathbf{p}} \delta n(\mathbf{p}) + \frac{1}{2V} \sum_{\mathbf{p}, \mathbf{k}} F_{\hat{\mathbf{p}}, \hat{\mathbf{k}}} \delta n(\mathbf{p}) \delta n(\mathbf{k}), \quad (9)$$

where V is the volume of the system. At a temperature $T \ll E_F$, $\delta n(\mathbf{p})$ is of order unity only in a window of momenta with $v_F |p - p_F| \sim T$ where $|\varepsilon_{\mathbf{p}}| \sim T$. Then, as we perform the radial integral in the first term in (3), we pick up a factor T from $\varepsilon_{\mathbf{p}}$, and a second factor of T from the limits on the integral: so the first term is of order T^2 . Landau's point is that the second term in (9) is also of order T^2 : there now are 2 integrals over radial momenta, and their product yields a factor of T^2 . This term describes the interaction between the quasiparticles and quasiholes, and is characterized by the unknown Landau interaction function $F_{\hat{\mathbf{p}}, \hat{\mathbf{k}}}$. To order T^2 , we can consistently assume that all the quasiparticles and quasiholes are practically on the Fermi surface in the interaction term, and so $F_{\hat{\mathbf{p}}, \hat{\mathbf{k}}}$ depends only upon the directions of \mathbf{p} and \mathbf{k} .

Although the quasiparticles and quasiholes are assumed to interact in Landau's functional, the interaction is conservative: *i.e.* it does not scatter quasiparticles between momenta, and change the quasiparticle distribution function. The main effect of the interaction term is that the change in the energy of the system upon adding a quasiparticle or quasihole depends upon the density of excitations already present. We will consider scattering processes of quasiparticles later in Section IC: these lead to a finite quasiparticle lifetime, but the corresponding corrections to the energy functional are higher order in T .

Landau's central point is that the values of m^* and $F_{\hat{\mathbf{p}}, \hat{\mathbf{k}}}$ are sufficient to provide a description of the low temperature properties of the interacting electron gas to order $(T/E_F)^2$, and all orders in the strength of the underlying Coulomb interactions.

C. Green's functions and quasiparticle lifetime

For further discussion of the properties of the Fermi liquid, and the nature of its corrections when we consider higher temperatures, it is useful to employ the language of Green's functions. We use the standard many-body Green's function defined in Ref. [1]. The most convenient definition starts from the Green's functions defined in imaginary time τ (ignoring the electron spin α)

$$G(\mathbf{p}, \tau) = - \langle T_{\tau} c_{\mathbf{p}}(\tau) c_{\mathbf{p}}^{\dagger}(0) \rangle \quad (10)$$

where T_{τ} is the time-ordering symbol. We can then Fourier transform this to the Matsubara frequencies $\omega_n = (2n+1)\pi T/\hbar$, n integer, to obtain $G(\mathbf{p}, i\omega_n)$. More generally, we can consider the Green's function in the complex z plane, $G(\mathbf{p}, z)$, obtained by analytic continuation of $G(\mathbf{p}, i\omega_n)$.

This Green's function obeys the spectral representation

$$G(\mathbf{p}, z) = \int_{-\infty}^{\infty} d\Omega \frac{\rho(\mathbf{p}, \Omega)}{z - \Omega} \quad (11)$$

where $\rho(\mathbf{p}, \Omega) = -(1/\pi)\text{Im}[G(\mathbf{p}, \Omega + i0^+)] > 0$ is the spectral density. We will also refer to the retarded Green's function $G^R(\mathbf{p}, \omega) = G(\mathbf{p}, \omega + i0^+)$, and more generally $G^R(\mathbf{p}, z) = G(\mathbf{p}, z)$ for z in the upper-half plane. Closely associated is the electron self-energy $\Sigma(\mathbf{p}, z)$, which is related to the Green's function by Dyson's equation

$$G(\mathbf{p}, z) = \frac{1}{z - \varepsilon_{\mathbf{p}}^0 - \Sigma(\mathbf{p}, z)} \quad (12)$$

where by $\varepsilon_{\mathbf{p}}^0$ we now denote the bare electron dispersion before the effects of electron-electron interactions are accounted for.

The postulates of Fermi liquid theory described above have strong implications for the structure of the Green's function in the complex frequency plane. Specifically, the existence of long-lived quasiparticles near the Fermi surface implies that the Green's function has a pole very close to the real frequency axis, at a frequency obeying $\text{Re}(z) = \varepsilon_{\mathbf{p}}$ for \mathbf{p} close to the Fermi surface. The existence of such a pole implies a free particle behavior of the Green's function at long times, representing the propagation of the quasiparticle. In this section, we wish to go beyond Fermi liquid theory and include a finite quasiparticle lifetime by taking the pole just off the real axis.

Actually, there is an important subtlety in the statement “there is a pole in the Green's function” that we need to keep in mind. The spectral definition (11) implies that $G(\mathbf{p}, z)$ is an analytic function for all z , with a branch cut on the real frequency axis, for an interacting system with a reasonably smooth spectral density $\rho(\mathbf{p}, \Omega)$. The pole is actually in a different Riemann sheet from the definition (11), and is reached by analytically continuing across the branch cut. So the retarded Green's function $G^R(\mathbf{p}, z)$ is analytic for all z in the upper-half plane, and the pole is obtained when we analytically continue $G^R(\mathbf{p}, z)$ to the lower-half plane (where it is *not* equal to the $G(\mathbf{p}, z)$ defined by (11)). For \mathbf{p} close to the Fermi surface in a Fermi liquid, this pole is at a frequency $z = \varepsilon_{\mathbf{p}} - i\gamma_{\mathbf{p}}$ where $\gamma_{\mathbf{p}} > 0$ is related to the quasiparticle lifetime $\tau_{\mathbf{p}} = 1/(2\gamma_{\mathbf{p}})$ because it leads to exponential decay for the Green's function in real time (the factor of 2 arises because we measure the *probability* of observing a quasiparticle a time $\tau_{\mathbf{p}}$ after creating it). Note that the pole is in the lower-half plane of the analytically continued $G^R(\mathbf{p}, z)$ for both signs of $\varepsilon_{\mathbf{p}}$ *i.e.* for both quasiparticles and quasiholes: see Fig. 4.

Ultimately, this complexity can be succinctly captured by initially restricting attention to the G Green's function on the imaginary frequency axis. Then, the existence of the quasiparticle implies that the Green's function defined by (11) obeys

$$G(\mathbf{p}, i\omega) = \frac{Z_{\mathbf{p}}}{i\omega - \varepsilon_{\mathbf{p}} + i\gamma_{\mathbf{p}} \text{sgn}(\omega)} + G_{\text{inc}}(\mathbf{p}, i\omega_n), \quad (13)$$

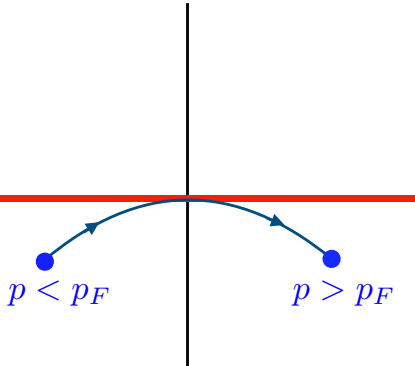


FIG. 4. The poles of the Green's function $G^R(\mathbf{p}, z)$ in the complex z plane. The poles are in the second Riemann sheet, and the horizontal line represents the branch cut implied by (11).

where $\varepsilon_{\mathbf{p}}^0$ is the 'bare' electron dispersion,

$$\varepsilon_{\mathbf{p}} = \varepsilon_{\mathbf{p}}^0 + \text{Re} [\Sigma(\mathbf{p}, 0)] \quad (14)$$

is the 'renormalized' quasiparticle dispersion, and

$$\gamma_{\mathbf{p}} = -\text{Im} [\Sigma(\mathbf{p}, \varepsilon_{\mathbf{p}} + i0^+)] > 0. \quad (15)$$

Consistency of the above definitions requires that the inverse lifetime of the quasiparticle is much smaller than its excitation energy, *i.e.*

$$\gamma_{\mathbf{p}} \ll |\varepsilon_{\mathbf{p}}|, \quad (16)$$

for \mathbf{p} close the Fermi surface. The Fourier transform of G has a slowly-decaying contribution which is just that of a free particle but with renormalized dispersion, and an amplitude suppressed by $Z_{\hat{\mathbf{p}}}$. Consequently, $Z_{\hat{\mathbf{p}}}$ is the quasiparticle residue, and it equals the square of the overlap between the free and quasiparticle wavefunctions. The G_{inc} term is the 'incoherent' contribution, associated with additional excitations created from the particle-hole continuum upon inserting a single particle into the system: this contribution decays rapidly in time, and can be ignored relative the quasiparticle contribution for the low energy physics.

From (13), we can now compute the momentum distribution function $n_e(\mathbf{p})$ of the underlying electrons;

$$n_e(\mathbf{p}) = \langle c_{\mathbf{p}}^\dagger c_{\mathbf{p}} \rangle, \quad (17)$$

where we are dropping the spin index. For a free electron gas

$$n_e(\mathbf{p}) = \theta(-\varepsilon_{\mathbf{p}}^0), \quad \text{free electrons, } T = 0, \quad (18)$$

where $\theta(x)$ is the unit step function. So there is a discontinuity of size unity on the Fermi surface in $n_e(\mathbf{p})$. For the interacting electron gas, it is important to distinguish $n_e(\mathbf{p})$ from the distribution

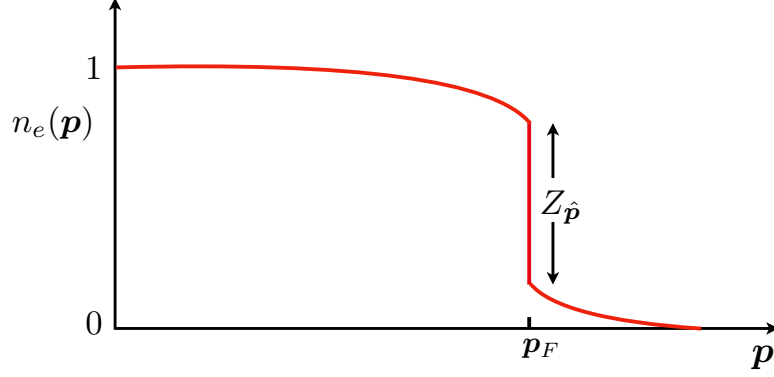


FIG. 5. The momentum distribution function of bare electrons in a Fermi liquid at $T = 0$. There is a discontinuity of size $Z_{\hat{\mathbf{p}}}$ on the Fermi surface.

function of quasiparticles $n(\mathbf{p})$ in (8). The *quasiparticle* momentum distribution function continues to have a discontinuity of size *unity* on the Fermi surface $\varepsilon_{\mathbf{p}} = 0$. For the electron momentum distribution function at $T = 0$, we need to evaluate

$$n_e(\mathbf{p}) = \int_{-\infty}^{\infty} \frac{d\omega}{2\pi} G(\mathbf{p}, i\omega) e^{i\omega 0^+} \quad (19)$$

Evaluating the integral in (19) using (13), we find a discontinuous contribution from the pole near the Fermi surface. There is no reason to expect a discontinuity from G_{inc} , and so we obtain

$$n_e(\mathbf{p}) = Z_{\hat{\mathbf{p}}} \theta(-\varepsilon_{\mathbf{p}}) + \dots, \quad \text{interacting electrons, } T = 0, \quad (20)$$

where \dots is the contribution from G_{inc} . We show a typical plot of $n_e(\mathbf{p})$ in Fig. 5. Because $n_e(\mathbf{p})$ must be positive and bounded by unity, we have a constraint on the quasiparticle residue

$$0 < Z_{\hat{\mathbf{p}}} \leq 1. \quad (21)$$

Note that a small $Z_{\hat{\mathbf{p}}}$ is not an indication that the Fermi liquid theory is not robust: it merely indicates a small overlap between the bare electron and the renormalized quasiparticle. Systems with very small $Z_{\hat{\mathbf{p}}}$ can be very good Fermi liquids: the heavy-fermion compounds discussed in Section V are of this type. Rather it is a short quasiparticle lifetime, or large $\gamma_{\mathbf{p}}$, and the failure of (16), which is a diagnostic of the breakdown of Fermi liquid theory. We will turn to ‘non-Fermi liquids’ (which also have $Z_{\hat{\mathbf{p}}} = 0$) in Section VII.

For an explicit evaluation of the inverse lifetime $\gamma_{\mathbf{p}}$, we have to consider processes beyond those present in Landau Fermi liquid theory. In particular, we have to evaluate the imaginary part of the self energy in (15) for \mathbf{p} near the Fermi surface. This requires a somewhat tedious evaluation of the relevant Feynman diagrams. For now, we will be satisfied here by ‘guessing’ the answer by

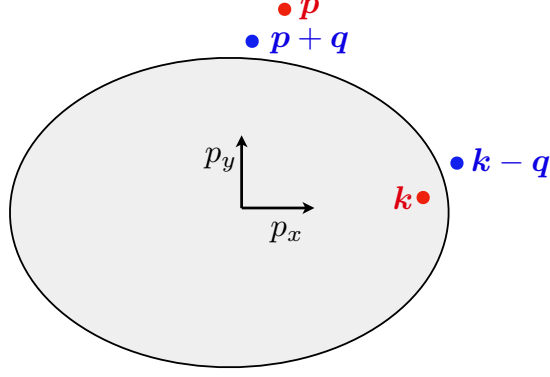


FIG. 6. Decay of a quasiparticle with momentum \mathbf{p} by scattering off a pre-existing quasiparticle with momentum \mathbf{k} to produce a quasiparticles of momenta $\mathbf{p} + \mathbf{q}$ and $\mathbf{k} - \mathbf{q}$.

Fermi's golden rule. Assuming only a contact interaction, U , between the quasiparticles, we can write down the inverse lifetime

$$\frac{1}{\tau_{\mathbf{p}}} = 2\gamma_{\mathbf{p}} = 2\pi U^2 \frac{1}{V^2} \sum_{\mathbf{k}, \mathbf{q}} f(\varepsilon_{\mathbf{k}}) [1 - f(\varepsilon_{\mathbf{p}+\mathbf{q}})] [1 - f(\varepsilon_{\mathbf{k}-\mathbf{q}})] \times \delta(\varepsilon_{\mathbf{p}} + \varepsilon_{\mathbf{k}} - \varepsilon_{\mathbf{p}+\mathbf{q}} - \varepsilon_{\mathbf{k}-\mathbf{q}}). \quad (22)$$

This obtained by employing Fermi's golden rule to the process sketched in Fig. 6, and including probabilities that the initial states are occupied, and the final states are empty. The momentum integrals in (22) are quite difficult to evaluate in general, but it is not difficult to see that the result becomes very small for \mathbf{p} near the Fermi surface and small T , because of the constraints imposed by the Fermi functions and the energy conserving delta function. A simple overestimate can be made by simply ignoring the constraints from momentum conservation, in which case we obtain

$$\begin{aligned} \gamma_{\varepsilon} &\sim U^2 [d(0)]^3 p_F^{-d} \int_{-\infty}^{\infty} d\varepsilon_1 d\varepsilon_2 d\varepsilon_3 f(\varepsilon_1) [1 - f(\varepsilon_2)] [1 - f(\varepsilon_3)] \\ &\quad \times \delta(\varepsilon + \varepsilon_1 - \varepsilon_2 - \varepsilon_3) \\ &= U^2 [d(0)]^3 p_F^{-d} \times \begin{cases} \pi^2 T^2 / 4 & \text{for } \varepsilon = 0 \\ \varepsilon^2 / 2 & \text{for } T = 0. \end{cases} \end{aligned} \quad (23)$$

More careful considerations of momentum conservations are needed to obtain the precise coefficients, but they show that the power-laws above in T and ε are correct. So at low temperatures, $\gamma_{\mathbf{p}} \sim T^2$ is always much smaller than $|\varepsilon_{\mathbf{p}}| \sim T$, and this justifies Fermi liquid theory.

We can also use these results to give a formal definition of the Fermi surface using Green's functions. Notice that γ_{ε} in (23) vanishes as $\varepsilon \rightarrow 0$ at $T = 0$. This follows from the vanishing of the phase space for the decay of an excitation with energy ε as $\varepsilon \rightarrow 0$. This is actually a special case of a more general phenomenon following from the stability of the ground state, and does not

even require excitations to be close to the Fermi surface. The more general statement is

$$\text{Im} [\Sigma(\mathbf{p}, \Omega + i0^+)] \rightarrow 0 \text{ as } \Omega \rightarrow 0 \text{ at } T = 0 \quad (24)$$

for any \mathbf{p} , and its validity can be checked by examining the structure of the Feynman graph expansion for Σ . We will see in Section VII A that (24) applies also to non-Fermi liquids without quasiparticle excitations. We can now define the Fermi surface by the pole in the Green's function which is determined by

$$G^{-1}(\mathbf{p}_F, i0^+) = 0 \text{ at } T = 0. \quad (25)$$

By (24), the left hand side of (25) is real, and so the solution of (25) determines a surface of co-dimension 1 in \mathbf{p} space, which is the Fermi surface. These definitions will be useful in establishing the Luttinger relation constraining the volume enclosed by the Fermi surface, which we will discuss next in Section I D.

D. The Luttinger relation

We will present a proof of the Luttinger relation following the classic text book treatments, but will use an approach which highlights its connections to the modern developments. Specifically, there is a fundamental connection between the Luttinger relation and U(1) symmetries [2, 3]: any many body quantum system has a Luttinger relation associated with each U(1) symmetry, and this connects the density of the U(1) charge in the ground state to the volume enclosed by its Fermi surfaces. This relation applies both to systems of fermions and bosons, or of mixtures of fermions and bosons. However, the relation does not apply if the U(1) symmetry is ‘broken’ or ‘Higgsed’ by the condensation of a boson carrying the U(1) charge. As bosons are usually condensed at low temperatures, the Luttinger relation is not often mentioned in the context of bosons. However, there can be situations when bosons do not condense *e.g.* if the bosons bind with fermions to form a fermionic molecule, and then the molecules form a Fermi surface: then we will have to apply the Luttinger relation to the boson density [2].

We begin by noting a simple argument on why there could even be a relation between a short time correlator (the density, given by an ‘ultraviolet’ (UV) equal-time correlator) and a long-time correlator (the Fermi surface is the locus of zero energy excitations in a Fermi liquid, an ‘infrared’ (IR) property). In the fermion path integral, the free particle term in the Lagrangian is

$$\mathcal{L}_c^0 = \sum_{\mathbf{p}} c_{\mathbf{p}}^\dagger \left(\frac{\partial}{\partial \tau} + \varepsilon_{\mathbf{p}}^0 - \mu \right) c_{\mathbf{p}}, \quad (26)$$

where we have now chosen to extract the chemical potential μ explicitly from the bare dispersion $\varepsilon_{\mathbf{p}}^0$. The expression in (26) is invariant under global U(1) symmetry

$$c_{\mathbf{p}} \rightarrow c_{\mathbf{p}} e^{i\theta} \quad , \quad c_{\mathbf{p}}^\dagger \rightarrow c_{\mathbf{p}}^\dagger e^{-i\theta} \quad (27)$$

as are the rest of the terms in the Lagrangian describing the interactions between the electrons. However, let us now ‘gauge’ this global symmetry by allowing θ to have a *linear* dependence on imaginary time τ :

$$c_{\mathbf{p}} \rightarrow c_{\mathbf{p}} e^{\mu\tau} \quad , \quad c_{\mathbf{p}}^{\dagger} \rightarrow c_{\mathbf{p}}^{\dagger} e^{-\mu\tau} \quad (28)$$

Note that in the Grassman path integral, $c_{\mathbf{p}}$ and $c_{\mathbf{p}}^{\dagger}$ are independent Grassman numbers and so the two transformations in (28) are not inconsistent with each other. The interaction terms in the Lagrangian are explicitly invariant under the time-dependent U(1) transformation in (28). The free particle Lagrangian in (26) is not invariant under (28) because of the presence of the time derivative term; however, application of (28) shows that μ cancels out of the transformed \mathcal{L}_c^0 , and so has completely dropped out of the path integral. We seem to have reached the absurd conclusion that the properties of the electron system are independent of μ : this is explicitly incorrect even for free particles.

What is wrong with the above argument which ‘gauges away’ μ by the transformation in (28)? The answer becomes clear from the expression for the total electron density

$$\rho_e = \frac{1}{V} \sum_{\mathbf{p}} \int_{-\infty}^{\infty} \frac{d\omega}{2\pi} G(\mathbf{p}, i\omega) e^{i\omega 0^+} . \quad (29)$$

The transformation in (28) corresponds to a shift in frequency $\omega \rightarrow \omega + i\mu$ of the contour of integration, and this is not permitted because of singularities in $G(\mathbf{p}, i\omega)$. However, as show below, it is possible to manipulate (29) into a part which contains the full answer, and a remainder which vanishes because manipulations similar to the failed frequency shift in (28) become legal.

The key step to extracting the non-zero part is to use the following simple identity which follows directly from Dyson’s equation (12)

$$\begin{aligned} G(\mathbf{p}, i\omega) &= G_{ff}(\mathbf{p}, i\omega) + G_{LW}(\mathbf{p}, i\omega) \\ G_{ff}(\mathbf{p}, i\omega) &\equiv i \frac{\partial}{\partial \omega} \ln [G(\mathbf{p}, i\omega)] \\ G_{LW}(\mathbf{p}, i\omega) &\equiv -i G(\mathbf{p}, i\omega) \frac{\partial}{\partial \omega} \Sigma(\mathbf{p}, i\omega) . \end{aligned} \quad (30)$$

The non-zero part is G_{ff} : it is a frequency derivative, and so its frequency integral in (29) is not difficult to evaluate exactly after carefully using the $e^{i\omega 0^+}$ convergence factor. The subscript of G_{ff} denotes that this the only term which is non-vanishing for free fermions; indeed we will see below that the frequency integral of G_{ff} has the same value for interacting fermions as for free fermions with the same Fermi surface. The remaining contribution from G_{LW} vanishes for free particles (which have vanishing Σ). Therefore, establishing the Luttinger relation, *i.e.* the invariance of the volume enclosed by the Fermi surface, reduces then to establishing that the contribution of G_{LW} to (29) vanishes.

We consider the latter important step first. We would like to show that

$$\sum_{\mathbf{p}} \int_{-\infty}^{\infty} \frac{d\omega}{2\pi} G_{LW}(\mathbf{p}, i\omega) = 0. \quad (31)$$

We now show that (31) follows from the transformations of G_{LW} under the gauge transformation in (28) for an imaginary chemical potential

$$c_{\mathbf{p}} \rightarrow c_{\mathbf{p}} e^{+i\omega_0\tau}, \quad c_{\mathbf{p}}^{\dagger} \rightarrow c_{\mathbf{p}}^{\dagger} e^{-i\omega_0\tau}. \quad (32)$$

The argument relies on the existence of a functional, $\Phi_{LW}[G(\mathbf{p}, i\omega)]$, of the Green's function, called the Luttinger-Ward functional, so that the self energy is its functional derivative

$$\Sigma(\mathbf{p}, i\omega) = \frac{\delta\Phi_{LW}}{\delta G(\mathbf{p}, i\omega)}. \quad (33)$$

The existence of such a functional can be seen diagrammatically, in which the Luttinger-Ward functional equals the interaction dependent terms for the free energy written in a 'skeleton' graph expansion in terms of the fully renormalized Green's function. Taking the functional derivative with respect to $G(\mathbf{p}, \omega)$ is equivalent to cutting a single G from all such graphs in all possible ways, and these are just the graphs for the self energy. For a more formal argument, see Ref. [4]. An important property of the Luttinger-Ward functional is its invariance under frequency shifts

$$\Phi[G(\mathbf{p}, i\omega + i\omega_0)] = \Phi[G(\mathbf{p}, i\omega)], \quad (34)$$

for any fixed ω_0 . Here, we are regarding Φ as functional of two distinct functions $f_{1,2}(\omega)$, with $f_1(\omega) \equiv G(\mathbf{p}, i\omega + i\omega_0)$ and $f_2(\omega) = G(\mathbf{p}, i\omega)$, and Φ evaluates to the same value for these two functions. Now note that this frequency shift is nothing but the gauge transformation in (32); therefore (34) follows from the fact that such frequency shifts are allowed in Φ_{LW} . The singularity on the real frequency axis is sufficiently weak so that the frequency shifts are legal in a Fermi liquid; but we note that in the non-Fermi liquid SYK model to be considered in Section VI, the Green's functions are significantly more singular at $\omega = 0$, and the analogs of (31) and (34) do not apply. For the Fermi liquid, we can now expand (34) to first order in ω_0 , using (33), and integrating by parts we establish (31).

Now that we have disposed of the offending term in (30), we can return to (29) and evaluate

$$\rho_e = \frac{i}{V} \sum_{\mathbf{p}} \int_{-\infty}^{\infty} \frac{d\omega}{2\pi} \frac{\partial}{\partial\omega} \ln[G(\mathbf{p}, i\omega)] e^{i\omega_0\tau}. \quad (35)$$

We will evaluate the ω integral by distorting the contour in the frequency plane. For this, we need to carefully understand the analytic structure of the integrand. This is subtle, because there are two types of branch cuts. One branch cut arises from the Green's function: $G(\mathbf{p}, z)$ has a branch cut

along the real axis $\text{Im}(z) = 0$, with $\text{Im}G(\mathbf{p}, z) \leq 0$ for $\text{Im}(z) = 0^+$, $\text{Im}G(\mathbf{p}, z) \geq 0$ for $\text{Im}(z) = 0^-$ and $\text{Im}G(\mathbf{p}, z) = 0$ for $z = 0$. The other branch cut is from the familiar $\ln(z)$ function: we take this on the positive real axis, with a discontinuity of $2i\pi$. First, we account for the branch cut in $G(\mathbf{p}, z)$, by distorting the contour of integration in (35) to pick up the discontinuity $\text{Im}G(\mathbf{p}, z)$

$$\rho_e = \frac{-i}{V} \sum_{\mathbf{p}} \int_{-\infty}^0 \frac{dz}{2\pi} \frac{\partial}{\partial z} \ln \left[\frac{G(\mathbf{p}, z + i0^+)}{G(\mathbf{p}, z + i0^-)} \right]. \quad (36)$$

Note from (12) and (24) that on real frequency axis $\text{Im}G(\mathbf{p}, z + i0^\pm) \rightarrow 0$ as $z \rightarrow 0$ or $-\infty$. Consequently the only possible values of $\ln[G(\mathbf{p}, z + i0^+)/G(\mathbf{p}, z + i0^-)]$ are $0, \pm 2\pi i$ as $z \rightarrow 0$ or $-\infty$, from the branch cut of the logarithm. So we obtain from (36)

$$\begin{aligned} \rho_e &= \frac{-i}{2\pi V} \sum_{\mathbf{p}} \ln \left[\frac{G(\mathbf{p}, i0^+)}{G(\mathbf{p}, i0^-)} \right] \\ &= \frac{1}{V} \sum_{\mathbf{p}} \theta(-\varepsilon_{\mathbf{p}}^0 + \mu - \Sigma(\mathbf{p}, i0^+)) \\ &= \frac{1}{V} \sum_{\mathbf{p}} \theta(-\varepsilon_{\mathbf{p}}), \end{aligned} \quad (37)$$

where we have used (14) and (24). Because the branch cut of the logarithm extends to $z = +\infty$, only negative values of $\varepsilon_{\mathbf{p}}$ contribute to the z integral extending from $z = -\infty$ to $z = 0$. Eqn. (37) is the celebrated Luttinger relation, equating the electron density to the volume enclosed by the Fermi surface of the quasiparticles $\varepsilon_{\mathbf{p}} = 0$. In the presence of a crystalline lattice, there can be additional bands which are either fully filled or fully occupied: such bands will yield a contribution of unity or zero respectively to (37).

To summarize, the Luttinger relation is intimately connected to the U(1) symmetry of electron number conservation. Indeed, we can obtain a Luttinger relation for each U(1) symmetry of any system consisting of fermions or bosons. The result follows from the invariance of the Luttinger-Ward functional under the transformation in (32), in which we gauge the global symmetry to a linear time dependence: in this respect, there is a resemblance to 'tHooft anomalies in quantum field theories. If the U(1) symmetry is 'broken' by the condensation of a boson which carries U(1) charge, then the Luttinger relation no longer applies.

II. QUANTUM PHASE TRANSITION OF ISING QUBITS

$$H = -J \sum_{\langle ij \rangle} Z_i Z_j - Jg \sum_i X_i$$

$i \rightarrow d$ -dimensional hypercubic lattice

$X_i, Z_i \rightarrow$ Pauli operators :

$$J > 0, g \geq 0.$$

Determine phase diagram as a function of g .

Will find a quantum phase transition at

$$g = g_c \text{ for all } d.$$

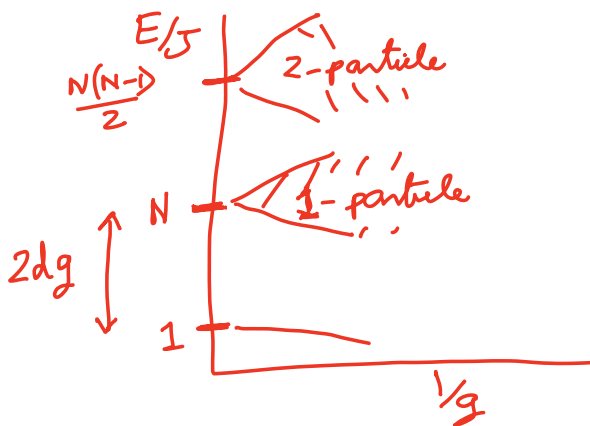
(i) $g \gg 1$.

Unique ground state $|\rightarrow \rightarrow \rightarrow \rightarrow \dots\rangle$

"Quantum paramagnet" ; $|\rightarrow\rangle = \frac{1}{\sqrt{2}}(|\uparrow\rangle + |\downarrow\rangle)$
 $|\leftarrow\rangle = \frac{1}{\sqrt{2}}(|\uparrow\rangle - |\downarrow\rangle)$

N -fold degenerate first excited states (N sites)
 at $g = \infty$

$|i\rangle = |\rightarrow \rightarrow \rightarrow \leftarrow_i \rightarrow \rightarrow \rightarrow \dots\rangle$



Use degenerate perturbation theory in $1/g$.

1- particle states

$$|\vec{k}\rangle = \frac{1}{\sqrt{N}} \sum_i e^{i\vec{k}\cdot\vec{r}_i} |i\rangle$$

$$\frac{\epsilon_k}{J} = -Ng + 2g - 2 \sum_{\alpha=1}^d \cos(k_\alpha a)$$

2- particle states

$$|\vec{k}_1, \vec{k}_2\rangle$$

Scattering and bound states...

(ii) $g \ll 1$

2-fold degenerate ferromagnetic ground states.

$$|\uparrow\uparrow\rangle = |\uparrow\uparrow\uparrow\uparrow\dots\rangle$$

$$|\downarrow\downarrow\rangle = |\downarrow\downarrow\downarrow\downarrow\dots\rangle$$

Cannot be smoothly connected to $g \gg 1$ at $N=\infty$
 \Rightarrow must be a quantum phase transition(s) at intermediate g

First excited states

$$\begin{array}{cccccc} \uparrow & \uparrow & \uparrow & \uparrow & \uparrow & \\ \uparrow & \uparrow & \boxed{\downarrow} & \uparrow & \uparrow & \\ \uparrow & \uparrow & \uparrow & \uparrow & \uparrow & \end{array}$$

"Flipped spin"
particle

$$\epsilon = 2dJ$$

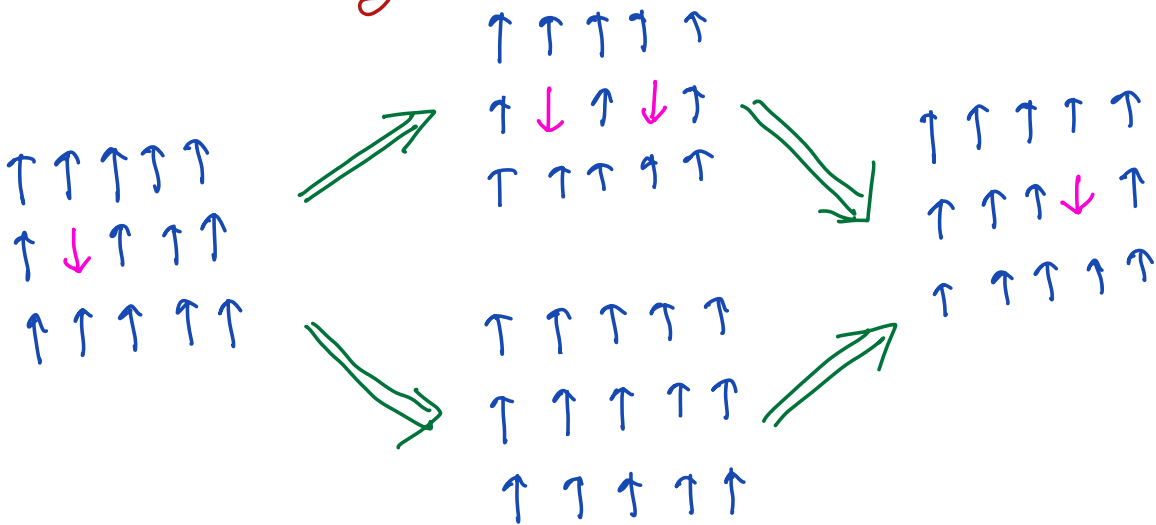
$d=1$ is special

$\uparrow\uparrow\uparrow\downarrow\uparrow\uparrow\uparrow\uparrow \implies \uparrow\uparrow\downarrow\downarrow\downarrow\downarrow\uparrow\uparrow\uparrow$

Flipped spin "fractionalizes" into
2 domain-wall particles.

Dispersion of flipped spin particle.

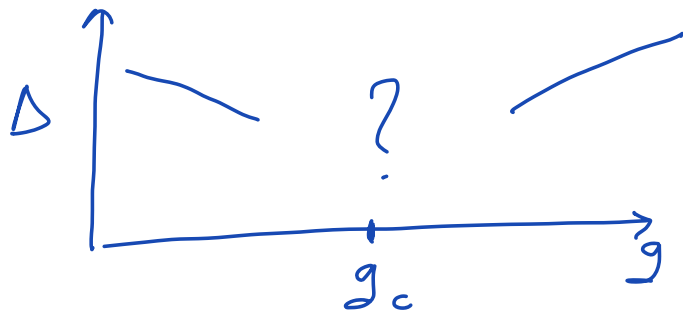
Have to use effective Hamiltonian method
to perform perturbation theory to
order g^2 .



Total matrix element is zero unless initial and
final flipped spins are nearest neighbors.

$$E_k = 2dJ + cJg^2 \sum_{\alpha=1}^d c_{\alpha}(k_{\alpha}a)$$

$\Delta =$ gap to first excited state



A single quantum phase transition at $g = g_c$ where Δ vanishes as

$$\Delta \sim |g - g_c|^{z\nu}$$

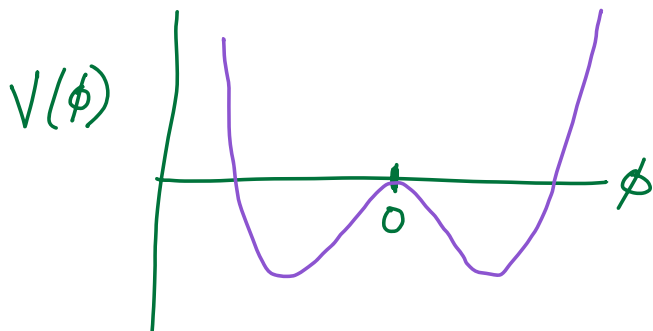
with $z=1$.

Mapping to ϕ^4 quantum field theory

Consider the following non-linear oscillator

$$H = \frac{1}{2m} \Pi_\phi^2 + V(\phi)$$

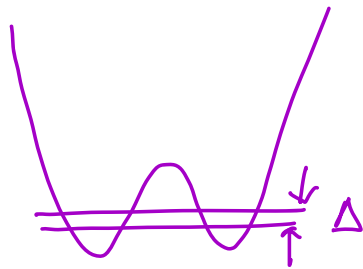
$$[\phi, \Pi_\phi] = i$$



Focus on 2 lowest energy states



Tunneling under the barrier will lift the degeneracy and produce a gap Δ



ground state

$$|\rightarrow\rangle = \frac{1}{\sqrt{2}} (\psi_u + \psi_D) \equiv \frac{1}{\sqrt{2}} (|\uparrow\rangle + |\downarrow\rangle)$$

$$|\leftarrow\rangle = \frac{1}{\sqrt{2}} (\psi_u - \psi_D) \equiv \frac{1}{\sqrt{2}} (|\uparrow\rangle - |\downarrow\rangle)$$

low energy Hamiltonian

$$H = -\frac{\Delta}{2} X$$

What is the operator ϕ in this low energy subspace?

$$|\phi\rangle \Rightarrow \frac{\phi}{\sqrt{2}} (\psi_u(\phi) + \psi_d(\phi))$$

π odd under $\phi \rightarrow -\phi$

$$\langle \rightarrow | \phi | \rightarrow \rangle = 0$$

$$\langle \leftarrow | \phi | \leftarrow \rangle = 0$$

$$\begin{aligned} \langle \leftarrow | \phi | \rightarrow \rangle &= \int_{-\infty}^{\infty} d\phi \frac{\phi}{2} (\psi_u^*(\phi) - \psi_d^*(\phi)) (\psi_u(\phi) + \psi_d(\phi)) \\ &= K \neq 0 \end{aligned}$$

$\Rightarrow \phi$ maps to Z !

Now consider a lattice of such non-linear oscillators and couple them together

$$H = \sum_i \frac{1}{2m} \pi_i^2 + \sum_i V(\phi_i) - \sum_{\langle ij \rangle} \tilde{J} \phi_i \phi_j$$

Provided the \tilde{J} is not too large, we can use the single-site mapping to obtain

$$H_{\text{eff}} = -\frac{\Delta}{2} \sum_i X_i - \tilde{J} K^2 \sum_{\langle ij \rangle} Z_i Z_j$$

From now on we will consider

$$H_\phi = \sum_i \frac{1}{2m} \Pi_{\phi_i}^2 + \sum_i \left(\frac{\lambda}{2} \phi_i^2 + \frac{u}{24} \phi_i^4 \right) - J \sum_{\langle ij \rangle} \phi_i \phi_j$$

In momentum space we can write

$$\phi_k = \frac{1}{\sqrt{N}} \sum_i \phi_i e^{ikx_i}$$

$$-J \sum_{\langle ij \rangle} \phi_i \phi_j = -J \sum_k |\phi_k|^2 \left(\sum_x 2 \cos(k_x a) \right)$$

$$\approx -2J \sum_k |\phi_k|^2 (2d - k^2 \dots) \quad \text{as } k \rightarrow 0.$$

Now take the continuum limit while

defining

$$\phi(x_i) = \frac{1}{\sqrt{a^d}} \phi_i$$

$$\Pi_\phi(x_i) = \frac{1}{\sqrt{a^d}} \Pi_{\phi_i}$$

so that

$$[\phi(x), \Pi_\phi(y)] = i \delta(x-y) \quad \text{as } a \rightarrow 0.$$

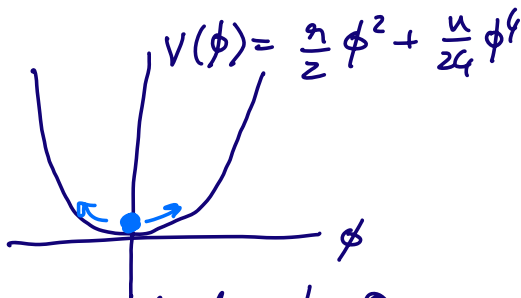
Then after various re-scalings

$$H_\phi = \int d^d x \left[\frac{1}{2} \Pi_\phi^2 + \frac{1}{2} (\vec{\nabla} \phi)^2 + \frac{\eta}{2} \phi^2 + \frac{u}{24} \phi^4 \right]$$

ϕ^4 quantum field theory!

Examine perturbation theory in u for $\eta < 0$ and $\eta > 0$.

(i) $\eta > 0$



ϕ will fluctuate about $\phi = 0$.

$$H = \sum_k \left(\frac{\Pi_k^2}{2} + \frac{\phi_k^2}{2} (\eta + k^2) \right)$$

One oscillator for each k

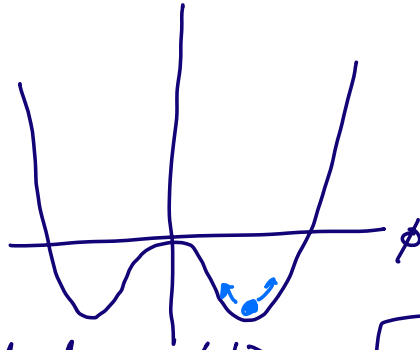
$$\epsilon_k = \sqrt{\eta + k^2}$$

Very similar to $g \gg 1$ Ising model

gap vanishes as $\eta \rightarrow 0$

$$\Delta = \sqrt{\eta} \quad ; \quad Z\nu = \frac{1}{2}$$

(ii) $\eta < 0$



ϕ fluctuates about $\langle \phi \rangle = \sqrt{-\frac{6\eta}{\mu}}$

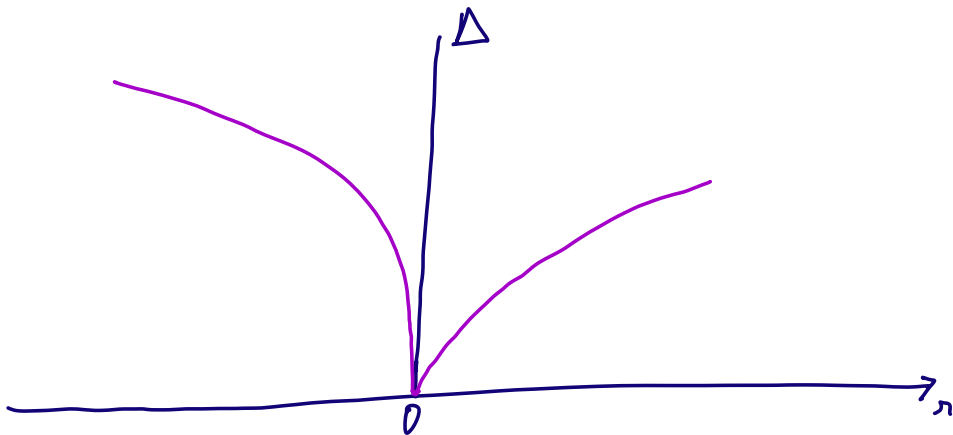
$$H_{\phi} = \sum_k \frac{|\phi_k|^2}{2} (2|\eta| + k^2) + \sum_k \frac{\pi_k^2}{2}$$

Similar to flipped spin quasiparticles at $g \ll 1$.

$$\epsilon_k = \sqrt{k^2 + 2|\eta|}$$

Energy gap vanishes as

$$\Delta = \sqrt{2|\eta|}$$



Quantum critical point at $z=0$

$$\varepsilon_k = k$$

Massless relativistic boson

$$z=1$$

Imaginary time path integral

Single particle path integral

$$H = \frac{m}{2} \Pi_\phi^2 + V(\phi)$$

$$Z = \text{Tr} e^{-\beta H} = \int_{\phi(0)=\phi(\beta)} \mathcal{D}\phi(\tau) e^{-S[\phi]}$$

$$S[\phi] = \int_0^\beta d\tau \left[\frac{m}{2} \left(\frac{d\phi}{d\tau} \right)^2 + V(\phi) \right]$$

$$H_\phi = \int d^d x \left[\frac{1}{2} \Pi_\phi^2 + \frac{1}{2} (\nabla\phi)^2 + \frac{g}{2} \phi^2 + \frac{u}{24} \phi^4 \right]$$

$$Z_\phi = \text{Tr} e^{-\beta H_\phi} = \int_{\phi(x,\beta)=\phi(x,0)} \mathcal{D}\phi(x,\tau) \exp\left(-\int d^d x d\tau \mathcal{L}[\phi]\right)$$

$$\begin{aligned}\mathcal{L}[\phi] &= \frac{1}{2}(\partial_t \phi)^2 + \frac{1}{2}(\nabla \phi)^2 + \frac{\eta}{2}\phi^2 + \frac{\mu}{24}\phi^4 \\ &= \frac{1}{2}(\partial_\mu \phi)^2 + \frac{\eta}{2}\phi^2 + \frac{\mu}{24}\phi^4\end{aligned}$$

Relativistic quantum field theory in
 $d+1$ spacetime dimensions.

III. ISING FERROMAGNETISM IN A METAL

See slides in Appendix A.

We now consider the onset of Ising ferromagnetic order in a metal. This can be described by coupling the Z_i to the σ^z ferromagnetic moment of a Fermi liquid of electrons c_i . So we are led to consider the Hamiltonian

$$H = \sum_{\mathbf{k},\alpha} \varepsilon_{\mathbf{k}} c_{\mathbf{k}\alpha}^\dagger c_{\mathbf{k}\alpha} - J \sum_{\langle ij \rangle} Z_i Z_j - h \sum_i X_i - g \sum_i Z_i c_{i\alpha}^\dagger \sigma_{\alpha\beta}^z c_{i\beta} \quad (38)$$

(we have changed notation, and now use h for the transverse field, and g for the fermion-Ising ‘Yukawa’ coupling). Near the quantum phase transition for the onset of ferromagnetism, we can represent the quantum Ising model by a ϕ^4 quantum field theory, as in Section II, and obtain the continuum Lagrangian

$$\begin{aligned} \mathcal{L} = & \sum_{\mathbf{k},\alpha} c_{\mathbf{k},\alpha}^\dagger \left[\frac{\partial}{\partial \tau} + \varepsilon_{\mathbf{k}} \right] c_{\mathbf{k},\alpha} + \int d^2 r \left\{ \frac{1}{2} [(\nabla \phi)^2 + (\partial_\tau \phi)^2 + s \phi^2] + \frac{u}{4!} \phi^4 \right\} \\ & - \int d^2 r g \phi c_\alpha^\dagger \sigma_{\alpha\beta}^z c_\beta \end{aligned} \quad (39)$$

The Yukawa coupling g between ϕ and the fermions c is relevant [5, 6], and we will consider its consequences in Section VII.

IV. SPIN DENSITY WAVE ORDER IN A METAL

See slides in Appendix A.

Let us now consider the onset of magnetism at a non-zero wavevector in a metal, often called a spin density wave (SDW). We will focus on the case where the wavevector of the SDW is $\mathbf{K} = (\pi, \pi)$ on the square lattice, and so the ordering has the same symmetry as the Néel state in an insulating antiferromagnet. The main ingredient here will be a bosonic collective mode representing antiferromagnetic spin fluctuations in the metal: this boson is the ‘paramagnon’.

Near the transition from the Fermi liquid to the antiferromagnetic metal, it is possible to derive a systematic approach to the paramagnon modes of a metal. We begin with an electronic Hubbard model

$$H = \sum_{\mathbf{k},\alpha} \varepsilon_{\mathbf{k}} c_{\mathbf{k}\alpha}^\dagger c_{\mathbf{k}\alpha} + U \sum_i n_{i\uparrow} n_{i\downarrow} \quad (40)$$

where $n_{i\uparrow} \equiv c_{i\uparrow}^\dagger c_{i\uparrow}$, and similarly for $n_{i\downarrow}$. Upon using the single-site identity

$$U \left(n_{i\uparrow} - \frac{1}{2} \right) \left(n_{i\downarrow} - \frac{1}{2} \right) = -\frac{2U}{3} \mathbf{S}_i^2 + \frac{U}{4}, \quad (41)$$

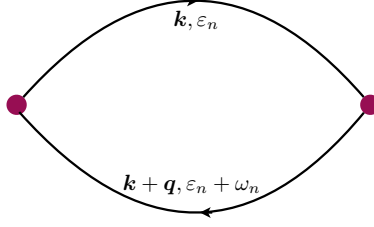


FIG. 7. Feynman diagram leading to (46).

(which is easily established from the electron commutation relations) it becomes possible to decouple the 4-fermion term in a particle-hole channel. We decouple the interaction term in the Hubbard model in (40), by the Hubbard-Stratonovich transformation

$$\exp\left(\frac{2U}{3}\sum_i\int d\tau\mathbf{S}_i^2\right)=\int\mathcal{D}\Phi_i(\tau)\exp\left(-\sum_i\int d\tau\left[\frac{3}{8U}\Phi_i^2-\Phi_i\cdot c_{i\alpha}^\dagger\frac{\sigma_{\alpha\beta}}{2}c_{i\beta}\right]\right)\quad(42)$$

We now have a new field $\Phi_i(\tau)$ which will play the role of the paramagnon field.

The path integral of the Hubbard model can now be written exactly as:

$$\mathcal{Z}=\int\mathcal{D}c_{i\alpha}(\tau)\mathcal{D}\Phi_i(\tau)\exp\left(-\int d\tau\left\{\sum_{\mathbf{k},\alpha}c_{\mathbf{k}\alpha}^\dagger\left[\frac{\partial}{\partial\tau}+\varepsilon_{\mathbf{k}}\right]c_{\mathbf{k}\alpha}+\sum_i\left[\frac{3}{8U}\Phi_i^2-\Phi_i\cdot c_{i\alpha}^\dagger\frac{\sigma_{\alpha\beta}}{2}c_{i\beta}\right]\right\}\right).\quad(43)$$

We can now formally integrate out the electrons, and obtain

$$\frac{\mathcal{Z}}{\mathcal{Z}_0}=\int\prod_i\mathcal{D}\Phi_i(\tau)\exp\left(-\mathcal{S}_{\text{paramagnon}}[\Phi_i(\tau)]\right),\quad(44)$$

where \mathcal{Z}_0 is the free electron partition function. Close to the onset of SDW order (but still on the non-magnetic side), we can expand the action in powers of Φ

$$\mathcal{S}_{\text{paramagnon}}[\Phi_i(\tau)]=\frac{T}{2}\sum_{\mathbf{q},\omega_n}|\Phi(\mathbf{q},\omega_n)|^2\left[\frac{3}{4U}-\frac{\chi_0(\mathbf{q},i\omega_n)}{2}\right]+\dots\quad(45)$$

where $\chi_0(\mathbf{q},\omega_n)$ is the frequency-dependent Lindhard susceptibility, given by the particle-hole bubble graph shown in Fig. 7

$$\chi_0(\mathbf{q},i\omega_n)=-\frac{T}{V}\sum_{\mathbf{p},\varepsilon_n}\frac{1}{(i\varepsilon_n-\varepsilon_{\mathbf{k}})(i\varepsilon_n+i\omega_n-\varepsilon_{\mathbf{k}+\mathbf{q}})}\quad(46)$$

Performing the sum over frequencies by partial fractions, we obtain

$$\chi_0(\mathbf{q},i\omega_n)=\frac{1}{V}\sum_{\mathbf{k}}\frac{f(\varepsilon_{\mathbf{k}+\mathbf{q}})-f(\varepsilon_{\mathbf{k}})}{i\omega_n+\varepsilon_{\mathbf{k}}-\varepsilon_{\mathbf{k}+\mathbf{q}}},\quad(47)$$

From the structure of the Φ propagator, it is clear that Φ will first condense at the wavevector \mathbf{q}_{\max} at which $\chi_0(\mathbf{q}, i\omega = 0)$ is a maximum, and \mathbf{q}_{\max} is then the wavevector of the SDW. In the mean field treatment of (45), the appearance of this condensate requires that U is large enough to obey the ‘Stoner criterion’:

$$\frac{3}{4U} - \frac{\chi_0(\mathbf{q}_{\max}, i\omega = 0)}{2} < 0. \quad (48)$$

This wavevector is in turn determined by the dispersion $\varepsilon_{\mathbf{k}}$ of the underlying fermions. For simplicity, we will only consider the case of a SDW with wavevector $\mathbf{K} = (\pi, \pi)$. The frequency dependence of $\chi_0(\mathbf{q}, i\omega)$ also has an important influence on the dynamics of the paramagnon fluctuations, related to the damping computed in Section VII for the Ising ferromagnetic case.

A. Fermi surface reconstruction

Let us now move into the antiferromagnetic metal phase, where there is a Φ condensate at wavevector $\mathbf{K} = (\pi, \pi)$

$$\langle \Phi_i \rangle = \eta_i \mathcal{N} \hat{z}, \quad (49)$$

with \mathcal{N} measuring the strength of the Néel ordered moment. We wish to describe the excitations of this state. One class of excitations are spin waves: these can be obtained by considering transverse fluctuations of Φ about the condensate in (49) using the full action in (44). However, there are also low energy fermionic excitations in the antiferromagnetic metal, which are gapped in the insulator. We can determine the spectrum of the fermions by inserting (49) into the Yukawa coupling; using $\eta_i = e^{i\mathbf{K} \cdot \mathbf{r}_i}$, with $\mathbf{K} = (\pi, \pi)$, we can write the fermion Hamiltonian in momentum space

$$H_{\text{AFM}} = \sum_{\mathbf{k}} \left[\varepsilon_{\mathbf{k}} c_{\mathbf{k}\alpha}^\dagger c_{\mathbf{k}\alpha} - \Delta c_{\mathbf{k}\alpha}^\dagger \sigma_{\alpha\alpha}^z c_{\mathbf{k}+\mathbf{K},\alpha} \right] + \text{constant}. \quad (50)$$

This is the analog of the BCS Hamiltonian for superconductivity, and the analog of the pairing gap is the energy

$$\Delta = \lambda \mathcal{N}. \quad (51)$$

But, in general, the spectrum of H_{AFM} does not have a gap, as we will see below. As in BCS theory, the value of \mathcal{N} has to be determined self-consistently from the mean-field equations.

To obtain the fermionic excitation spectrum, we have to perform the analog of the Bogoliubov rotation in BCS theory. This is achieved by writing H_{AFM} in a 2×2 matrix form by using the fact that $2\mathbf{K}$ is a reciprocal lattice vector, and so $\varepsilon_{\mathbf{k}+2\mathbf{K}} = \varepsilon_{\mathbf{k}}$; correspondingly, the prime over the summation indicates that it only extends over half the Brillouin zone of the underlying lattice, shown in the left panel of Fig. 8, which is the Brillouin zone of the lattice with Néel order.

$$H_{\text{AFM}} = \sum_{\mathbf{k}} (c_{\mathbf{k}\alpha}^\dagger, c_{\mathbf{k}+\mathbf{K},\alpha}^\dagger) \begin{pmatrix} \varepsilon_{\mathbf{k}} & -\Delta \sigma_{\alpha\alpha}^z \\ -\Delta \sigma_{\alpha\alpha}^z & \varepsilon_{\mathbf{k}+\mathbf{K}} \end{pmatrix} \begin{pmatrix} c_{\mathbf{k}\alpha} \\ c_{\mathbf{k}+\mathbf{K},\alpha} \end{pmatrix}. \quad (52)$$

Square-lattice Hubbard model with no doping

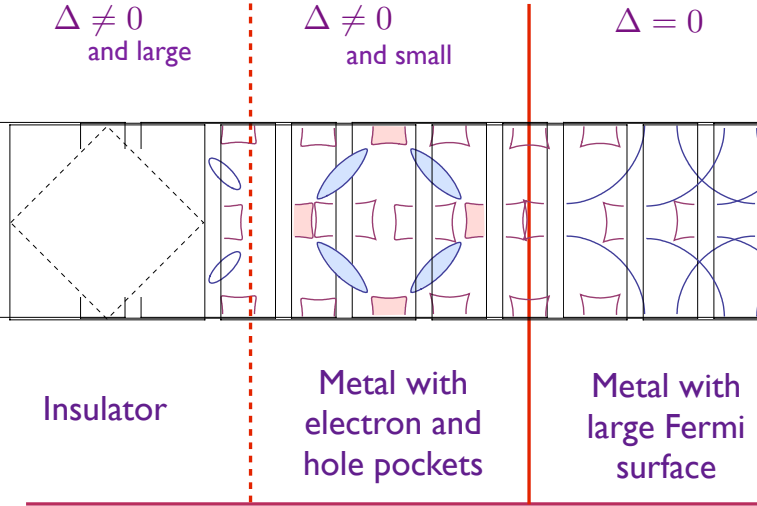


FIG. 8. Fermi surfaces of the Néel state at doping $p = 0$. The pockets intersecting the diagonals of the Brillouin zone have both bands in (53) empty and so form hole pockets, while the remaining pockets have both bands occupied and form electron pockets. The dashed line in the insulator shows the boundary of the Brillouin zone of the Néel state

It is now easy to diagonalize the 2×2 matrix in (52), and we obtain

$$E_{\mathbf{k}\pm} = \frac{\varepsilon_{\mathbf{k}} + \varepsilon_{\mathbf{k}+\mathbf{K}}}{2} \pm \left[\left(\frac{\varepsilon_{\mathbf{k}} - \varepsilon_{\mathbf{k}+\mathbf{K}}}{2} \right)^2 + \Delta^2 \right]^{1/2} \quad (53)$$

Unlike the BCS spectrum, the spectrum in (53) is not gapped, or even positive definite. Rather, it is the spectrum of a metal, in which the negative energy states are filled, and bounded by a Fermi surface. The Fermi surfaces so obtained is shown in Figs. 8, 9, 10 for different values of p .

We observe that the ‘large’ Fermi surface of the paramagnetic metal has ‘reconstructed’ into small pocket Fermi surfaces in the SDW state. The excitations of the SDW metal are hole-like quasiparticles on the Fermi surfaces surrounding the hole pockets, and electron-like quasiparticles on the Fermi surfaces surrounding the electron pockets. The spin wave excitations interact rather weakly with the fermionic quasiparticle excitations: this can be seen from a somewhat involved computation from the effective action.

Finally we discuss the fate of the Luttinger relation of Section ID in this metal. The Luttinger relation connects the volume enclosed by the Fermi surface to the density of electrons, modulo 2 electrons per unit cell. It should be applied in the Brillouin zone of the Néel state, which is half the size of the Brillouin zone of the underlying square lattice, as shown in Fig. 8. In real space, this corresponds to the fact that the unit cell has doubled, and so the density of electrons per unit

Square-lattice Hubbard model with hole doping

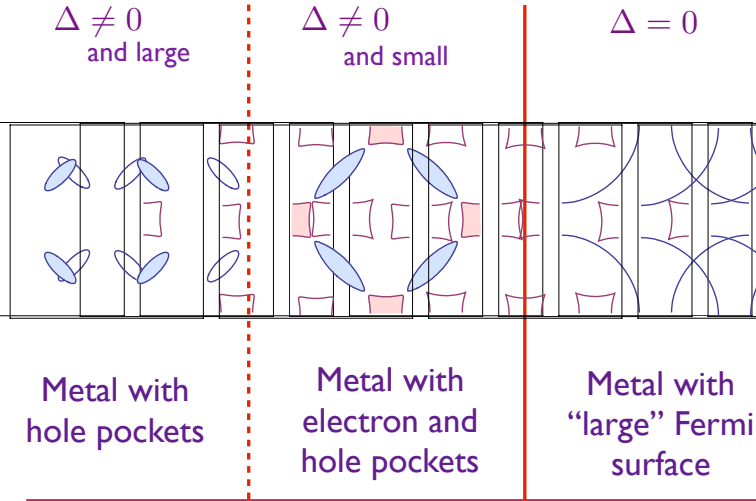


FIG. 9. Fermi surfaces of the Néel state at $p > 0$. The pockets are as in Fig. 8.

Square-lattice Hubbard model with electron doping

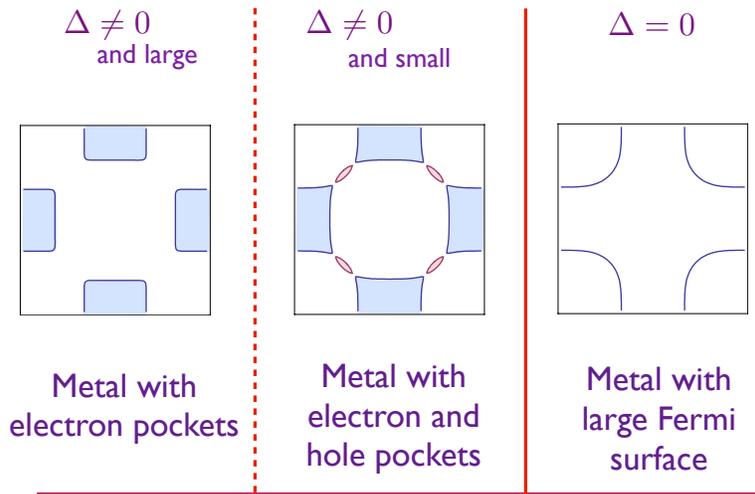


FIG. 10. Fermi surfaces of the Néel state at $p < 0$, with pockets as in Figs. 8.

cell is $2(1 - p)$. For spinful electrons, the Luttinger relations measures electron density modulo 2, and so the density appearing in the Luttinger relation is $-2p$. This has to be equated to twice the volumes enclosed by the electron and hole pockets within the diamond shaped Brillouin zone in Fig. 8. Let \mathcal{A}_h be the area of a single elliptical hole pocket: there are 4 such pockets in the complete Brillouin zone of the square lattice or 2 pockets in the Brillouin zone of the Néel state,

as is apparent from Figs. 8, 9, 10. Similarly, let \mathcal{A}_e be the area of a single elliptical electron pocket: there are 2 such pockets in the complete Brillouin zone of the square lattice or 1 pocket in the Brillouin zone of the Néel state. These arguments show that the Luttinger relation becomes

$$2 \times \frac{1}{(2\pi)^2/2} \times (-2\mathcal{A}_h + \mathcal{A}_e) = -2p. \quad (54)$$

On the left hand side, the first factor is the spin degeneracy, and the second factor is the inverse of the volume of the Brillouin zone of the Néel state. To reiterate, this is the conventional Luttinger relation applied after accounting for the doubling of the unit cell, and it determines a linear constraint on the areas of the electron and hole pockets.

V. FERMI VOLUME CHANGE IN A METAL

See slides in Appendix B.

VI. THE SYK MODEL

See slides in Appendix C.

The Hamiltonian of a version of a SYK model is illustrated in Fig. 11. A system with fermions c_i , $i = 1 \dots N$ states is assumed. Depending upon physical realizations, the label i could be position or an orbital, and it is best to just think of it as an abstract label of a fermionic qubit with the two states $|0\rangle$ and $c_i^\dagger |0\rangle$. $\mathcal{Q}N$ fermions are placed in these states, so that a density $\mathcal{Q} \approx 1/2$ is occupied, as shown in Fig. 11. The quantum dynamics is restricted to *only* have a ‘collision’ term between the fermions, analogous to the right-hand-side of the Boltzmann equation. However, in stark contrast to the Boltzmann equation, statistically independent collisions are not assumed, and quantum interference between successive collisions is accounted for: this is the key to building up a many-body state with non-trivial entanglement. So a collision in which fermions move from sites i and j to sites k and ℓ is characterized not by a probability, but by a quantum amplitude $U_{ij;k\ell}$, which is a complex number.

The model so defined has a Hilbert space of order 2^N states, and a Hamiltonian determined by order N^4 numbers $U_{ij;k\ell}$. Determining the spectrum or dynamics of such a Hamiltonian for large N seems like an impossibly formidable task. But with the assumption that the $U_{ij;k\ell}$ are statistically independent random numbers, remarkable progress is possible. Note that an ensemble of SYK models with different $U_{ij;k\ell}$ is not being considered, but a single fixed set of $U_{ij;k\ell}$. Most physical properties of this model are self-averaging at large N , and so as a technical tool, they can be rapidly obtained by computations on an ensemble of random $U_{ij;k\ell}$. In any case, the analytic results described below have been checked by numerical computations on a computer for a fixed

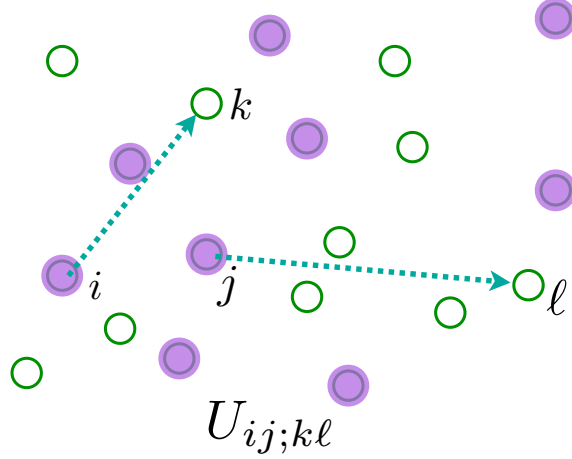


FIG. 11. The SYK model: fermions undergo the transition (‘collision’) shown with quantum amplitude $U_{ij;kl}$.

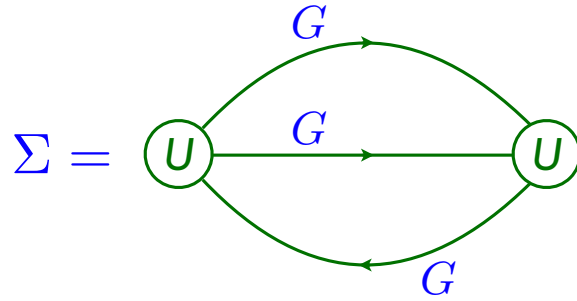


FIG. 12. Self-energy for the fermions of \mathcal{H} in (55) in the limit of large N . The intermediate Green’s functions are fully renormalized.

set of $U_{ij;kl}$. Recall that, even for the Boltzmann equation, there was an ensemble average over the initial positions and momenta of the molecules that was implicitly performed.

Specifically, the Hamiltonian in a chemical potential μ is

$$\mathcal{H} = \frac{1}{(2N)^{3/2}} \sum_{i,j,k,\ell=1}^N U_{ij;kl} c_i^\dagger c_j^\dagger c_k c_\ell - \mu \sum_i c_i^\dagger c_i \quad (55)$$

$$c_i c_j + c_j c_i = 0 \quad , \quad c_i c_j^\dagger + c_j^\dagger c_i = \delta_{ij} \quad (56)$$

$$\mathcal{Q} = \frac{1}{N} \sum_i c_i^\dagger c_i; \quad [\mathcal{H}, \mathcal{Q}] = 0; \quad 0 \leq \mathcal{Q} \leq 1, \quad (57)$$

and its large N limit is most simply taken graphically, order-by-order in $U_{ij;kl}$, and averaging over $U_{ij;kl}$ as independent random variables with $\overline{U_{ij;kl}} = 0$ and $\overline{|U_{ij;kl}|^2} = U^2$. This expansion can be

used to compute graphically the Green's function in imaginary time τ

$$G(\tau) = -\frac{1}{N} \sum_i \overline{\langle \mathcal{T} (c_i(\tau) c_i^\dagger(0)) \rangle}, \quad (58)$$

where \mathcal{T} is the time-ordering symbol, the angular brackets are a quantum average for any given $U_{ij;k\ell}$, and the over-line denotes an average over the ensemble of $U_{ij;k\ell}$. (It turns out that the last average is not needed for large N , because the quantum observable is self-averaging.) In the large N limit, only the graph for the Dyson self energy, Σ , in Fig. 12 survives, and the on-site fermion Green's function is given by the solution of the following equations

$$\begin{aligned} G(i\omega_n) &= \frac{1}{i\omega_n + \mu - \Sigma(i\omega_n)} \\ \Sigma(\tau) &= -U^2 G^2(\tau) G(-\tau) \\ G(\tau = 0^-) &= \mathcal{Q}, \end{aligned} \quad (59)$$

where ω_n is a fermionic Matsubara frequency. The first equation in (59) is the usual Dyson relation between the Green's function and self energy in quantum field theory, the second equation in (59) is the Feynman graph in Fig. 12, and the last determines the chemical potential μ from the charge density \mathcal{Q} . These equations can also be obtained as saddle-point equations of the following exact representation of the disordered-averaged partition function, expressed as a ' $G - \Sigma$ ' theory [7–10]:

$$\begin{aligned} \mathcal{Z} &= \int \mathcal{D}G(\tau_1, \tau_2) \mathcal{D}\Sigma(\tau_1, \tau_2) \exp(-NI) \\ I &= \ln \det [\delta(\tau_1 - \tau_2)(\partial_{\tau_1} + \mu) - \Sigma(\tau_1, \tau_2)] \\ &\quad + \int d\tau_1 d\tau_2 [\Sigma(\tau_1, \tau_2) G(\tau_2, \tau_1) + (U^2/2) G^2(\tau_2, \tau_1) G^2(\tau_1, \tau_2)] \end{aligned} \quad (60)$$

This is a path-integral over bi-local in time functions $G(\tau_1, \tau_2)$ and $\Sigma(\tau_1, \tau_2)$, whose saddle point values are the Green's function $G(\tau_1 - \tau_2)$, and the self energy $\Sigma(\tau_1 - \tau_2)$. This bi-local G can be viewed as a composite quantum operator corresponding to an on-site fermion bilinear

$$G(\tau_1, \tau_2) = -\frac{1}{N} \sum_i \mathcal{T} (c_i(\tau_1) c_i^\dagger(\tau_2)) \quad (61)$$

that is averaged in (58).

For general ω and T , the equations in (59) have to be solved numerically. But an exact analytic solution is possible in the limit $\omega, T \ll U$. At $T = 0$, the asymptotic forms can be obtained straightforwardly [11]

$$G(i\omega) \sim -i \operatorname{sgn}(\omega) |\omega|^{-1/2}, \quad \Sigma(i\omega) - \Sigma(0) \sim -i \operatorname{sgn}(\omega) |\omega|^{1/2}, \quad (62)$$

and a more complete analysis of (59) gives the exact form at non-zero T ($\hbar = k_B = 1$) [12]

$$G(\omega) = \frac{-iC e^{-i\theta} \Gamma\left(\frac{1}{4} - \frac{i\omega}{2\pi T} + i\mathcal{E}\right)}{(2\pi T)^{1/2} \Gamma\left(\frac{3}{4} - \frac{i\omega}{2\pi T} + i\mathcal{E}\right)} \quad |\omega|, T \ll U. \quad (63)$$

Here, \mathcal{E} is a dimensionless number which characterizes the particle-hole asymmetry of the spectral function; both \mathcal{E} and the pre-factor C are determined by an angle $-\pi/4 < \theta < \pi/4$

$$e^{2\pi\mathcal{E}} = \frac{\sin(\pi/4 + \theta)}{\sin(\pi/4 - \theta)} \quad , \quad C = \left(\frac{\pi}{U^2 \cos(2\theta)}\right)^{1/4} \quad , \quad (64)$$

and the value of θ is determined by a Luttinger relation to the density \mathcal{Q} [7]

$$\mathcal{Q} = \frac{1}{2} - \frac{\theta}{\pi} - \frac{\sin(2\theta)}{4}. \quad (65)$$

A notable property of (63) at $\mathcal{E} = 0$ is that it equals the temporal Fourier transform of the spatially local correlator of a fermionic field of dimension $1/4$ in a conformal field theory in 1+1 spacetime dimensions. A theory in 0+1 dimensions is considered here, where conformal transformations map the temporal circle onto itself, as reviewed in Appendices A and B of Ref. [13]; such transformations allow a non-zero \mathcal{E} . An important consequence of this conformal invariance is that (63) is a scaling function of $\hbar\omega/(k_B T)$ (after restoring fundamental constants); in other words, the characteristic frequency scale of (63) is determined solely by $k_B T/\hbar$, is independent of the value of U/\hbar . A careful study of the consequences of this conformal invariance have established the following properties of the SYK model (more complete references to the literature are given in other reviews [13, 14]):

- There are no quasiparticle excitations, and the SYK model exhibits quantum dynamics with a ‘Planckian’ relaxation time of order $\hbar/(k_B T)$ at $T \ll U$. In particular, the relaxation time is *independent* of U , a feature not present in any ordinary metal with quasiparticles. While the Planckian relaxation in (63) implies the absence of quasiparticles with the same quantum numbers as the c fermion, it does not rule out the possibility that c has fractionalized into some emergent quasiparticles; this possibility is ruled out by the exponentially large number of low energy states, as discussed below.
- At large N , the many-body density of states at fixed \mathcal{Q} is [9, 10, 15–18] (see Fig. 13a)

$$D(E) \sim \frac{1}{N} \exp(N s_0) \sinh\left(\sqrt{2N\gamma E}\right) \quad , \quad (66)$$

where the ground state energy has been set to zero. Here s_0 is a universal number dependent only on \mathcal{Q} ($s_0 = 0.4648476991708051\dots$ for $\mathcal{Q} = 1/2$), $\gamma \sim 1/U$ is the only parameter

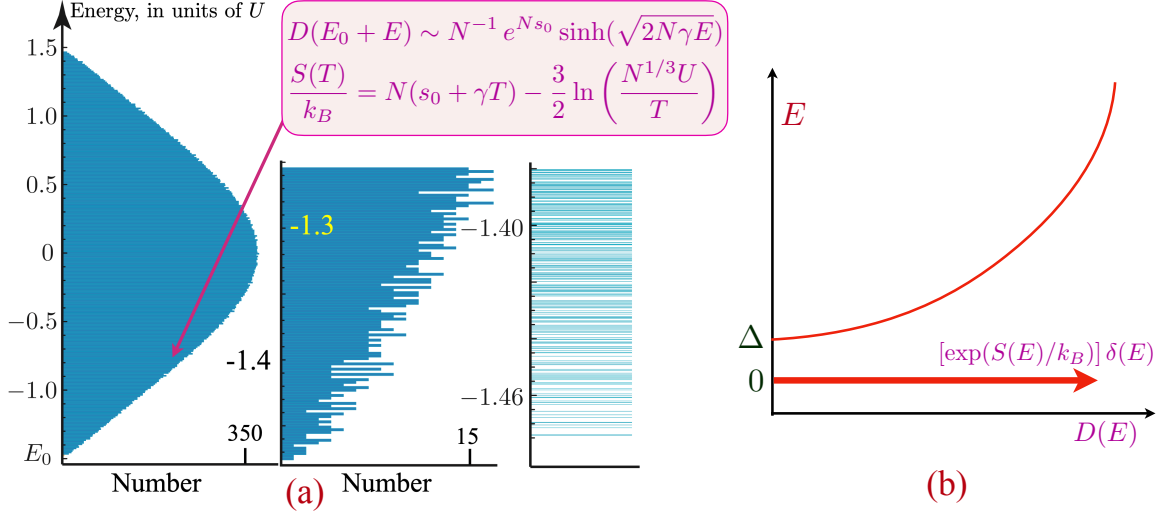


FIG. 13. (a) Plot of the 65536 many-body eigenvalues of a $N = 32$ Majorana SYK Hamiltonian; however, the analytical results quoted here are for the SYK model with complex fermions which has a similar spectrum. The coarse-grained low-energy and low-temperature behavior is described by (66) and (68). (b) Schematic of the lower energy density of states of a supersymmetric generalization of the SYK model [17, 19]. There is a delta function at $E = 0$, and the energy gap Δ is proportional to the inverse of $S(E = 0)$.

dependent upon the strength of the interactions, and the N dependence of the pre-factor is discussed in Ref. [18]. Given $D(E)$, the partition function can be computed from

$$\mathcal{Z} = \int_{0^-}^{\infty} dE D(E) \exp\left(-\frac{E}{k_B T}\right). \quad (67)$$

at a temperature T , and hence the low- T dependence of the entropy at fixed Q is given by

$$\frac{S(T)}{k_B} = N(s_0 + \gamma k_B T) - \frac{3}{2} \ln\left(\frac{U}{k_B T}\right) - \frac{\ln N}{2} + \dots \quad (68)$$

The thermodynamic limit $\lim_{N \rightarrow \infty} S(T)/N$ yields the microcanonical entropy

$$S(E)/k_B = N s_0 + \sqrt{2N\gamma E}, \quad (69)$$

and this connects to the extensive E limit of (66) after using Boltzmann's formula. The limit

$$\lim_{T \rightarrow 0} \lim_{N \rightarrow \infty} \frac{1}{N} S(T) = k_B s_0 \quad (70)$$

is non-zero, which can be realized by an energy-level spacing exponentially small in N near the ground state. The density of states (66) implies that any small energy interval near the

ground state contains an exponentially large number of energy eigenstates (see Fig. 13a). This is very different from systems with quasiparticle excitations, whose energy level spacing vanishes with a positive power of $1/N$ near the ground state, as quasiparticles have order N quantum numbers. The exponentially small level spacing therefore rules out the existence of quasiparticles in the SYK model.

- However, it is important to note that there is no exponentially large degeneracy of the ground state itself in the SYK model, unlike that in a supersymmetric generalization of the SYK model (see Fig. 13b) and the ground states in Pauling’s model of ice [20]. So the SYK model realizes the extensive zero temperature entropy in (70) *without* an exponentially large ground state degeneracy, and was the first model to do so. Computing the ground-state degeneracy requires the opposite order of limits between T and N in (70), and numerical studies show that the entropy density does vanish in such a limit for the SYK model. The many-particle wavefunctions of the low-energy eigenstates in Fock space change chaotically from one state to the next, providing a realization of maximal many-body quantum chaos [21] in a precise sense. This structure of eigenstates is very different from systems with quasiparticles, for which the lowest energy eigenstates differ only by adding and removing a few quasiparticles.
- The E dependence of the density of states in (66) is associated with a time reparameterization mode, and (66) shows that its effects are important when $E \sim 1/N$. The low energy quantum fluctuations of (60) can be expressed in terms of a path integral which reparameterizes imaginary time $\tau \rightarrow f(\tau)$, in a manner analogous to the quantum theory of gravity being expressed in terms of the fluctuations of the spacetime metric. There are also quantum fluctuations of a phase mode $\phi(\tau)$, whose time derivative is the charge density, and the path integral in (60) reduces to the partition function

$$\mathcal{Z}_{\text{SYK-TR}} = e^{N s_0} \int \mathcal{D}f \mathcal{D}\phi \exp \left(-\frac{1}{\hbar} \int_0^{\hbar/(k_B T)} d\tau \mathcal{L}_{\text{SYK-TR}}[f, \phi] \right) \quad (71)$$

The Lagrangian $\mathcal{L}_{\text{SYK-TR}}$ is known, and involves a Schwarzian of $f(\tau)$. Remarkably, despite its non-quadratic Lagrangian, the path integral in (71) can be performed exactly [17], and leads to (66).

A. The Yukawa-SYK model

The SYK model defined above is a 0+1 dimensional theory with no spatial structure, and so cannot be directly applied to transport of strange metals in non-zero spatial dimensions. A great deal of work has been undertaken on generalizing the SYK model to non-zero spatial dimensions [13], but this effort has ultimately not been successful: although ‘bad metal’ states have been

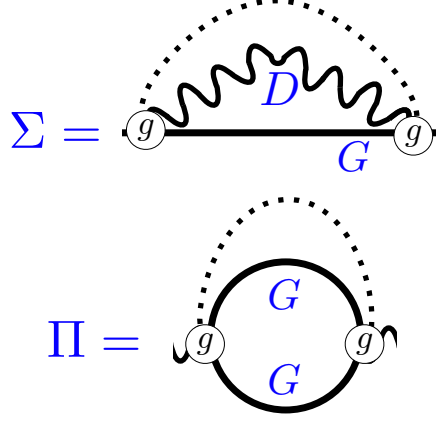


FIG. 14. Self-energies of the fermions and bosons in the Hamiltonian \mathcal{H}_Y in (72). The intermediate Green's functions are fully renormalized.

obtained, low T strange metals have not. But another effort based upon a variation of the SYK model, the 0+1 dimensional ‘Yukawa-SYK’ model [19, 22–32], has been a much better starting point for a non-zero spatial dimensional theory, as shown in Section VIII. The present subsection describes the basic properties of the simplest realization [26, 30–32] of the Yukawa-SYK model.

In the spirit of (55), a model of fermions c_i ($i = 1 \dots N$) and bosons ϕ_ℓ ($\ell = 1 \dots N$) with a Yukawa coupling $g_{ij\ell}$ between them is now considered

$$\mathcal{H}_Y = -\mu \sum_i c_i^\dagger c_i + \sum_\ell \frac{1}{2} (\pi_\ell^2 + \omega_0^2 \phi_\ell^2) + \frac{1}{N} \sum_{ij\ell} g_{ij\ell} c_i^\dagger c_j \phi_\ell, \quad (72)$$

with $g_{ij\ell}$ independent random numbers with zero mean and r.m.s. value g . The bosons are oscillators with the same frequency ω_0 , while the fermions have no one-particle hopping. The large N limit of (72) can be taken just as for the SYK model in (55). The self-energy graph in Fig. 12 is replaced by those in Fig. 14: the phonon Green's function is D , while the phonon self-energy is Π .

Continuing the parallel with the SYK model, the disorder-averaged partition function of the Yukawa-SYK model is a bi-local G - Σ - D - Π theory, analogous to (60):

$$\begin{aligned} \mathcal{Z} &= \int \mathcal{D}G \mathcal{D}\Sigma \mathcal{D}D \mathcal{D}\Pi \exp(-N S_{\text{all}}) \\ S_{\text{all}} &= -\ln \det(\partial_\tau - \mu + \Sigma) + \frac{1}{2} \ln \det(-\partial_\tau^2 + \omega_0^2 - \Pi) \\ &+ \int d\tau \int d\tau' \left[-\Sigma(\tau'; \tau) G(\tau, \tau') + \frac{1}{2} \Pi(\tau', \tau) D(\tau, \tau') + \frac{g^2}{2} G(\tau, \tau') G(\tau', \tau) D(\tau, \tau') \right]. \end{aligned} \quad (73)$$

The large N saddle-point equations replacing (59) are:

$$\begin{aligned} G(i\omega_n) &= \frac{1}{i\omega_n + \mu - \Sigma(i\omega_n)} \quad , \quad D(i\omega_n) = \frac{1}{\omega_n^2 + \omega_0^2 - \Pi(i\omega_n)} \\ \Sigma(\tau) &= g^2 G(\tau) D(\tau) \quad , \quad \Pi(\tau) = -g^2 G(\tau) G(-\tau) \end{aligned} \quad (74)$$

The solution of (73) and (74) leads to a critical state with properties very similar to that of the SYK model [26, 30–32]. Only the low-frequency behavior of the Green's functions at $T = 0$, is quoted analogous to (62):

$$G(i\omega) \sim -i \operatorname{sgn}(\omega) |\omega|^{-(1-2\Delta)} \quad , \quad D(i\omega) \sim |\omega|^{1-4\Delta} \quad , \quad \frac{1}{4} < \Delta < \frac{1}{2}. \quad (75)$$

Inserting the ansatz (75) into (74) fixes the value of the critical exponent Δ .

$$\frac{4\Delta - 1}{2(2\Delta - 1)[\sec(2\pi\Delta) - 1]} = 1 \quad , \quad \Delta = 0.42037\dots \quad (76)$$

Although the fermion Green's function has an exponent which differs from that of the SYK model, the thermodynamic properties have the same structure as that of the SYK model, including the presence of the Schwarzian mode and the form of the many-body density of states.

VII. QUANTUM CRITICALITY OF CLEAN METALS

See slides in Appendix D.

Following the example of the Yukawa-SYK model in Section VIA, it was argued [26, 28, 33] that problems of fermions coupled to a critical boson could also be addressed by examining ensembles of theories with different Yukawa couplings. It is also possible to choose the ensemble so that the couplings are spatially independent, and this maintains full translational symmetry in each member of the ensemble. If most members of the ensemble flow to the same universal low energy theory, then we can access the low energy behavior by studying the average over the ensemble. We also obtain the added benefit of a G - Σ action with large N prefactor, which allows for a systematic treatment of the theory.

Here we consider the case of an order parameter of a broken symmetry at zero momentum, such as Ising ferromagnetism of Section III. Similar analyses apply to the cases in Sections IV and V, but will not be discussed here. So we consider the following generalization of the theory (39)

$$\begin{aligned} \mathcal{L} &= \sum_{\alpha=1}^N \sum_{\mathbf{k}} c_{\mathbf{k},\alpha}^\dagger \left[\frac{\partial}{\partial \tau} + \varepsilon(\mathbf{k}) \right] c_{\mathbf{k},\alpha} + \int d^2r \sum_{\gamma=1}^M \left\{ \frac{1}{2} [(\nabla \phi_\gamma)^2 + (\partial_\tau \phi_\gamma)^2 + s \phi_\gamma^2] \right\} \\ &\quad - \int d^2r \sum_{\gamma=1}^M \sum_{\alpha,\beta=1}^N \frac{g_{\alpha\beta\gamma}}{N} \phi_\gamma c_\alpha^\dagger c_\beta. \end{aligned} \quad (77)$$

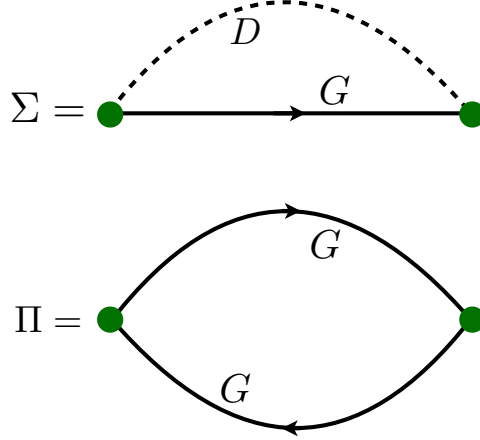


FIG. 15. Saddle point equations for the fermion self energy Σ and boson self energy Π , expressed in terms of the renormalized fermion Green's function G and boson Green's function D . The filled circle is the Yukawa coupling $g_{\alpha\beta\gamma}$.

Here the fermion has N components, the boson has M components, and we take the large N limit with

$$\lambda = \frac{M}{N} \quad (78)$$

fixed. The Yukawa coupling is taken to be a random function of the flavor indices with

$$\overline{g_{\alpha\beta\gamma}} = 0, \quad g_{\alpha\beta\gamma}^* = g_{\beta\alpha\gamma}, \quad \overline{|g_{\alpha\beta\gamma}|^2} = g^2. \quad (79)$$

We have dropped the quartic self-coupling u of the the scalar field for simplicity: it is unimportant for the leading critical behavior, but is needed for certain sub-leading effects at non-zero temperature [33]. The original theory in (39) has a $\phi \rightarrow -\phi$ symmetry which is only statistically present in (77): we can maintain this symmetry in each member of the ensemble by dividing the indices into groups of 2, but we avoid this complexity because it does not modify the large N results. We consider an ensemble of complex couplings because it simplifies the analysis, but real couplings lead to essentially the same results.

We can now proceed with the large N analysis following the script of the Yukawa-SYK model. As in Section VIA, the large N saddle point equations are most easily obtained by a diagrammatic perturbation theory in g , in which we average each graph order-by-order. In the large N limit, only the graphs shown in Fig. 15 survive, and yield the following saddle point equations

$$\begin{aligned}
\Sigma(\mathbf{r}, \tau) &= g^2 \lambda D(\mathbf{r}, \tau) G(\mathbf{r}, \tau), \\
\Pi(\mathbf{r}, \tau) &= -g^2 G(-\mathbf{r}, -\tau) G(\mathbf{r}, \tau), \\
G(\mathbf{k}, i\omega_n) &= \frac{1}{i\omega_n - \varepsilon(\mathbf{k}) - \Sigma(\mathbf{k}, i\omega_n)}, \\
D(\mathbf{q}, i\Omega_m) &= \frac{1}{\Omega_m^2 + q^2 + s - \Pi(\mathbf{q}, i\Omega_m)}.
\end{aligned} \tag{80}$$

Here G is the Green's function for the fermion c , and Σ its self energy, and D is the Green's function for the boson f , and Π is its self energy.

The equations (80) are the analog of the Yukawa-SYK equations in (74), but the Green's functions now involve both spatial and temporal arguments. For completeness, we also write down the path integral of the averaged theory using bilocal Green's functions, the analog of (60) for the SYK model. We introduce the spacetime co-ordinate $X \equiv (\tau, x, y)$, and all Green's functions and self energies in the path integral are functions of two spacetime co-ordinates X_1 and X_2 . Then we have

$$\begin{aligned}
\bar{\mathcal{Z}} &= \int \mathcal{D}G(X_1, X_2) \mathcal{D}\Sigma(X_1, X_2) \mathcal{D}D(X_1, X_2) \\
&\quad \times \mathcal{D}\Pi(X_1, X_2) \exp[-NI(G, \Sigma, D, \Pi)].
\end{aligned} \tag{81}$$

The G - Σ - D - Π action is now

$$\begin{aligned}
I(G, \Sigma, D, \Pi) &= \frac{g^2 \lambda}{2} \text{Tr}(G \cdot [GD]) - \text{Tr}(G \cdot \Sigma) + \frac{\lambda}{2} \text{Tr}(D \cdot \Pi) \\
&\quad - \ln \det [(\partial_{\tau_1} + \varepsilon(-i\nabla_1)) \delta(X_1 - X_2) + \Sigma(X_1, X_2)] \\
&\quad + \frac{\lambda}{2} \ln \det [(-\partial_{\tau_1}^2 - \nabla_1^2 + s) \delta(X_1 - X_2) - \Pi(X_1, X_2)].
\end{aligned} \tag{82}$$

where we have introduced notation

$$\text{Tr}(f \cdot g) \equiv \int dX_1 dX_2 f(X_2, X_1) g(X_1, X_2). \tag{83}$$

Note the crucial pre-factor of N before I in the path-integral. It can be verified that the saddle point equations of (82) reduce to (80).

Remarkably, an exact solution of the low energy scaling behavior is possible for (80), just as it was for the Yukawa-SYK model. For details, see Chapter 34 in *Quantum Phases of Matter*, by S. S., Cambridge University Press (2023). At the critical point $s = 0$, and at $T = 0$, we obtain the fermion self energy

$$\begin{aligned}
\Sigma(i\omega) &= -i \frac{g^2 \lambda}{3v_F \sqrt{3}} \left(\frac{2\pi v_F \kappa}{g^2} \right)^{1/3} \int \frac{d\Omega}{2\pi} \frac{\text{sgn}(\omega + \Omega)}{|\Omega|^{1/3}} \\
&= -iB \text{sgn}(\omega) |\omega|^{2/3} \quad s = 0, T = 0,
\end{aligned} \tag{84}$$

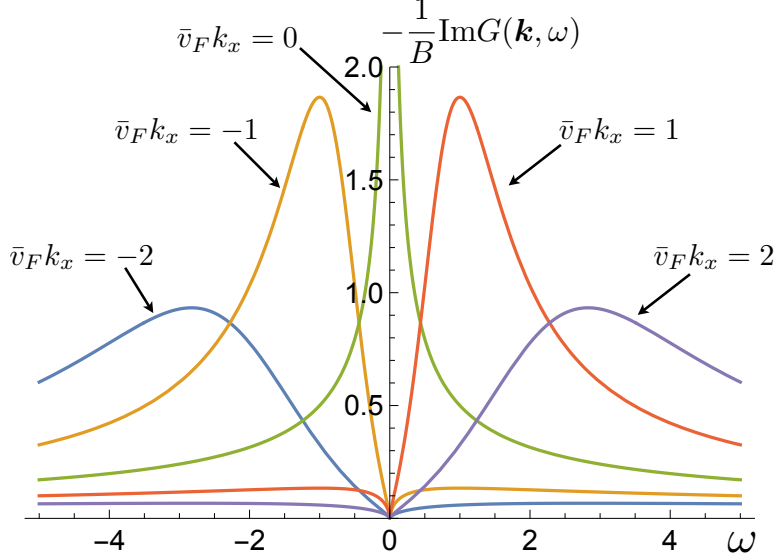


FIG. 16. Plot of fermion spectral density from (86) at wavevectors $\mathbf{k} = \mathbf{k}_0 + (k_x, 0)$ across the Fermi surface without quasiparticles. Here $\bar{v}_F = v_F/B$.

with

$$B = \frac{g^2 \lambda}{2\pi v_F \sqrt{3}} \left(\frac{2\pi v_F \kappa}{g^2} \right)^{1/3}. \quad (85)$$

It is instructive to examine the frequency and momentum dependence of the $T = 0$ fermion Green's function across the Fermi surface. In the scaling limit, we can write the real frequency axis Green's function near the Fermi surface as

$$G(\mathbf{k}, \omega) = \frac{1}{-v_F k_x - \kappa k_y^2/2 + iB e^{-i\pi \text{sgn}(\omega)/3} |\omega|^{2/3}}. \quad (86)$$

As in the SYK model, we can drop the bare ω term in G^{-1} because it is subleading with respect to the frequency-dependent self energy. Note also the distinction in the singularity structure from that of the one-dimensional Tomonaga Luttinger liquid—the singularity here is entirely in the frequency dependence of the self energy, as in the SYK model. We show a plot of $-\text{Im}G$ in Fig. 16. On the Fermi surface $k_x = 0$, $k_y = 0$ we have $\text{Im}G \sim -1/|\omega|^{2/3}$, which is similar to the $\text{Im}G \sim -1/|\omega|^{1/2}$ behavior of the SYK model. Unlike the Fermi liquid, there is no delta function in ω on the Fermi surface, indicating the absence of quasiparticles. Away from the Fermi surface, $\text{Im}G$ actually vanishes on the Fermi surface (see Fig. 16), and there is a broad spectral feature which disperses as $\omega = [(2v_F/(\sqrt{3}B))k_x]^{2/3}$. Note that the position of the Fermi surface is still given by the vanishing of the inverse Green's function at zero frequency, as in (25).

We can compute the momentum distribution function of the electrons from (86), and it leads to result similar in form to that of a Tomonaga-Luttinger liquid

$$n(\mathbf{k}) \sim -\text{sgn}(v_F k_x + \kappa k_y^2/2) |v_F k_x + \kappa k_y^2/2|^{1/2}, \quad (87)$$

with a power-law singularity on the Fermi surface. But recall that the frequency dependent form of (86) is quite different from that for the one-dimensional electron gas.

At non-zero T , the SYK model displays simple ω/T scaling in its spectral function. There are ‘quantum’ contributions which do indeed scale as ω/T for the critical Fermi surface, but there are also additional corrections which arise from classical thermal fluctuations of ϕ which are important. So the $T > 0$ situation is rather complex [28, 33–35].

A. Luttinger relation

The strong damping and breakdown of quasiparticles implied by (84) and (85) nevertheless does not remove the sharp Fermi surface [36]. There is no singular momentum dependence in these expressions, and the frequency dependence still obeys (24). Consequently, there is still a Fermi surface specified by (25).

We now show that this Fermi surface obeys the same Luttinger relation as that of a Fermi liquid. The argument proceeds just as in Section ID. The evaluation of (35) proceeds as before, as the self energy all the needed properties. We only need to examine more carefully the fate of the Luttinger-Ward term in (31):

$$I_2 = -i \int_{-\infty}^{\infty} \int \frac{d^2k}{4\pi^2} \frac{d\omega}{2\pi} G(\mathbf{k}, i\omega) \frac{d}{d\omega} \Sigma(i\omega) e^{-i\omega 0^+}. \quad (88)$$

As the self energy of the critical Fermi surface is singular, it is possible that there is an anomalous contribution at $\omega = 0$ that leads to a non-vanishing I_2 . However, that is not the case here because the singularity of the Green’s function is much weaker as a result of its momentum dependence; the low energy Green’s function is

$$G^{-1}(\mathbf{k}, i\omega) = -v_F k_x - \frac{\kappa}{2} k_y^2 - \Sigma(i\omega), \quad (89)$$

and this diverges at $\omega = 0$ only on the Fermi surface $v_F k_x + \kappa k_y^2/2 = 0$. Indeed, with this form, the local density of states is a constant at the Fermi level. Consequently, there is no anomaly at $T = 0$, and $I_2 = 0$ from the Luttinger-Ward functional analysis. Incidentally, we note that the Luttinger-Ward functional in the large N limit is just the first term in the action I in Eq. (82), similar to the SYK model.

To complete this discussion, we add a few remarks on the structure of the Luttinger-Ward functional, and its connection to global U(1) symmetries [2, 3]. Consider the general case where there are multiple Green’s functions (of bosons or fermions) $G_\alpha(k_\alpha, \omega_\alpha)$. Let the α ’th particle have a charge q_α under a global U(1) symmetry. Then for each such U(1) symmetry, the Luttinger-Ward functional will obey the identity

$$\Phi_{LW} [G_\alpha(\mathbf{k}_\alpha, \omega_\alpha)] = \Phi_{LW} [G_\alpha(\mathbf{k}_\alpha, \omega_\alpha + q_\alpha \Omega)]. \quad (90)$$

Here, we are regarding Φ_{LW} as functional of two distinct sets of functions $f_{1,2\alpha}(\omega_\alpha)$, with $f_{1\alpha}(\omega_\alpha) \equiv G_\alpha(k_\alpha, \omega_\alpha + q_\alpha\Omega)$ and $f_{2\alpha}(\omega) \equiv G_\alpha(k_\alpha, \omega_\alpha)$, and Φ_{LW} evaluates to the same value for these two sets of functions. Expanding (90) to first order in Ω , and integrating by parts, we establish the corresponding $I_2 = 0$.

B. Transport

The highly singular self energy in (84) suggests that there will be strong scattering of charge carriers, and hence a low T resistivity which is larger than the $\sim T^2$ resistivity of a Fermi liquid. Indeed, it was argued in an early work [37] that the resistivity $\sim T^{4/3}$; this is weaker than $\Sigma \sim T^{2/3}$, because of the $(1 - \cos(\theta))$ factor in the transport scattering time, for scattering by an angle θ , and the dominance of forward scattering.

However, this argument ignores the strong constraints placed by momentum conservation [38–43] in a theory of critical fluctuations which is described by a translationally invariant continuum field theory. If we set up an initial state at $t = 0$ with a non-zero current, such a state necessarily has a non-zero momentum, which will remain the same for $t > 0$. The current will decay to a non-zero value which maximizes the entropy subject to the constraint of a non-zero momentum. This non-zero current as $t \rightarrow \infty$ implies that the d.c. conductivity is actually infinite. These considerations are similar to those of ‘phonon drag’ [44, 45] leading to the absence of resistivity from electron-phonon scattering. In practice, phonon drag is observed only in very clean samples [46], because otherwise the phonons rapidly lose their momentum to impurities. But the electron-phonon coupling is weak, allowing for phonon-impurity interactions before there are multiple electron-phonon interactions. In contrast, for the critical Fermi surface, the fermion-boson coupling is essentially infinite because it leads to the breakdown of electronic quasiparticles. So the critical Fermi surface must be studied in the limit of strong drag, with vanishing d.c. resistivity in the critical theory.

More remarkable and subtle is the fact that the non-Fermi liquid structure of (84) also does *not* feed into the optical conductivity, which remains very similar to that of a Fermi liquid [47–52] with the form:

$$\sigma(\omega) \sim \frac{1}{-i\omega} + |\omega|^0 + \dots \quad (\omega^{-2/3} \text{ term has vanishing co-efficient}) \quad (91)$$

There has been a claim [53] of a $\omega^{-2/3}$ contribution to the conductivity, but its co-efficient vanishes after evaluation of all the graphs in Fig. 17 [50, 51]. This cancellation can be understood as a consequence of Kohn’s theorem [54], which states that in a Galilean-invariant system only the first term of the right-hand-side of (91) is non-zero. A Galilean-invariant system is not considered here, but all contributions to the possible $\omega^{-2/3}$ term arise from long-wavelength processes in the vicinity of patches of the Fermi surface, and these patches can be embedded in a system which is

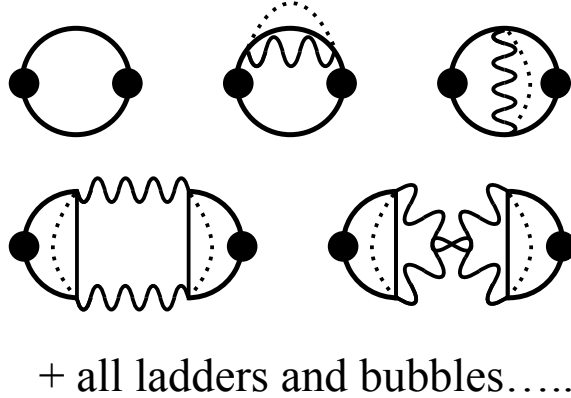


FIG. 17. Diagrams for the conductivity for the theory $\mathcal{L}_c + \mathcal{L}_v + \mathcal{L}_\phi$.

Galilean-invariant also at higher energies.

A detailed analysis of the nature of the fluctuation spectrum of a critical Fermi surface in the particle-hole channel has been provided by Guo [43], and this sheds light on the various regimes at finite time and frequency scales.

VIII. UNIVERSAL THEORY OF STRANGE METALS: THE 2d-YSYK MODEL

See slides in Appendix D.

Mechanisms extrinsic to the theory in Section VII are required to relax the current and obtain a finite d.c. conductivity. In a system with strong interactions, such processes are most conveniently addressed by a ‘memory matrix’ approach that has been reviewed elsewhere [42]; this approach also has close connections to holographic approaches [55, 56]. Various mechanisms have been considered [39, 40, 57–60] involving spatial disorder or umklapp processes, and these do lead to a singular resistivity at low T . Here we focus on the results [50, 61, 62] obtained by including spatial disorder in Yukawa coupling.

We will add spatial disorder to the theory of Ising ferromagnetism in Section III, as described by the large N action in (77). We will not explicitly consider the models of quantum phase transitions in metals in Sections IV and V. The three cases in Sections III, IV, and V lead to distinct universality classes of quantum phase transitions in the clean limit. However, a remarkable fact is that the universality classes become the *same* once spatial disorder is included. This happens because: (i) the Fermi surface becomes ‘fuzzy’ because of elastic scattering, and constraints from momentum conservation become unimportant at distances larger than the fermion mean-free path, and (ii) the boson propagator has the diffusive form in (94) in all three cases.

The most important source of spatial disorder in the theory of disordered Fermi liquids is potential scattering, and so it is natural to include that here in the present theory. A form

amenable to the large N limit being described here is the random potential action, which we add to the action in (77)

$$\mathcal{S}_v = \frac{1}{\sqrt{N}} \sum_{\alpha, \beta=1}^N \int d^2r d\tau v_{\alpha\beta}(\mathbf{r}) \psi_\alpha^\dagger(\mathbf{r}, \tau) \psi_\beta(\mathbf{r}, \tau)$$

$$\overline{v_{\alpha\beta}(\mathbf{r})} = 0, \quad \overline{v_{\alpha\beta}^*(\mathbf{r}) v_{\gamma\delta}(\mathbf{r}') } = v^2 \delta(\mathbf{r} - \mathbf{r}') \delta_{\alpha\gamma} \delta_{\beta\delta} \quad (92)$$

The solution of the corresponding large N saddle point equations shows [61, 62] that the boson polarizability is

$$\Pi(\mathbf{q}, i\Omega_n) \sim -\frac{g^2}{v^2} |\Omega_n|, \quad (93)$$

which leads to $z = 2$ diffusive behavior in the boson propagator, with

$$[D(\mathbf{q}, i\Omega_n)]^{-1} \sim q^2 + \gamma |\Omega_n|. \quad (94)$$

The corresponding fermion self energy is modified from (84): it a familiar elastic impurity scattering contribution Σ_v also present in a disordered Fermi liquid, along with an inelastic term Σ_g [50] with the ‘marginal Fermi liquid’ form [63]

$$\Sigma_v(i\omega_n) \sim -iv^2 \text{sgn}(\omega_n), \quad \Sigma_g(i\omega_n) \sim -\frac{g^2}{v^2} \omega_n \ln(1/|\omega_n|). \quad (95)$$

Despite the promising singularity in Σ_g , (95) does not translate [50] into interesting behavior in the transport: the scattering is mostly forward, and the resistivity is Fermi liquid-like with $\rho(T) = \rho(0) + AT^2$. At larger disorder, the potential scattering v can lead to electron localization effects [64, 65], but these are much weaker than the boson localization effects [66, 67] discussed below.

Much more interesting and appealing behavior results when we add spatial randomness in the Yukawa coupling. Such randomness will be generated by the potential randomness $v_{\alpha\beta}(x)$ considered above, but it has to included at the outset in the large N limit. More explicitly, we recall that the Yukawa coupling invariably arises from a Hubbard-Stratonovich decoupling of a four-fermion interaction: we can decouple such an interaction via a ϕ^2 term which is spatially uniform, and then all the spatial disorder is transferred to the Yukawa term.

We can also view spatial disorder in the Yukawa coupling as a form of ‘Harris’ disorder *i.e.* disorder in the local position of the quantum critical point. Such disorder is usually include as a spatially random contribution $\delta s(\mathbf{r})$ to the boson ‘mass’ s in (77). However, direct treatment of $\delta s(\mathbf{r})$ by the present large N method leads to unphysical results. We have argued [61, 62, 66] that random mass disorder should be treated exactly by rescaling ϕ so that the co-efficient of ϕ^2 is spatially independent. This rescaling induces spatial disorder in all other terms in (77), and the most relevant is the one in the Yukawa coupling.

So we *add* to the spatially independent Yukawa couplings $g_{\alpha\beta\gamma}$ in (77) a second coupling $g'_{\alpha\beta\gamma}(\mathbf{r})$ which has both spatial and flavor randomness with action

$$\begin{aligned} \mathcal{S}_{g'} &= \frac{1}{N} \int d^2r d\tau g'_{\alpha\beta\gamma}(\mathbf{r}) \psi_\alpha^\dagger(\mathbf{r}, \tau) \psi_\beta(\mathbf{r}, \tau) \phi_\gamma(\mathbf{r}, \tau) \\ \overline{g'_{\alpha\beta\gamma}(\mathbf{r})} &= 0, \quad \overline{g'^*_{\alpha\beta\gamma}(\mathbf{r}) g'_{\delta\rho\sigma}(\mathbf{r}')} = g'^2 \delta(\mathbf{r} - \mathbf{r}') \delta_{\alpha\delta} \delta_{\beta\rho} \delta_{\gamma\sigma}. \end{aligned} \quad (96)$$

The complete action of the 2d-YSYK model is given by the sum of (77), (92), and (96), and the large N equations (80) are now modified to

$$\begin{aligned} \Sigma(\mathbf{r}, \tau) &= g^2 \lambda D(\mathbf{r}, \tau) G(\mathbf{r}, \tau) + v^2 G(\tau, \mathbf{r}) \delta^2(\mathbf{r}) + g'^2 G(\tau, \mathbf{r}) D(\tau, \mathbf{r}) \delta^2(\mathbf{r}), \\ \Pi(\mathbf{r}, \tau) &= -g^2 G(-\mathbf{r}, -\tau) G(\mathbf{r}, \tau) - g'^2 G(-\tau, \mathbf{r}) G(\tau, \mathbf{r}) \delta^2(\mathbf{r}), \\ G(\mathbf{k}, i\omega_n) &= \frac{1}{i\omega_n - \varepsilon(\mathbf{k}) - \Sigma(\mathbf{k}, i\omega_n)}, \\ D(\mathbf{q}, i\Omega_m) &= \frac{1}{\Omega_m^2 + q^2 + s - \Pi(\mathbf{q}, i\Omega_m)}. \end{aligned} \quad (97)$$

From the g'^2 terms in (97) we obtain additional contributions to the boson and fermion self energies [28, 33, 61, 62, 67]

$$\Pi_{g'}(\mathbf{q}, i\Omega_n) \sim -g'^2 |\Omega_n|, \quad \Sigma_{g'}(i\omega_n) \sim -ig'^2 \omega_n \ln(1/|\omega_n|), \quad (98)$$

so that the boson propagator retains the crucial diffusive $z = 2$ form in (94). Now the marginal Fermi liquid self energy does contribute significantly to transport [61, 62, 67], with a linear- T resistivity $\sim g'^2 T$, while the residual resistivity is determined primarily by v . It is notable that it is the disorder in the interactions, v , which determines the slope of the linear- T resistivity, while it is the potential scattering disorder which determines the residual resistivity. Other attractive features of this theory are that it has an anomalous optical conductivity $\sigma(\omega)$ with $\text{Re}[1/\sigma(\omega)] \sim \omega$ and a $T \ln(1/T)$ specific heat [61, 62, 67]. A full solution of the large N equations in (97) for $g = 0$ was provided recently by Li *et al.* [62]; at $g = 0$, the self energies depend only upon frequencies, and this enabled the numerical analysis. The optical conductivity was also computed, and the results reproduce key aspects of observations in the cuprates as analyzed by Michon *et al.* [68].

Recent works [66, 67] have examined the crossover to strong Harris disorder at low temperatures. Two distinct regimes emerged:

- At higher energies, both fermion and boson states are extended, for which the application of self-averaging SYK methods in (97) works well.
- At very low energy, the Harris disorder leads to localized overdamped bosonic modes, while the fermions remain extended. The SYK methods cannot be applied in this regime, and the behavior is similar to that expected from the strong disorder renormalization group [69]. This emergent low temperature regime has been argued to explain the ‘foot’ feature which extends strange metal behavior at low T beyond the usual quantum critical region [70, 71].

-
- [1] H. Bruus and K. Flensberg, *Many-Body Quantum Theory in Condensed Matter Physics: An Introduction*, Oxford Graduate Texts (OUP Oxford, 2004).
- [2] S. Powell, S. Sachdev, and H. P. Büchler, *Depletion of the Bose-Einstein condensate in Bose-Fermi mixtures*, *Phys. Rev. B* **72**, 024534 (2005), [cond-mat/0502299](#).
- [3] P. Coleman, I. Paul, and J. Rech, *Sum rules and Ward identities in the Kondo lattice*, *Phys. Rev. B* **72**, 094430 (2005), [cond-mat/0503001](#).
- [4] M. Potthoff, *Non-perturbative construction of the Luttinger-Ward functional*, *Condens. Mat. Phys* **9**, 557 (2006), [arXiv:cond-mat/0406671](#).
- [5] J. A. Hertz, *Quantum critical phenomena*, *Phys. Rev. B* **14**, 1165 (1976).
- [6] A. J. Millis, *Effect of a nonzero temperature on quantum critical points in itinerant fermion systems*, *Phys. Rev. B* **48**, 7183 (1993).
- [7] A. Georges, O. Parcollet, and S. Sachdev, *Quantum fluctuations of a nearly critical Heisenberg spin glass*, *Phys. Rev. B* **63**, 134406 (2001), [arXiv:cond-mat/0009388](#) [[cond-mat.str-el](#)].
- [8] S. Sachdev, *Bekenstein-Hawking Entropy and Strange Metals*, *Phys. Rev. X* **5**, 041025 (2015), [arXiv:1506.05111](#) [[hep-th](#)].
- [9] A. Kitaev and S. J. Suh, *The soft mode in the Sachdev-Ye-Kitaev model and its gravity dual*, *JHEP* **05**, 183, [arXiv:1711.08467](#) [[hep-th](#)].
- [10] J. Maldacena and D. Stanford, *Remarks on the Sachdev-Ye-Kitaev model*, *Phys. Rev. D* **94**, 106002 (2016), [arXiv:1604.07818](#) [[hep-th](#)].
- [11] S. Sachdev and J. Ye, *Gapless spin-fluid ground state in a random quantum Heisenberg magnet*, *Phys. Rev. Lett.* **70**, 3339 (1993), [arXiv:cond-mat/9212030](#) [[cond-mat](#)].
- [12] O. Parcollet and A. Georges, *Non-Fermi-liquid regime of a doped Mott insulator*, *Phys. Rev. B* **59**, 5341 (1999), [arXiv:cond-mat/9806119](#) [[cond-mat.str-el](#)].
- [13] D. Chowdhury, A. Georges, O. Parcollet, and S. Sachdev, *Sachdev-Ye-Kitaev models and beyond: Window into non-Fermi liquids*, *Rev. Mod. Phys.* **94**, 035004 (2022), [arXiv:2109.05037](#) [[cond-mat.str-el](#)].
- [14] S. Sachdev, *Quantum Phases of Matter*, 1st ed. (Cambridge University Press, Cambridge, UK, 2023).
- [15] J. S. Cotler, G. Gur-Ari, M. Hanada, J. Polchinski, P. Saad, S. H. Shenker, D. Stanford, A. Streicher, and M. Tezuka, *Black Holes and Random Matrices*, *JHEP* **05**, 118, [Erratum: *JHEP* 09, 002 (2018)], [arXiv:1611.04650](#) [[hep-th](#)].
- [16] D. Bagrets, A. Altland, and A. Kamenev, *Power-law out of time order correlation functions in the SYK model*, *Nucl. Phys. B* **921**, 727 (2017), [arXiv:1702.08902](#) [[cond-mat.str-el](#)].
- [17] D. Stanford and E. Witten, *Fermionic Localization of the Schwarzian Theory*, *Journal of High Energy Physics* **10**, 008 (2017), [arXiv:1703.04612](#) [[hep-th](#)].

- [18] Y. Gu, A. Kitaev, S. Sachdev, and G. Tarnopolsky, *Notes on the complex Sachdev-Ye-Kitaev model*, *Journal of High Energy Physics* **02**, 157 (2020), [arXiv:1910.14099 \[hep-th\]](#).
- [19] W. Fu, D. Gaiotto, J. Maldacena, and S. Sachdev, *Supersymmetric Sachdev-Ye-Kitaev models*, *Phys. Rev. D* **95**, 026009 (2017), [Addendum: *Phys. Rev. D* 95, 069904 (2017)], [arXiv:1610.08917 \[hep-th\]](#).
- [20] L. Pauling, *The Structure and Entropy of Ice and of Other Crystals with Some Randomness of Atomic Arrangement*, *Journal of the American Chemical Society* **57**, 2680 (1935).
- [21] J. Maldacena, S. H. Shenker, and D. Stanford, *A bound on chaos*, *JHEP* **08**, 106, [arXiv:1503.01409 \[hep-th\]](#).
- [22] J. Murugan, D. Stanford, and E. Witten, *More on Supersymmetric and 2d Analogs of the SYK Model*, *JHEP* **08**, 146, [arXiv:1706.05362 \[hep-th\]](#).
- [23] A. A. Patel and S. Sachdev, *Critical strange metal from fluctuating gauge fields in a solvable random model*, *Phys. Rev. B* **98**, 125134 (2018), [arXiv:1807.04754 \[cond-mat.str-el\]](#).
- [24] E. Marcus and S. Vandoren, *A new class of SYK-like models with maximal chaos*, *JHEP* **01**, 166, [arXiv:1808.01190 \[hep-th\]](#).
- [25] Y. Wang, *Solvable Strong-coupling Quantum Dot Model with a Non-Fermi-liquid Pairing Transition*, *Phys. Rev. Lett.* **124**, 017002 (2020), [arXiv:1904.07240 \[cond-mat.str-el\]](#).
- [26] I. Esterlis and J. Schmalian, *Cooper pairing of incoherent electrons: an electron-phonon version of the Sachdev-Ye-Kitaev model*, *Phys. Rev. B* **100**, 115132 (2019), [arXiv:1906.04747 \[cond-mat.str-el\]](#).
- [27] Y. Wang and A. V. Chubukov, *Quantum Phase Transition in the Yukawa-SYK Model*, *Phys. Rev. Res.* **2**, 033084 (2020), [arXiv:2005.07205 \[cond-mat.str-el\]](#).
- [28] E. E. Aldape, T. Cookmeyer, A. A. Patel, and E. Altman, *Solvable theory of a strange metal at the breakdown of a heavy Fermi liquid*, *Phys. Rev. B* **105**, 235111 (2022), [arXiv:2012.00763 \[cond-mat.str-el\]](#).
- [29] W. Wang, A. Davis, G. Pan, Y. Wang, and Z. Y. Meng, *Phase diagram of the spin-1/2 Yukawa-Sachdev-Ye-Kitaev model: Non-Fermi liquid, insulator, and superconductor*, *Phys. Rev. B* **103**, 195108 (2021), [arXiv:2102.10755 \[cond-mat.str-el\]](#).
- [30] D. Valentinis, G. A. Inkof, and J. Schmalian, *Correlation between phase stiffness and condensation energy across the non-Fermi to Fermi-liquid crossover in the Yukawa-Sachdev-Ye-Kitaev model on a lattice*, *Physical Review Research* **5**, 043007 (2023), [arXiv:2302.13134 \[cond-mat.supr-con\]](#).
- [31] D. Valentinis, G. A. Inkof, and J. Schmalian, *BCS to incoherent superconductivity crossover in the Yukawa-Sachdev-Ye-Kitaev model on a lattice*, *Phys. Rev. B* **108**, L140501 (2023), [arXiv:2302.13138 \[cond-mat.supr-con\]](#).
- [32] H. Hosseinabadi, S. P. Kelly, J. Schmalian, and J. Marino, *Thermalization of non-Fermi-liquid electron-phonon systems: Hydrodynamic relaxation of the Yukawa-Sachdev-Ye-Kitaev model*, *Phys. Rev. B* **108**, 104319 (2023), [arXiv:2306.03898 \[cond-mat.str-el\]](#).
- [33] I. Esterlis, H. Guo, A. A. Patel, and S. Sachdev, *Large N theory of critical Fermi surfaces*, *Phys.*

- Rev. B **103**, 235129 (2021), [arXiv:2103.08615 \[cond-mat.str-el\]](#).
- [34] J. A. Damia, M. Solís, and G. Torroba, *How non-Fermi liquids cure their infrared divergences*, *Phys. Rev. B* **102**, 045147 (2020), [arXiv:2004.05181 \[cond-mat.str-el\]](#).
- [35] Y. Wang, A. Abanov, B. L. Altshuler, E. A. Yuzbashyan, and A. V. Chubukov, *Superconductivity near a Quantum-Critical Point: The Special Role of the First Matsubara Frequency*, *Phys. Rev. Lett.* **117**, 157001 (2016), [arXiv:1606.01252 \[cond-mat.supr-con\]](#).
- [36] G. E. Volovik, *Topology of quantum vacuum*, *Lecture Notes in Physics* **870**, 343 (2013), [arXiv:1111.4627 \[hep-ph\]](#).
- [37] P. A. Lee, *Gauge field, Aharonov-Bohm flux, and high- T_c superconductivity*, *Phys. Rev. Lett.* **63**, 680 (1989).
- [38] S. A. Hartnoll, P. K. Kovtun, M. Muller, and S. Sachdev, *Theory of the Nernst effect near quantum phase transitions in condensed matter, and in dyonic black holes*, *Phys. Rev. B* **76**, 144502 (2007), [arXiv:0706.3215 \[cond-mat.str-el\]](#).
- [39] D. L. Maslov, V. I. Yudson, and A. V. Chubukov, *Resistivity of a Non-Galilean-Invariant Fermi Liquid near Pomeranchuk Quantum Criticality*, *Phys. Rev. Lett.* **106**, 106403 (2011), [arXiv:1012.0069 \[cond-mat.str-el\]](#).
- [40] S. A. Hartnoll, R. Mahajan, M. Punk, and S. Sachdev, *Transport near the Ising-nematic quantum critical point of metals in two dimensions*, *Phys. Rev.* **B89**, 155130 (2014), [arXiv:1401.7012 \[cond-mat.str-el\]](#).
- [41] A. Eberlein, I. Mandal, and S. Sachdev, *Hyperscaling violation at the Ising-nematic quantum critical point in two dimensional metals*, *Phys. Rev. B* **94**, 045133 (2016), [arXiv:1605.00657 \[cond-mat.str-el\]](#).
- [42] S. A. Hartnoll, A. Lucas, and S. Sachdev, *Holographic quantum matter*, MIT Press, Cambridge MA (2016), [arXiv:1612.07324 \[hep-th\]](#).
- [43] H. Guo, *Fluctuation Spectrum of Critical Fermi Surfaces*, (2024), [arXiv:2406.12967 \[cond-mat.str-el\]](#).
- [44] R. Peierls, *Zur Theorie der elektrischen und thermischen Leitfähigkeit von Metallen*, *Annalen der Physik* **396**, 121 (1930).
- [45] R. Peierls, *Zur Frage des elektrischen Widerstandsgesetzes für tiefe Temperaturen*, *Annalen der Physik* **404**, 154 (1932).
- [46] C. W. Hicks, A. S. Gibbs, A. P. Mackenzie, H. Takatsu, Y. Maeno, and E. A. Yelland, *Quantum Oscillations and High Carrier Mobility in the Delafossite $PdCoO_2$* , *Phys. Rev. Lett.* **109**, 116401 (2012), [arXiv:1207.5402 \[cond-mat.str-el\]](#).
- [47] H. K. Pal, V. I. Yudson, and D. L. Maslov, *Resistivity of non-Galilean-invariant Fermi- and non-Fermi liquids*, *Lithuanian Journal of Physics and Technical Sciences* **52**, 142 (2012), [arXiv:1204.3591 \[cond-mat.str-el\]](#).
- [48] D. L. Maslov and A. V. Chubukov, *Optical response of correlated electron systems*, *Reports on Progress in Physics* **80**, 026503 (2017), [arXiv:1608.02514 \[cond-mat.str-el\]](#).

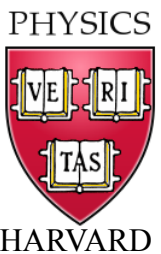
- [49] A. V. Chubukov and D. L. Maslov, *Optical conductivity of a two-dimensional metal near a quantum critical point: The status of the extended Drude formula*, *Phys. Rev. B* **96**, 205136 (2017), [arXiv:1707.07352 \[cond-mat.str-el\]](#).
- [50] H. Guo, A. A. Patel, I. Esterlis, and S. Sachdev, *Large- N theory of critical Fermi surfaces. II. Conductivity*, *Phys. Rev. B* **106**, 115151 (2022), [arXiv:2207.08841 \[cond-mat.str-el\]](#).
- [51] Z. D. Shi, D. V. Else, H. Goldman, and T. Senthil, *Loop current fluctuations and quantum critical transport*, *SciPost Phys.* **14**, 113 (2023), [arXiv:2208.04328 \[cond-mat.str-el\]](#).
- [52] H. Guo, D. Valentinis, J. Schmalian, S. Sachdev, and A. A. Patel, *Cyclotron resonance and quantum oscillations of critical Fermi surfaces*, *Phys. Rev. B* **109**, 075162 (2024), [arXiv:2308.01956 \[cond-mat.str-el\]](#).
- [53] Y. B. Kim, A. Furusaki, X.-G. Wen, and P. A. Lee, *Gauge-invariant response functions of fermions coupled to a gauge field*, *Phys. Rev. B* **50**, 17917 (1994), [arXiv:cond-mat/9405083 \[cond-mat\]](#).
- [54] W. Kohn, *Cyclotron Resonance and de Haas-van Alphen Oscillations of an Interacting Electron Gas*, *Phys. Rev.* **123**, 1242 (1961).
- [55] A. Lucas, *Conductivity of a strange metal: from holography to memory functions*, *JHEP* **03**, 071, [arXiv:1501.05656 \[hep-th\]](#).
- [56] A. Lucas and S. Sachdev, *Memory matrix theory of magnetotransport in strange metals*, *Phys. Rev.* **B91**, 195122 (2015), [arXiv:1502.04704 \[cond-mat.str-el\]](#).
- [57] A. A. Patel and S. Sachdev, *DC resistivity at the onset of spin density wave order in two-dimensional metals*, *Phys. Rev.* **B90**, 165146 (2014), [arXiv:1408.6549 \[cond-mat.str-el\]](#).
- [58] X. Wang and E. Berg, *Scattering mechanisms and electrical transport near an Ising nematic quantum critical point*, *Phys. Rev. B* **99**, 235136 (2019), [arXiv:1902.04590 \[cond-mat.str-el\]](#).
- [59] D. V. Else and T. Senthil, *Strange Metals as Ersatz Fermi Liquids*, *Phys. Rev. Lett.* **127**, 086601 (2021), [arXiv:2010.10523 \[cond-mat.str-el\]](#).
- [60] P. A. Lee, *Low-temperature T -linear resistivity due to umklapp scattering from a critical mode*, *Phys. Rev. B* **104**, 035140 (2021), [arXiv:2012.09339 \[cond-mat.str-el\]](#).
- [61] A. A. Patel, H. Guo, I. Esterlis, and S. Sachdev, *Universal theory of strange metals from spatially random interactions*, *Science* **381**, 6659 (2023), [arXiv:2203.04990 \[cond-mat.str-el\]](#).
- [62] C. Li, D. Valentinis, A. A. Patel, H. Guo, J. Schmalian, S. Sachdev, and I. Esterlis, *Strange metal and superconductor in the two-dimensional Yukawa-Sachdev-Ye-Kitaev model*, (2024), [arXiv:2406.07608 \[cond-mat.str-el\]](#).
- [63] C. M. Varma, P. B. Littlewood, S. Schmitt-Rink, E. Abrahams, and A. E. Ruckenstein, *Phenomenology of the normal state of Cu-O high-temperature superconductors*, *Phys. Rev. Lett.* **63**, 1996 (1989).
- [64] P. A. Lee and T. V. Ramakrishnan, *Disordered electronic systems*, *Rev. Mod. Phys.* **57**, 287 (1985).
- [65] T. C. Wu, Y. Liao, and M. S. Foster, *Quantum interference of hydrodynamic modes in a dirty marginal Fermi liquid*, *Phys. Rev. B* **106**, 155108 (2022), [arXiv:2206.01762 \[cond-mat.str-el\]](#).

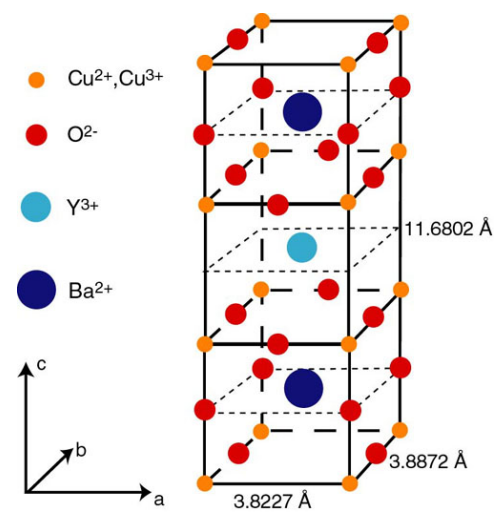
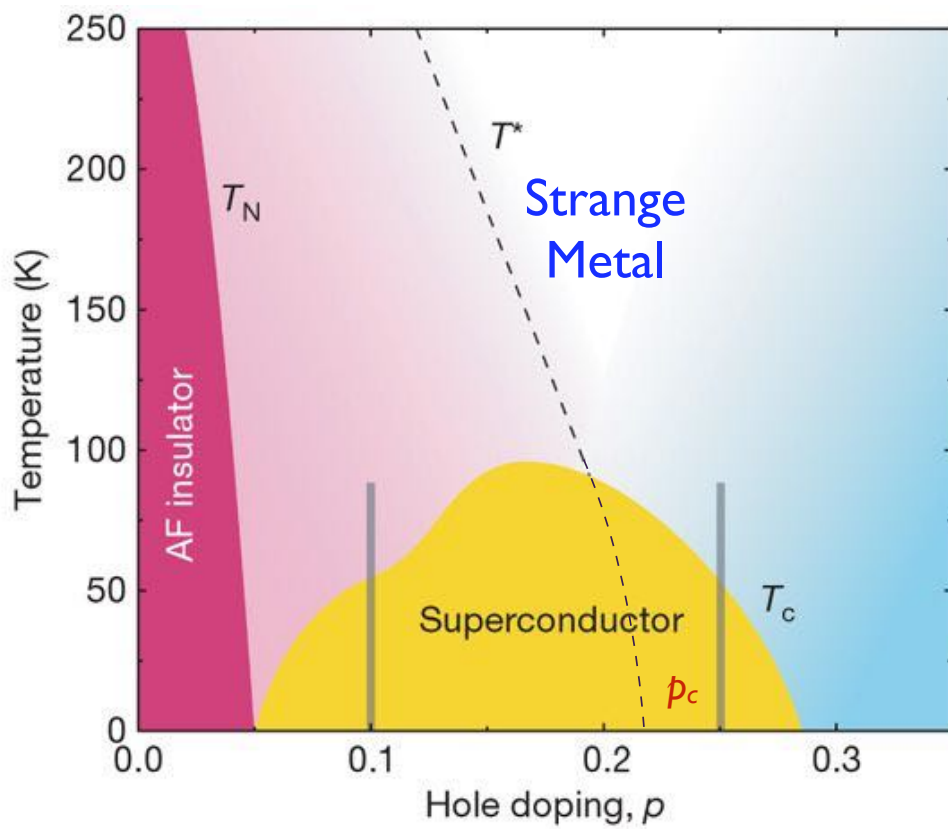
- [66] A. A. Patel, P. Lunts, and S. Sachdev, *Localization of overdamped bosonic modes and transport in strange metals*, *Proceedings of the National Academy of Science* **121**, e2402052121 (2024), [arXiv:2312.06751 \[cond-mat.str-el\]](#).
- [67] A. A. Patel, P. Lunts, and M. Albergo, *Strange metals with spatially random interactions: a hybrid Monte Carlo study*, *Talk at ICTS, Bengaluru* (2024).
- [68] B. Michon, C. Berthod, C. W. Rischau, A. Ataei, L. Chen, S. Komiyama, S. Ono, L. Taillefer, D. van der Marel, and A. Georges, *Reconciling scaling of the optical conductivity of cuprate superconductors with Planckian resistivity and specific heat*, *Nature Communications* **14**, 3033 (2023), [arXiv:2205.04030 \[cond-mat.str-el\]](#).
- [69] J. A. Hoyos, C. Kotabage, and T. Vojta, *Effects of Dissipation on a Quantum Critical Point with Disorder*, *Phys. Rev. Lett.* **99**, 230601 (2007), [arXiv:0705.1865 \[cond-mat.str-el\]](#).
- [70] R. A. Cooper, Y. Wang, B. Vignolle, O. J. Lipscombe, S. M. Hayden, Y. Tanabe, T. Adachi, Y. Koike, M. Nohara, H. Takagi, C. Proust, and N. E. Hussey, *Anomalous Criticality in the Electrical Resistivity of $La_{2-x}Sr_xCuO_4$* , *Science* **323**, 603 (2009).
- [71] L. Taillefer, *Scattering and Pairing in Cuprate Superconductors*, *Annual Review of Condensed Matter Physics* **1**, 51 (2010), [arXiv:1003.2972 \[cond-mat.supr-con\]](#).

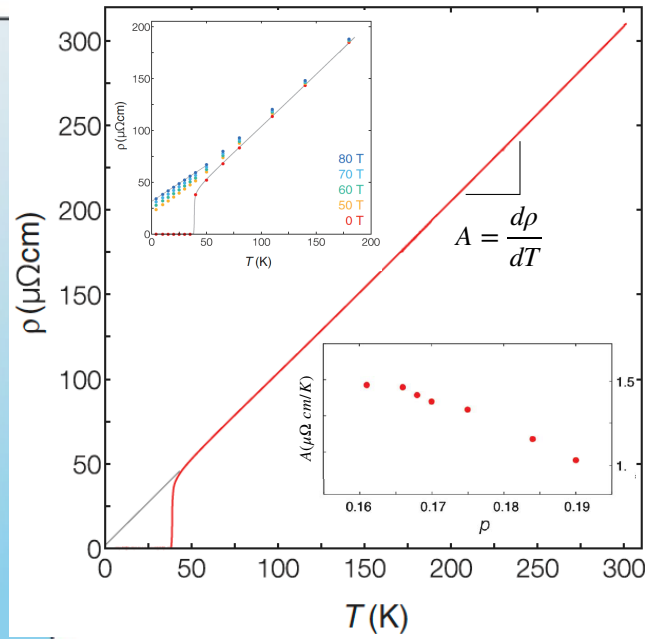
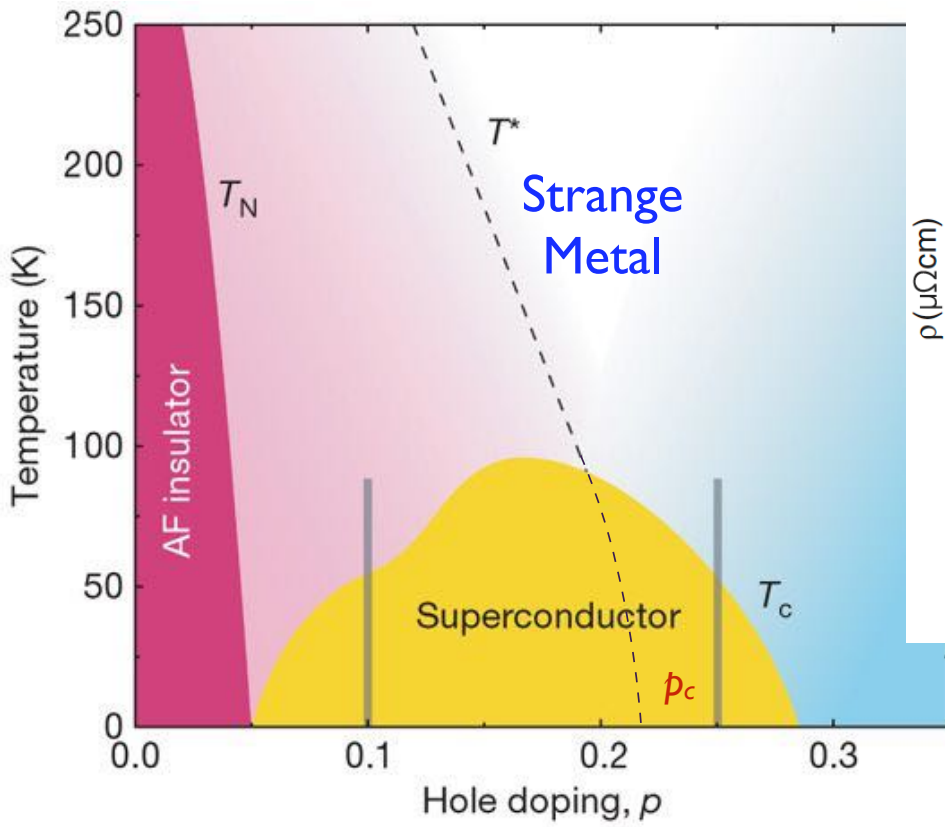
Appendix A: Hertz-Millis transitions in metals

Quantum phase transitions of metals

Subir Sachdev







LSCO: Giraldo-Gallo et al. 2018

Reconciling scaling of the optical conductivity of cuprate superconductors with Planckian resistivity and specific heat

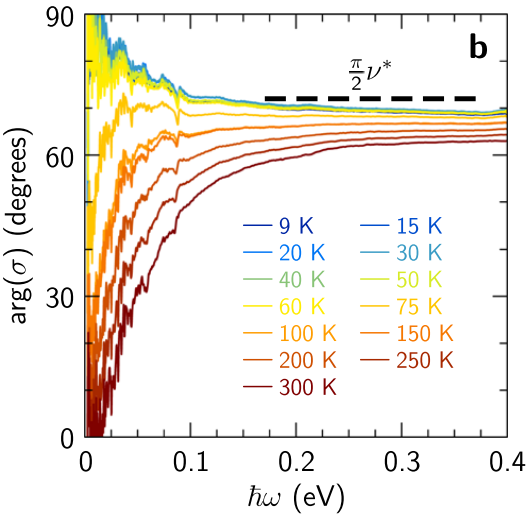
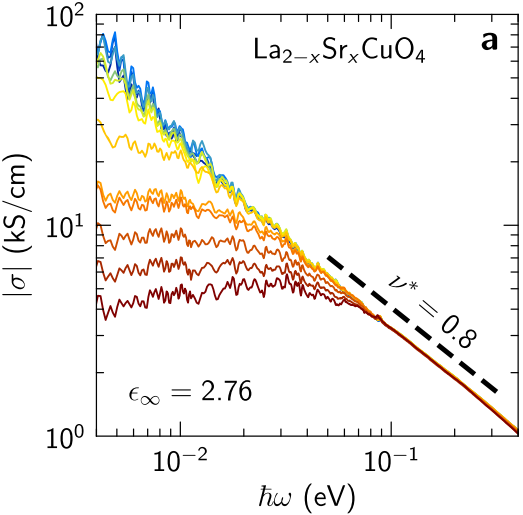
B. Michon, C. Berthod, C. W. Rischau, A. Ataei, L. Chen, S. Komiya, S. Ono, L. Taillefer, D. van der Marel, A. Georges
Nature Communications **14**, Article number: 3033 (2023)

$$\sigma(\omega) = i \frac{e^2 K / (\hbar d_c)}{\hbar \omega \frac{m^*(\omega)}{m} + i \frac{\hbar}{\tau(\omega)}}$$

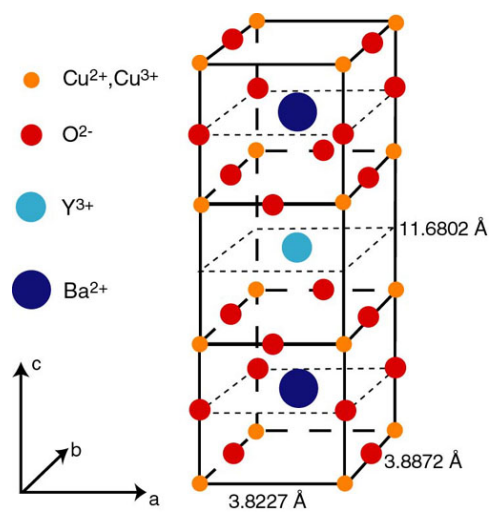
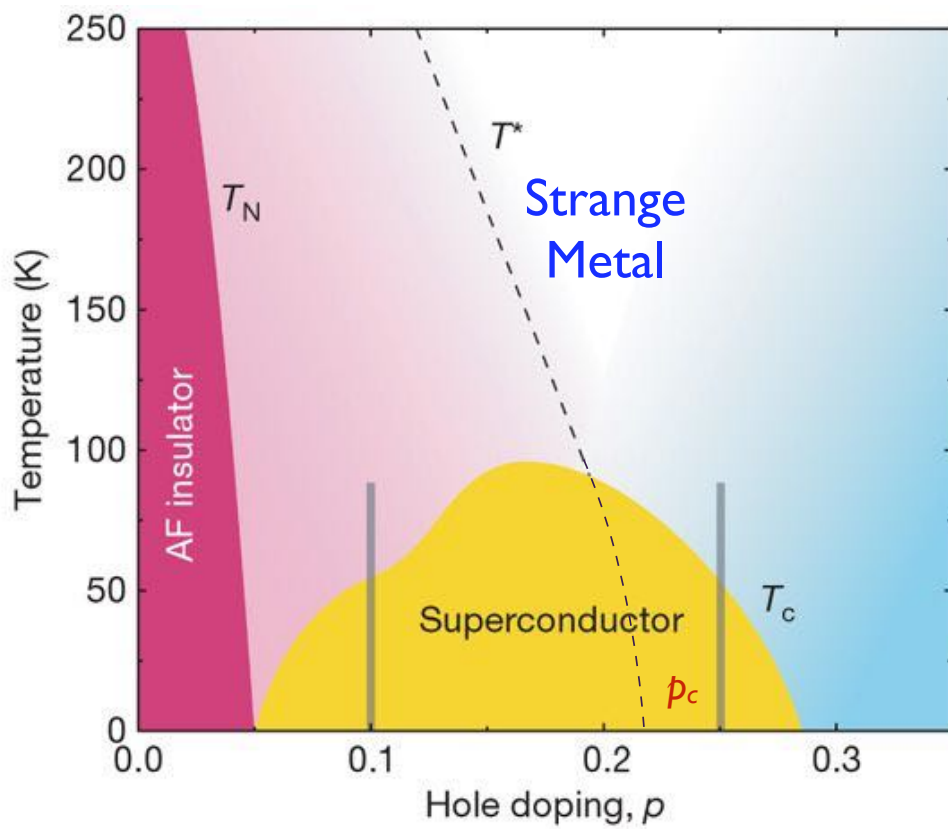
Planckian dynamics!

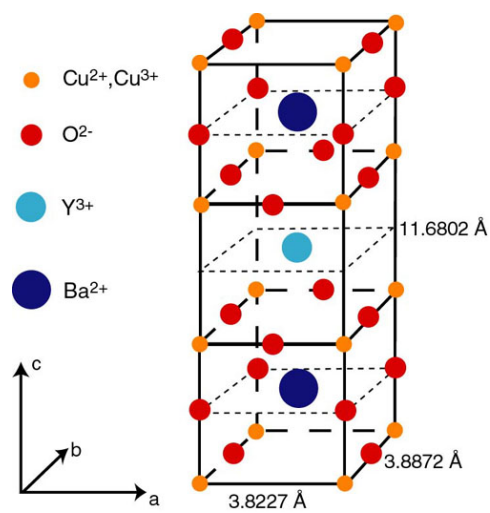
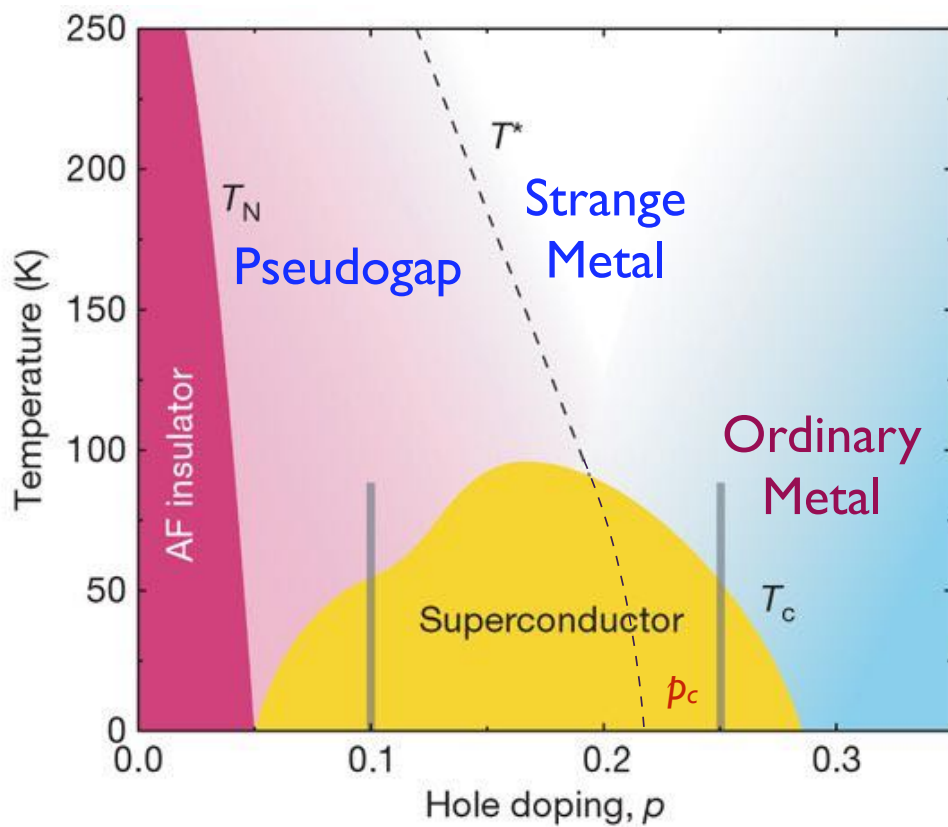
$$\tau(\omega) = \frac{\hbar}{k_B T} F\left(\frac{\hbar \omega}{k_B T}\right)$$
 and entropy

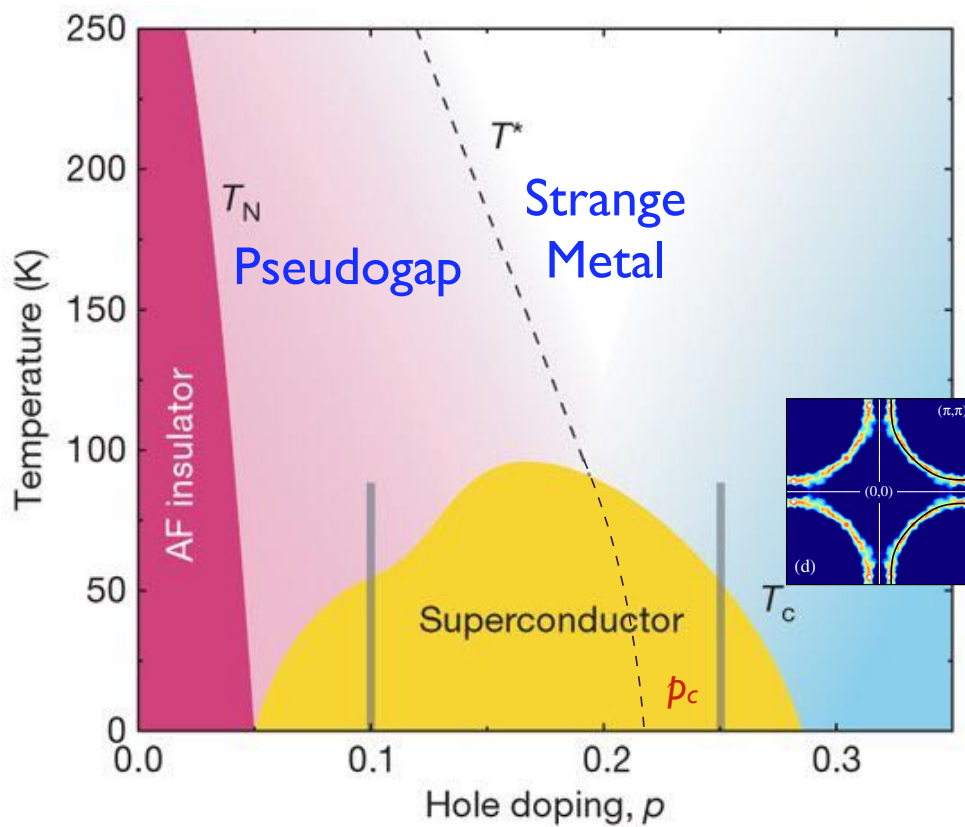
$$S(T \rightarrow 0) \sim T \ln(1/T).$$



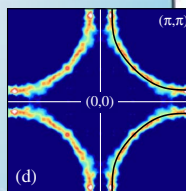
$\text{La}_{2-x}\text{Sr}_x\text{CuO}_4$
 $p = 0.24$
 $T_c = 19 \text{ K}$

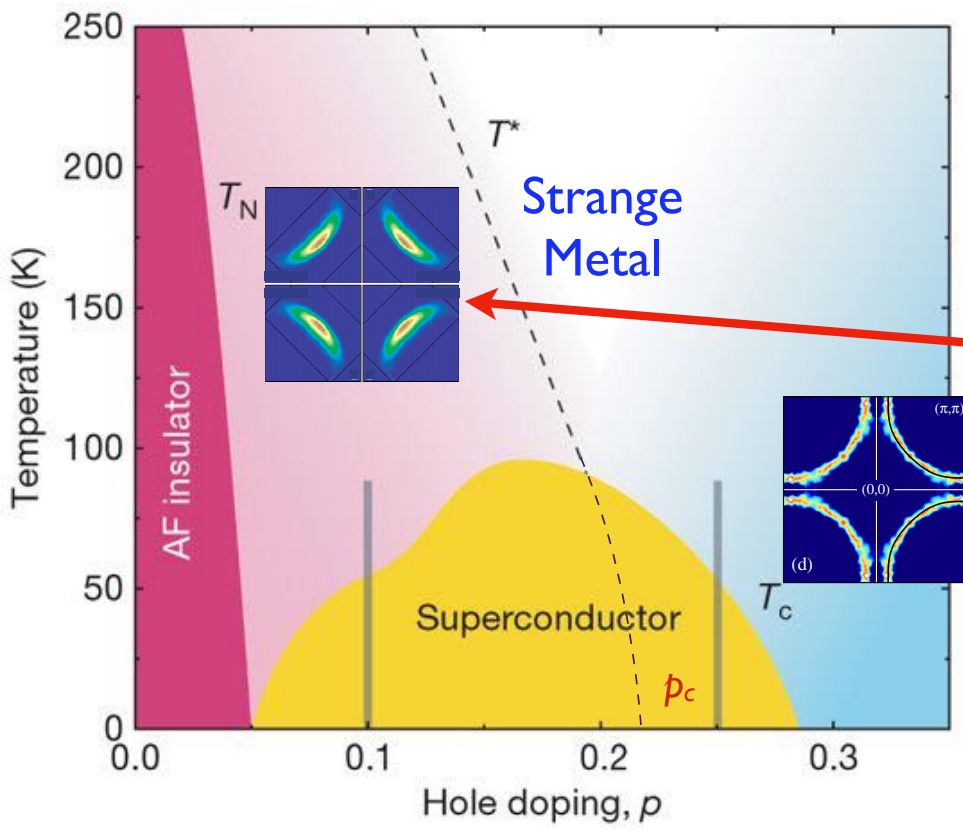




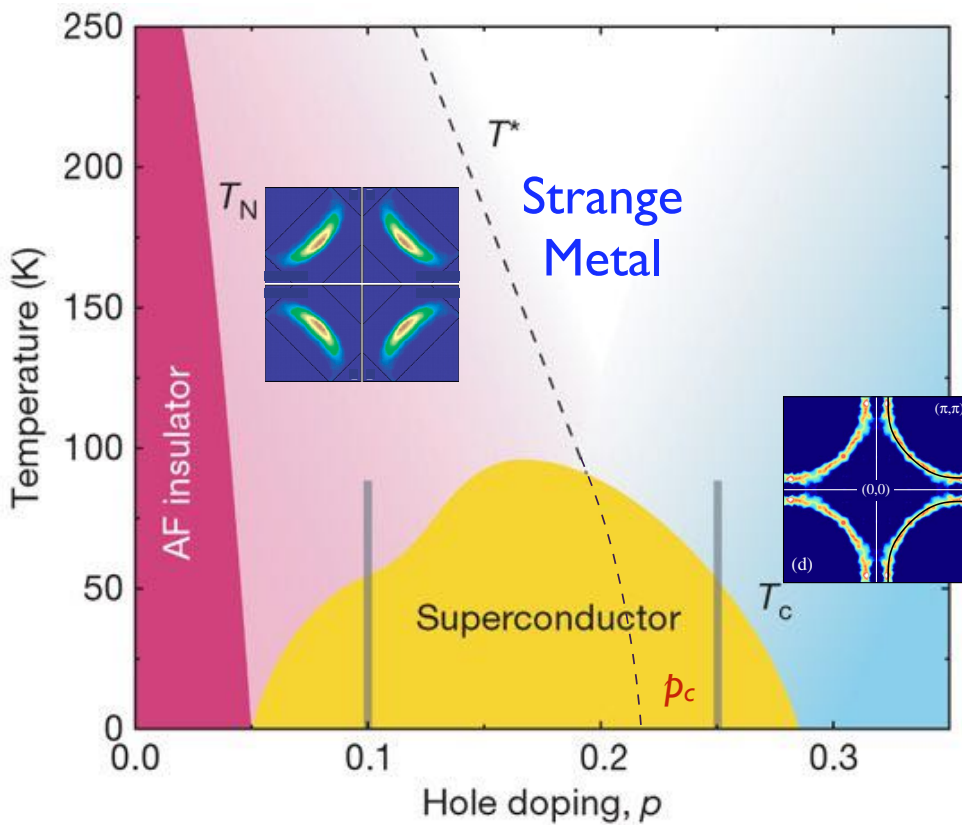


Fermi surface
as expected
in a model
of free electrons





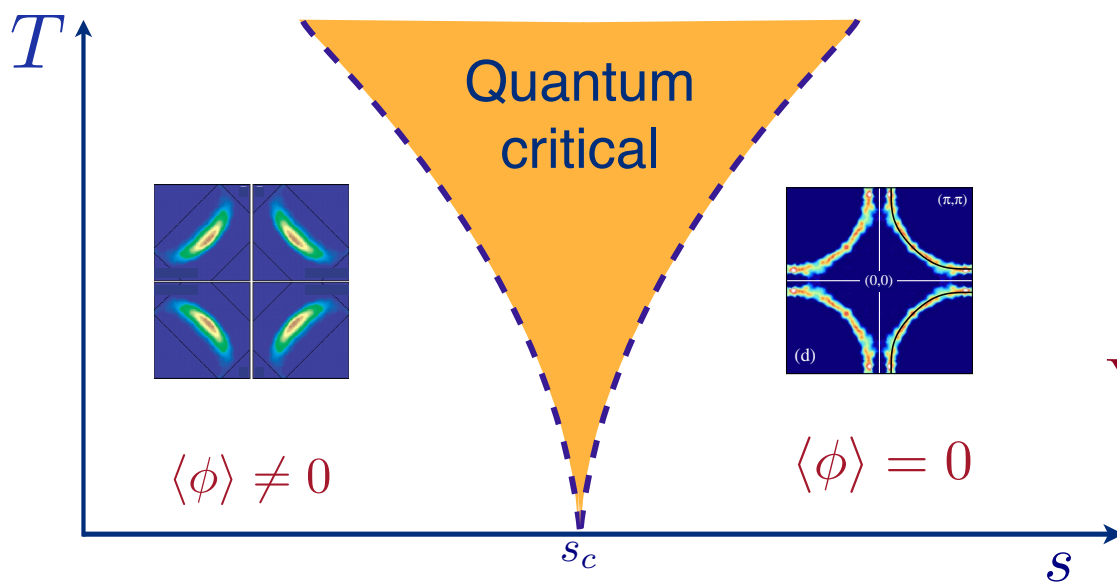
“Pseudogap metal”
Fermi surface
modified by
electron-electron
interactions



View the strange metal as a property of a $T = 0$ quantum phase transition involving change in the Fermi surface.

The onset of superconductivity may “hide” this quantum transition.

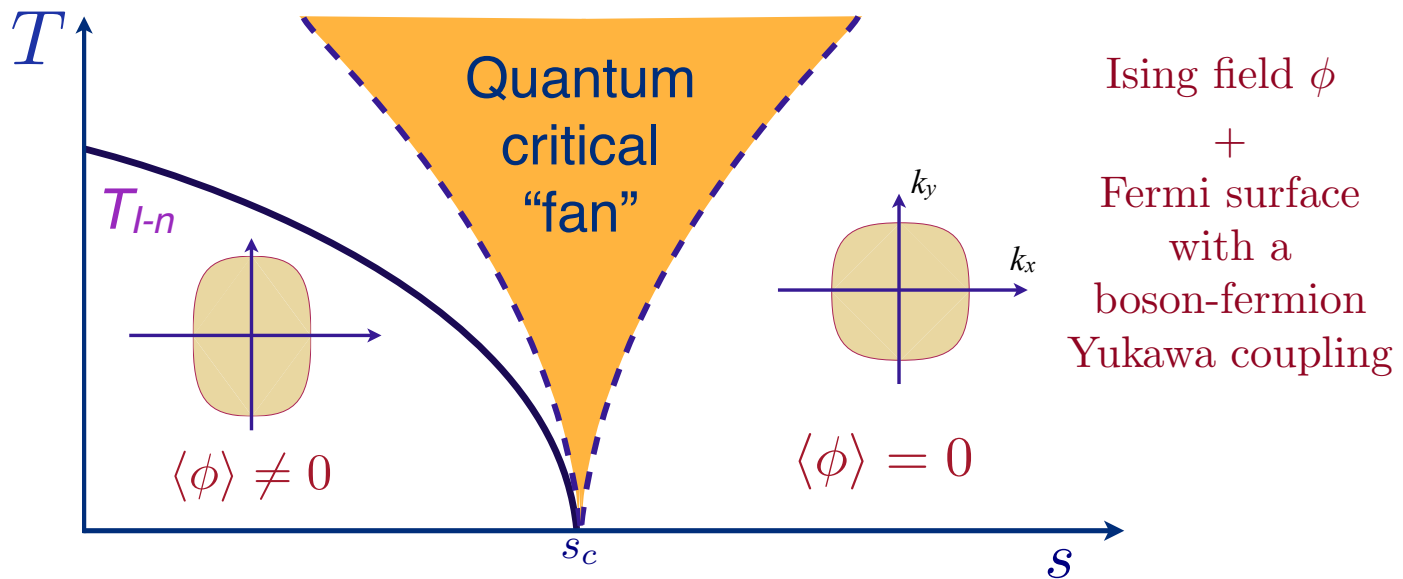
Quantum phase transitions of Fermi surface change



Fermi surface
+
scalar field ϕ
with a 'mass' s
and
a boson-fermion
Yukawa coupling g .

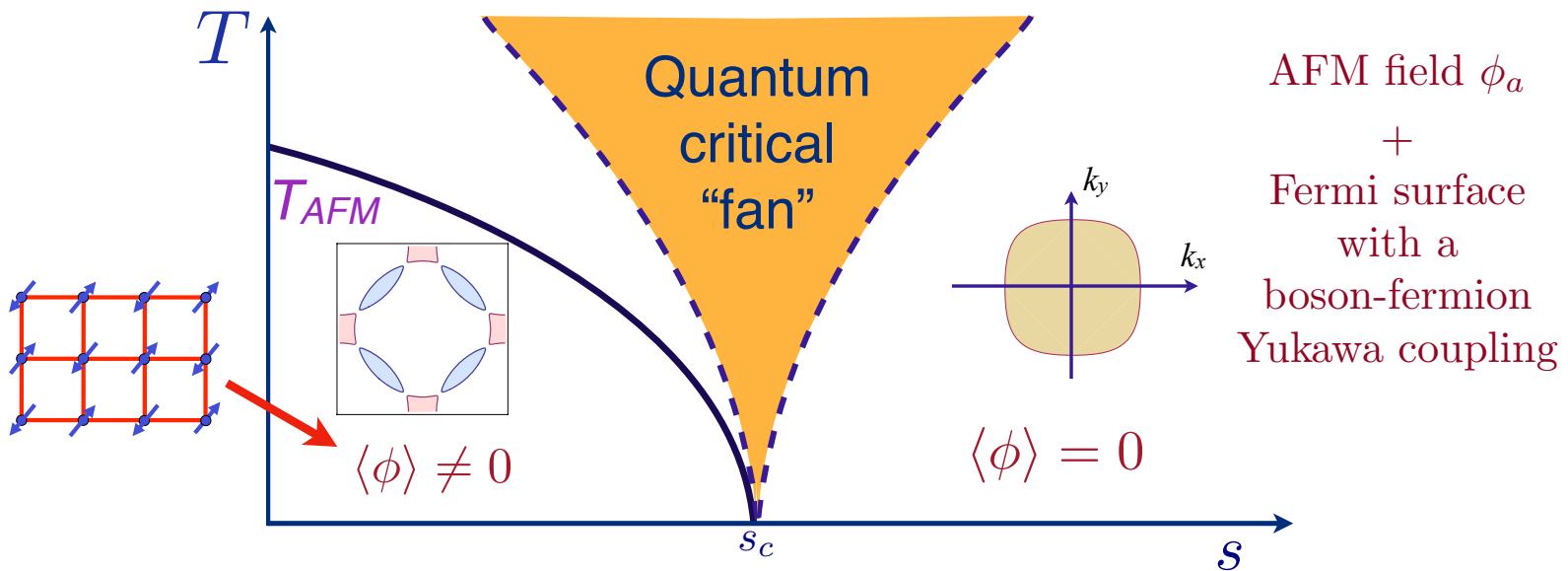
Quantum phase transitions in two-dimensional metals

Type I: Fermi surface deformation



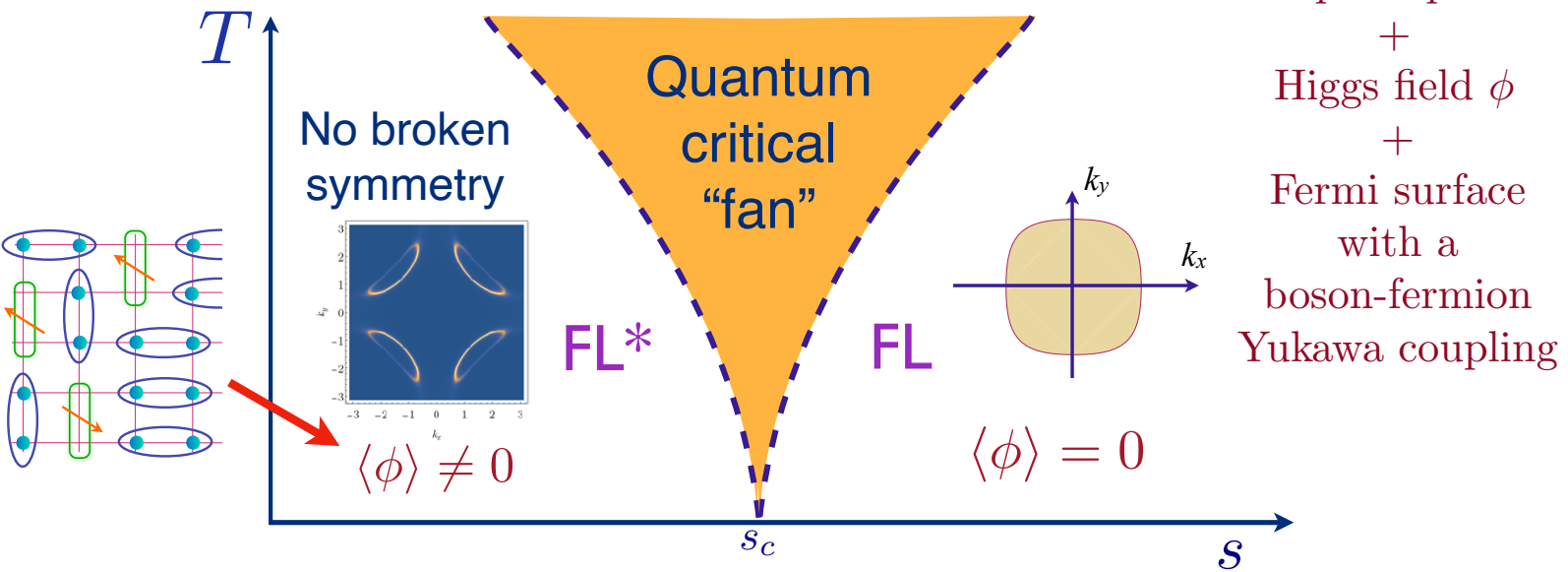
Quantum phase transitions in two-dimensional metals

Type II: Fermi surface reconstruction



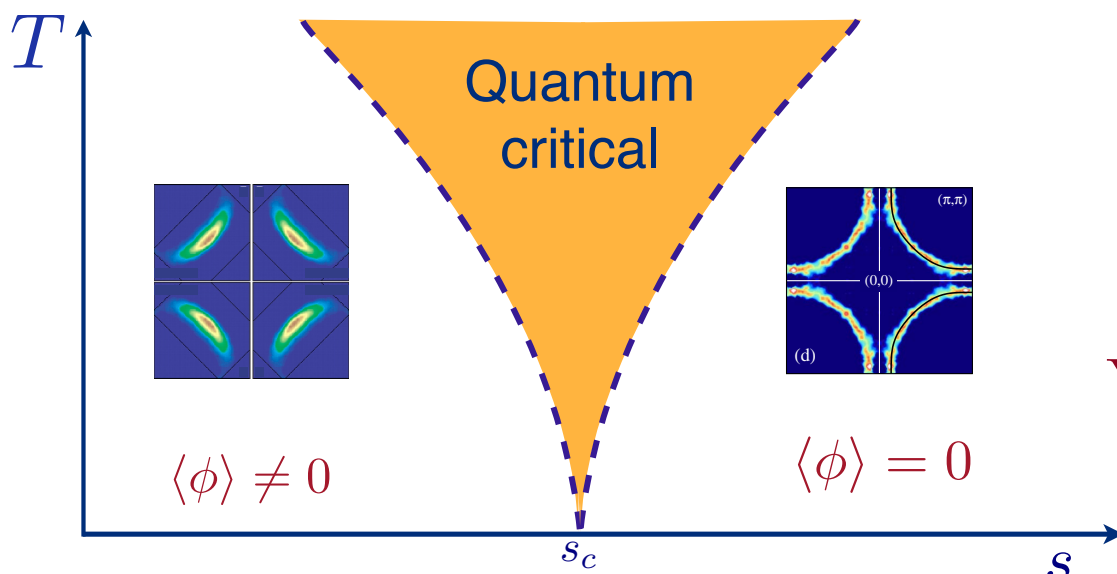
Quantum phase transitions in two-dimensional metals

Type III: Fermi surface jump



Applies to hole-doped cuprates

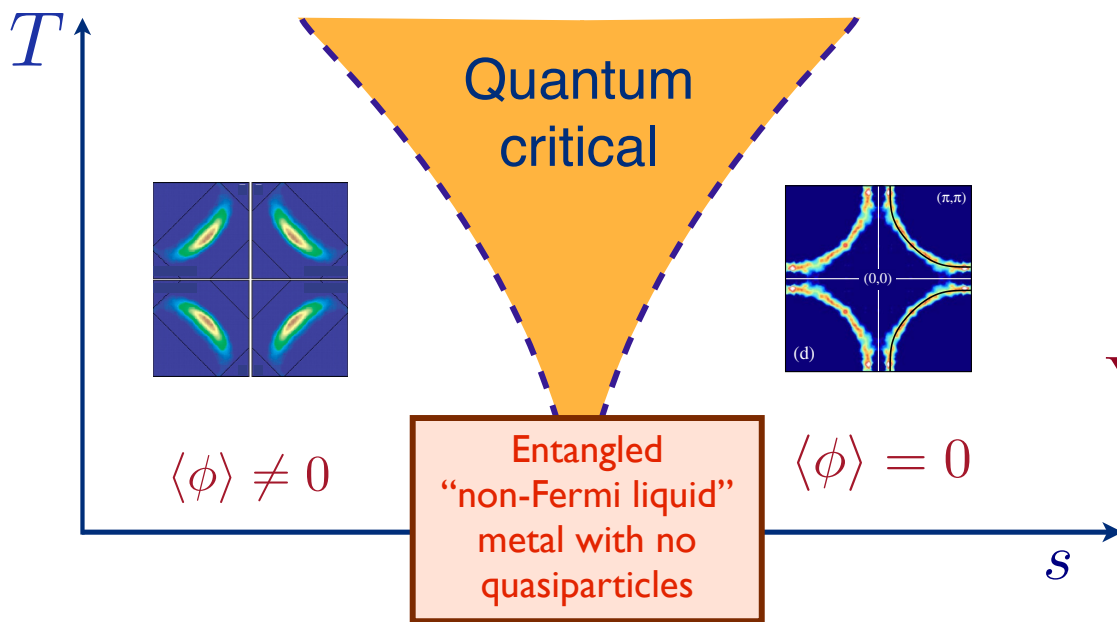
Quantum phase transitions of Fermi surface change



Fermi surface
+
scalar field ϕ
with a 'mass' s
and
a boson-fermion
Yukawa coupling g .

ϕ could represent
e.g. Ising-nematic order,
spin-density wave order,
Higgs boson for Fermi-volume
changing transition

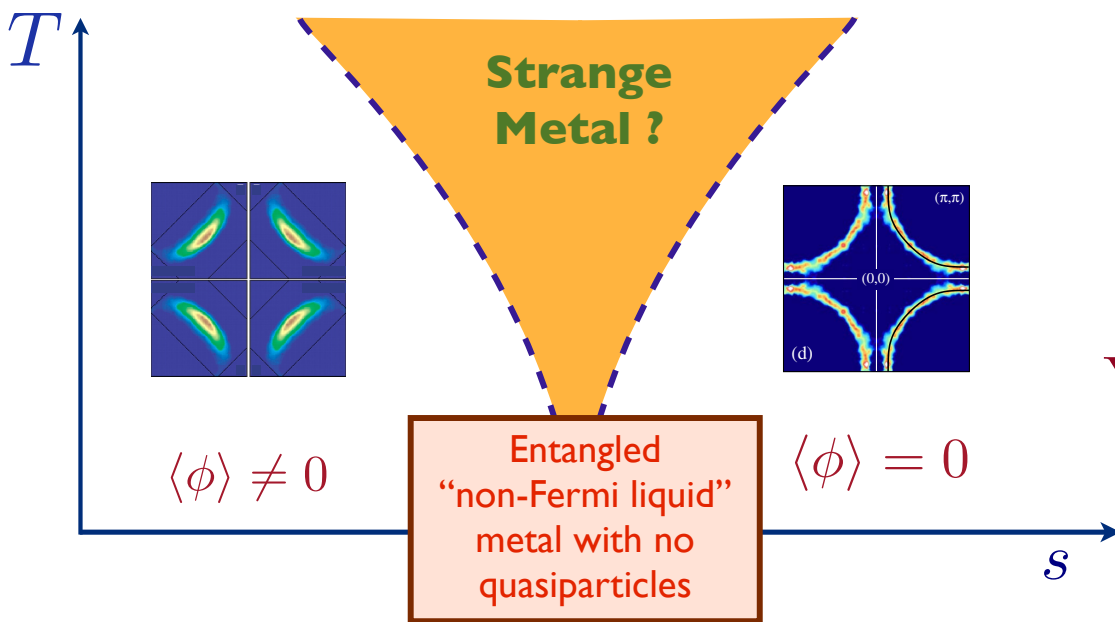
Quantum phase transitions of Fermi surface change



Fermi surface
+
scalar field ϕ
with a 'mass' s
and
a boson-fermion
Yukawa coupling g .

ϕ could represent
e.g. Ising-nematic order,
spin-density wave order,
Higgs boson for Fermi-volume
changing transition

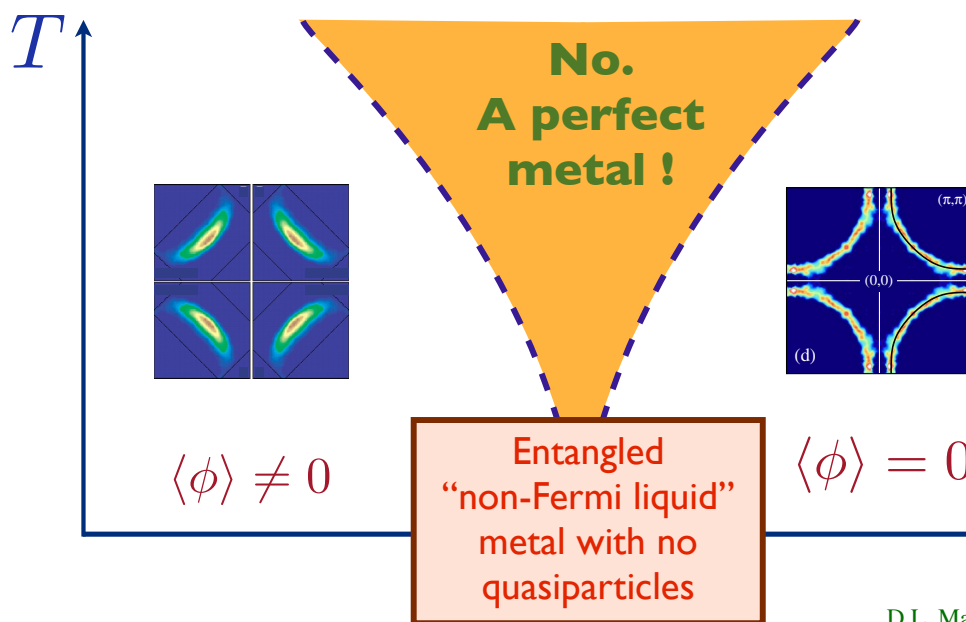
Quantum phase transitions of Fermi surface change



Fermi surface
+
scalar field ϕ
with a 'mass' s
and
a boson-fermion
Yukawa coupling g .

ϕ could represent
e.g. Ising-nematic order,
spin-density wave order,
Higgs boson for Fermi-volume
changing transition

Quantum phase transitions of Fermi surface change

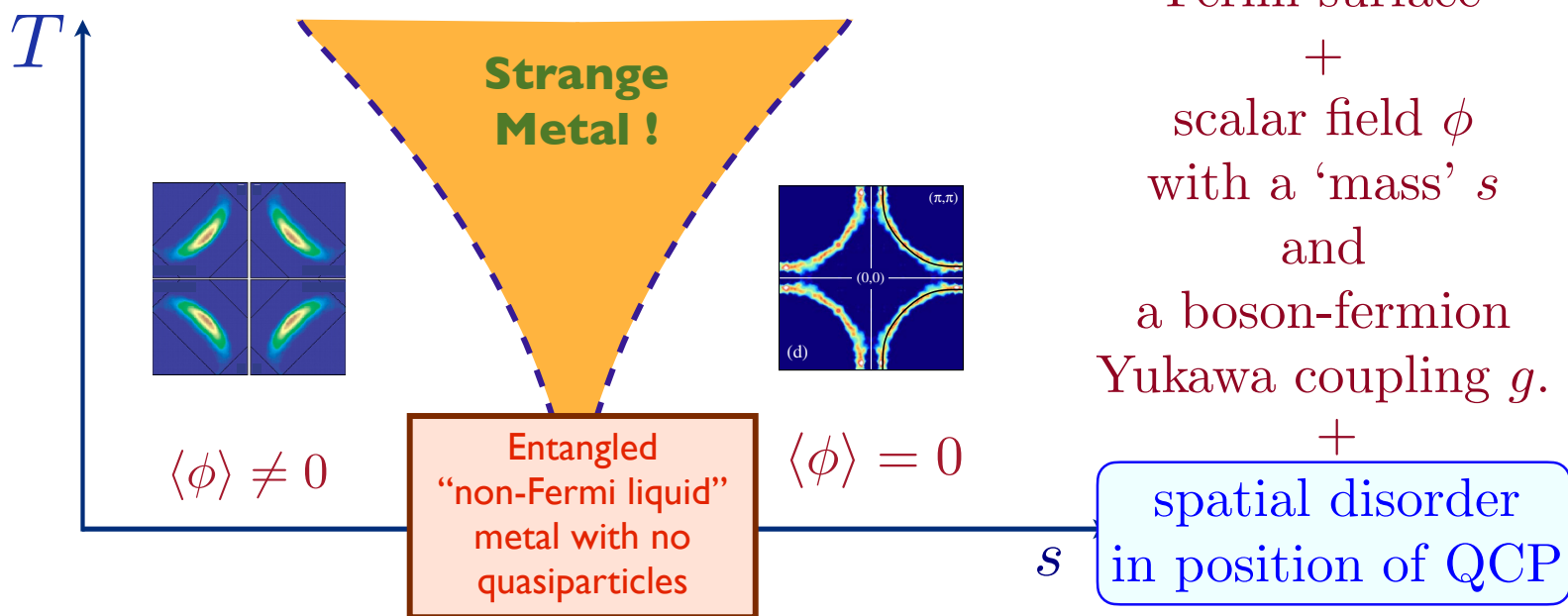


Fermi surface
+
scalar field ϕ
with a 'mass' s
and
a boson-fermion
Yukawa coupling g .

S. A. Hartnoll, P. K. Kovtun, M. Muller, and S.S. PRB **76**, 144502 (2007); Haoyu Guo, Aavishkar Patel, Ilya Esterlis, S.S., PRB **106**, 115151 (2022); Haoyu Guo, Davide Valentini, J. Schmalian, S.S., Aavishkar Patel, PRB **109**, 075162 (2024);

D.L. Maslov and A.V. Chubukov, Rep. Prog. Phys. **80**, 026503 (2017); Zhengyan Darius Shi, Dominic V. Else, Hart Goldman, T. Senthil, SciPost Phys. **14**, 113 (2023)

Quantum phase transitions of Fermi surface change



I. Quantum phase transitions with Fermi surface deformation and broken symmetry

Hertz 1976
Millis 1993

II. Quantum phase transitions with Fermi surface reconstruction and broken translational symmetry

III. Quantum phase transitions with Fermi volume change and no broken symmetry

**I. Quantum phase transitions
with
Fermi surface deformation
and
broken symmetry**

Ising ferromagnetism

$$H = -J \sum_{\langle ij \rangle} Z_i Z_j - h \sum_i X_i$$

Field theory near the quantum critical point

$$\mathcal{L} = \int d^2r \left\{ \frac{1}{2} [(\nabla\phi)^2 + (\partial_\tau\phi)^2 + s\phi^2] + \frac{u}{4!}\phi^4 \right\}$$

$\langle Z \rangle \neq 0$

Wilson-Fisher CFT3
No quasiparticles!

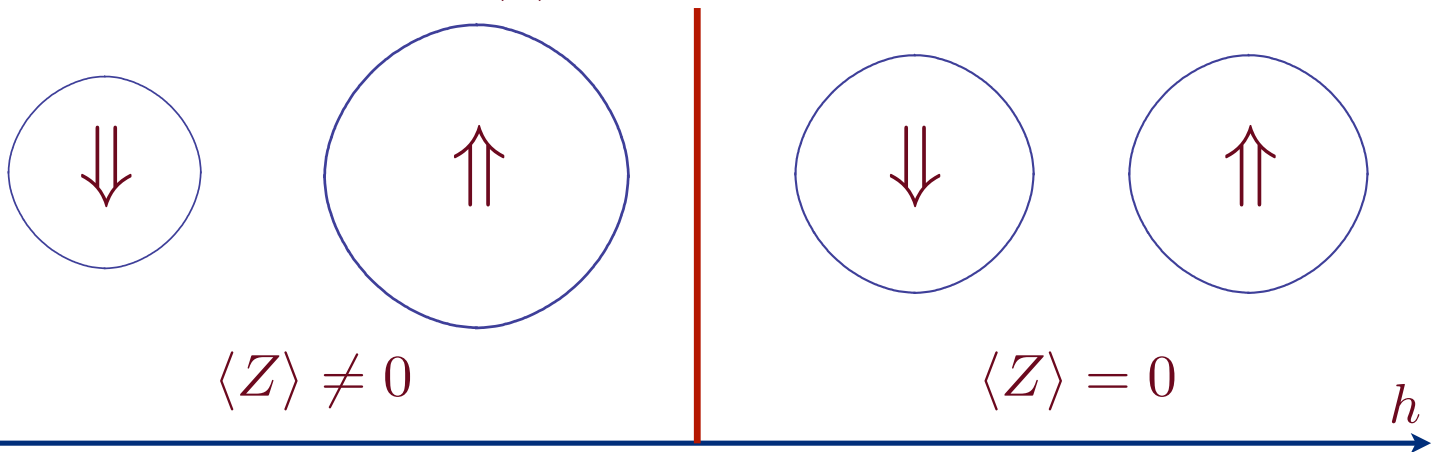
$\langle Z \rangle = 0$

h

Ising ferromagnetism in a metal

Couple the Ising model to a Fermi surface:

$$H = \sum_{\mathbf{k}, \alpha} \varepsilon_{\mathbf{k}} c_{\mathbf{k}\alpha}^\dagger c_{\mathbf{k}\alpha} - J \sum_{\langle ij \rangle} Z_i Z_j - h \sum_i X_i - g \sum_i Z_i c_{i\alpha}^\dagger \sigma_{\alpha\beta}^z c_{i\beta}$$



$U(1) \times U(1)$ symmetry: Luttinger volume Fermi surfaces for \uparrow and \downarrow electrons.

Ising ferromagnetism in a metal

Couple the Ising model to a Fermi surface:

$$H = \sum_{\mathbf{k}, \alpha} \varepsilon_{\mathbf{k}} c_{\mathbf{k}\alpha}^\dagger c_{\mathbf{k}\alpha} - J \sum_{\langle ij \rangle} Z_i Z_j - h \sum_i X_i - g \sum_i Z_i c_{i\alpha}^\dagger \sigma_{\alpha\beta}^z c_{i\beta}$$

Field theory near the quantum critical point

$$\begin{aligned} \mathcal{L} = & \sum_{\mathbf{k}, \alpha} c_{\mathbf{k}, \alpha}^\dagger \left[\frac{\partial}{\partial \tau} + \varepsilon_{\mathbf{k}} \right] c_{\mathbf{k}, \alpha} + \int d^2 r \left\{ \frac{1}{2} [(\nabla \phi)^2 + (\partial_\tau \phi)^2 + s \phi^2] + \frac{u}{4!} \phi^4 \right\} \\ & - \int d^2 r g \phi c_\alpha^\dagger \sigma_{\alpha\beta}^z c_\beta \end{aligned}$$

Hertz effective action

Integrate out the fermions to obtain the Hertz effective action

$$\begin{aligned}\mathcal{S}_H[\phi] &= \sum_{\mathbf{k}, \omega} |\phi(\mathbf{k}, i\omega)|^2 [s + k^2 - g^2 \chi(\mathbf{k}, i\omega)] + \dots \\ &= \sum_{\mathbf{k}, \omega} |\phi(\mathbf{k}, i\omega)|^2 \left[s + k^2 + \frac{|\omega|}{k} \right] + \dots\end{aligned}$$

**II. Quantum phase transitions
with
Fermi surface reconstruction
and
broken translational symmetry**

The Hubbard Model

$$H = - \sum_{i < j} t_{ij} c_{i\alpha}^\dagger c_{j\alpha} + U \sum_i \left(n_{i\uparrow} - \frac{1}{2} \right) \left(n_{i\downarrow} - \frac{1}{2} \right) - \mu \sum_i c_{i\alpha}^\dagger c_{i\alpha}$$

$t_{ij} \rightarrow$ “hopping”. $U \rightarrow$ local repulsion, $\mu \rightarrow$ chemical potential

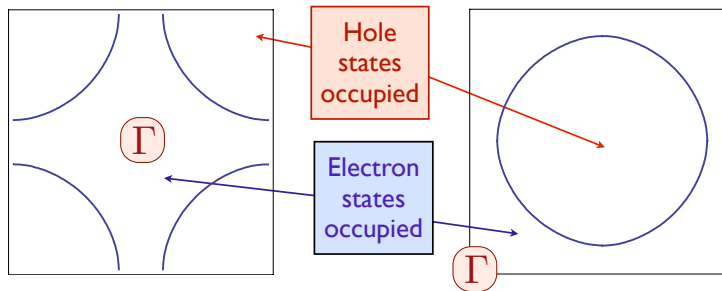
Spin index $\alpha = \uparrow, \downarrow$

$$n_{i\alpha} = c_{i\alpha}^\dagger c_{i\alpha}$$

$$\begin{aligned} c_{i\alpha}^\dagger c_{j\beta} + c_{j\beta} c_{i\alpha}^\dagger &= \delta_{ij} \delta_{\alpha\beta} \\ c_{i\alpha} c_{j\beta} + c_{j\beta} c_{i\alpha} &= 0 \end{aligned}$$

Will study on the square lattice

Fermi surfaces in electron- and hole-doped cuprates



Effective Hamiltonian for quasiparticles:

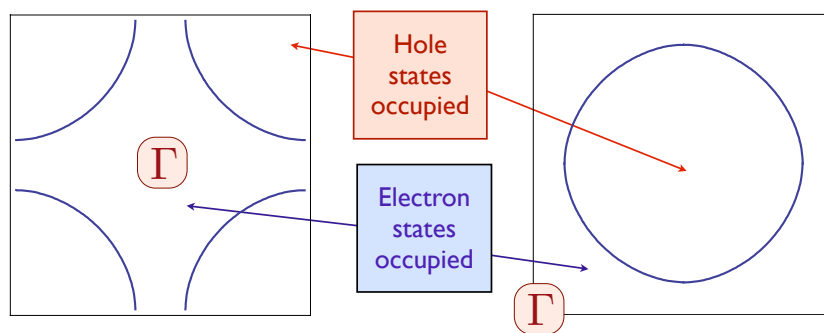
$$H_0 = - \sum_{i < j} t_{ij} c_{i\alpha}^\dagger c_{j\alpha} \equiv \sum_{\mathbf{k}} \varepsilon_{\mathbf{k}} c_{\mathbf{k}\alpha}^\dagger c_{\mathbf{k}\alpha}$$

with t_{ij} non-zero for first, second and third neighbor, leads to satisfactory agreement with experiments. The area of the occupied electron states, \mathcal{A}_e , from Luttinger's theory is

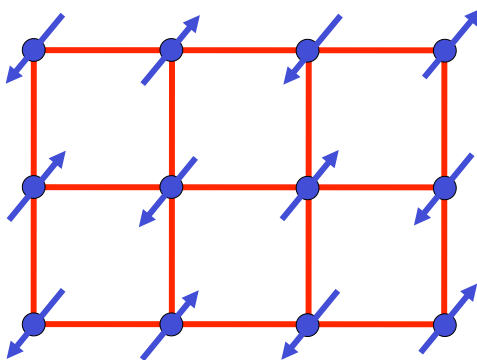
$$\frac{2\mathcal{A}_e}{4\pi^2} = \begin{cases} (1-x) & \text{for hole-doping } x \\ (1+p) & \text{for electron-doping } p \end{cases}$$

The area of the occupied hole states, \mathcal{A}_h , which form a closed Fermi surface and so appear in quantum oscillation experiments is $\mathcal{A}_h = 4\pi^2 - \mathcal{A}_e$.

Fermi surface+antiferromagnetism



+



The electron spin polarization obeys

$$\langle \vec{S}(\mathbf{r}, \tau) \rangle = \vec{\varphi}(\mathbf{r}, \tau) e^{i\mathbf{K} \cdot \mathbf{r}}$$

where $\mathbf{K} = (\pi, \pi)$ is the ordering wavevector.

Fermi surface+antiferromagnetism

We use the operator equation (valid on each site i):

$$U \left(n_{\uparrow} - \frac{1}{2} \right) \left(n_{\downarrow} - \frac{1}{2} \right) = -\frac{2U}{3} \vec{S}^2 + \frac{U}{4} \quad (1)$$

Then we decouple the interaction via

$$\exp \left(\frac{2U}{3} \sum_i \int d\tau \vec{S}_i^2 \right) = \int \mathcal{D}\vec{J}_i(\tau) \exp \left(- \sum_i \int d\tau \left[\frac{3}{8U} J_i^2 - \vec{J}_i \vec{S}_i \right] \right) \quad (2)$$

We now integrate out the fermions, and look for the saddle point of the resulting effective action for \vec{J}_i . At the saddle-point we find that the lowest energy is achieved when the vector has opposite orientations on the A and B sublattices. Anticipating this, we look for a continuum limit in terms of a field $\vec{\varphi}_i$ where

$$\vec{J}_i = \vec{\varphi}_i e^{i\mathbf{K} \cdot \mathbf{r}_i} \quad (3)$$

Fermi surface+antiferromagnetism

In this manner, we obtain the “spin-fermion” model

$$\begin{aligned}\mathcal{Z} &= \int \mathcal{D}c_\alpha \mathcal{D}\vec{\varphi} \exp(-\mathcal{S}) \\ \mathcal{S} &= \int d\tau \sum_{\mathbf{k}} c_{\mathbf{k}\alpha}^\dagger \left(\frac{\partial}{\partial \tau} - \varepsilon_{\mathbf{k}} \right) c_{\mathbf{k}\alpha} \\ &\quad - \lambda \int d\tau \sum_i c_{i\alpha}^\dagger \vec{\varphi}_i \cdot \vec{\sigma}_{\alpha\beta} c_{i\beta} e^{i\mathbf{K}\cdot\mathbf{r}_i} \\ &\quad + \int d\tau d^2r \left[\frac{1}{2} (\nabla_r \vec{\varphi})^2 + \frac{1}{2} (\partial_\tau \vec{\varphi})^2 + \frac{s}{2} \vec{\varphi}^2 + \frac{u}{4} \vec{\varphi}^4 \right]\end{aligned}$$

Fermi surface+antiferromagnetism

In the Hamiltonian form (ignoring, for now, the time dependence of $\vec{\varphi}$), the coupling between $\vec{\varphi}$ and the electrons takes the form

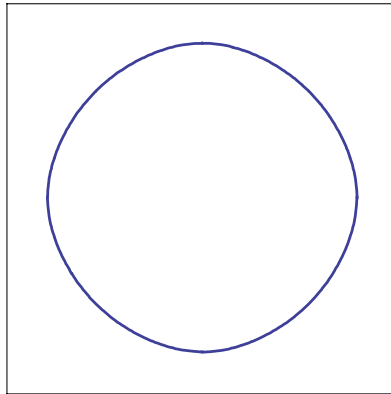
$$H_{\text{sdw}} = \lambda \sum_{\mathbf{k}, \mathbf{q}, \alpha, \beta} \vec{\varphi}_{\mathbf{q}} \cdot c_{\mathbf{k}+\mathbf{q}, \alpha}^{\dagger} \vec{\sigma}_{\alpha\beta} c_{\mathbf{k}+\mathbf{K}, \beta}$$

where $\vec{\sigma}$ are the Pauli matrices, the boson momentum \mathbf{q} is small, while the fermion momentum \mathbf{k} extends over the entire Brillouin zone. In the antiferromagnetically ordered state, we may take $\vec{\varphi} \propto (0, 0, 1)$, and the electron dispersions obtained by diagonalizing $H_0 + H_{\text{sdw}}$ are

$$E_{\mathbf{k}\pm} = \frac{\varepsilon_{\mathbf{k}} + \varepsilon_{\mathbf{k}+\mathbf{K}}}{2} \pm \sqrt{\left(\frac{\varepsilon_{\mathbf{k}} - \varepsilon_{\mathbf{k}+\mathbf{K}}}{2}\right)^2 + \lambda^2 |\vec{\varphi}|^2}$$

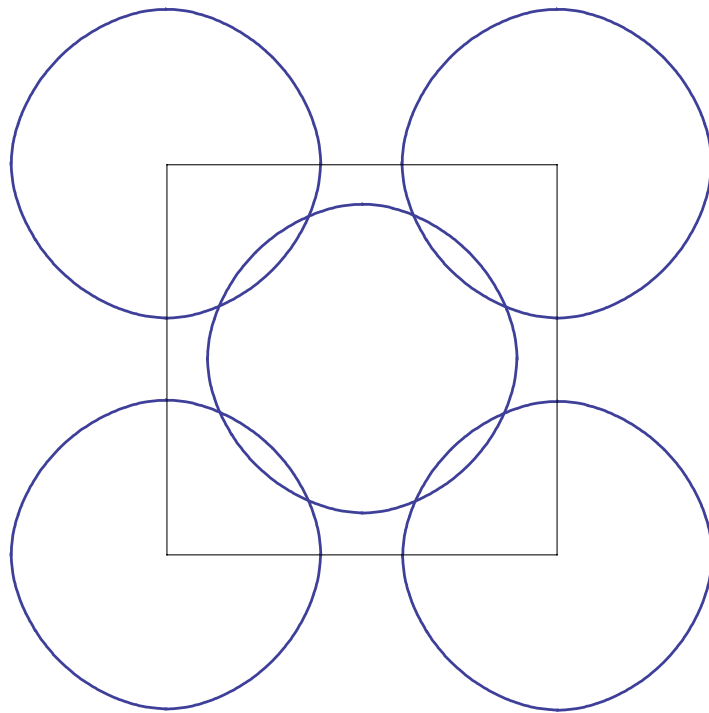
This leads to the Fermi surfaces shown in the following slides as a function of increasing $|\vec{\varphi}|$.

Fermi surface+antiferromagnetism



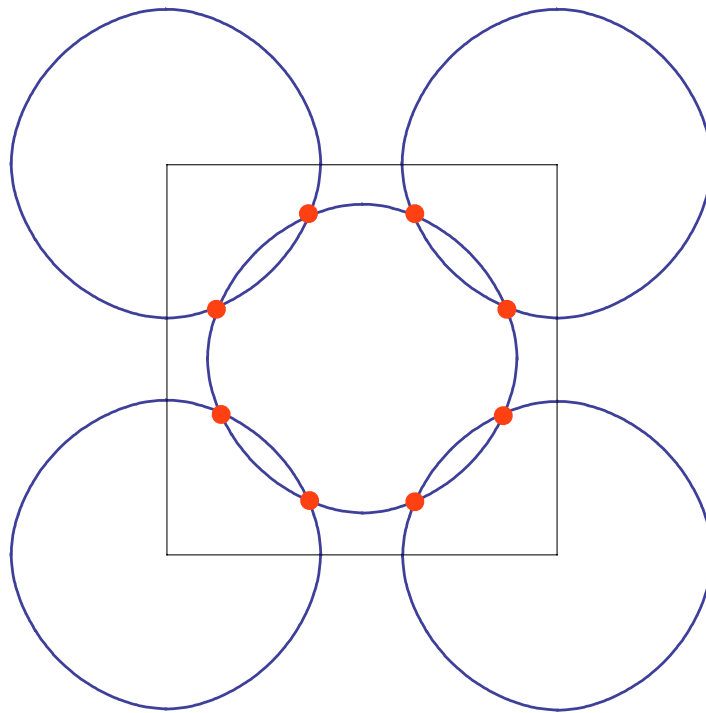
Metal with “large” Fermi surface

Fermi surface+antiferromagnetism



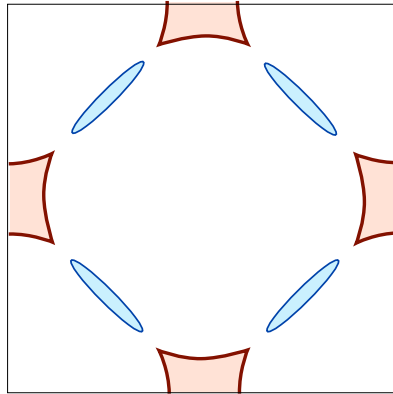
Fermi surfaces translated by $\mathbf{K} = (\pi, \pi)$.

Fermi surface+antiferromagnetism



“Hot” spots

Fermi surface+antiferromagnetism

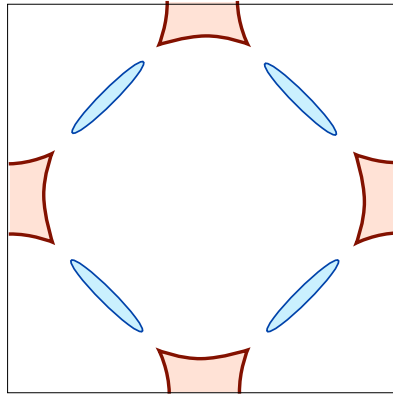


Electron and hole pockets in
antiferromagnetic phase with $\langle \vec{\varphi} \rangle \neq 0$

Fermi surface+antiferromagnetism

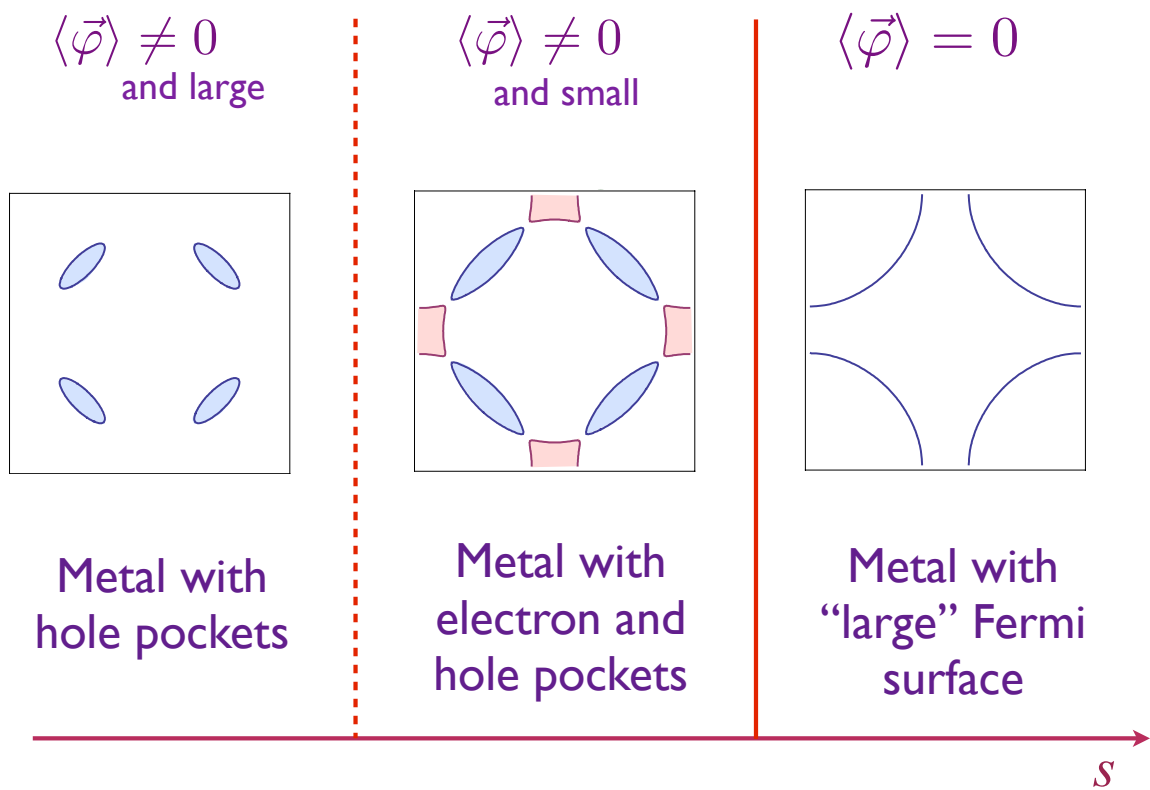
Obeys Luttinger volume
in reduced Brillouin zone:

$$2 \times \frac{1}{(2\pi)^2/2} \times (-2\mathcal{A}_h + \mathcal{A}_e) = -2p.$$

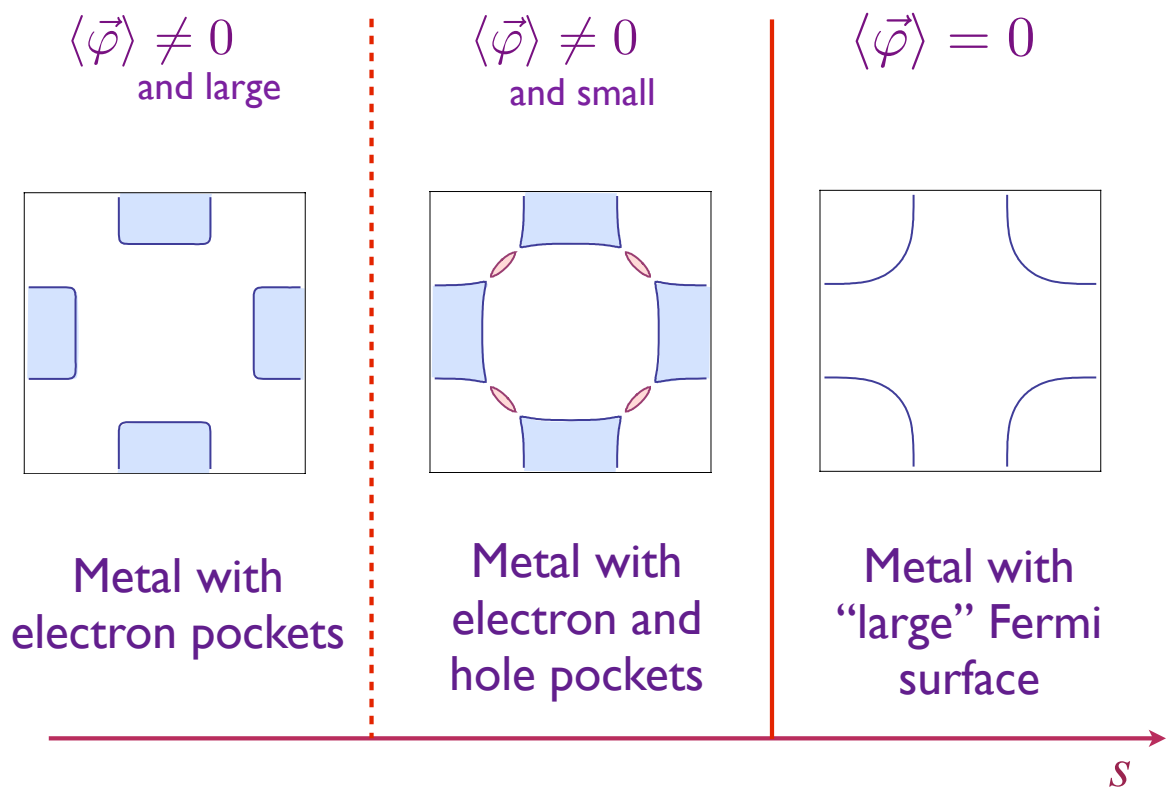


Electron and hole pockets in
antiferromagnetic phase with $\langle \vec{\varphi} \rangle \neq 0$

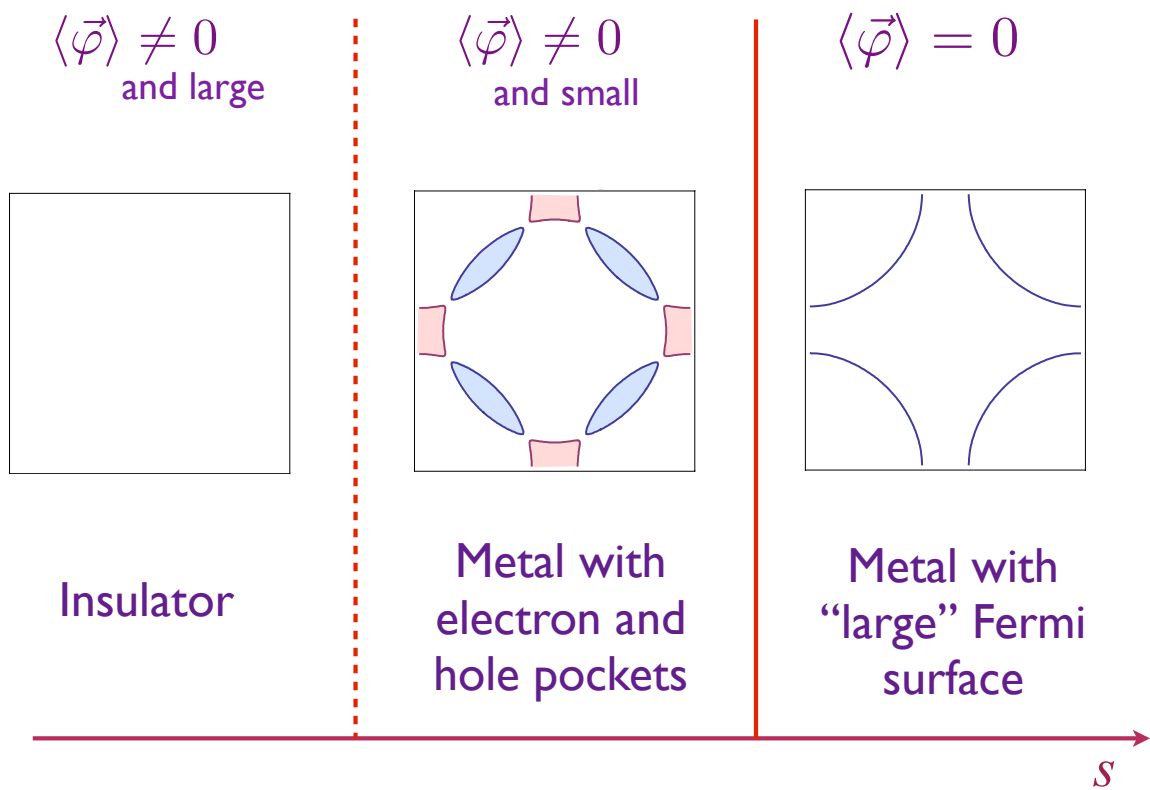
Square lattice Hubbard model with hole doping



Square lattice Hubbard model with electron doping



Square lattice Hubbard model with no doping



Fermi surface+antiferromagnetism

We use the operator equation (valid on each site i):

$$U \left(n_{\uparrow} - \frac{1}{2} \right) \left(n_{\downarrow} - \frac{1}{2} \right) = -\frac{2U}{3} \vec{S}^2 + \frac{U}{4} \quad (1)$$

Then we decouple the interaction via

$$\exp \left(\frac{2U}{3} \sum_i \int d\tau \vec{S}_i^2 \right) = \int \mathcal{D}\vec{J}_i(\tau) \exp \left(- \sum_i \int d\tau \left[\frac{3}{8U} J_i^2 - \vec{J}_i \vec{S}_i \right] \right) \quad (2)$$

We now integrate out the fermions, and look for the saddle point of the resulting effective action for \vec{J}_i . At the saddle-point we find that the lowest energy is achieved when the vector has opposite orientations on the A and B sublattices. Anticipating this, we look for a continuum limit in terms of a field $\vec{\varphi}_i$ where

$$\vec{J}_i = \vec{\varphi}_i e^{i\mathbf{K} \cdot \mathbf{r}_i} \quad (3)$$

Hertz effective action

Integrate out the fermions to obtain the Hertz effective action

$$\begin{aligned}\mathcal{S}_H[\vec{\varphi}] &= \sum_{\mathbf{k}, \omega} |\vec{\varphi}(\mathbf{k}, i\omega)|^2 \left[\frac{3}{8U} - \chi(\mathbf{K} + \mathbf{k}, i\omega) \right] + \dots \\ &= \sum_{\mathbf{k}, \omega} |\vec{\varphi}(\mathbf{k}, i\omega)|^2 [k^2 + |\omega| + s] + \dots\end{aligned}$$

Appendix B: Transitions from a Fermi liquid to a fractionalized Fermi liquid (FL*)

III. Quantum phase transitions with Fermi volume change and no broken symmetry

Ya-Hui Zhang and S. Sachdev, *Phys. Rev. Res.* **2**, 023172 (2020)

Maine Christos, Zhu-Xi Luo, Henry Shackleton, Ya-Hui Zhang,
Mathias Scheurer, and S. Sachdev, *Proc. Nat. Acad. Sci.* **120**, e2302701120 (2023)

Maine Christos and S. Sachdev, *npj Quantum Materials* **9**, 4 (2024)

M. Christos, H. Shackleton, S. Sachdev, and Zhu-Xi Luo, arXiv:2402.09502

Pietro M. Bonetti, Maine Christos, S. Sachdev (BCS), arXiv: 2405.08817

Jia-Xin Zhang, S. Sachdev, arXiv:2406.12964

1. Spin liquids on the Kondo lattice:
non-Luttinger volume Fermi surfaces (FL*)

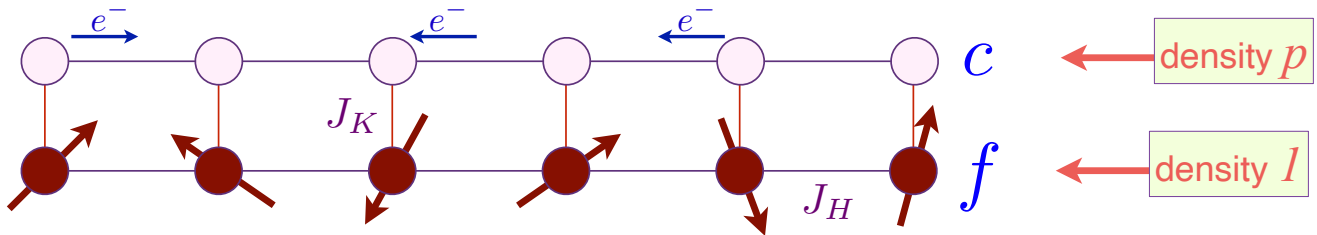
2. Doping square lattice spin liquids for $t \gg J$:
FL* in a single-band model

3. FL* theory of the pseudogap metal of the cuprates

4. Nodal fermionic quasiparticles in d-wave SC

5. Quantum oscillations in hole-doped cuprates

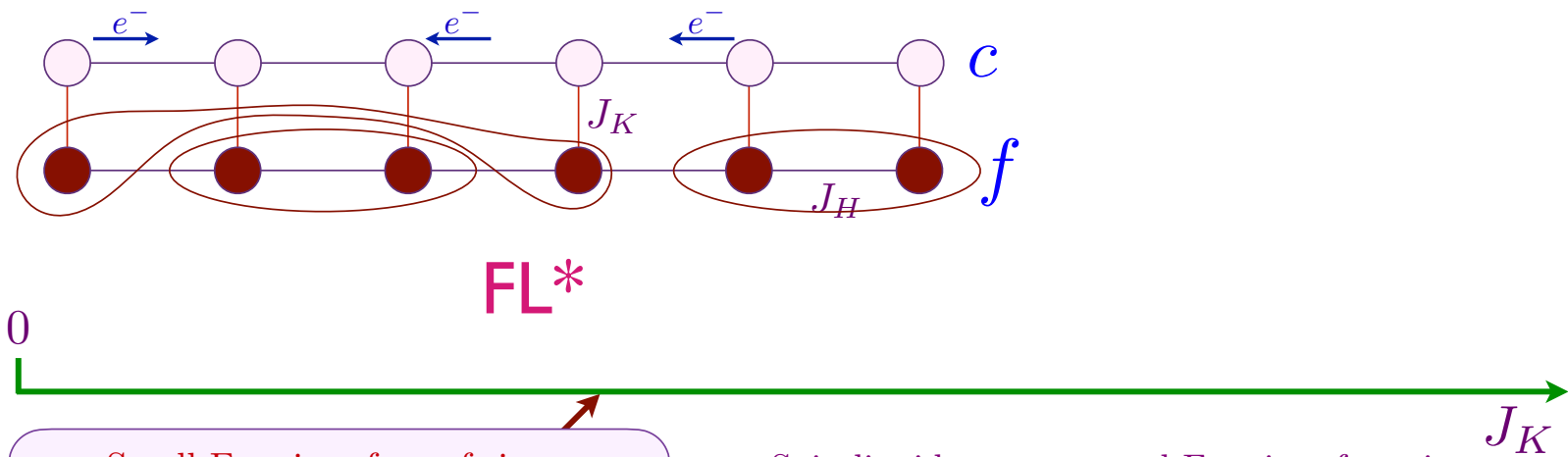
$$\mathcal{H}_{KL} = \sum_{\mathbf{p}} \varepsilon_{\mathbf{p}} c_{\mathbf{p}\sigma}^\dagger c_{\mathbf{p}\sigma} + \sum_i J_K c_{i\sigma}^\dagger \frac{\tau_{\sigma\sigma'}}{2} c_{i\sigma'} \cdot \mathbf{S}_i + \sum_{\langle ij \rangle} J_H \mathbf{S}_i \cdot \mathbf{S}_j$$



Assume J_H is chosen so that at $J_K = 0$ the \mathbf{S}_i spins have a fractionalized spin liquid ground state.

Represent \mathbf{S}_i by fermionic spinons: $\mathbf{S}_i = \frac{1}{2} f_{i\sigma}^\dagger \frac{\tau_{\sigma\sigma'}}{2} f_{i\sigma'}$
 $\sum_{\sigma} f_{i\sigma}^\dagger f_{i\sigma} = 1$ for all i .

$$\mathcal{H}_{KL} = \sum_{\mathbf{p}} \epsilon_{\mathbf{p}} c_{\mathbf{p}\sigma}^\dagger c_{\mathbf{p}\sigma} + \sum_i J_K c_{i\sigma}^\dagger \frac{\boldsymbol{\tau}_{\sigma\sigma'}}{2} c_{i\sigma'} \cdot \mathbf{S}_i + \sum_{\langle ij \rangle} J_H \mathbf{S}_i \cdot \mathbf{S}_j$$



Small Fermi surface of size p

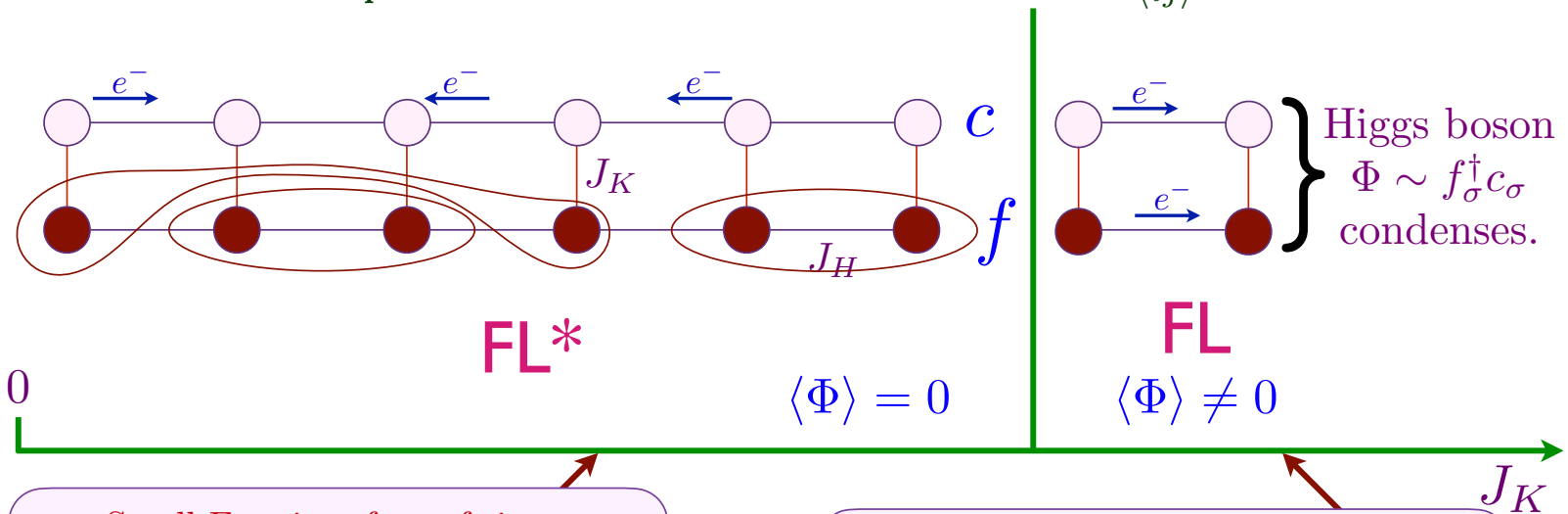
$|\text{FL}^*\rangle = [\text{Projection onto one } f \text{ per site}]$
 $\propto |\text{Slater determinant of } f\rangle$
 $\otimes |\text{Slater determinant of } c\rangle$

Spin liquid structure and Fermi surface size are stable for a finite range of J_K

Note: nevertheless, density of f electrons may change with J_K in an Anderson lattice model!

N. Andrei and P. Coleman, PRL **62**, 595 (1989); S. Burdin, D. R. Grempel, and A. Georges, PRB **66**, 045111 (2002); T. Senthil, M. Vojta, and S. Sachdev, PRB **69**, 035111 (2004); A. Paramekanti and A. Vishwanath, PRB **70**, 245118 (2004)

$$\mathcal{H}_{KL} = \sum_{\mathbf{p}} \epsilon_{\mathbf{p}} c_{\mathbf{p}\sigma}^\dagger c_{\mathbf{p}\sigma} + \sum_i J_K c_{i\sigma}^\dagger \frac{\tau_{\sigma\sigma'}}{2} c_{i\sigma'} \cdot \mathbf{S}_i + \sum_{\langle ij \rangle} J_H \mathbf{S}_i \cdot \mathbf{S}_j$$



Small Fermi surface of size p

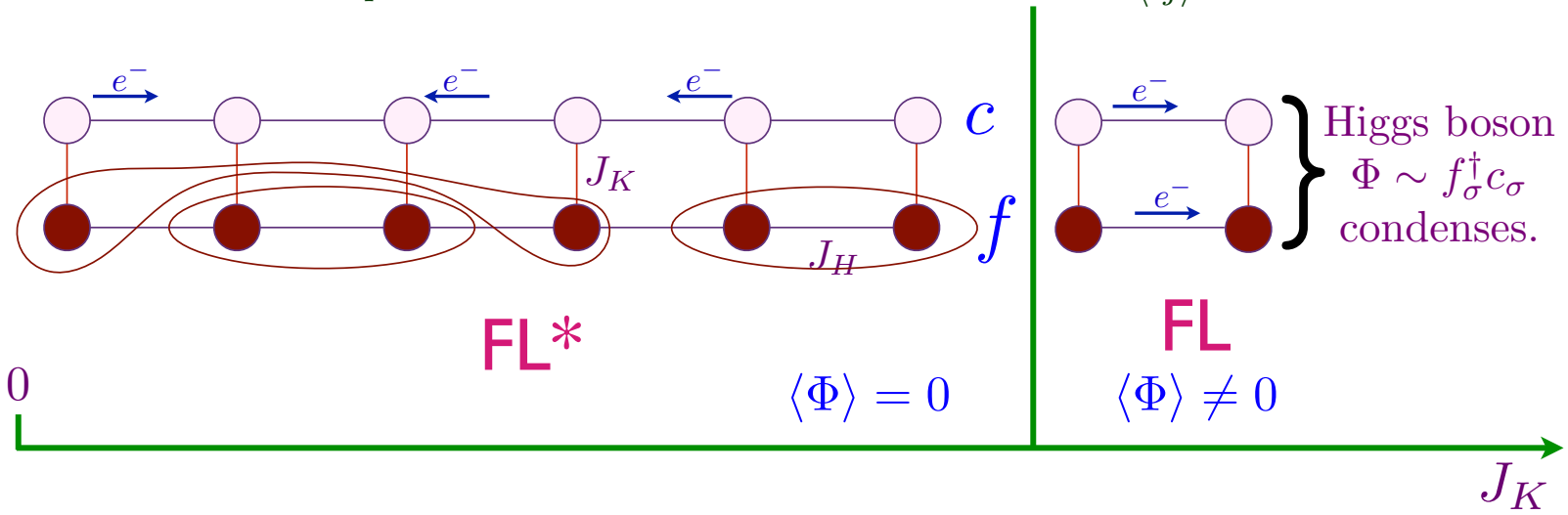
$|\text{FL}^*\rangle = [\text{Projection onto one } f \text{ per site}]$
 $\propto |\text{Slater determinant of } f\rangle$
 $\otimes |\text{Slater determinant of } c\rangle$

Large Fermi surface of size $1 + p$

$|\text{HFL}\rangle = [\text{Projection onto one } f \text{ per site}]$
 $\propto |\text{Slater determinant of } (c, f)\rangle$

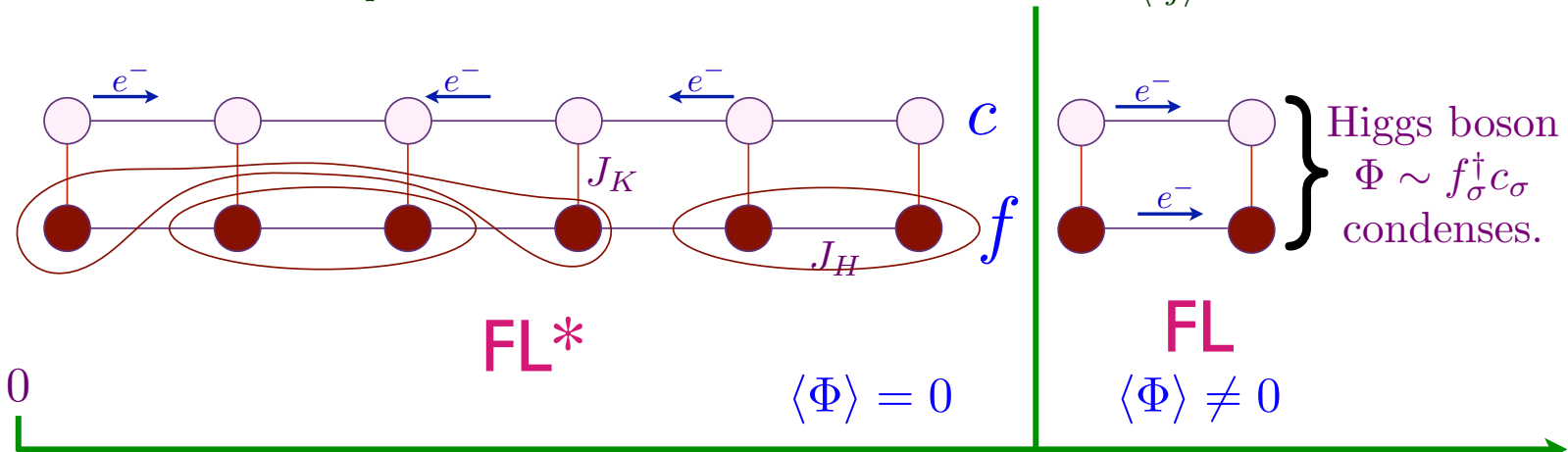
Coleman, Read, Newns, Millis, P.A. Lee, Auerbach, Levin

$$\mathcal{H}_{KL} = \sum_{\mathbf{p}} \varepsilon_{\mathbf{p}} c_{\mathbf{p}\sigma}^\dagger c_{\mathbf{p}\sigma} + \sum_i J_K c_{i\sigma}^\dagger \frac{\tau_{\sigma\sigma'}}{2} c_{i\sigma'} \cdot \mathbf{S}_i + \sum_{\langle ij \rangle} J_H \mathbf{S}_i \cdot \mathbf{S}_j$$



$$H_{\text{mf}} = - \sum_{i,j} t_{ij} c_{i\sigma}^\dagger c_{j\sigma} - \sum_{i,j} t_{1,ij} f_{i\sigma}^\dagger f_{j\sigma} - \sum_i \Phi (c_{i\sigma}^\dagger f_{i\sigma} + f_{i\sigma}^\dagger c_{i\sigma})$$

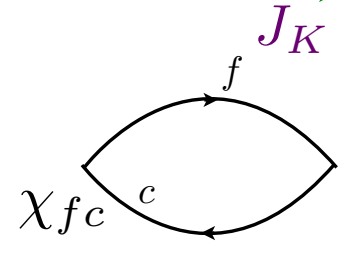
$$\mathcal{H}_{KL} = \sum_{\mathbf{p}} \epsilon_{\mathbf{p}} c_{\mathbf{p}\sigma}^\dagger c_{\mathbf{p}\sigma} + \sum_i J_K c_{i\sigma}^\dagger \frac{\tau_{\sigma\sigma'}}{2} c_{i\sigma'} \cdot \mathbf{S}_i + \sum_{\langle ij \rangle} J_H \mathbf{S}_i \cdot \mathbf{S}_j$$



Higgs boson
 $\Phi \sim f_\sigma^\dagger c_\sigma$
 condenses.

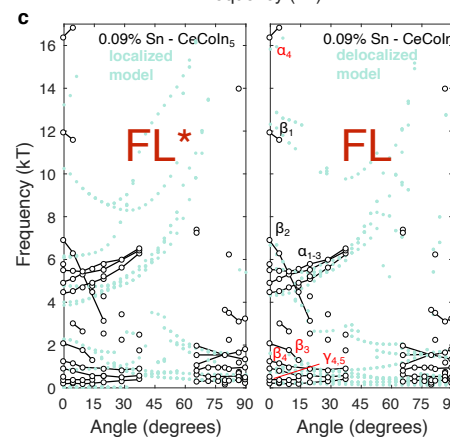
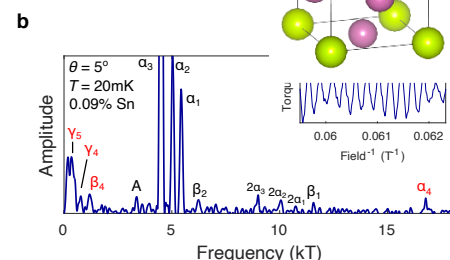
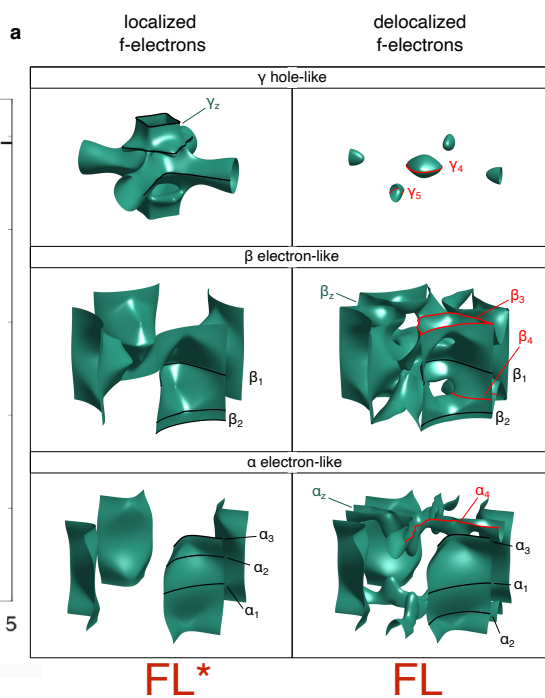
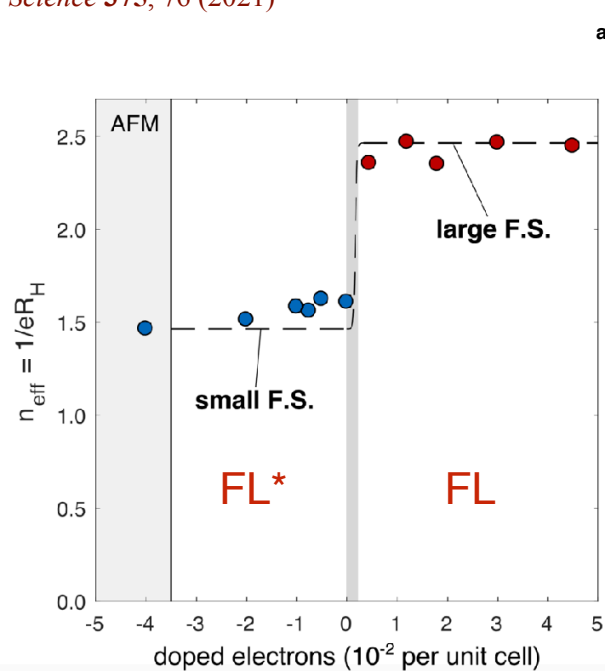
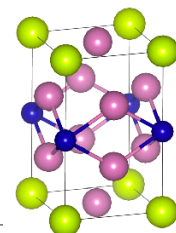
Effective action for Φ : $\mathcal{L}[\Phi] = s|\Phi|^2 + \dots$ with $s \sim \frac{1}{J_K} - \chi_{fc}$.

No singularity in χ_{fc} because Fermi surfaces do not match.
 \Rightarrow FL* is stable for small J_K



Evidence for a delocalization quantum phase transition without symmetry breaking in CeCoIn₅

Nikola Maksimovic, Daniel H. Eilbott, Tessa Cookmeyer.....Ehud Altman, Alessandra Lanzara, James G. Analytis, *Science* **375**, 76 (2021)



1. Spin liquids on the Kondo lattice:
non-Luttinger volume Fermi surfaces (FL*)

2. Doping square lattice spin liquids for $t \gg J$:
FL* in a single-band model

3. FL* theory of the pseudogap metal of the cuprates

4. Nodal fermionic quasiparticles in d-wave SC

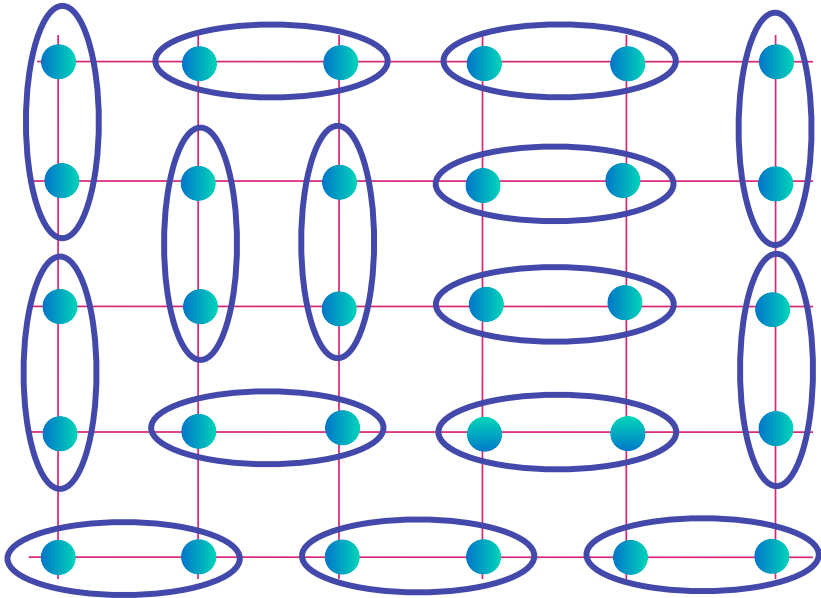
5. Quantum oscillations in hole-doped cuprates

The dance of electrons on Cu atoms in YBCO

P.W. Anderson (1973)

Spin liquid

Electrons form entangled pairs, and the pairs entangle across the entire sample



$$\text{[Diagram of two electrons in an oval]} = |\uparrow\downarrow\rangle - |\downarrow\uparrow\rangle$$

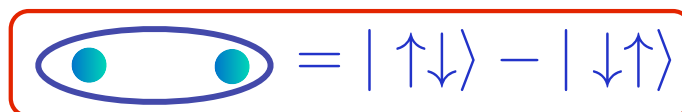
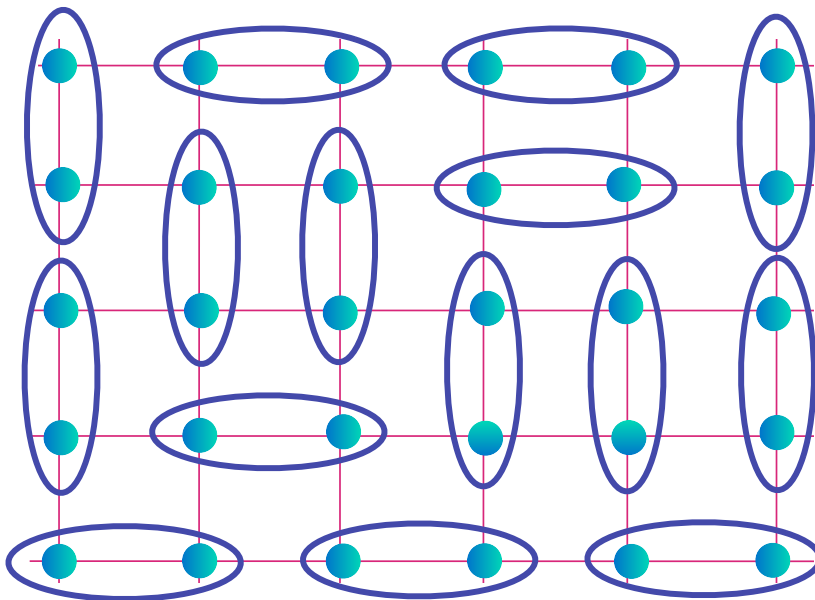
G. Baskaran, Z. Zou, P.W. Anderson, *Solid State Comm.* **63**, 973 (1987)
 S.A. Kivelson, D.S. Rokhsar and J.P. Sethna, *Phys. Rev. B* **35**, 8865 (1987)
 D. Rokhsar and S.A. Kivelson, *Phys. Rev. Lett.* **61**, 2376 (1988)
 E. Fradkin and S.A. Kivelson, *Mod. Phys. Lett. B* **4**, 225 (1990)

The dance of electrons on Cu atoms in YBCO

P.W. Anderson (1973)

Spin liquid

Electrons form entangled pairs, and the pairs entangle across the entire sample



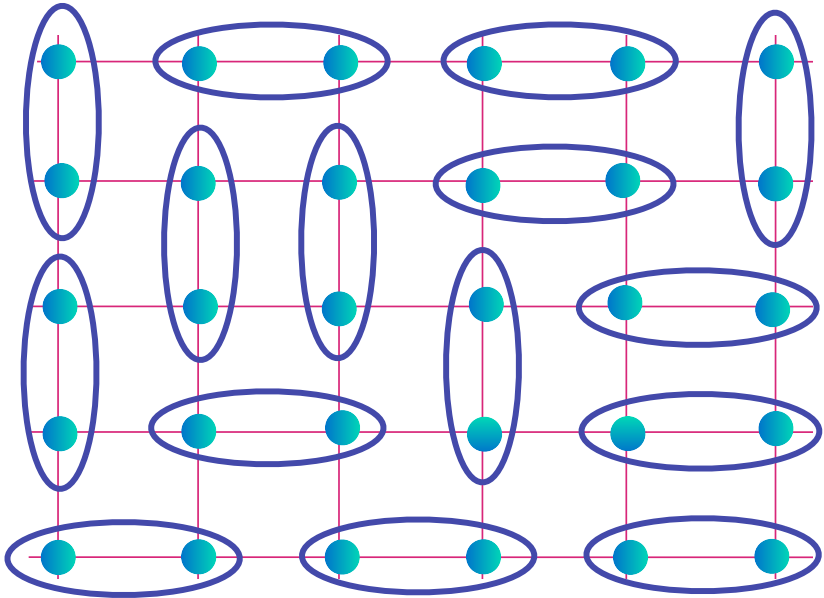
G. Baskaran, Z. Zou, P.W. Anderson,
Solid State Comm. **63**, 973 (1987)
 S.A. Kivelson, D.S. Rokhsar and J.P. Sethna,
Phys. Rev. B **35**, 8865 (1987)
 D. Rokhsar and S.A. Kivelson,
Phys. Rev. Lett. **61**, 2376 (1988)
 E. Fradkin and S.A. Kivelson,
Mod. Phys. Lett. B **4**, 225 (1990)

The dance of electrons on Cu atoms in YBCO

P.W. Anderson (1973)

Spin liquid

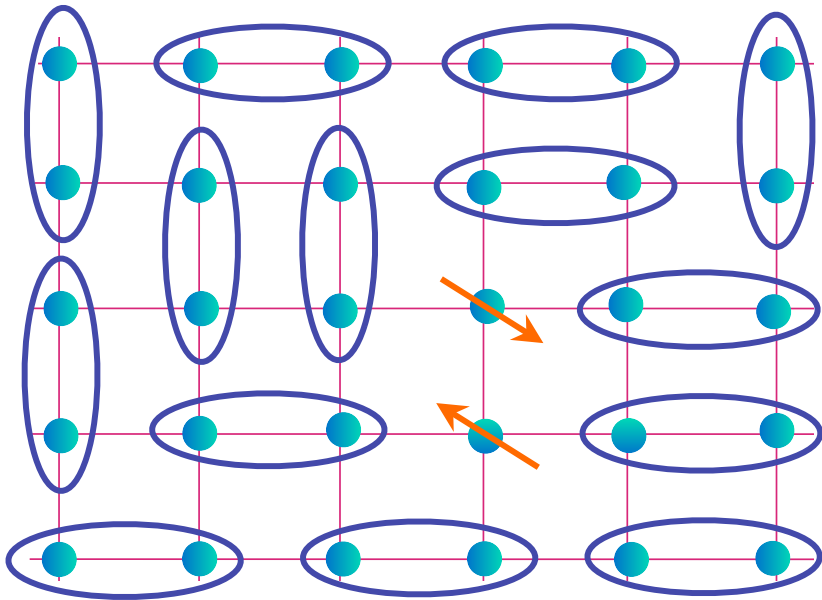
Electrons form entangled pairs, and the pairs entangle across the entire sample



$$\text{[Oval with two dots]} = |\uparrow\downarrow\rangle - |\downarrow\uparrow\rangle$$

G. Baskaran, Z. Zou, P.W. Anderson, *Solid State Comm.* **63**, 973 (1987)
 S.A. Kivelson, D.S. Rokhsar and J.P. Sethna, *Phys. Rev. B* **35**, 8865 (1987)
 D. Rokhsar and S.A. Kivelson, *Phys. Rev. Lett.* **61**, 2376 (1988)
 E. Fradkin and S.A. Kivelson, *Mod. Phys. Lett. B* **4**, 225 (1990)

The dance of electrons on Cu atoms in YBCO



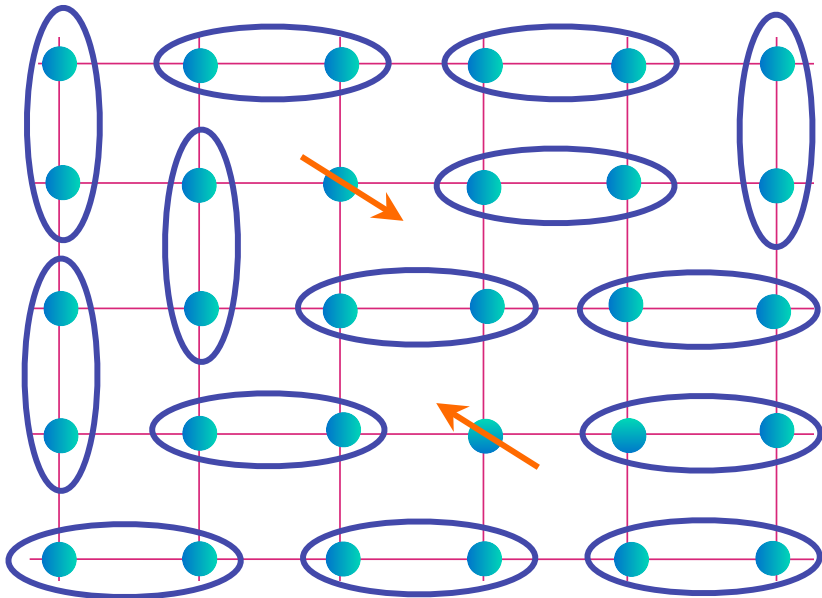
Spin liquid

Fractionalized spinon excitations with spin $S=1/2$ and charge 0.

$$\text{Oval with two dots} = |\uparrow\downarrow\rangle - |\downarrow\uparrow\rangle$$

G. Baskaran, Z. Zou, P.W. Anderson, *Solid State Comm.* **63**, 973 (1987)
 S.A. Kivelson, D.S. Rokhsar and J.P. Sethna, *Phys. Rev. B* **35**, 8865 (1987)
 D. Rokhsar and S.A. Kivelson, *Phys. Rev. Lett.* **61**, 2376 (1988)
 E. Fradkin and S.A. Kivelson, *Mod. Phys. Lett. B* **4**, 225 (1990)

The dance of electrons on Cu atoms in YBCO



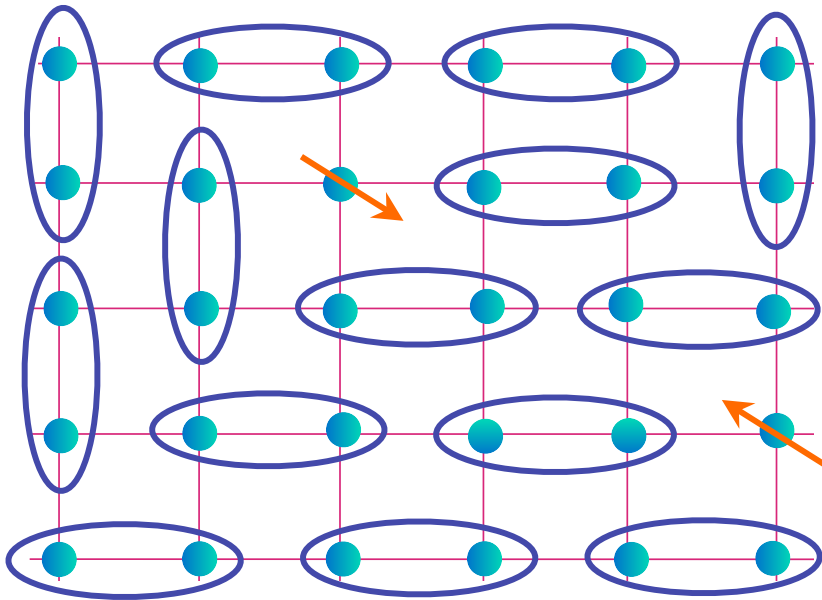
Spin liquid

Fractionalized spinon excitations with spin $S=1/2$ and charge 0.

$$\text{Oval with two dots} = |\uparrow\downarrow\rangle - |\downarrow\uparrow\rangle$$

G. Baskaran, Z. Zou, P.W. Anderson, *Solid State Comm.* **63**, 973 (1987)
 S.A. Kivelson, D.S. Rokhsar and J.P. Sethna, *Phys. Rev. B* **35**, 8865 (1987)
 D. Rokhsar and S.A. Kivelson, *Phys. Rev. Lett.* **61**, 2376 (1988)
 E. Fradkin and S.A. Kivelson, *Mod. Phys. Lett. B* **4**, 225 (1990)

The dance of electrons on Cu atoms in YBCO



Spin liquid

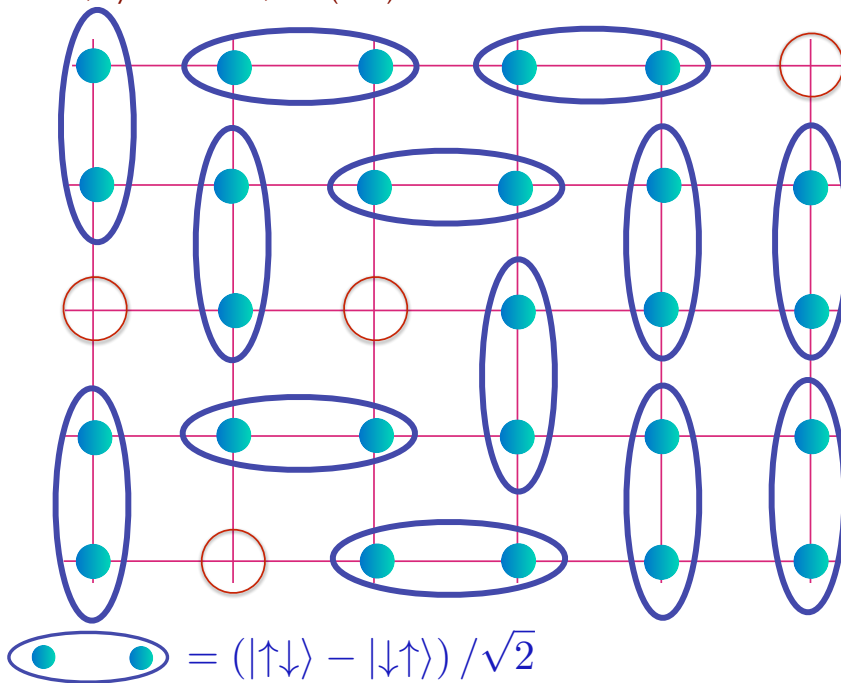
Fractionalized spinon excitations with spin $S=1/2$ and charge 0.

$$\text{Oval with two dots} = |\uparrow\downarrow\rangle - |\downarrow\uparrow\rangle$$

G. Baskaran, Z. Zou, P.W. Anderson, *Solid State Comm.* **63**, 973 (1987)
 S.A. Kivelson, D.S. Rokhsar and J.P. Sethna, *Phys. Rev. B* **35**, 8865 (1987)
 D. Rokhsar and S.A. Kivelson, *Phys. Rev. Lett.* **61**, 2376 (1988)
 E. Fradkin and S.A. Kivelson, *Mod. Phys. Lett. B* **4**, 225 (1990)

Holons

G. Baskaran, Z. Zou, P.W. Anderson, *Solid State Comm.* **63**, 973 (1987)
S.A. Kivelson, D.S. Rokhsar and J.P. Sethna, *Phys. Rev. B* **35**, 8865 (1987)
D. Rokhsar and S.A. Kivelson, *Phys. Rev. Lett.* **61**, 2376 (1988)

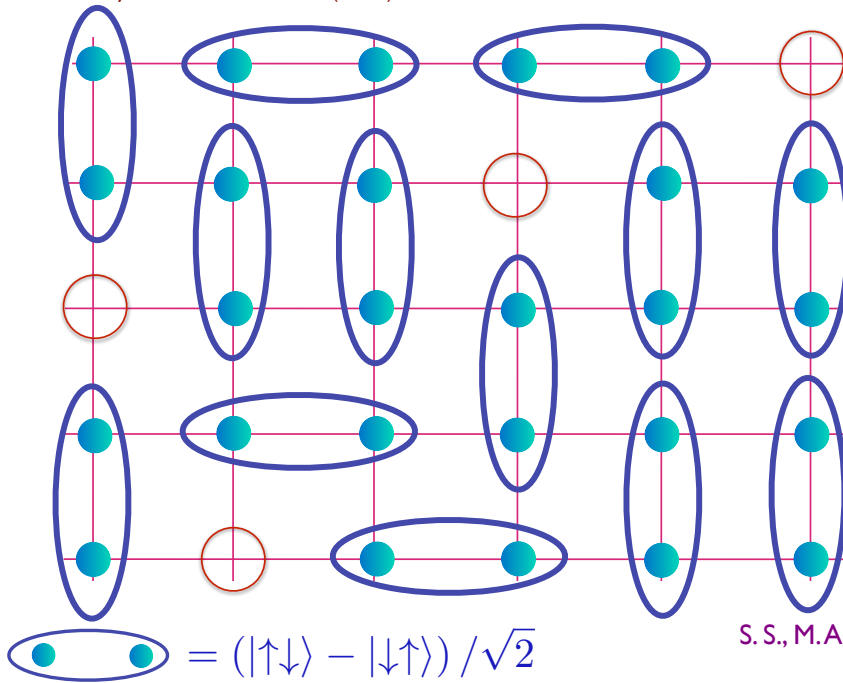


Spin liquid

Fractionalized
holon excitations
with spin $S=0$
and charge $+e$.

Holon metal

G. Baskaran, Z. Zou, P.W. Anderson, *Solid State Comm.* **63**, 973 (1987)
 S.A. Kivelson, D.S. Rokhsar and J.P. Sethna, *Phys. Rev. B* **35**, 8865 (1987)
 D. Rokhsar and S.A. Kivelson, *Phys. Rev. Lett.* **61**, 2376 (1988)

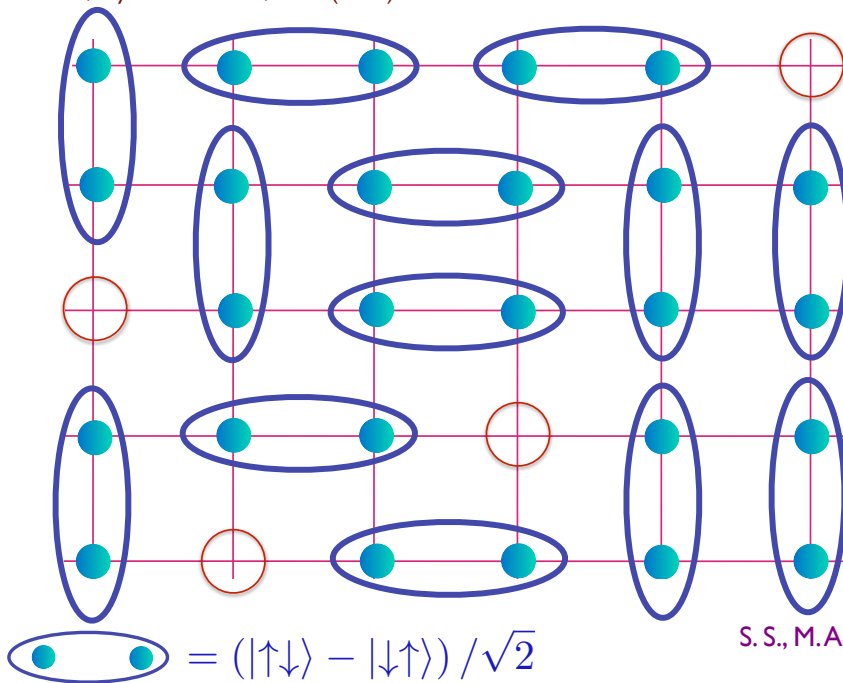


If each holon is a fermion, we obtain a Fermi surface of holons of size p

S. S., M.A. Metlitski, Y. Qi, and C. Xu, *PRB* **80**, 155129 (2009)
 M. S. Scheurer, S. Chatterjee, Wei Wu, M. Ferrero, A. Georges, and S. S., *PNAS* **115**, E3665 (2018)
 Pietro M. Bonetti and Walter Metzner, *PRB* **106**, 205152 (2022)

Holon metal

G. Baskaran, Z. Zou, P.W. Anderson, *Solid State Comm.* **63**, 973 (1987)
 S.A. Kivelson, D.S. Rokhsar and J.P. Sethna, *Phys. Rev. B* **35**, 8865 (1987)
 D. Rokhsar and S.A. Kivelson, *Phys. Rev. Lett.* **61**, 2376 (1988)

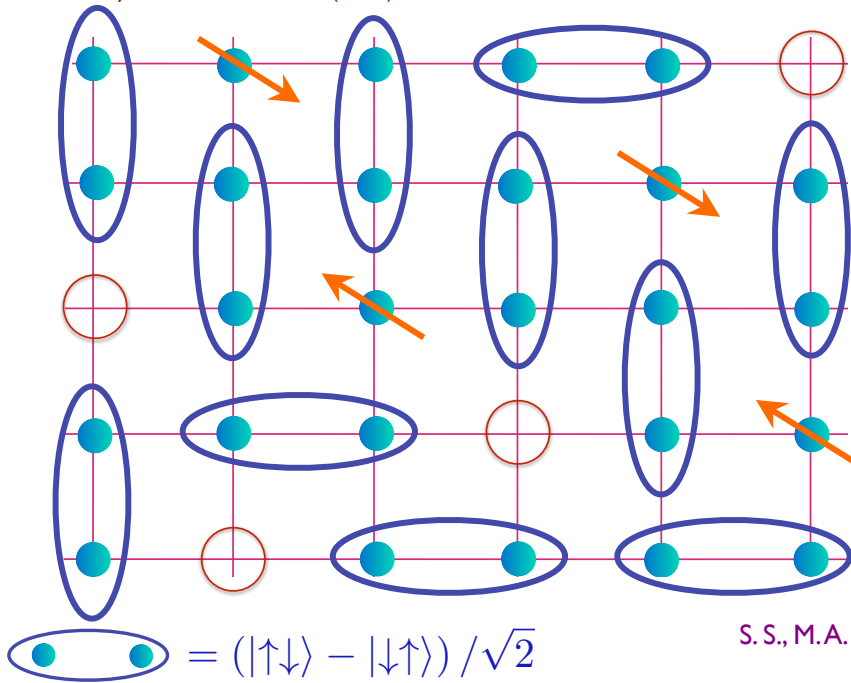


If each holon is a fermion, we obtain a Fermi surface of holons of size p

S. S., M.A. Metlitski, Y. Qi, and C. Xu, *PRB* **80**, 155129 (2009)
 M. S. Scheurer, S. Chatterjee, Wei Wu, M. Ferrero, A. Georges, and S. S., *PNAS* **115**, E3665 (2018)
 Pietro M. Bonetti and Walter Metzner, *PRB* **106**, 205152 (2022)

Holon metal

G. Baskaran, Z. Zou, P.W. Anderson, *Solid State Comm.* **63**, 973 (1987)
 S.A. Kivelson, D.S. Rokhsar and J.P. Sethna, *Phys. Rev. B* **35**, 8865 (1987)
 D. Rokhsar and S.A. Kivelson, *Phys. Rev. Lett.* **61**, 2376 (1988)

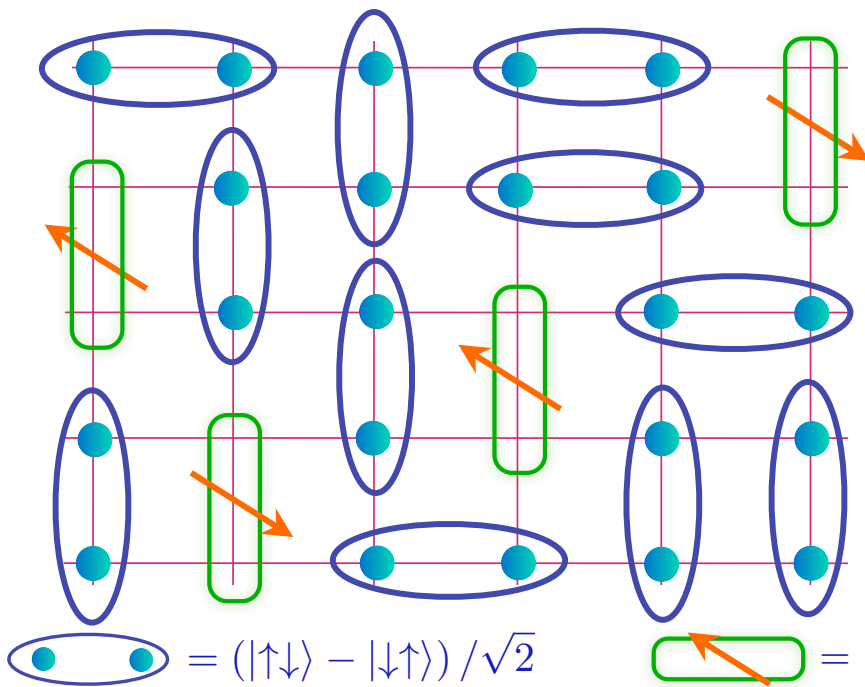


There is an energy cost of order J to create spinons in a holon metal

S. S., M.A. Metlitski, Y. Qi, and C. Xu, *PRB* **80**, 155129 (2009)
 M. S. Scheurer, S. Chatterjee, Wei Wu, M. Ferrero, A. Georges, and S. S., *PNAS* **115**, E3665 (2018)
 Pietro M. Bonetti and Walter Metzner, *PRB* **106**, 205152 (2022)

FL* in a **one-band** model

S. Sachdev *Phys. Rev. B* **49**, 6770 (1994); X.-G. Wen and P.A. Lee *Phys. Rev. Lett.* **76**, 503 (1996)
 R. K. Kaul, A. Kolezhuk, M. Levin, S. Sachdev, and T. Senthil, *Phys. Rev. B* **75**, 235122 (2007)



There is an energy gain of order t in the formation of spinon-holon bound states

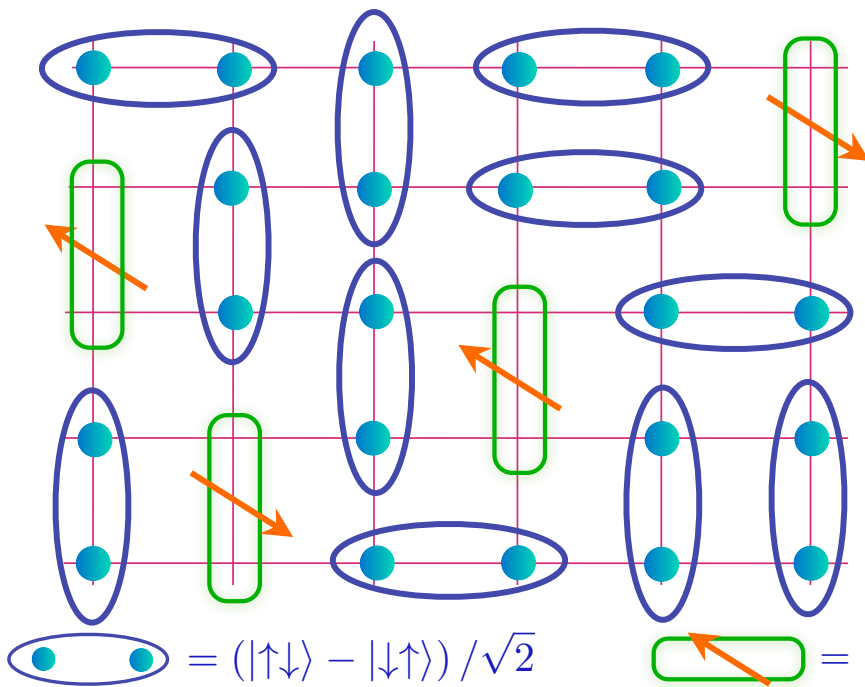
Spinon-holon bound state



Yang Qi and S. Sachdev, *Phys. Rev. B* **81**, 115129 (2010); M. Punk, A. Allais, and S. Sachdev, *Proc. Nat. Acad. Sci.* **112**, 9552 (2015)

FL* in a **one-band** model

S. Sachdev *Phys. Rev. B* **49**, 6770 (1994); X.-G. Wen and P.A. Lee *Phys. Rev. Lett.* **76**, 503 (1996)
 R. K. Kaul, A. Kolezhuk, M. Levin, S. Sachdev, and T. Senthil, *Phys. Rev. B* **75**, 235122 (2007)



Metal with electron-like quasiparticles on a Fermi surface of size ρ , and emergent gauge fields

Spinon-holon bound state

$$\text{Blue oval} = (|\uparrow\downarrow\rangle - |\downarrow\uparrow\rangle) / \sqrt{2}$$

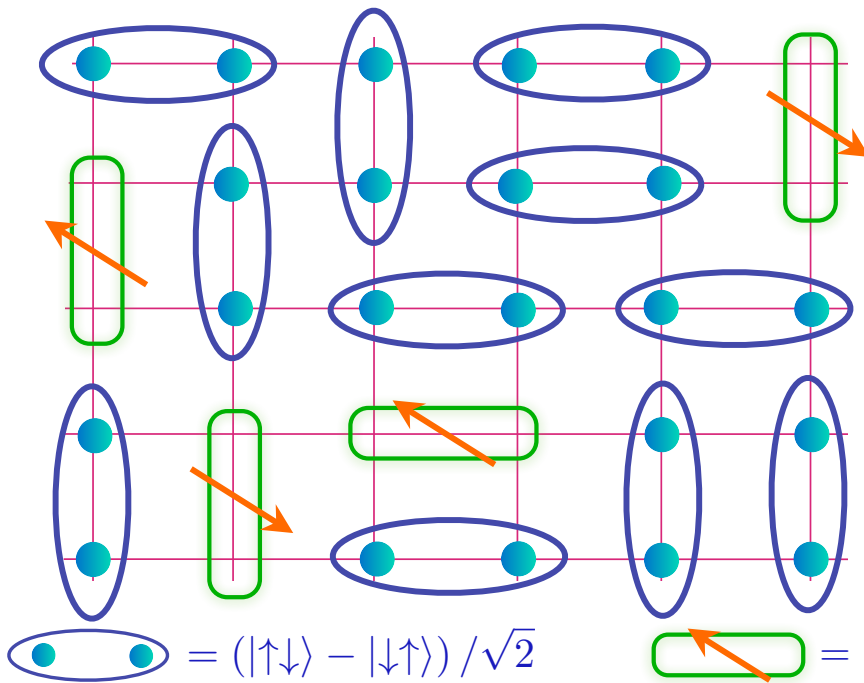
$$\text{Green oval with arrow} = (|\uparrow\circ\rangle + |\circ\uparrow\rangle) / \sqrt{2}$$



Yang Qi and S. Sachdev, *Phys. Rev. B* **81**, 115129 (2010); M. Punk, A. Allais, and S. Sachdev, *Proc. Nat. Acad. Sci.* **112**, 9552 (2015)

FL* in a **one-band** model

S. Sachdev *Phys. Rev. B* **49**, 6770 (1994); X.-G. Wen and P.A. Lee *Phys. Rev. Lett.* **76**, 503 (1996)
 R. K. Kaul, A. Kolezhuk, M. Levin, S. Sachdev, and T. Senthil, *Phys. Rev. B* **75**, 235122 (2007)



Metal with electron-like quasiparticles on a Fermi surface of size ρ , and emergent gauge fields

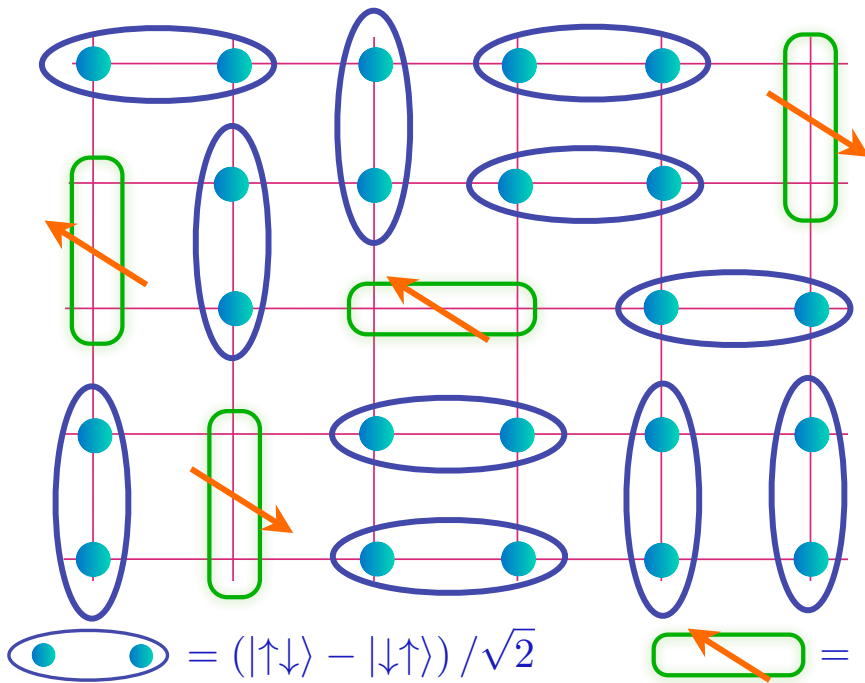
Spinon-holon bound state



Yang Qi and S. Sachdev, *Phys. Rev. B* **81**, 115129 (2010); M. Punk, A. Allais, and S. Sachdev, *Proc. Nat. Acad. Sci.* **112**, 9552 (2015)

FL* in a **one-band** model

S. Sachdev *Phys. Rev. B* **49**, 6770 (1994); X.-G. Wen and P.A. Lee *Phys. Rev. Lett.* **76**, 503 (1996)
 R. K. Kaul, A. Kolezhuk, M. Levin, S. Sachdev, and T. Senthil, *Phys. Rev. B* **75**, 235122 (2007)



Metal with electron-like quasiparticles on a Fermi surface of size ρ , and emergent gauge fields

Spinon-holon bound state

$$\text{Blue oval} = (|\uparrow\downarrow\rangle - |\downarrow\uparrow\rangle) / \sqrt{2} \quad \text{Green oval with arrow} = (|\uparrow\circ\rangle + |\circ\uparrow\rangle) / \sqrt{2}$$



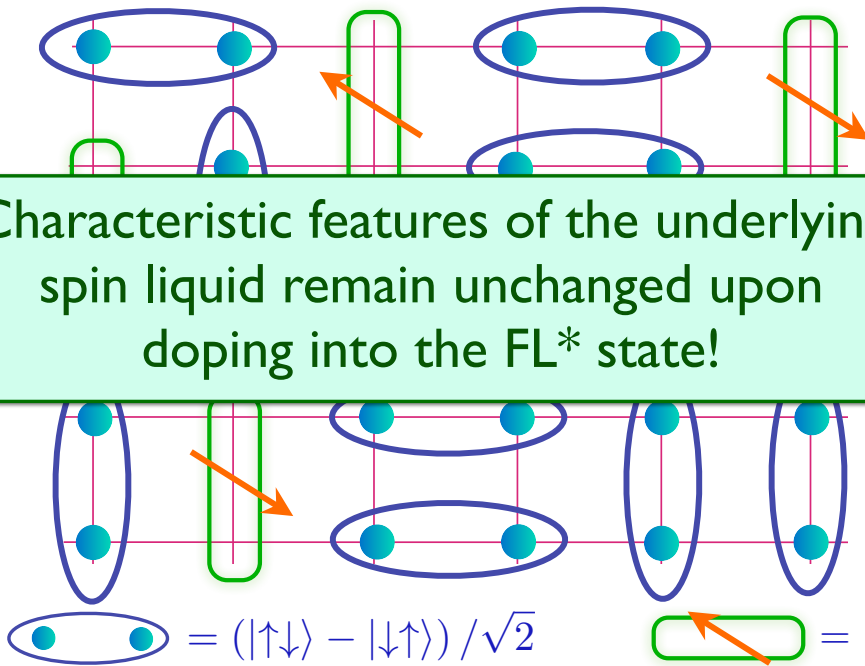
Yang Qi and S. Sachdev, *Phys. Rev. B* **81**, 115129 (2010); M. Punk, A. Allais, and S. Sachdev, *Proc. Nat. Acad. Sci.* **112**, 9552 (2015)

FL* in a **one-band** model

S. Sachdev *Phys. Rev. B* **49**, 6770 (1994); X.-G. Wen and P.A. Lee *Phys. Rev. Lett.* **76**, 503 (1996)
 R. K. Kaul, A. Kolezhuk, M. Levin, S. Sachdev, and T. Senthil, *Phys. Rev. B* **75**, 235122 (2007)

Metal with
 electron-like
 quasiparticles
 on a Fermi
 surface of size
 ρ , and
 emergent
 gauge fields

Characteristic features of the underlying
 spin liquid remain unchanged upon
 doping into the FL* state!



Spinon-holon
 bound state

$$\text{Spinon} = (|\uparrow\downarrow\rangle - |\downarrow\uparrow\rangle) / \sqrt{2}$$

$$\text{Spinon-holon bound state} = (|\uparrow\circ\rangle + |\circ\uparrow\rangle) / \sqrt{2}$$

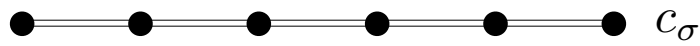


Yang Qi and S. Sachdev, *Phys. Rev. B* **81**, 115129 (2010); M. Punk, A. Allais, and S. Sachdev, *Proc. Nat. Acad. Sci.* **112**, 9552 (2015)

FL* from a doped spin liquid

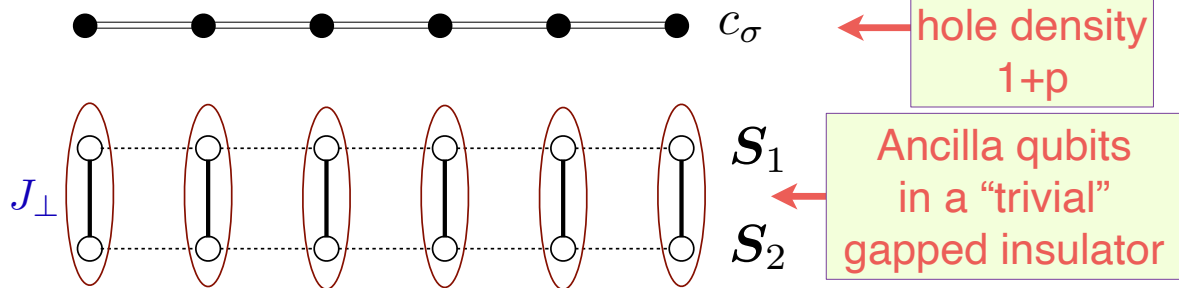
1. Begin with a spin liquid insulator at half-filling. This has a ‘spinon’ anyon superselection sector \mathcal{S} with spin $S = 1/2$ and charge 0.
2. Now consider the expanded Hilbert space of the doped spin liquid. This will have a ‘holon’ sector \mathcal{H} with charge e and spin $S = 0$ such that the \mathcal{S} - \mathcal{H} composite has the same quantum numbers and statistics as the electron.
3. For $t \gg J$, it is invariably the case that the binding energy of a \mathcal{S} - \mathcal{H} bound state compensates the energy to create a \mathcal{S} excitation. Then the doped charges will appear as \mathcal{S} - \mathcal{H} ‘polarons’.
4. For doping density p , the \mathcal{S} - \mathcal{H} polarons will form Fermi surfaces of size p with electron-like quasiparticles.
5. This is FL* because (i) the Fermi surface size is p (and not the Fermi liquid value of $1 + p$), and (ii) the spinon sector \mathcal{S} of excitations is still present.

Ancilla theory of the Hubbard model



← Hubbard
model of
hole density
 $1+p$

Ancilla theory of the Hubbard model (Luttinger-Oshikawa anomalies for dummies)



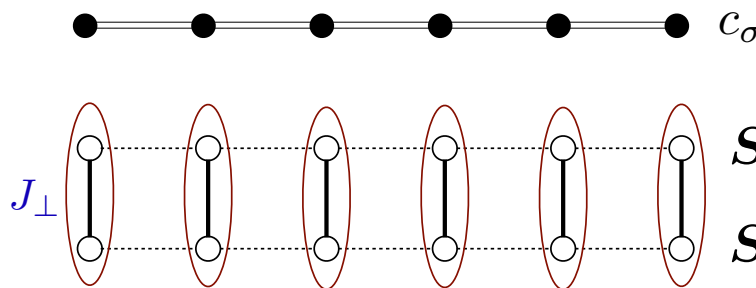
$$\mathcal{H}_{\text{Hubbard}} + \mathcal{H}_{\text{trivial insulator}}$$

Ya-Hui Zhang



Ya-Hui Zhang and S. Sachdev, PRR **2**, 023172 (2020)
A. Nikolaenko, M. Tikhanovskaya, S. Sachdev, and Ya-Hui Zhang, PRB **103**, 235138 (2021)

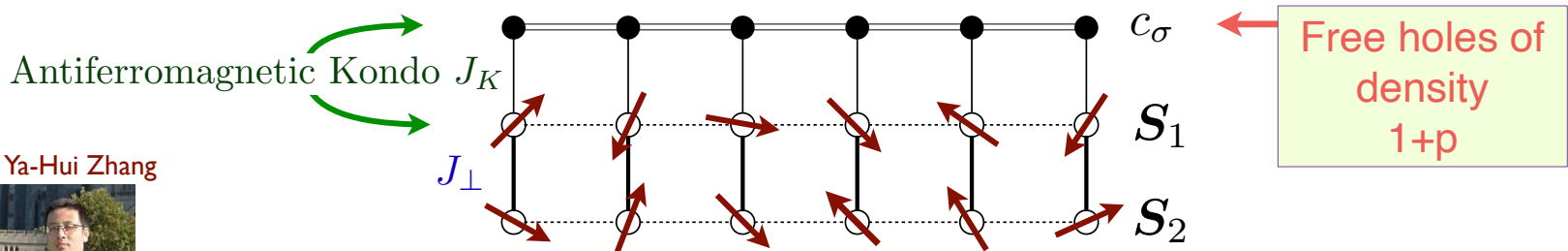
Ancilla theory of the Hubbard model (Luttinger-Oshikawa anomalies for dummies)



Hubbard model of hole density $1+p$

Ancilla qubits in a "trivial" gapped insulator

$$\mathcal{U} (\mathcal{H}_{\text{Hubbard}} + \mathcal{H}_{\text{trivial insulator}}) \mathcal{U}^{-1} = \mathcal{H}_{\text{ancilla}}$$



Antiferromagnetic Kondo J_K

Free holes of density $1+p$

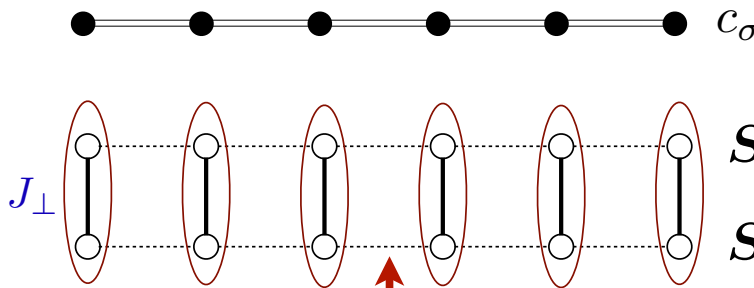
Ya-Hui Zhang



Ya-Hui Zhang and S. Sachdev, PRR **2**, 023172 (2020)

A. Nikolaenko, M. Tikhanovskaya, S. Sachdev, and Ya-Hui Zhang, PRB **103**, 235138 (2021)

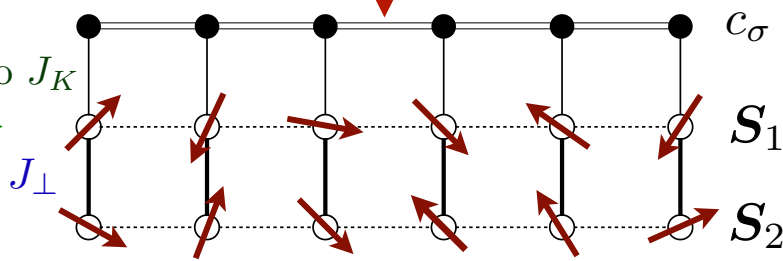
Ancilla theory of the Hubbard model (Luttinger-Oshikawa anomalies for dummies)



Hubbard model of hole density $1+p$

Ancilla qubits in a "trivial" gapped insulator

Schrieffer-Wolff transformation at large J_\perp yields $U = \frac{3J_K^2}{8J_\perp} + \frac{3J_K^3}{16J_\perp^2} + \dots$



Free holes of density $1+p$

Antiferromagnetic Kondo J_K

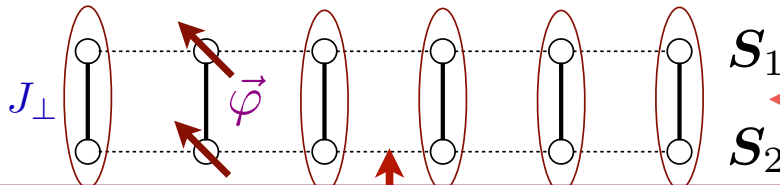


Ya-Hui Zhang and S. Sachdev, PRR **2**, 023172 (2020)
A. Nikolaenko, M. Tikhanovskaya, S. Sachdev, and Ya-Hui Zhang, PRB **103**, 235138 (2021)

Ancilla theory of the Hubbard model (Luttinger-Oshikawa anomalies for dummies)

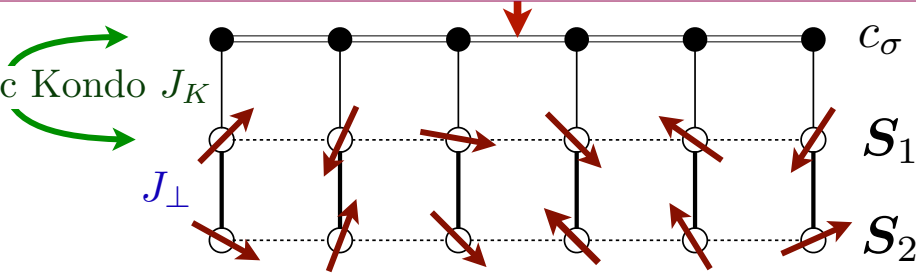


Hubbard model of hole density $1+p$



Ancilla qubits in a "trivial" gapped insulator

Hubbard-Stratonovich transformation:
 $U n_{i\uparrow} n_{i\downarrow} \Rightarrow (3/(8U)) \vec{\varphi}_i^2 - \vec{\varphi}_i \cdot c_{i\sigma}^\dagger (\tau_{\sigma\sigma'}/2) c_{i\sigma'}$.
 Then fractionalize paramagnon $\vec{\varphi}$ into $S = 1/2$ spins, $\vec{\varphi} \sim S_1 - S_2$.



Free holes of density $1+p$

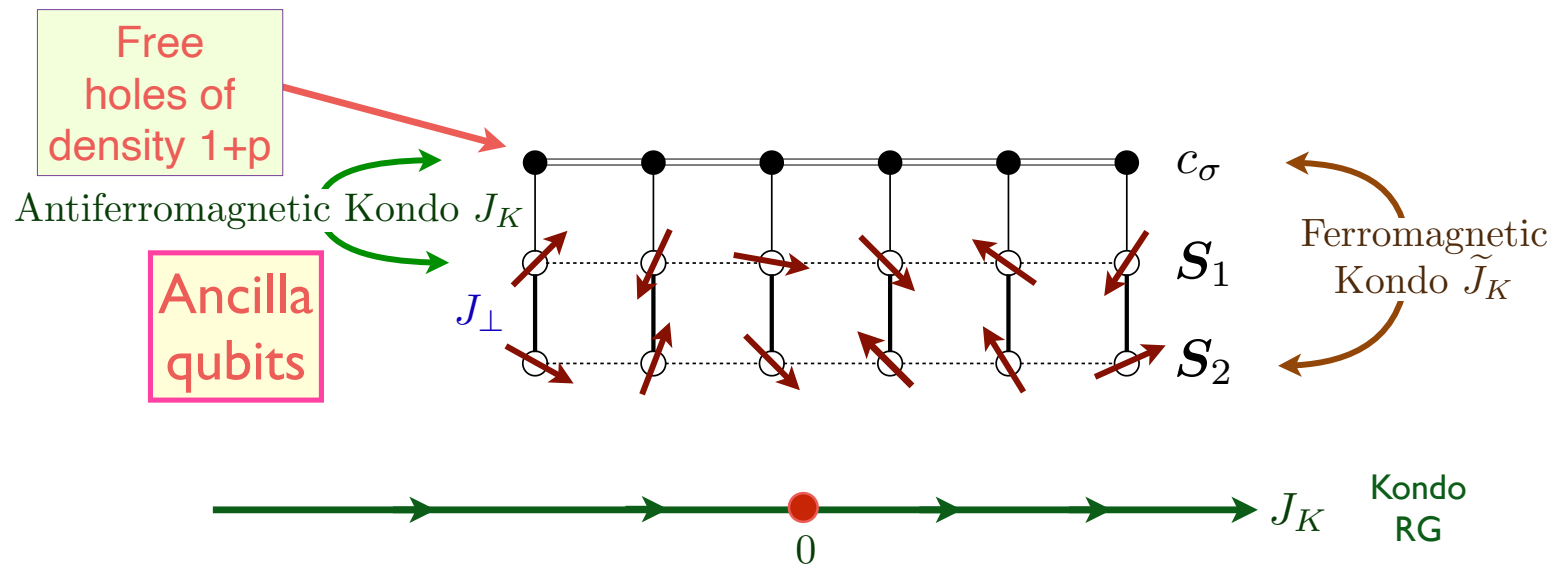
Antiferromagnetic Kondo J_K



Ya-Hui Zhang and S. Sachdev, PRR **2**, 023172 (2020)
 A. Nikolaenko, M. Tikhanovskaya, S. Sachdev, and Ya-Hui Zhang, PRB **103**, 235138 (2021)

Ancilla theory of the Hubbard model

Ya-Hui Zhang and S. Sachdev,
Phys. Rev. Res. **2**, 023172 (2020)



Ya-Hui Zhang



$$\mathcal{H}_{\text{ancilla}} = \sum_{\mathbf{p}} \varepsilon_{\mathbf{p}} c_{\mathbf{p}\sigma}^\dagger c_{\mathbf{p}\sigma} + J_K \sum_i c_{i\sigma}^\dagger \frac{\tau_{\sigma\sigma'}}{2} c_{i\sigma'} \cdot \mathbf{S}_{1i} + J_{\perp} \sum_i \mathbf{S}_{1i} \cdot \mathbf{S}_{2i}$$

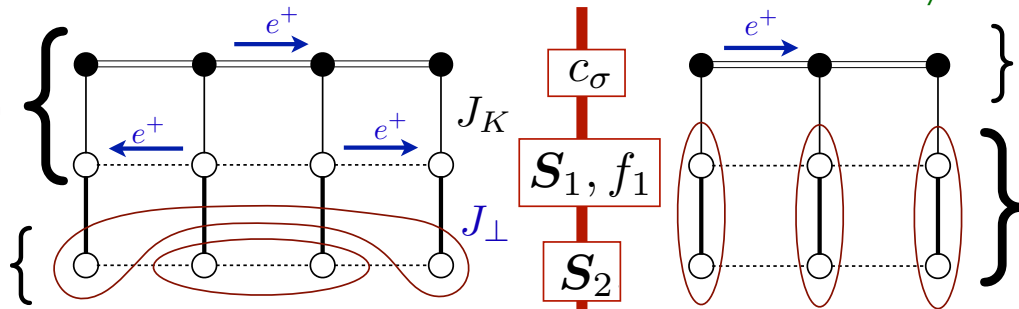
Ancilla theory of the Hubbard model

Ya-Hui Zhang and S. Sachdev,
Phys. Rev. Res. **2**, 023172 (2020)

Kondo lattice heavy
Fermi liquid.
Size $1 + p + 1$
 $= p \pmod{2}$.
Small Fermi surface!

$$\langle \Phi \rangle \neq 0$$

Spin liquid



Large
Fermi surface.
Size: $1 + p$

Trivial
insulator

FL*

$$\langle \Phi \rangle \neq 0$$

$$\langle \Phi \rangle = 0$$

FL

J_K

doping p

Pseudogap metal =
Kondo Lattice Heavy
Fermi Liquid
 \oplus
Spin Liquid

Fractionalized excitations of layer S_1 confined
by condensation of Higgs boson $\Phi \sim f_{1\sigma}^\dagger c_\sigma$.

Fractionalized excitations of layer S_2 remain deconfined

Ya-Hui
Zhang



Kondo lattice

FL*

$$\langle \Phi \rangle = 0$$

$$\langle \Phi \rangle \neq 0$$

FL

Small Fermi surface of size p

Large Fermi surface of size $1 + p$

0

J_K

Single band model

FL*

$$\langle \Phi \rangle \neq 0$$

$$\langle \Phi \rangle = 0$$

FL

Small Fermi surface of size p

Large Fermi surface of size $1 + p$

J_K

0

Note the inversion: in the Kondo lattice (single band model)
the large J_K phase with $\langle \Phi \rangle \neq 0$ is FL (FL*).

Single band model has a 'flipped' Kondo lattice transition!

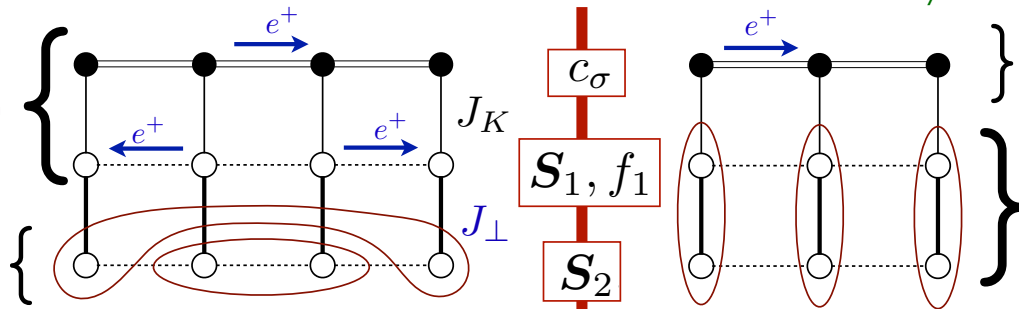
Ancilla theory of the Hubbard model

Ya-Hui Zhang and S. Sachdev,
Phys. Rev. Res. **2**, 023172 (2020)

Kondo lattice heavy
Fermi liquid.
Size $1 + p + 1$
 $= p \pmod{2}$.
Small Fermi surface!

$$\langle \Phi \rangle \neq 0$$

Spin liquid



Large
Fermi surface.
Size: $1 + p$

Trivial
insulator

FL*

$$\langle \Phi \rangle \neq 0$$

$$\langle \Phi \rangle = 0$$

FL

J_K

doping p

Pseudogap metal =
Kondo Lattice Heavy
Fermi Liquid
 \oplus
Spin Liquid

Fractionalized excitations of layer S_1 confined
by condensation of Higgs boson $\Phi \sim f_{1\sigma}^\dagger c_\sigma$.

Fractionalized excitations of layer S_2 remain deconfined

Ya-Hui
Zhang



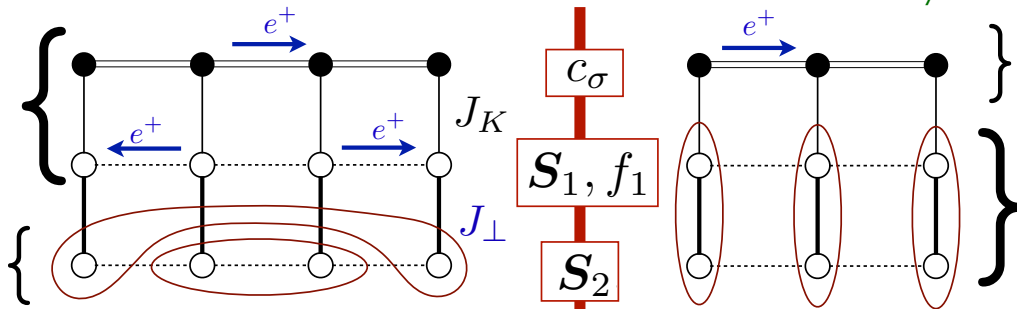
Ancilla theory of the Hubbard model

Ya-Hui Zhang and S. Sachdev,
Phys. Rev. Res. **2**, 023172 (2020)

Kondo lattice heavy
Fermi liquid.
Size $1 + p + 1$
 $= p \pmod{2}$.
Small Fermi surface!

$$\langle \Phi \rangle \neq 0$$

Spin liquid



Large
Fermi surface.
Size: $1 + p$

Trivial
insulator

FL*

$$\langle \Phi \rangle \neq 0$$

$$\langle \Phi \rangle = 0$$

FL

J_K

doping p

Pseudogap metal =
Kondo Lattice Heavy
Fermi Liquid
 \oplus
Spin Liquid

$$H_{mf} = - \sum_{i,j} t_{ij} c_{i\sigma}^\dagger c_{j\sigma} - \sum_{i,j} t_{1,ij} f_{1i\sigma}^\dagger f_{1j\sigma} - \sum_i \Phi (c_{i\sigma}^\dagger f_{1i\sigma} + f_{1i\sigma}^\dagger c_{i\sigma})$$

Ya-Hui
Zhang



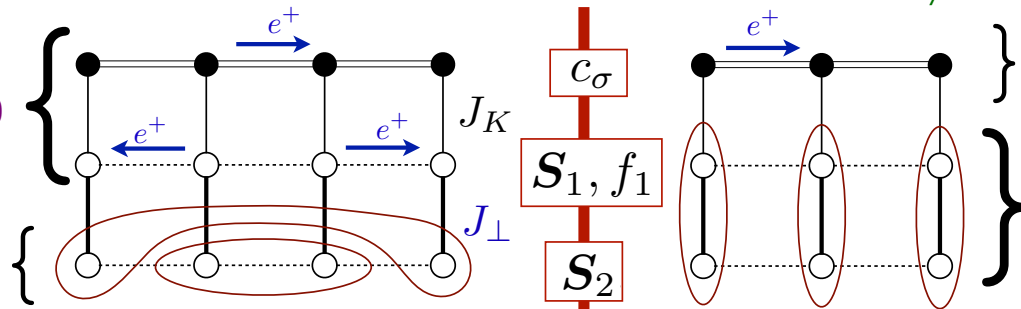
Ancilla theory of the Hubbard model

Ya-Hui Zhang and S. Sachdev,
Phys. Rev. Res. **2**, 023172 (2020)

Kondo lattice heavy
Fermi liquid.
Size $1 + p + 1$
 $= p \pmod{2}$.
Small Fermi surface!

$$\langle \Phi \rangle \neq 0$$

Spin liquid



Large
Fermi surface.
Size: $1 + p$

Trivial
insulator

FL*

$$\langle \Phi \rangle \neq 0$$

$$\langle \Phi \rangle = 0$$

FL

J_K

doping p

Pseudogap metal =
Kondo Lattice Heavy
Fermi Liquid
 \oplus
Spin Liquid

$$|FL^*\rangle = [\text{Projection onto rung singlets of } S_1, S_2] \\ \otimes |\text{Slater determinant of } (c, f_1)\rangle \\ \otimes |\text{Spin liquid of } S_2\rangle$$

Replacement for “vanilla” Gutzwiller-projected Fermi liquid in the underdoped regime

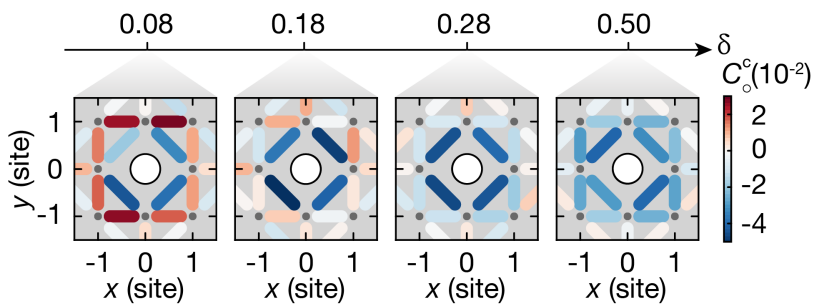
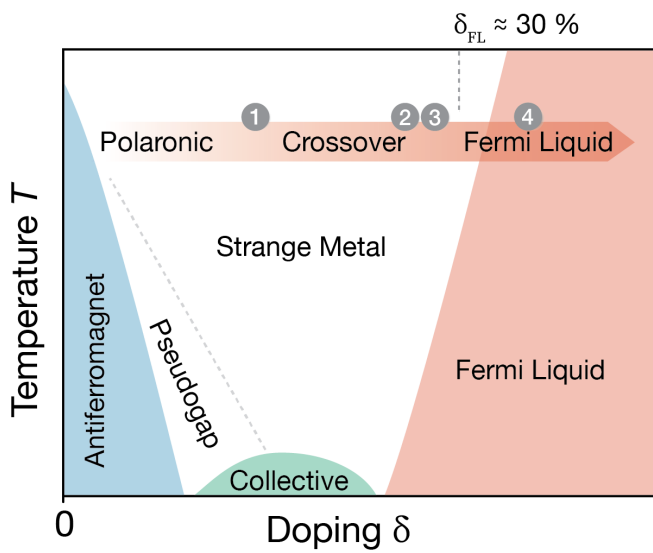


Ultracold fermionic atoms in optical lattices

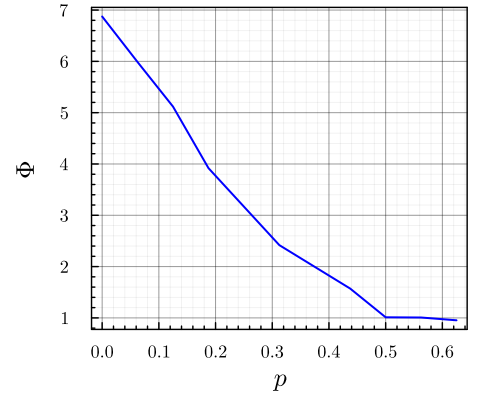
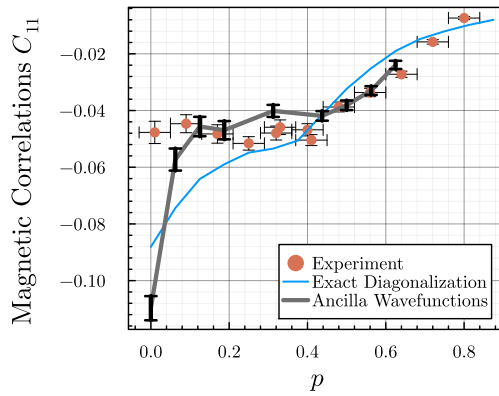
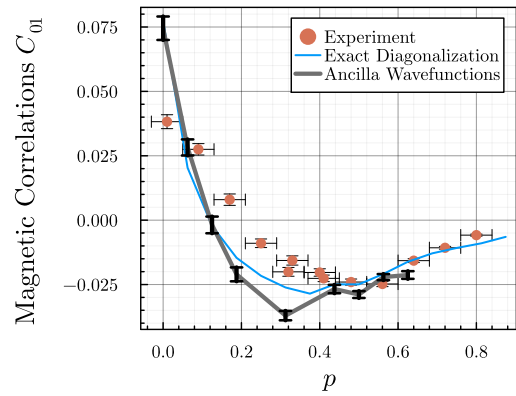
Microscopic evolution of doped Mott insulators from polaronic metal to Fermi liquid

Joannis Koepsell, Dominik Bourgund, Pimonpan Sompert, Sarah Hirthe, Annabelle Bohrdt, Yao Wang, Fabian Grusdt, Eugene Demler, Guillaume Salomon, Christian Gross, Immanuel Bloch

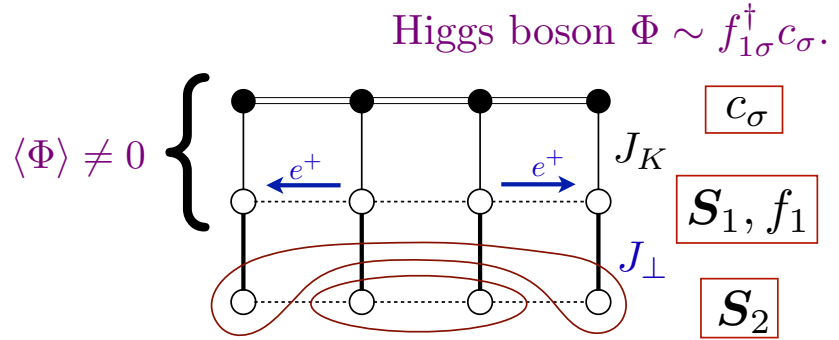
Science **374** (2021) 82



Max Planck Institute of
Quantum Optics,
Garching

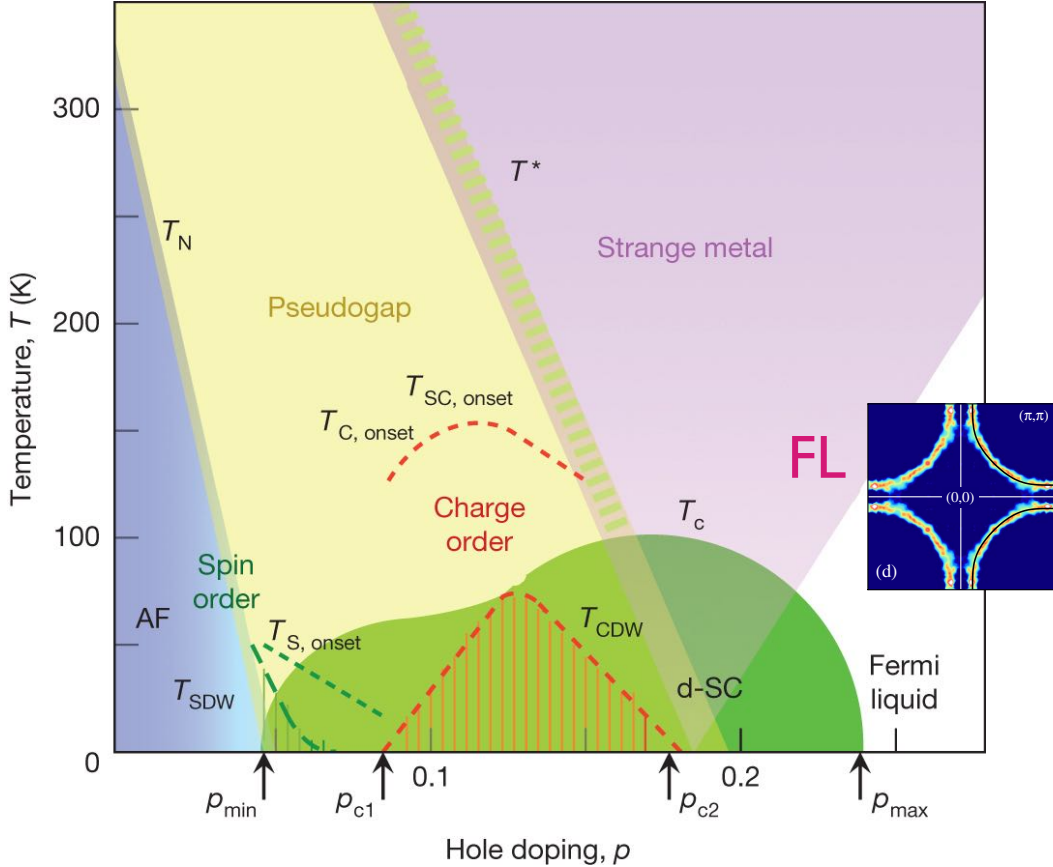


H. Shackleton and Shiwei Zhang, arXiv:2408.02190
 (Tobias Müller, Yasir Iqbal, S.S., Ronny Thomale, arXiv:2408.01492)



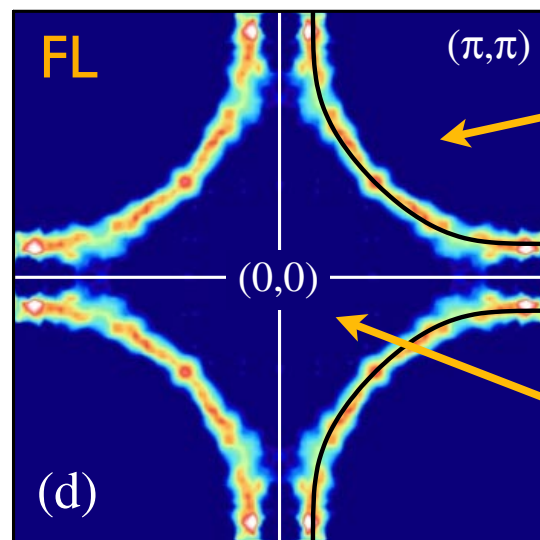
1. Spin liquids on the Kondo lattice:
non-Luttinger volume Fermi surfaces (FL*)
2. Doping square lattice spin liquids for $t \gg J$:
FL* in a single-band model
3. FL* theory of the pseudogap metal of the cuprates
4. Nodal fermionic quasiparticles in d-wave SC
5. Quantum oscillations in hole-doped cuprates

Keimer, Kivelson, Norman, Uchida, and Zaanen, *Nature* **518**, 179 (2015)



Fermi liquid
in the
overdoped metal

Photoemission at large p



$l+p$ holes

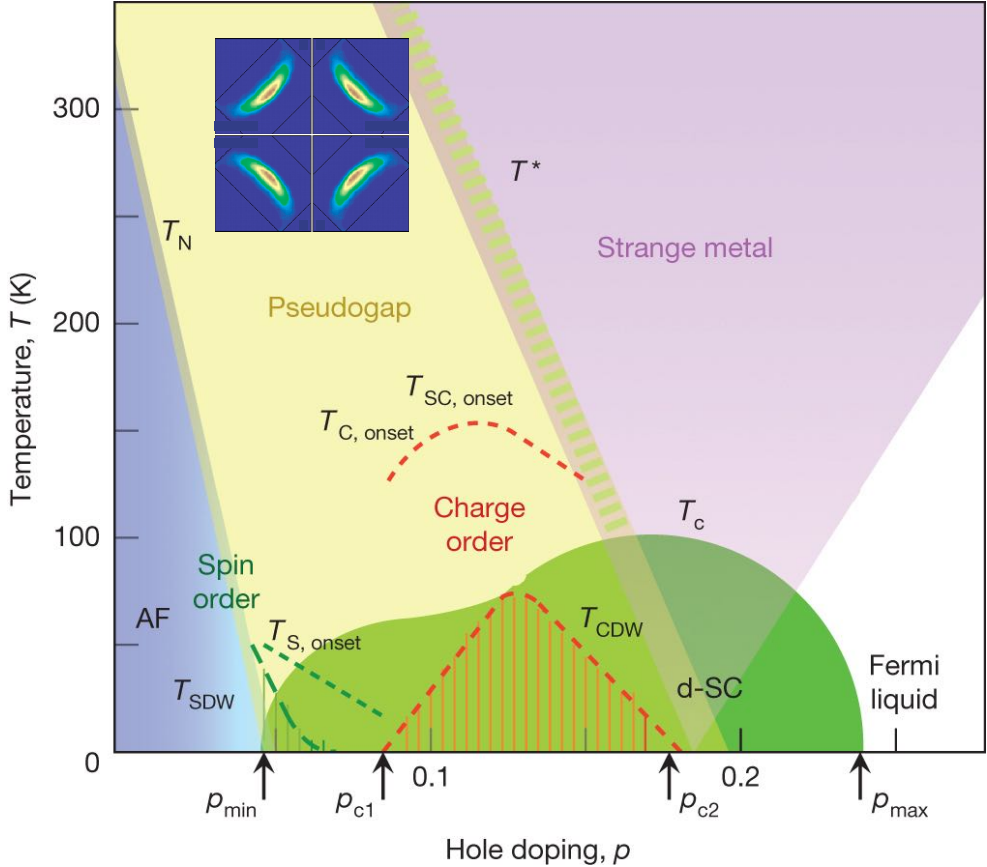
Overdoped $\text{Tl}_2\text{Ba}_2\text{CuO}_{6+\delta}$
 $T_c = 30\text{K}$

$l-p$ electrons

$l+p$ mobile holes in a filled band of 2 electrons per site

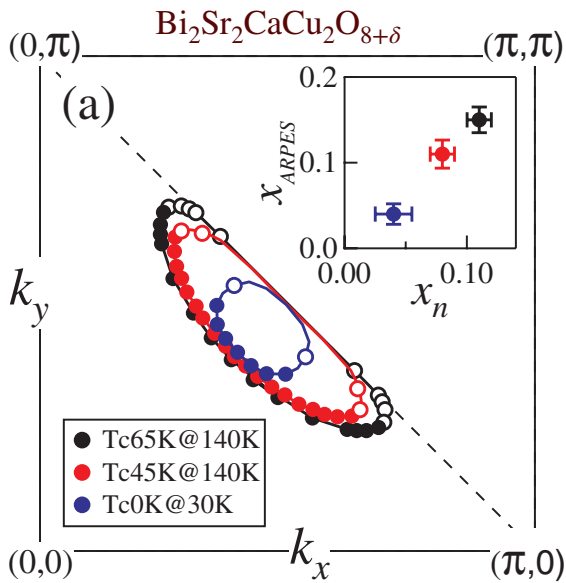
M. Platé, J. D. F. Mottershead, I. S. Elfimov, D. C. Peets, Ruixing Liang, D. A. Bonn, W. N. Hardy, S. Chiuzaian, M. Falub, M. Shi, L. Patthey, and A. Damascelli, Phys. Rev. Lett. **95**, 077001 (2005)

Keimer, Kivelson, Norman, Uchida, and Zaanen, *Nature* **518**, 179 (2015)



Pseudogap metal with “Fermi arcs”

Photoemission expts at small p

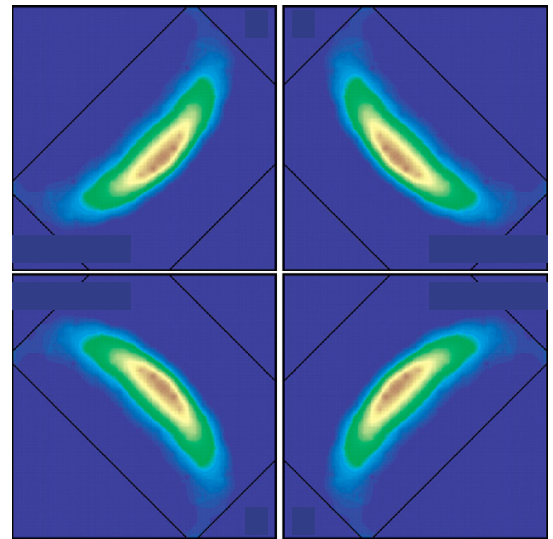


Reconstructed Fermi Surface of Underdoped $\text{Bi}_2\text{Sr}_2\text{CaCu}_2\text{O}_{8+\delta}$ Cuprate Superconductors,

H.-B. Yang, J. D. Rameau, Z.-H. Pan, G. D. Gu, P. D. Johnson, H. Claus, D. G. Hinks, and T. E. Kidd, PRL **107**, 047003 (2011).

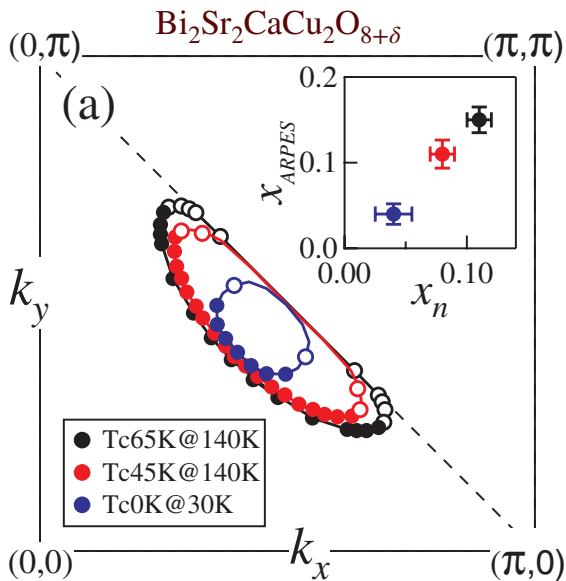
Photoemission expts at small p

$\text{Ca}_{2-x}\text{Na}_x\text{CuO}_2\text{Cl}_2$ at $x = 0.10$



Kyle M. Shen, F. Ronning, D. H. Lu, F. Baumberger, N. J. C. Ingle, W. S. Lee, W. Meevasana, Y. Kohsaka, M. Azuma, M. Takano, H. Takagi, Z.-X. Shen, Science **307**, 901 (2005)

Photoemission expts at small p



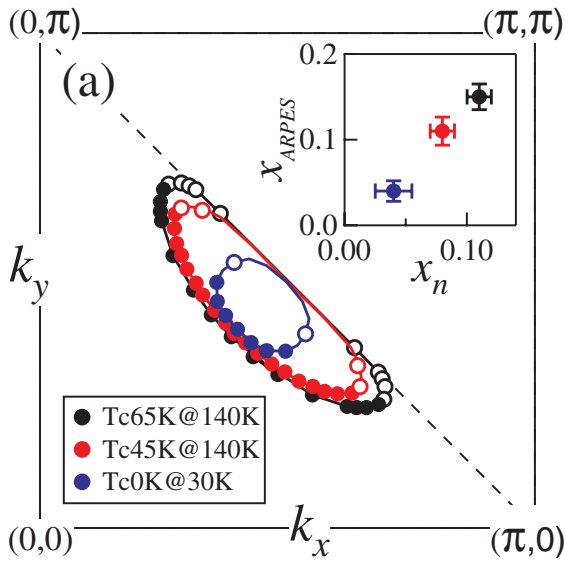
Reconstructed Fermi Surface of Underdoped $\text{Bi}_2\text{Sr}_2\text{CaCu}_2\text{O}_{8+\delta}$ Cuprate Superconductors,
 H.-B. Yang, J. D. Rameau, Z.-H. Pan, G. D. Gu,
 P. D. Johnson, H. Claus, D. G. Hinks,
 and T. E. Kidd, PRL **107**, 047003 (2011).

“DMFT” theories at small p

- Kai-Yu Yang, T. M. Rice, Fu-Chun Zhang,
Phys. Rev. B **73**, 174501 (2006).
 T. D. Stanescu and G. Kotliar,
Phys. Rev. B **74**, 125110 (2006).
 C. Berthod, T. Giamarchi, S. Biermann, and A. Georges,
Phys. Rev. Lett. **97**, 136401 (2006).
 S. Sakai, Y. Motome, M. Imada,
Phys. Rev. Lett. **102**, 056404 (2009).
 G. E. Volovik, *Physics-Uspekhi* **61**, 89 (2018).
 N. J. Robinson, P. D. Johnson, T. M. Rice, A. M. Tsvelik,
Rep. Prog. Phys. **82**, 126501 (2019).
 J. Skolimowski and M. Fabrizio,
Phys. Rev. B **106**, 045109 (2022).
 N. Wagner... A. Georges, G. Sangiovanni,
Nature Communication **14**, 7531 (2023)
 Jinchao Zhao, Gabriele La Nave, Philip Phillips,
Phys. Rev. B **108**, 165135
 Jing-Yu Zhao, Zheng-Yu Weng, arXiv:2309.11556

Green function zeros.....

Photoemission expts at small p



Reconstructed Fermi Surface of Underdoped $\text{Bi}_2\text{Sr}_2\text{CaCu}_2\text{O}_{8+\delta}$ Cuprate Superconductors,

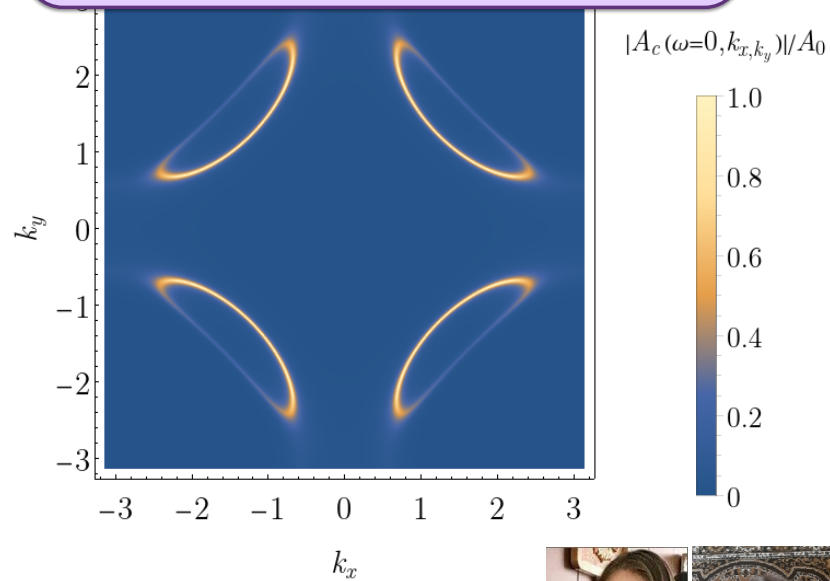
H.-B. Yang, J. D. Rameau, Z.-H. Pan, G. D. Gu,

P. D. Johnson, H. Claus, D. G. Hinks,

and T. E. Kidd, PRL **107**, 047003 (2011).

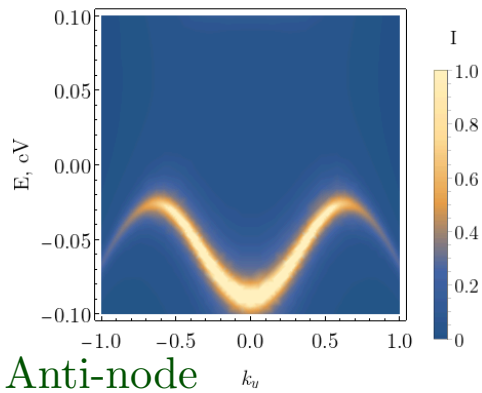
E. Mascot, A. Nikolaenko, M. Tikhanovskaya, Ya-Hui Zhang,
D. K. Morr, and S. S., PRB **105**, 075146 (2022)

Ancilla theory at small p

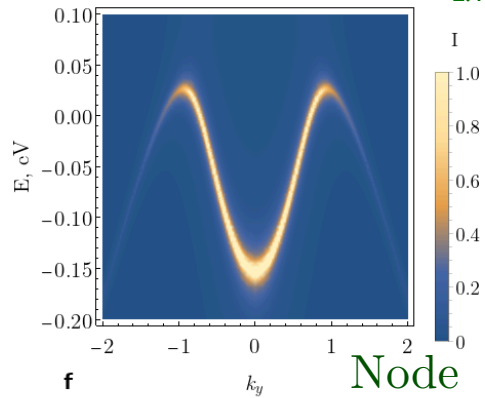


$$H_{mf} = - \sum_{i,j} t_{ij} c_{i\sigma}^\dagger c_{j\sigma} - \sum_{i,j} t_{1,ij} f_{1i\sigma}^\dagger f_{1j\sigma} - \sum_i \Phi (c_{i\sigma}^\dagger f_{1i\sigma} + f_{1i\sigma}^\dagger c_{i\sigma})$$

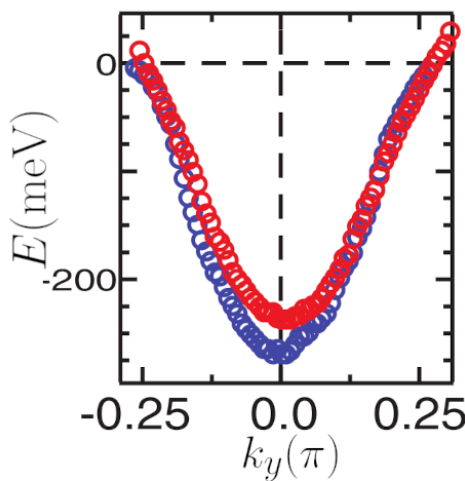
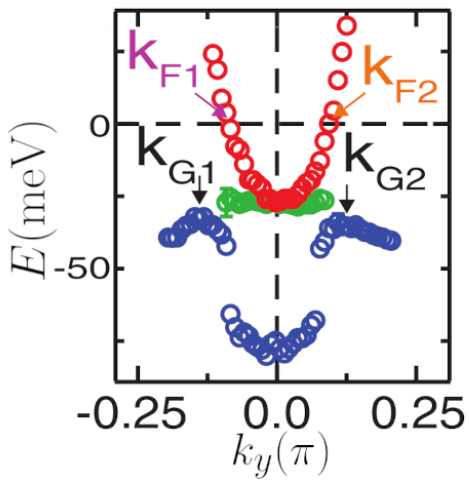




Anti-node



Node



E. Mascot, A. Nikolaenko, M. Tikhanovskaya, Ya-Hui Zhang, D. K. Morr, and S. S., PRB **105**, 075146 (2022)

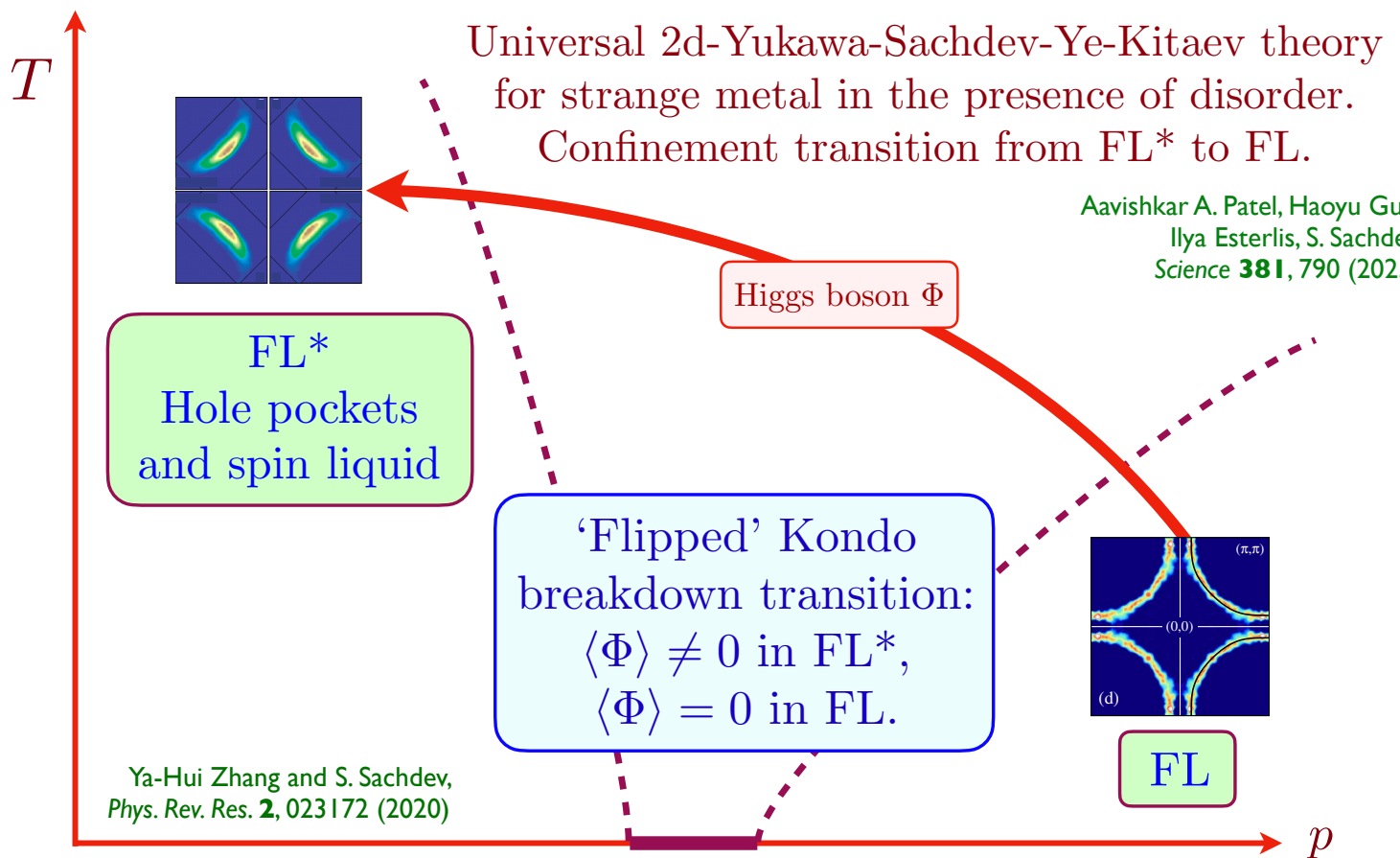
Ancilla theory of antinodal region

$$H_{mf} = - \sum_{i,j} t_{ij} c_{i\sigma}^\dagger c_{j\sigma} - \sum_{i,j} t_{1,ij} f_{1i\sigma}^\dagger f_{1j\sigma} - \sum_i \Phi (c_{i\sigma}^\dagger f_{1i\sigma} + f_{1i\sigma}^\dagger c_{i\sigma})$$

R.-H. He, M. Hashimoto, H. Karapetyan, J. D. Koralek, J. P. Hinton, J. P. Testaud, V. Nathan, Y. Yoshida, H. Yao, K. Tanaka, W. Meevasana, R. G. Moore, D. H. Lu, S. K. Mo, M. Ishikado, H. Eisaki, Z. Hussain, T. P. Devereaux, S. A. Kivelson, J. Orenstein, A. Kapitulnik, and Z.-X. Shen, Science **331**, 1579 (2011)

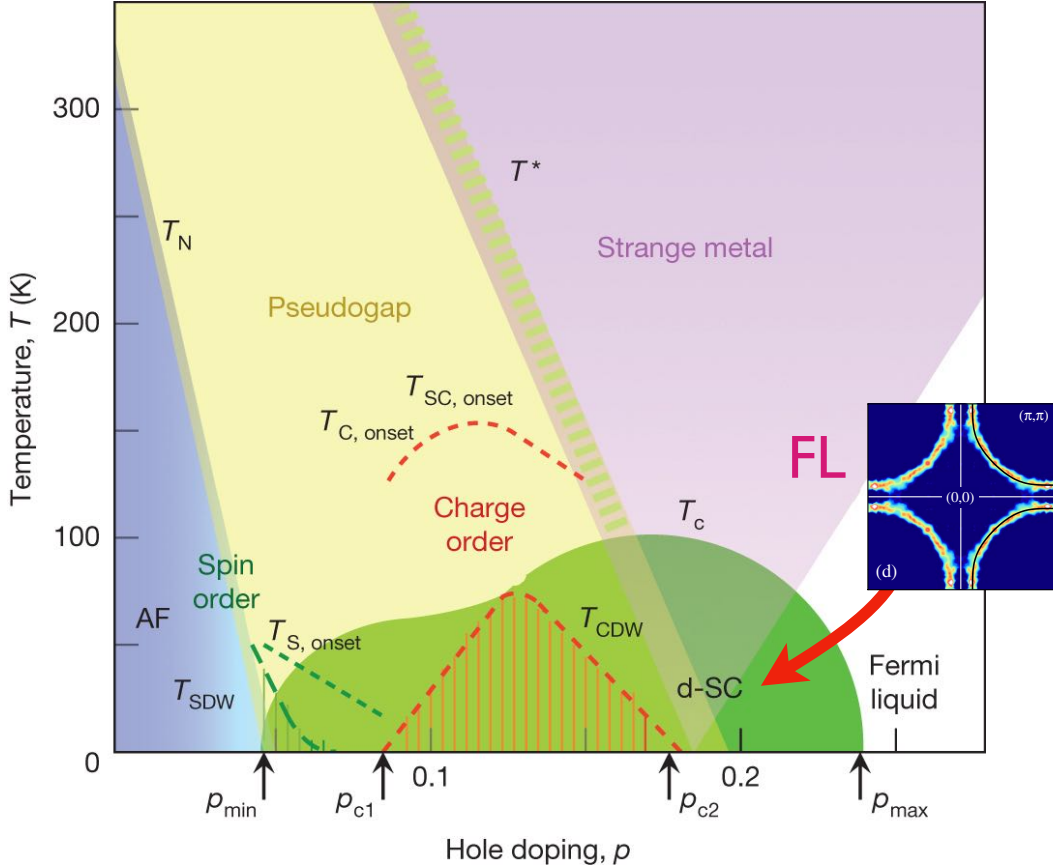
ARPES on Bi2201





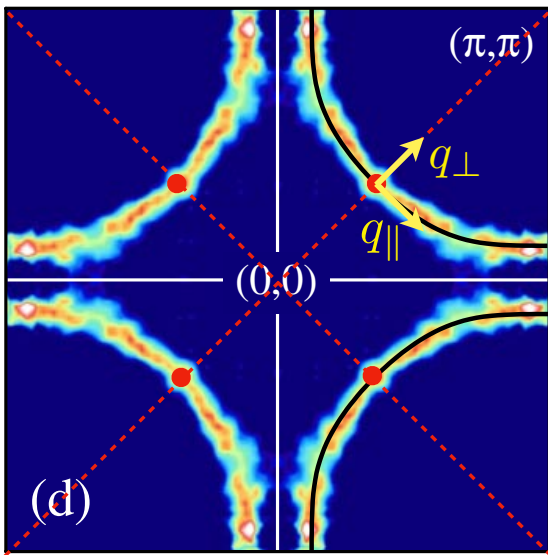
1. Spin liquids on the Kondo lattice:
non-Luttinger volume Fermi surfaces (FL*)
2. Doping square lattice spin liquids for $t \gg J$:
FL* in a single-band model
3. FL* theory of the pseudogap metal of the cuprates
4. Nodal fermionic quasiparticles in d-wave SC
5. Quantum oscillations in hole-doped cuprates

Keimer, Kivelson, Norman, Uchida, and Zaanen, *Nature* **518**, 179 (2015)



BCS-type theory of *d*-wave superconductivity (and charge order) induced by antiferromagnetic spin fluctuations.

FL → dSC



BCS/Bogoliubov quasiparticles
in a *d*-wave superconductor

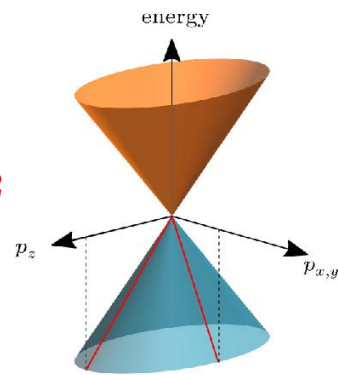
$$E_{\mathbf{k}} = (\varepsilon_{\mathbf{k}}^2 + \Delta_{\mathbf{k}}^2)^{1/2}$$

$$\Delta_{\mathbf{k}} = \Delta_0 (\cos k_x - \cos k_y)$$

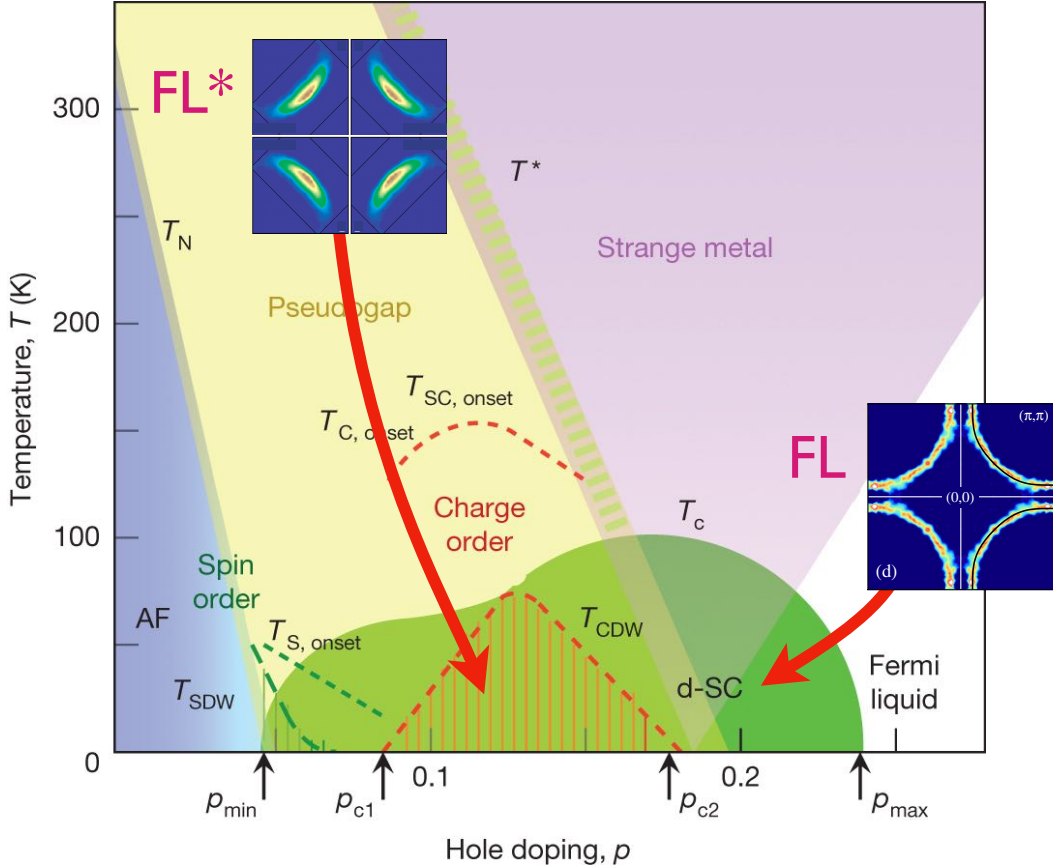
4 nodal points where

$$E_{\mathbf{k}_0 + \mathbf{q}} = \left(v_F^2 q_{\perp}^2 + v_{\Delta}^2 q_{\parallel}^2 \right)^{1/2}$$

with $v_F \gg v_{\Delta}$.



Keimer, Kivelson, Norman, Uchida, and Zaanen, *Nature* **518**, 179 (2015)



Obtain *d*-wave superconductor and charge order from a theory of *confinement* instabilities of FL*.

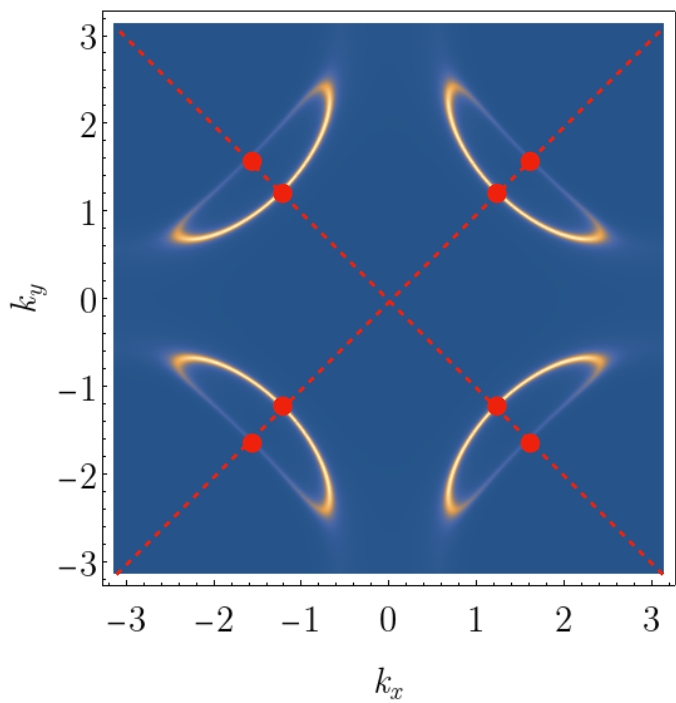
The resulting low *T* ordered states should be adiabatically connected to the corresponding states obtained from instabilities of FL.

Early work described the emergence of nodal d -wave superconductivity from a spin liquid with spinons with a Dirac dispersion: in this approach, the spinons of the spin liquid are directly transformed into the nodal Bogoliubov quasiparticles of the d -wave superconductor.

F.C. Zhang, C. Gros, T.M. Rice and H. Shiba,
Superconductor Science and Technology **1** (1988) 36
[cond-mat/0311604].

This leads to a d -wave superconductor with $v_F \approx v_\Delta$, in contrast to observations.

FL* → dSC*

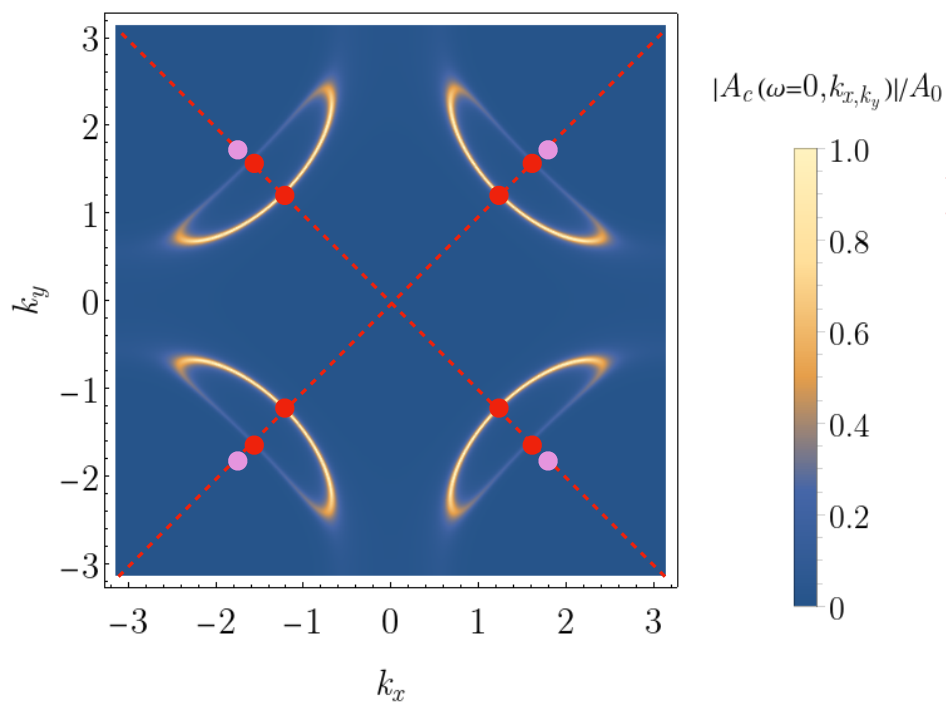


$|A_c(\omega=0, k_x, k_y)|/A_0$

$$E_{\mathbf{k}} = (\varepsilon_{\mathbf{k}}^2 + \Delta_{\mathbf{k}}^2)^{1/2}$$
$$\Delta_{\mathbf{k}} = \Delta_0 (\cos k_x - \cos k_y)$$

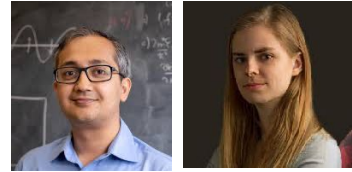
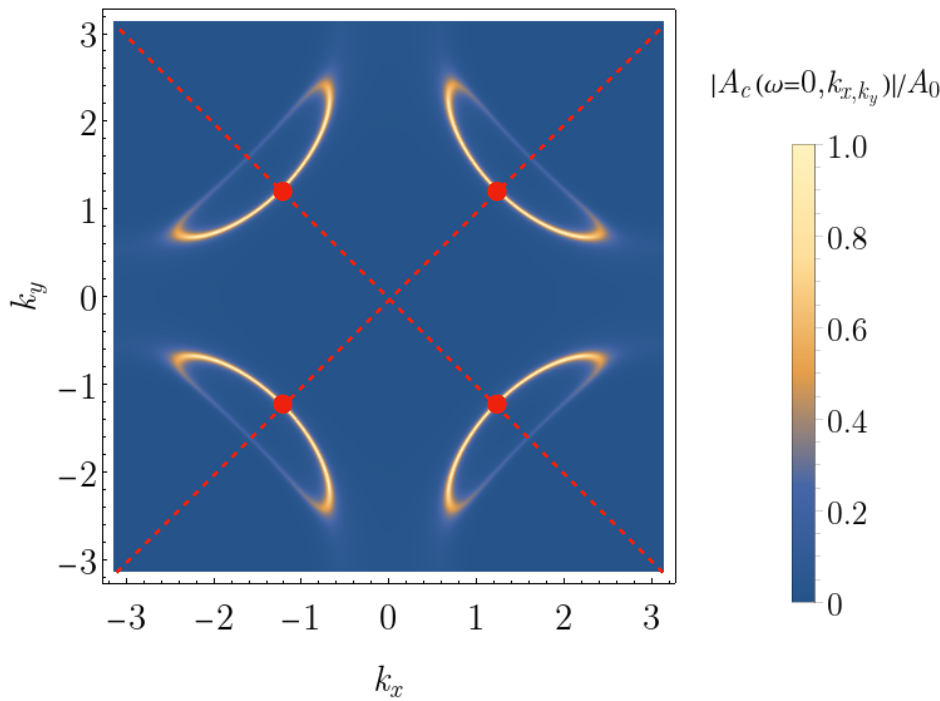
Adding *d*-wave pairing
to the hole pockets
leads to 8 nodal points of
Bogoliubov quasiparticles???

FL* \rightarrow dSC*



8 nodal points of
Bogoliubov quasiparticles
from the Fermi pockets
and
4 nodal points of
spinons from
the π -flux spin liquid

FL* → dSC

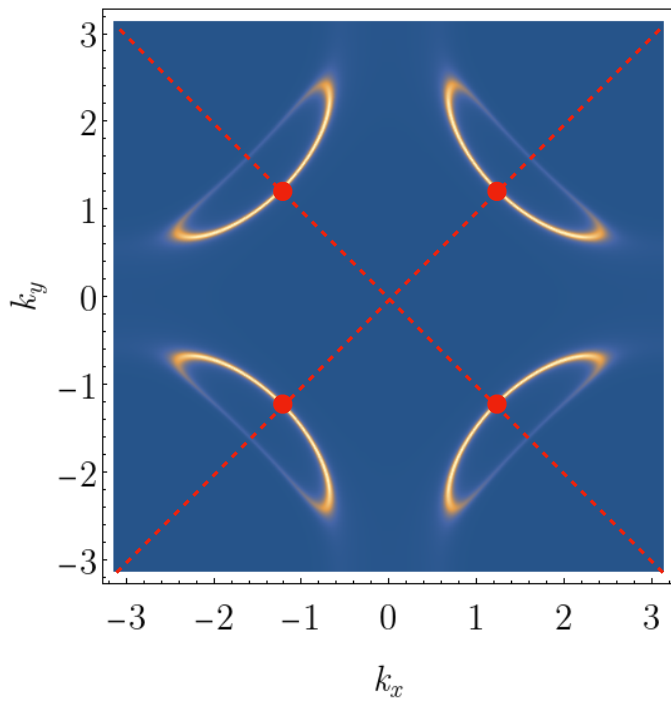


A B Higgs condensate allows spinons and Bogoliubov quasiparticles to hybridize:

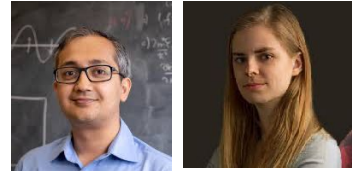
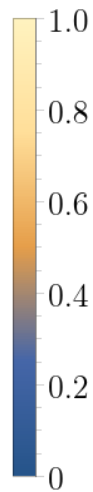
8 nodal points annihilate each other, leaving 4 nodal points with anisotropic velocities, just as in a BCS d -wave state.

Shubhayu Chatterjee and S. Sachdev,
PRB **94**, 205117 (2016)
Maine Christos and S. Sachdev,
npj Quantum Materials **9**, 4 (2024)

FL* → dSC



$|A_c(\omega=0, k_x, k_y)|/A_0$



The spinons do *not* become the Bogoliubov quasiparticles, they *annihilate* the unwanted Bogoliubov quasiparticles. This leads to a *d*-wave superconductor with 4 nodal Bogoliubov quasiparticles, with $v_F \gg v_\Delta$, consistent with observations.

Shubhayu Chatterjee and S. Sachdev,
PRB **94**, 205117 (2016)
Maine Christos and S.Sachdev,
npj Quantum Materials **9**, 4 (2024)

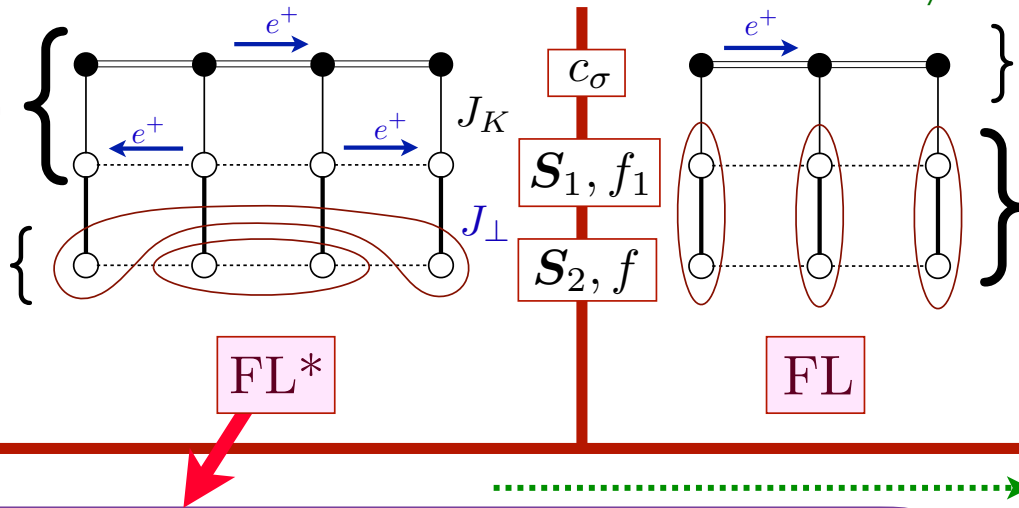
Ancilla theory of the Hubbard model

Ya-Hui Zhang and S. Sachdev,
Phys. Rev. Res. **2**, 023172 (2020)

Kondo lattice heavy
Fermi liquid.
Size $1 + p + 1$
 $= p \pmod{2}$.
Small Fermi surface!

$$\langle \Phi \rangle \neq 0$$

Spin liquid



Large
Fermi surface.
Size: $1 + p$
Trivial
insulator

J_K

FL*

FL

doping p

1. Choose Néel-VBS DQCP spin liquid: f_σ spinons moving in π -flux coupled to $SU(2)_N$ gauge field. Note $\Phi \sim f_{1\sigma}^\dagger c_\sigma$ is condensed.

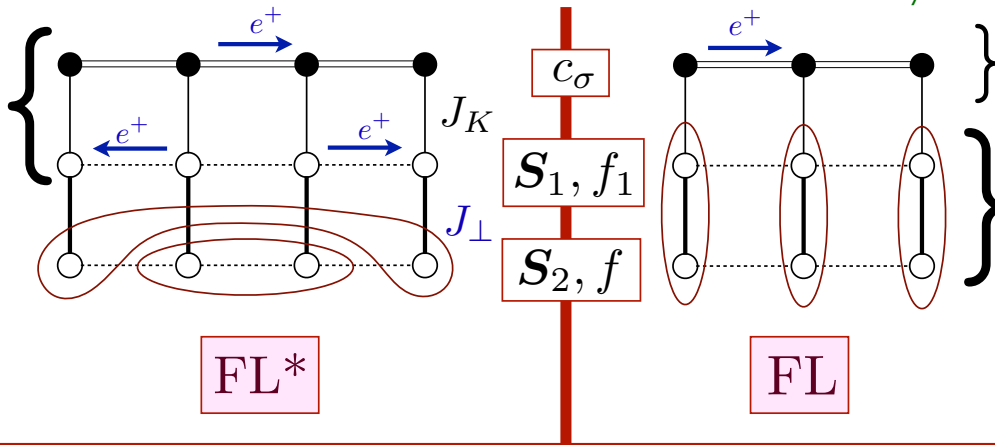
Ancilla theory of the Hubbard model

Ya-Hui Zhang and S. Sachdev,
Phys. Rev. Res. **2**, 023172 (2020)

Kondo lattice heavy
Fermi liquid.
Size $1 + p + 1$
 $= p \pmod{2}$.
Small Fermi surface!

$$\langle \Phi \rangle \neq 0$$

B



Large
Fermi surface.
Size: $1 + p$

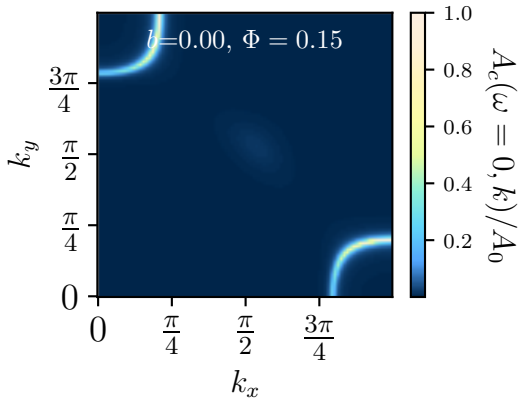
Trivial
insulator

J_K

doping p

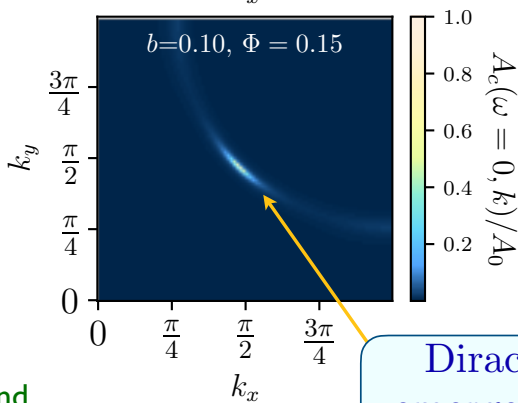
$$\begin{aligned}
 H_{\text{mf}} = & - \sum_{i,j} t_{ij} c_{i\sigma}^\dagger c_{j\sigma} - \sum_{i,j} t_{1,ij} f_{1i\sigma}^\dagger f_{1j\sigma} - \sum_{i,j} \tilde{t}_{ij} f_{i\sigma}^\dagger f_{j\sigma} \\
 & - \sum_i \Phi (c_{i\sigma}^\dagger f_{1i\sigma} + f_{1i\sigma}^\dagger c_{i\sigma}) - \sum_i \left(B_{1i}^* f_{1i\sigma}^\dagger f_{i\sigma} + B_{2i}^* \varepsilon_{\sigma\sigma'} f_{1i\sigma}^\dagger f_{i\sigma'} + \text{H.c.} \right)
 \end{aligned}$$

Electron spectral density in electron-doped cuprates



FL*

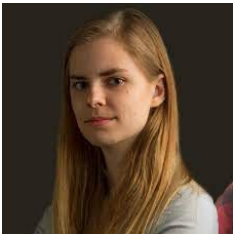
d-wave superconductor obtained by condensing charge-*e*, SU(2) fundamental boson.



dSC

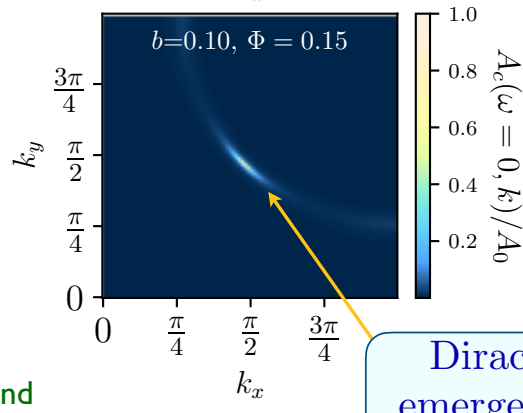
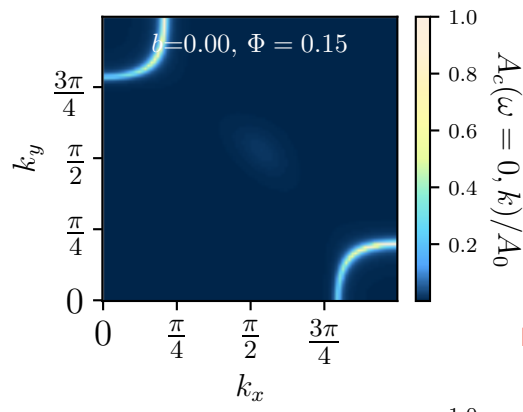
In the electron-doped case, nodes of the *d*-wave superconductor *are* remnants of the spinons of the π -flux state.

Dirac node emerges inside normal state gap

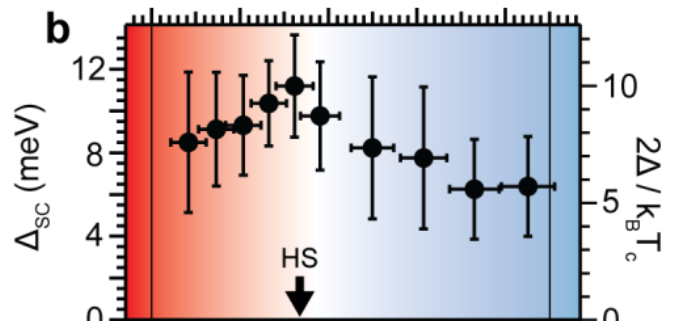


Maine Christos and S.Sachdev, npj Quantum Materials **9**, 4 (2024)

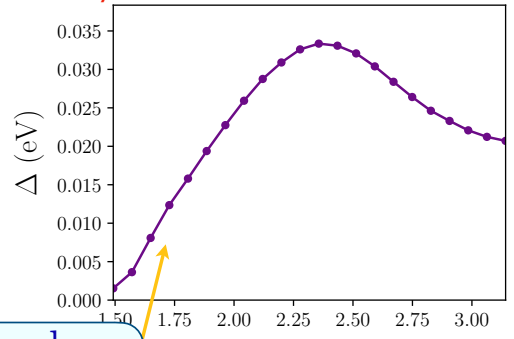
Electron spectral density in electron-doped cuprates



Dirac node emerges inside normal state gap



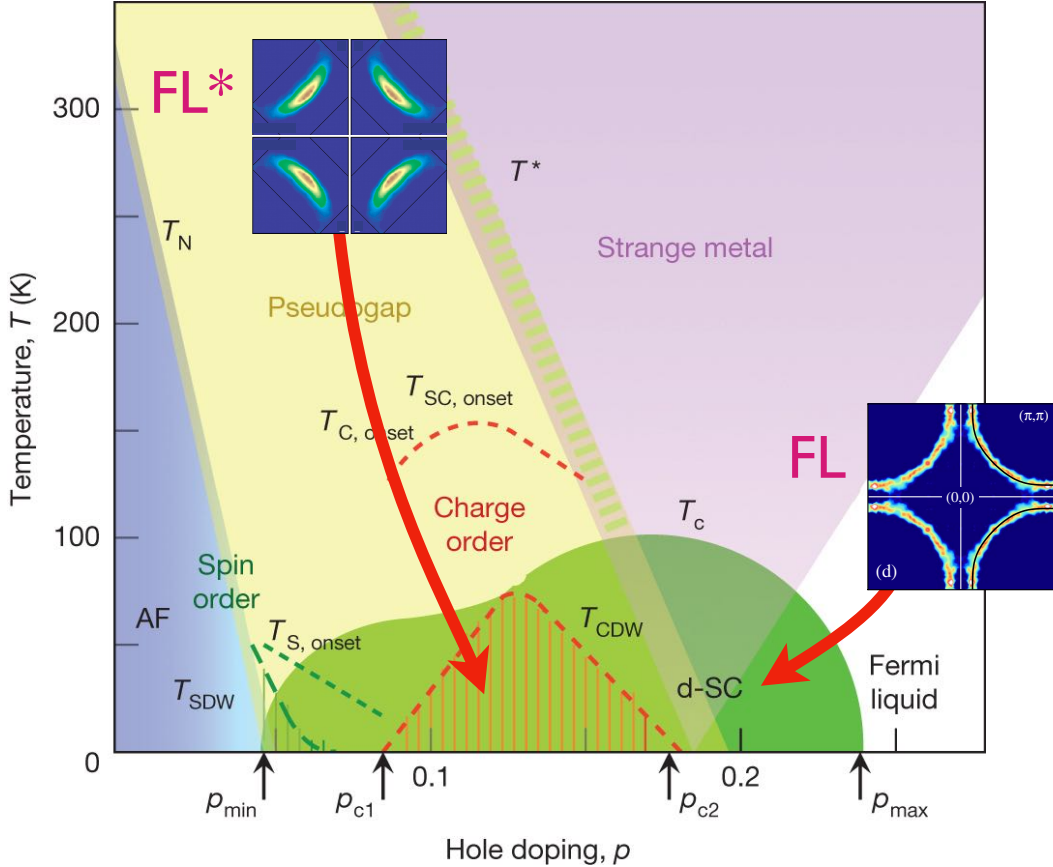
Bogoliubov Quasiparticle on the Gossamer Fermi Surface in Electron-Doped Cuprates, Ke-Jun Xu.....Z.-X. Shen, arXiv:2308.05313; Nature Physics



Maine Christos and S.Sachdev, npj Quantum Materials 9, 4 (2024)

1. Spin liquids on the Kondo lattice:
non-Luttinger volume Fermi surfaces (FL*)
2. Doping square lattice spin liquids for $t \gg J$:
FL* in a single-band model
3. FL* theory of the pseudogap metal of the cuprates
4. Nodal fermionic quasiparticles in d-wave SC
5. Quantum oscillations in hole-doped cuprates

Keimer, Kivelson, Norman, Uchida, and Zaanen, *Nature* **518**, 179 (2015)



Obtain *d*-wave superconductor and charge order from a theory of *confinement* instabilities of FL*.

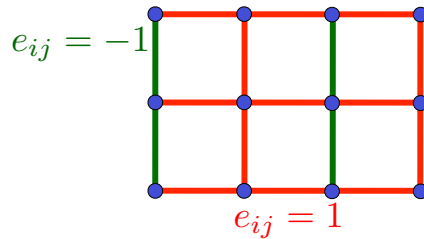
The resulting low *T* ordered states should be adiabatically connected to the corresponding states obtained from instabilities of FL.

Confinement of $SU(2)_N$ gauge theory by charge fluctuations

- Begin with the π -flux spin liquid in the fermionic spinon description.

$$H_f = iJ \sum_{\langle ij \rangle} e_{ij} \left(f_{i\sigma}^\dagger f_{j\sigma} - f_{j\sigma}^\dagger f_{i\sigma} \right) = iJ \sum_{\langle ij \rangle} e_{ij} \left(\Psi_i^\dagger U_{ij} \Psi_j - \Psi_j^\dagger U_{ji} \Psi_i \right); \quad \Psi_i = \begin{pmatrix} f_{i\uparrow} \\ f_{i\downarrow} \end{pmatrix}$$

H_f is invariant under $SU(2)$ rotations in spin and $SU(2)_N$ rotations in Nambu space; U_{ij} is the $SU(2)_N$ gauge field.



- Introduce a charge e , $SU(2)_N$ fundamental boson B_i such that the composite of B_i and Ψ_i is an electron. The projective symmetries require

$$H_B = r \sum_i B_i^\dagger B_i + iw \sum_{\langle ij \rangle} e_{ij} \left(B_i^\dagger U_{ij} B_j - B_j^\dagger U_{ji} B_i \right) + \dots$$

M. Christos, Zhu-Xi Luo, H. Shackleton, Ya-Hui Zhang, M. Scheurer, and S. S., *PNAS* **120**, e2302701120 (2023)

Confinement of $SU(2)_N$ gauge theory by charge fluctuations

$$\mathcal{L}(B) = H_B + \frac{u}{2} \sum_i \rho_i^2 + V_1 \sum_i \rho_i (\rho_{i+\hat{x}} + \rho_{i+\hat{y}}) + g \sum_{\langle ij \rangle} |\Delta_{ij}|^2 + J_1 \sum_{\langle ij \rangle} Q_{ij}^2 + K_1 \sum_{\langle ij \rangle} J_{ij}^2.$$

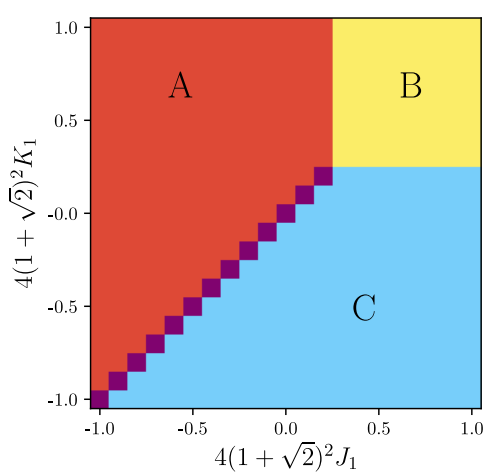
site charge density: $\langle c_{i\alpha}^\dagger c_{i\alpha} \rangle \sim \rho_i = B_i^\dagger B_i$

bond density: $\langle c_{i\alpha}^\dagger c_{j\alpha} + c_{j\alpha}^\dagger c_{i\alpha} \rangle \sim Q_{ij} = Q_{ji} = \text{Im} \left(B_i^\dagger e_{ij} U_{ij} B_j \right)$

bond current: $i \langle c_{i\alpha}^\dagger c_{j\alpha} - c_{j\alpha}^\dagger c_{i\alpha} \rangle \sim J_{ij} = -J_{ji} = \text{Re} \left(B_i^\dagger e_{ij} U_{ij} B_j \right)$

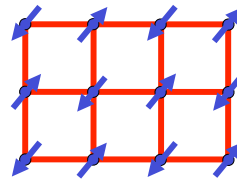
Pairing: $\langle \varepsilon_{\alpha\beta} c_{i\alpha} c_{j\beta} \rangle \sim \Delta_{ij} = \Delta_{ji} = \varepsilon_{ab} B_{ai} e_{ij} U_{ij} B_{bj}.$

Global phase diagram of $SU(2)_N$ gauge theory

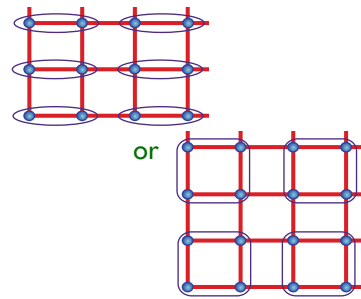


$\langle B \rangle \neq 0$

$\langle B \rangle = 0$



Confining phase:
Néel order



Confining phase:
VBS order

s

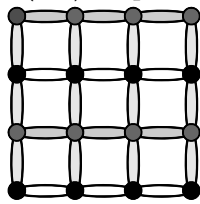
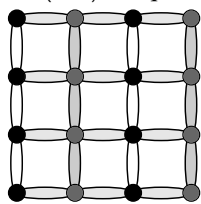
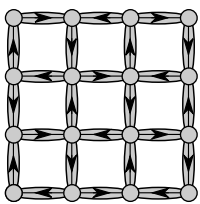
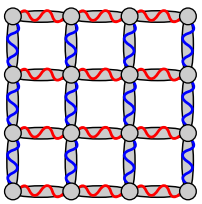
γ

Phase B
 d -wave SC

Phase C
 d -density

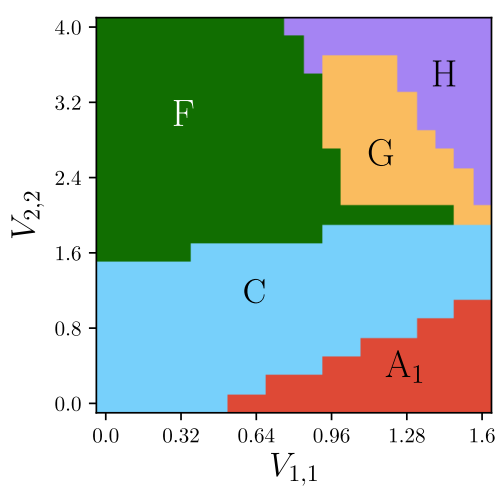
Phase A
 $(\pi, 0)$ stripe

Phase A
 $(0, \pi)$ stripe



At half filling:
possible CFT/DQCP with
 $N_f = 2$ Dirac fermions and
 $N_b = 2$ complex scalars coupled
to $SU(2)_N$ gauge field.
M. Christos, H. Shackleton, S. S.,
and Zhu-Xi Luo, PRR **6**, 033018 (2024).

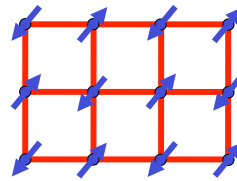
Global phase diagram of $SU(2)_N$ gauge theory



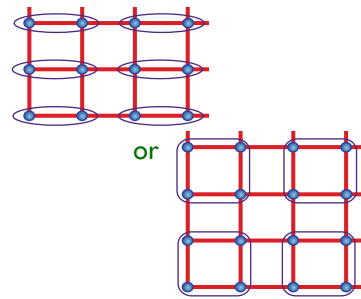
$\langle B \rangle \neq 0$

Including further-neighbor couplings in B

$\langle B \rangle = 0$



Confining phase: Néel order

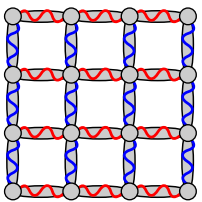


Confining phase: VBS order

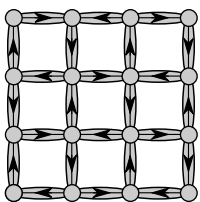
s

r

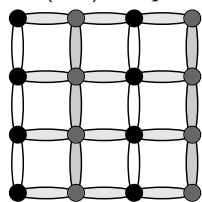
Phase B
 d -wave SC



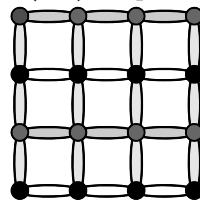
Phase C
 d -density



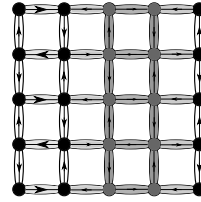
Phase A
 $(\pi, 0)$ stripe



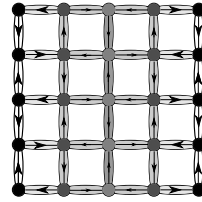
Phase A
 $(0, \pi)$ stripe



Phase F
Period 4 bond centered stripe + d -density



Phase G
Period 4 site centered stripe + d -density



M. Christos, Zhu-Xi Luo, H. Shackleton, Ya-Hui Zhang, M. Scheurer, and S. S., *PNAS* **120**, e2302701120 (2023)

C. Proust and L. Taillefer, *The Remarkable Underlying Ground States of Cuprate Superconductors*, [Annual Review of Condensed Matter Physics](#) **10**, 409 (2019),

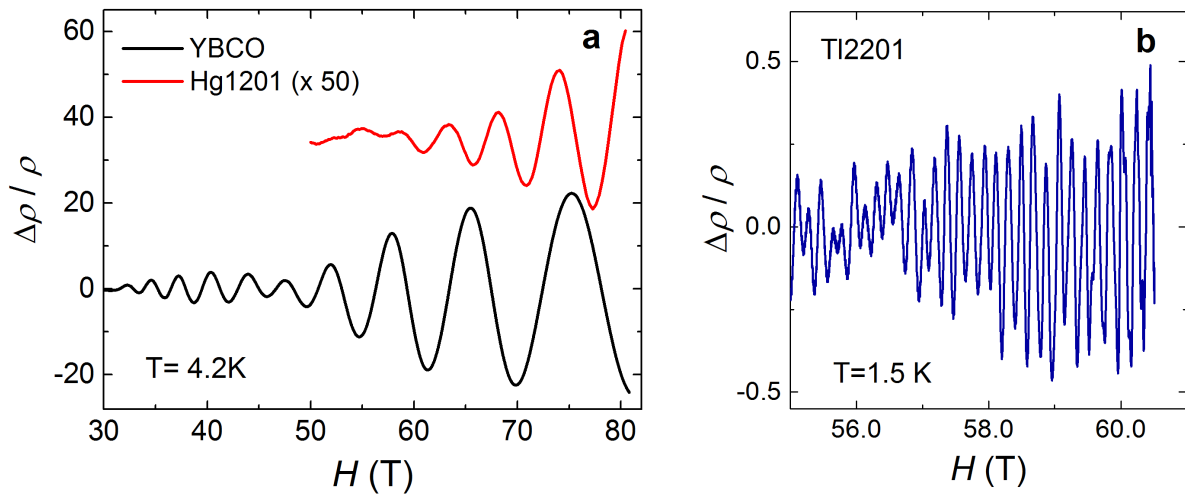


Figure 4

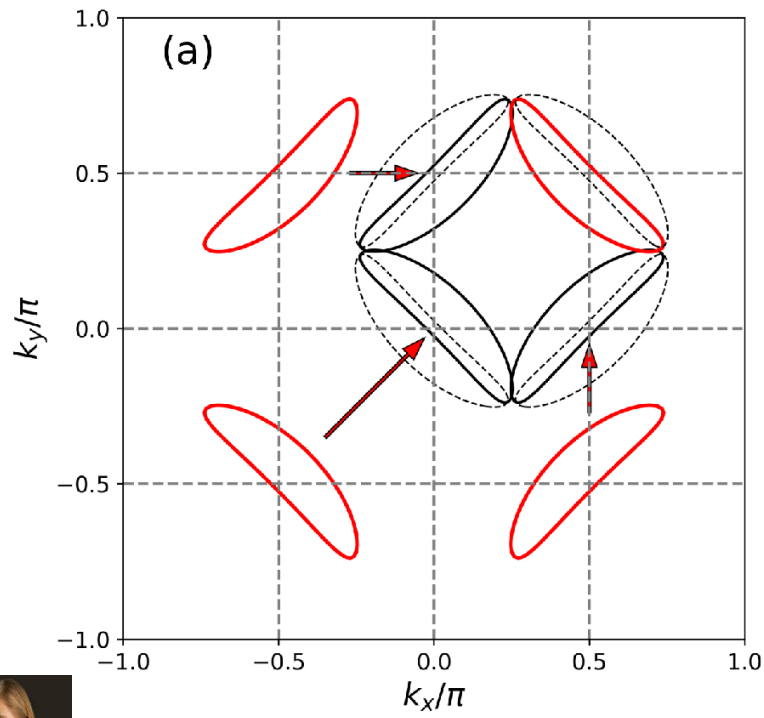
Quantum oscillations in cuprates. **a)** Underdoped YBCO ($p = 0.11$, $T_c = 62$ K) (black (22)) and Hg1201 ($p \simeq 0.1$, $T_c = 72$ K) (red (33), $\times 50$). **b)** Overdoped Tl2201 ($p \simeq 0.3$, $T_c \approx 10$ K) (28).

22. Vignolle B, et al. 2013. *C. R. Physique* 14:39–52

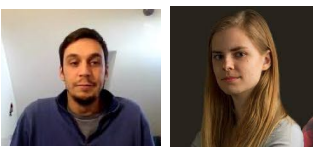
28. Vignolle B, et al. 2008. *Nature* 455:952–955

33. Barisic N, et al. 2013. *Nat. Phys.* 9:761–764

FL*



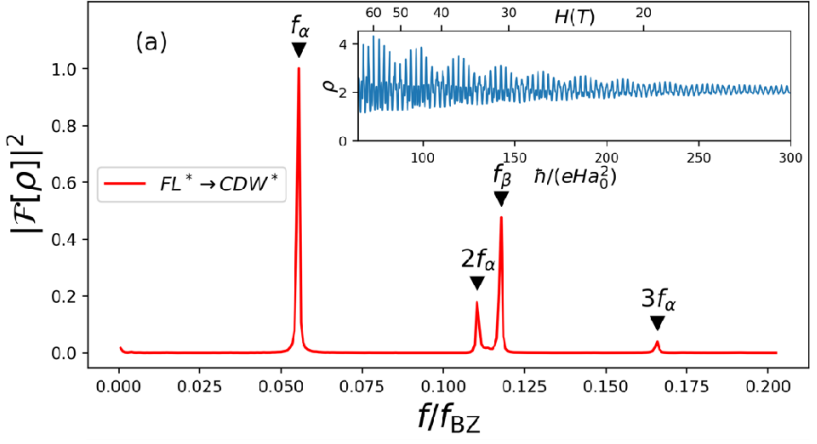
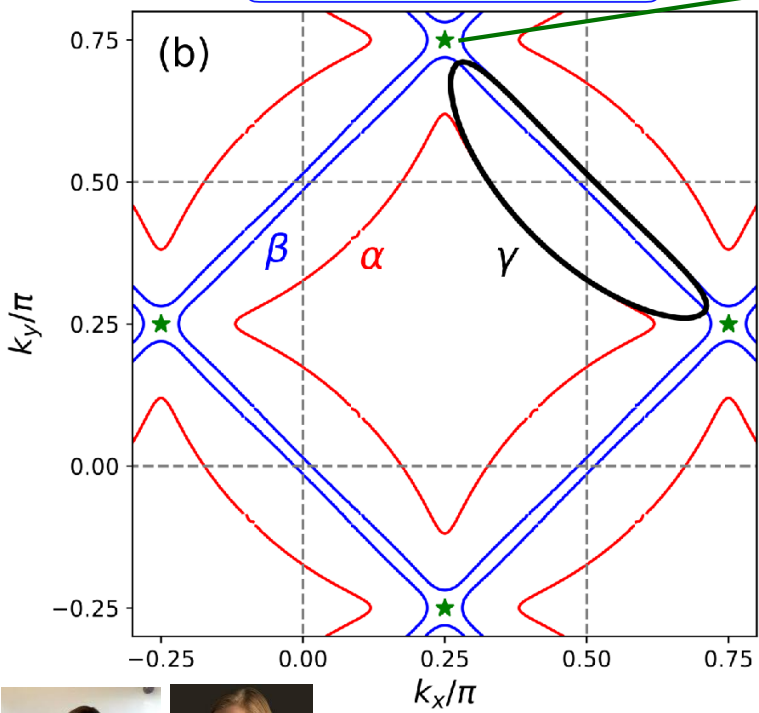
N. Harrison and S. Sebastian
electron pocket
(PRL **106**, 226402 (2011))



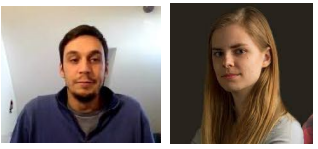
Pietro Bonetti, Maine Christos and S.S. (**BCS**), arXiv:2405.08817

FL* → CDW*

Spinon

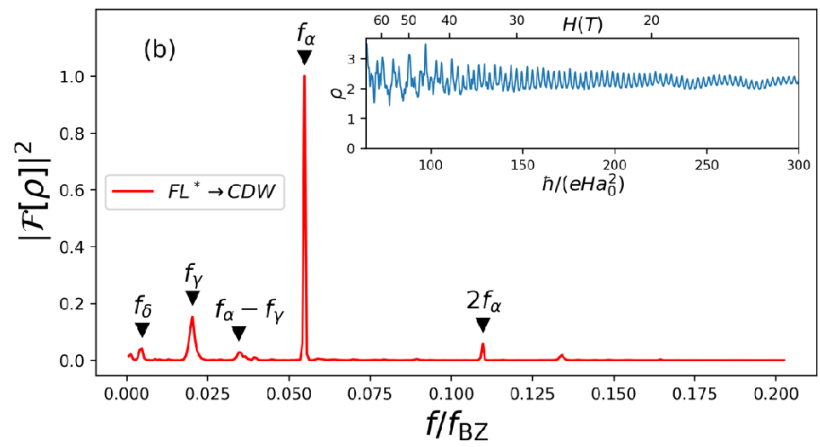
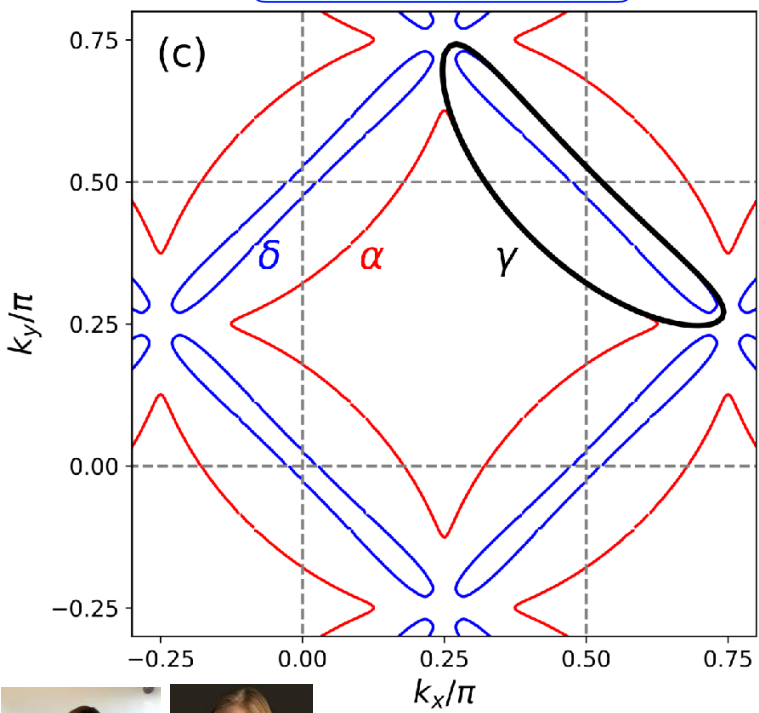


Computation does not account for spinons.
 α and β pockets
 show clear quantum oscillations.
 Long Zhang and Jia-Wei Mei,
 EPL **114**, 47008 (2016)

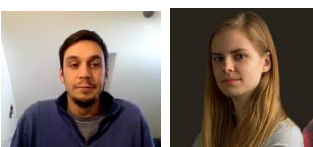


Pietro Bonetti, Maine Christos and S.S. (BCS), arXiv:2405.08817

FL* → CDW



Period 4 CDW obtained by condensing B .
 SU(2) gauge theory allows CDW with
 vanishing Δ_{ij} and J_{ij} .
 Mixing between electrons and
 spinons removes β pocket.



Pietro Bonetti, Mainie Christos and S.S. (BCS), arXiv:2405.08817

Summary

Ancilla theory of pseudogap metal with hole pockets and underlying π -flux spin liquid yields:

- Theory for Fermi arcs in hole-doped pseudogap metal.
- ADMR in pseudogap.
- Anti-nodal and nodal electronic dispersion.
- *d*-wave superconductor with 4 nodal points in both electron- and hole-doped cuprates.
- Near-equality of dSC and charge order onset temperatures
- Multipoint correlators measured by cold atom experiments
- Theory for strange metal in the crossover from FL* to FL
- Theory for quantum oscillations in hole-doped cuprates

Appendix C: The SYK model

SYK model

The Sachdev-Ye-Kitaev (SYK) model

(See also: the “2-Body Random Ensemble” in nuclear physics; did not obtain the large N limit;
T.A. Brody, J. Flores, J.B. French, P.A. Mello, A. Pandey, and S.S.M. Wong, Rev. Mod. Phys. **53**, 385 (1981))

$$\mathcal{H} = \frac{1}{(2N)^{3/2}} \sum_{\alpha, \beta, \gamma, \delta=1}^N U_{\alpha\beta; \gamma\delta} c_{\alpha}^{\dagger} c_{\beta}^{\dagger} c_{\gamma} c_{\delta} - \mu \sum_{\alpha} c_{\alpha}^{\dagger} c_{\alpha}$$

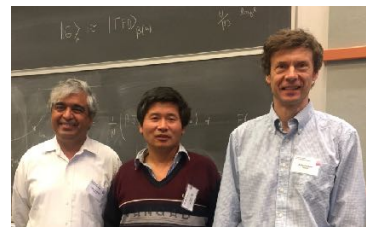
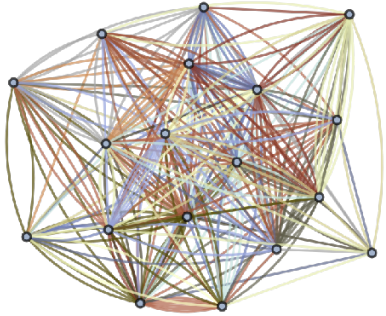
$$c_{\alpha} c_{\beta} + c_{\beta} c_{\alpha} = 0 \quad , \quad c_{\alpha} c_{\beta}^{\dagger} + c_{\beta}^{\dagger} c_{\alpha} = \delta_{\alpha\beta}$$

$$\mathcal{Q} = \frac{1}{N} \sum_{\alpha} c_{\alpha}^{\dagger} c_{\alpha}; \quad [\mathcal{H}, \mathcal{Q}] = 0; \quad 0 \leq \mathcal{Q} \leq 1$$

$U_{\alpha\beta; \gamma\delta}$ are independent random variables with $\overline{U_{\alpha\beta; \gamma\delta}} = 0$ and $\overline{|U_{\alpha\beta; \gamma\delta}|^2} = U^2$
 $N \rightarrow \infty$ yields critical strange metal.

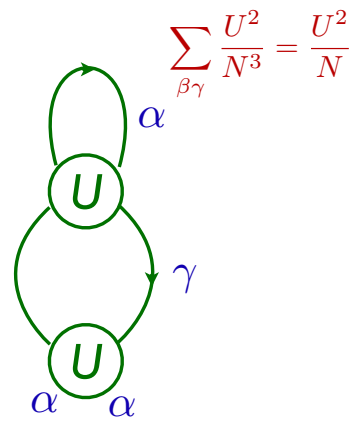
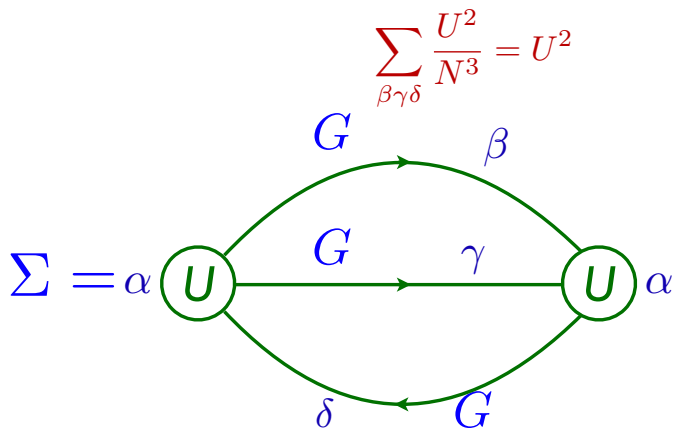
S. Sachdev and J. Ye, PRL **70**, 3339 (1993)

A. Kitaev, unpublished; S. Sachdev, PRX **5**, 041025 (2015)



The Sachdev-Ye-Kitaev (SYK) model

Feynman graph expansion in $U_{\alpha\beta;\gamma\delta}$, and graph-by-graph average



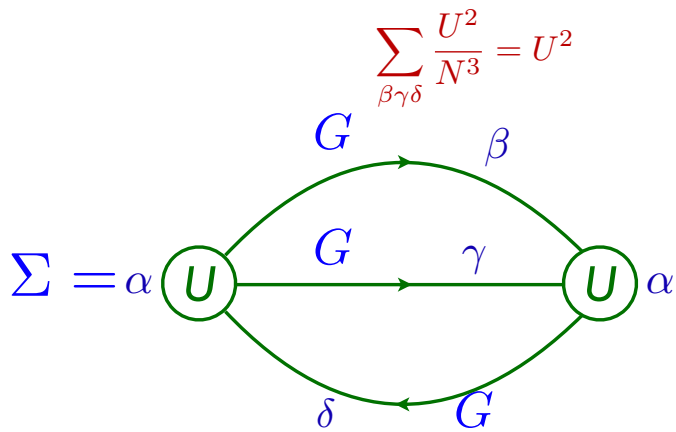
S. Sachdev and J. Ye,
PRL **70**, 3339 (1993)



The Sachdev-Ye-Kitaev (SYK) model

Feynman graph expansion in $U_{\alpha\beta;\gamma\delta}$, and graph-by-graph average, yields exact equations in the large N limit:

$$G(i\omega) = \frac{1}{i\omega + \mu - \Sigma(i\omega)} \quad , \quad \Sigma(\tau) = -U^2 G^2(\tau) G(-\tau)$$
$$G(\tau = 0^-) = \mathcal{Q}.$$



S. Sachdev and J. Ye,
PRL **70**, 3339 (1993)



The complex SYK model

Solution of these equations, and of the free energy, yields universal results for the SYK model:

- At long times, and at $T = 0$, $G(\tau) \sim |\tau|^{-1/2}$ (\Rightarrow indication there are no quasiparticles)
- At general charge \mathcal{Q} , there is a particle-hole asymmetry determined by a parameter \mathcal{E} :

$$G(\tau) \sim \begin{cases} -\tau^{-1/2} & \tau > 0 \\ e^{-2\pi\mathcal{E}}(-\tau)^{-1/2} & \tau < 0 \end{cases}, \quad T = 0$$

S. Sachdev and J. Ye,
PRL **70**, 3339 (1993)

- There is a universal ‘Luttinger relation’ between $-\infty < \mathcal{E} < \infty$ and the total charge $0 < \mathcal{Q} < 1$

$$e^{2\pi\mathcal{E}} = \frac{\sin(\pi/4 + \theta)}{\sin(\pi/4 - \theta)}$$
$$\mathcal{Q} = \frac{1}{2} - \frac{\theta}{\pi} - \frac{\sin(2\theta)}{4}$$

A. Georges, O. Parcollet,
and S. Sachdev,
PRB **63**, 134406 (2001)

The SYK model

Consequences of emergent time-reparameterization and conformal symmetries
in low-energy theory in 0+1 spacetime dimensions:

1. Planckian dynamics!

$$\tau(\omega) = \frac{\hbar}{k_B T} F\left(\frac{\hbar\omega}{k_B T}\right)$$

S. Sachdev and J. Ye, PRL **70**, 3339 (1993)

A. Georges and O. Parcollet PRB **59**, 5341 (1999)

The complex SYK model

$$G_*(\tau) = -C \frac{e^{-2\pi\mathcal{E}T\tau}}{\sqrt{1 + e^{-4\pi\mathcal{E}}}} \left(\frac{T}{\sin(\pi T\tau)} \right)^{1/2}.$$

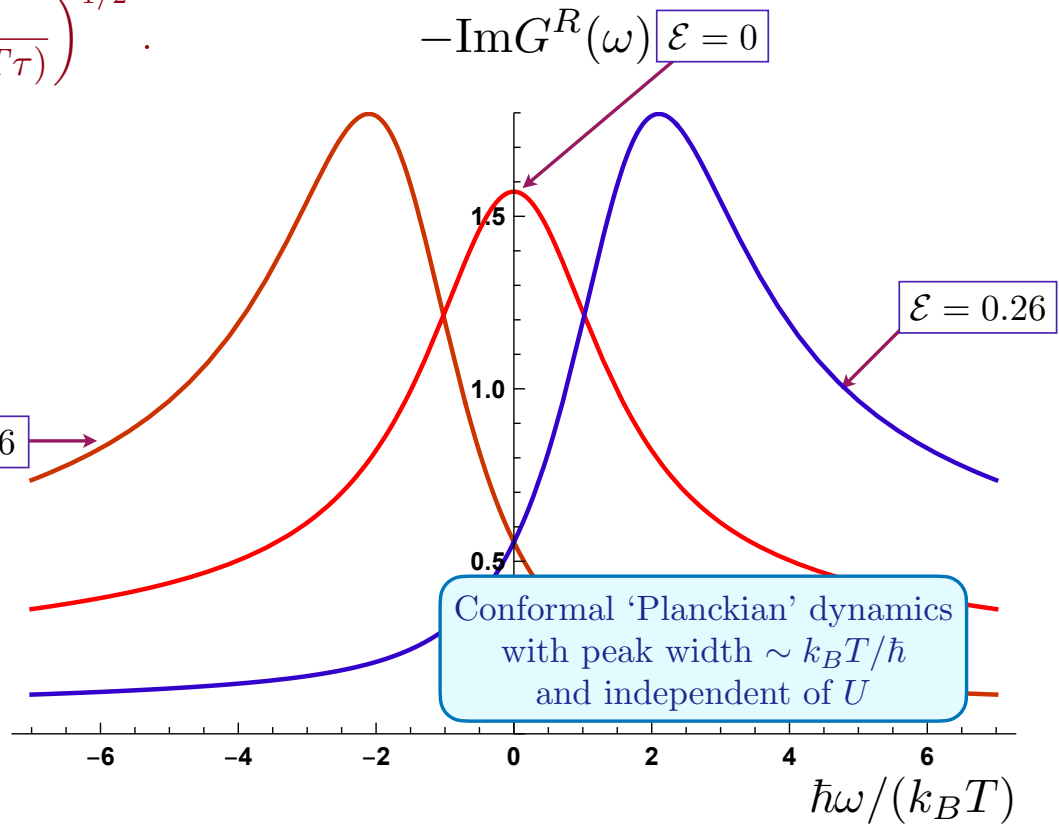
$$G_*^R(\omega) = \frac{-iC e^{-i\theta} \Gamma\left(\frac{1}{4} - \frac{i\omega}{2\pi T} + i\mathcal{E}\right)}{(2\pi T)^{1/2} \Gamma\left(\frac{3}{4} - \frac{i\omega}{2\pi T} + i\mathcal{E}\right)}.$$

$$e^{2\pi\mathcal{E}} = \frac{\sin(\pi/4 + \theta)}{\sin(\pi/4 - \theta)}$$

$$C = \left(\frac{\pi}{U^2 \cos(2\theta)} \right)^{1/4}$$

\mathcal{E} is a known function of \mathcal{Q}
(Luttinger relation)

S. Sachdev and J. Ye, PRL **70**, 3339 (1993)
A. Georges and O. Parcollet PRB **59**, 5341 (1999)
S. Sachdev, PRX **5**, 041025 (2015)



The SYK model

Consequences of emergent time-reparameterization and conformal symmetries in low-energy theory in 0+1 spacetime dimensions:

1. Planckian dynamics!

$$\tau(\omega) = \frac{\hbar}{k_B T} F\left(\frac{\hbar\omega}{k_B T}\right)$$



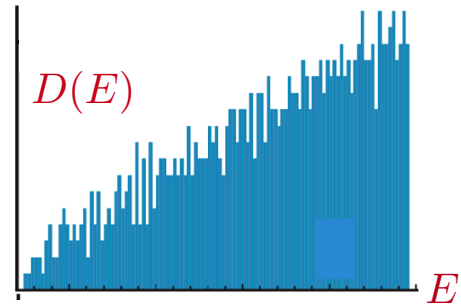
S. Sachdev and J. Ye, PRL **70**, 3339 (1993)

A. Georges and O. Parcollet PRB **59**, 5341 (1999)

2. Zero temperature entropy without exponential ground state degeneracy!

$$\lim_{T \rightarrow 0} \lim_{N \rightarrow \infty} \frac{1}{N} S(T) = s_0 \quad , \quad D(E \rightarrow 0) \sim e^{N s_0} f_{\text{smooth}}(E)$$

$$s_0 = 0.46484769917080510749\dots \text{ for } Q = 1/2.$$



A. Georges, O. Parcollet, and S. Sachdev, PRB **63**, 134406 (2001)

Yukawa-SYK model

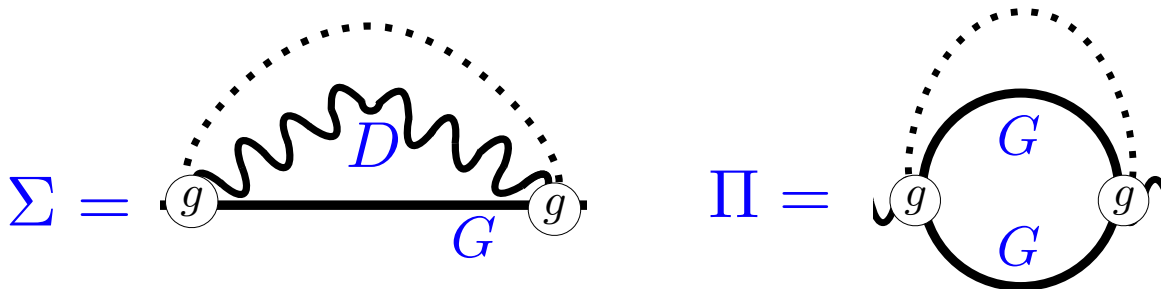
Yukawa-SYK model

$$\mathcal{H} = -\mu \sum_i \psi_i^\dagger \psi_i + \sum_\ell \frac{1}{2} (\pi_\ell^2 + \omega_0^2 \phi_\ell^2) + \frac{1}{N} \sum_{ij\ell} g_{ij\ell} \psi_i^\dagger \psi_j \phi_\ell$$

with $g_{ij\ell}$ independent random numbers with zero mean. The large N equations for the Green's functions and self energies of the fermions (G, Σ) and bosons (D, Π) are

$$G(i\omega_n) = \frac{1}{i\omega_n + \mu - \Sigma(i\omega_n)} \quad , \quad D(i\omega_n) = \frac{1}{\omega_n^2 + \omega_0^2 - \Pi(i\omega_n)}$$

$$\Sigma(\tau) = g^2 G(\tau) D(\tau) \quad , \quad \Pi(\tau) = -g^2 G(\tau) G(-\tau)$$



I. Esterlis and J. Schmalian,
PRB **100**, 115132 (2019)
See also Yuxuan Wang,
PRL **124**, 017002 (2020)

Yukawa-SYK model

$$\mathcal{H} = -\mu \sum_i \psi_i^\dagger \psi_i + \sum_\ell \frac{1}{2} (\pi_\ell^2 + \omega_0^2 \phi_\ell^2) + \frac{1}{N} \sum_{ij\ell} g_{ij\ell} \psi_i^\dagger \psi_j \phi_\ell$$

with $g_{ij\ell}$ independent random numbers with zero mean. The large N equations for the Green's functions and self energies of the fermions (G, Σ) and bosons (D, Π) are

$$G(i\omega_n) = \frac{1}{i\omega_n + \mu - \Sigma(i\omega_n)} \quad , \quad D(i\omega_n) = \frac{1}{\omega_n^2 + \omega_0^2 - \Pi(i\omega_n)}$$

$$\Sigma(\tau) = g^2 G(\tau) D(\tau) \quad , \quad \Pi(\tau) = -g^2 G(\tau) G(-\tau)$$

Make the low frequency ansatz

$$G(i\omega) \sim -i \operatorname{sgn}(\omega) |\omega|^{-(1-2\Delta)} \quad , \quad D(i\omega) \sim |\omega|^{1-4\Delta} \quad , \quad \frac{1}{4} < \Delta < \frac{1}{2}$$

A consistent solution exists for

$$\frac{4\Delta - 1}{2(2\Delta - 1)[\sec(2\pi\Delta) - 1]} = 1 \quad , \quad \Delta = 0.42037\dots$$

I. Esterlis and J. Schmalian,
PRB **100**, 115132 (2019)
See also Yuxuan Wang,
PRL **124**, 017002 (2020)

The SYK model and black holes

Semiclassical connection first proposed by S.S. in Physical Review Letters **105**, 151602 (2010): SYK model and charged black holes exhibit Planckian dynamics and zero temperature entropy.

Fully quantum connection established in 2015 by A. Kitaev, J. Maldacena, D. Stanford....

Black Holes Obey Information-Emission Limits

April 22, 2021 • *Physics 14*, s47 –Christopher Crockett

G. Carullo, D. Laghi, J. Veitch, W. Del Pozzo, *Phys. Rev. Lett.* **126**, 161102 (2021)

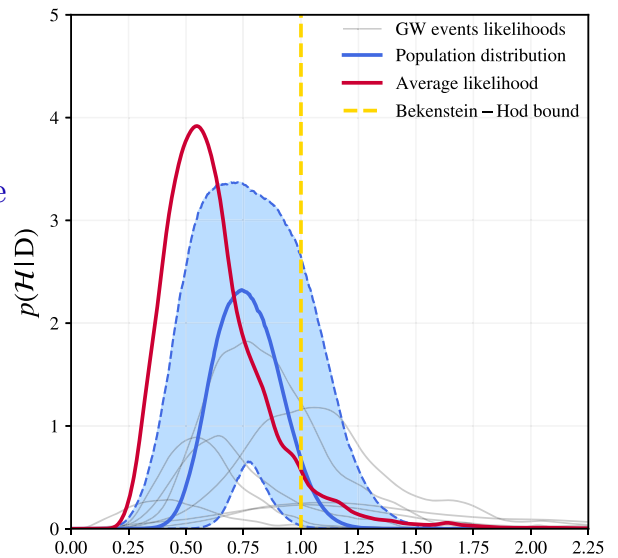
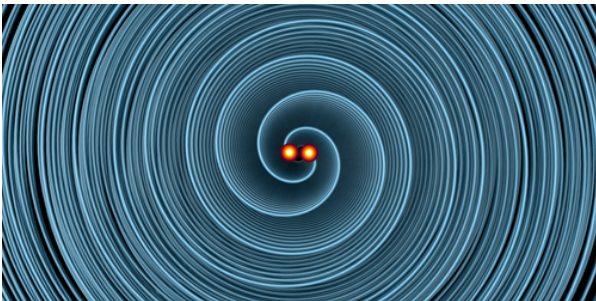
An analysis of the gravitational waves emitted from black hole mergers confirms that black holes are the fastest known information dissipaters.

Planckian dynamics!

$$\tau(\omega) = \frac{\hbar}{k_B T} F\left(\frac{\hbar\omega}{k_B T}\right)$$

Gravity wave observations of 8 different black holes show a relaxation time

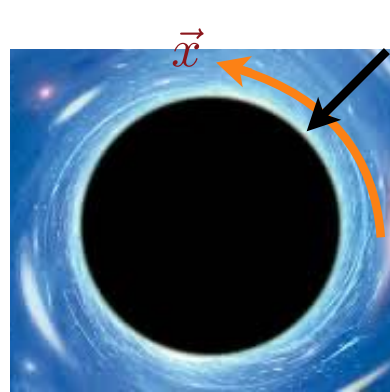
$$\tau \sim \frac{\hbar}{k_B T}$$



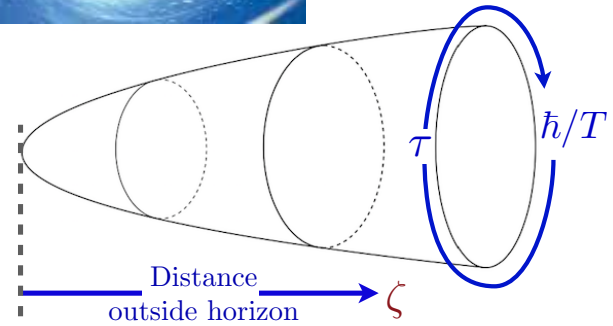
$$\mathcal{H} = \frac{1}{\pi} \frac{\hbar/\tau}{k_B T}$$

Thermodynamics of quantum black holes with charge Q :

$$\mathcal{Z}(Q, T) = \int \mathcal{D}g_{\mu\nu} \mathcal{D}A_{\mu} \exp \left(-\frac{1}{\hbar} I_{\text{Einstein gravity+Maxwell EM}}^{(3+1)}[g_{\mu\nu}, A_{\mu}] \right)$$



A. Chamblin, R. Emparan,
C.V. Johnson, and R.C. Myers,
PRD **60**, 064018 (1999)



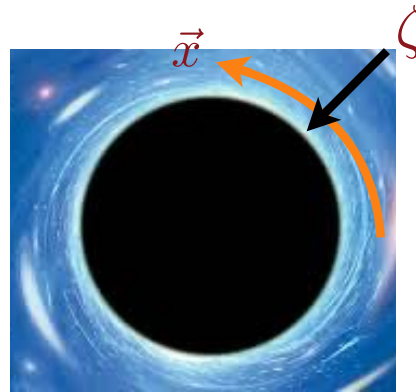
Thermodynamics of quantum black holes with charge Q :

$$\mathcal{Z}(Q, T) = \int \mathcal{D}g_{\mu\nu} \mathcal{D}A_\mu \exp \left(-\frac{1}{\hbar} I_{\text{Einstein gravity+Maxwell EM}}^{(3+1)}[g_{\mu\nu}, A_\mu] \right)$$

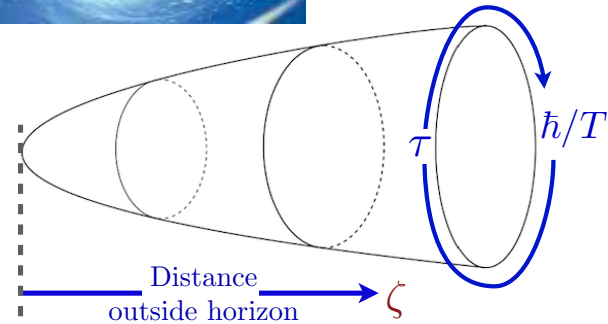
$$\approx \exp \left(\frac{A_0 c^3}{4\hbar G} \right)$$

$A_0 = 2GQ^2/c^4$ is the area of the charged black hole horizon at $T = 0$.

The Bekenstein-Hawking entropy $A_0 c^3 / (4\hbar G)$ is the analog of the $T \rightarrow 0$ GPS entropy, Ns_0 , of the SYK model.



A. Chamblin, R. Emparan,
C.V. Johnson, and R.C. Myers,
PRD **60**, 064018 (1999)



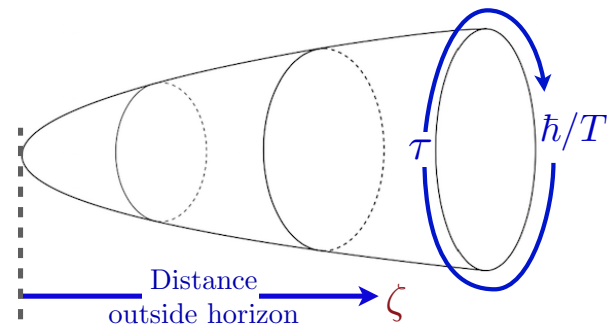
Sachdev (2010)

Thermodynamics of quantum black holes with charge Q :

$$\begin{aligned} \mathcal{Z}(Q, T) &= \int \mathcal{D}g_{\mu\nu} \mathcal{D}A_\mu \exp \left(-\frac{1}{\hbar} I_{\text{Einstein gravity+Maxwell EM}}^{(3+1)}[g_{\mu\nu}, A_\mu] \right) \\ &\approx \exp \left(\frac{A_0 c^3}{4\hbar G} \right) \int \mathcal{D}g_{\mu\nu} \mathcal{D}A_\mu \exp \left(-\frac{1}{\hbar} I_{\text{JT gravity of AdS}_2+\text{boundary graviton}}^{(1+1)}[g_{\mu\nu}, A_\mu] \right) \end{aligned}$$

$A_0 = 2GQ^2/c^4$ is the area of the charged black hole horizon at $T = 0$.

The Bekenstein-Hawking entropy $A_0 c^3 / (4\hbar G)$ is the analog of the $T \rightarrow 0$ GPS entropy, Ns_0 , of the SYK model.



Kitaev (2015); Maldacena, Stanford, Yang (2016)

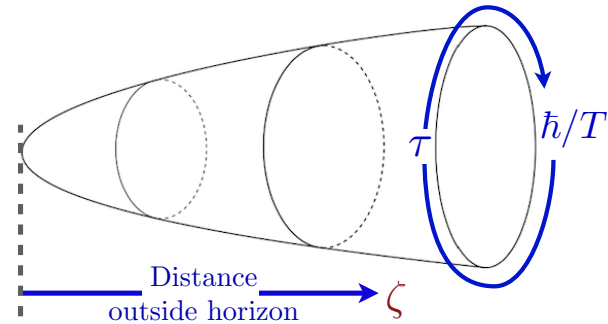
Thermodynamics of quantum black holes with charge Q :

$$\begin{aligned}
 \mathcal{Z}(Q, T) &= \int \mathcal{D}g_{\mu\nu} \mathcal{D}A_\mu \exp \left(-\frac{1}{\hbar} I_{\text{Einstein gravity+Maxwell EM}}^{(3+1)}[g_{\mu\nu}, A_\mu] \right) \\
 &\approx \exp \left(\frac{A_0 c^3}{4\hbar G} \right) \int \mathcal{D}g_{\mu\nu} \mathcal{D}A_\mu \exp \left(-\frac{1}{\hbar} I_{\text{JT gravity of AdS}_2+\text{boundary graviton}}^{(1+1)}[g_{\mu\nu}, A_\mu] \right) \\
 &= \exp \left(\frac{A_0 c^3}{4\hbar G} \right) \int \mathcal{D}f(\tau) \mathcal{D}\phi(\tau) \exp \left(-\frac{1}{\hbar} I_{\text{SYK}}^{(0+1)}[\text{time reparameterizations } f(\tau), \text{ phase } \phi(\tau)] \right)
 \end{aligned}$$

The path integral over the action $I_{\text{SYK}}^{(0+1)}$ can be evaluated exactly,

and leads to a computation of $D(E)$

$$\mathcal{Z}(Q, T) = \int dE D(E) \exp \left(-\frac{E}{k_B T} \right)$$



Kitaev (2015) Maldacena, Stanford, Yang (2016); Cotler et al. (2017)

D(E) of charged black holes from the SYK model

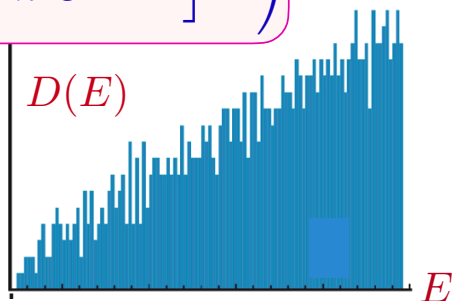
- For generic charged black holes in 3+1 dimensions with horizon area A_0 at $T = 0$ and fixed charge Q ($A_0 = 2GQ^2/c^4$), the density of quantum states at small energy E is

$$D(E) \sim \left(\frac{A_0 c^3}{\hbar G}\right)^{-347/90} \exp\left(\frac{A_0 c^3}{4\hbar G}\right) \sinh\left(\left[\frac{\sqrt{\pi} A_0^{3/2} c^2}{\hbar^2 G} E\right]^{1/2}\right)$$

Bekenstein-Hawking

Iliesiu, Murthy, Turiaci (2022)

Developments from the SYK model

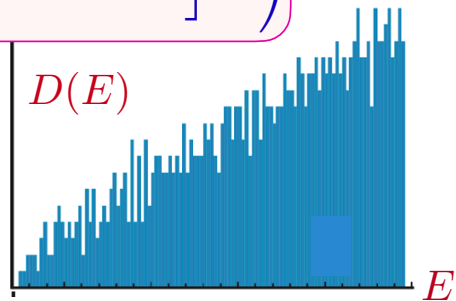


D(E) of charged black holes from the SYK model

- For generic charged black holes in 3+1 dimensions with horizon area A_0 at $T = 0$ and fixed charge Q ($A_0 = 2GQ^2/c^4$), the density of quantum states at small energy E is

$$D(E) \sim \left(\frac{A_0 c^3}{\hbar G} \right)^{-347/90} \exp \left(\frac{A_0 c^3}{4\hbar G} \right) \sinh \left(\left[\frac{\sqrt{\pi} A_0^{3/2} c^2}{\hbar^2 G} E \right]^{1/2} \right)$$

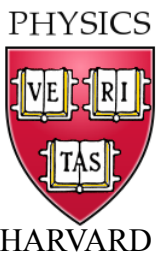
For supersymmetric charged black holes or SYK models: $D(E) = e^S \delta(E)$
i.e. exponential ground state degeneracy.



Appendix D: Quantum criticality of metals

Universal theory of strange metals: the two-dimensional Yukawa-Sachdev-Ye-Kitaev model

Subir Sachdev

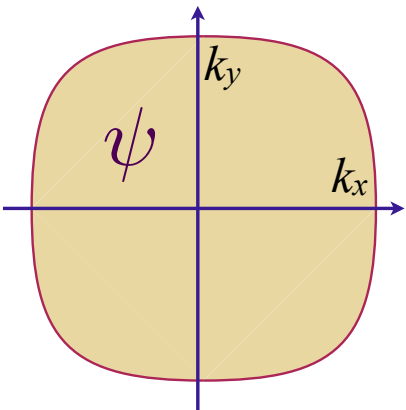


Quantum criticality in clean metals

Fermi surface + critical boson with no spatial disorder

$$\mathcal{L}_\psi = \psi_{\mathbf{k}}^\dagger \left(\frac{\partial}{\partial \tau} + \varepsilon(\mathbf{k}) \right) \psi_{\mathbf{k}}$$

Type I: a critical boson ϕ
e.g. Ising ferromagnetism

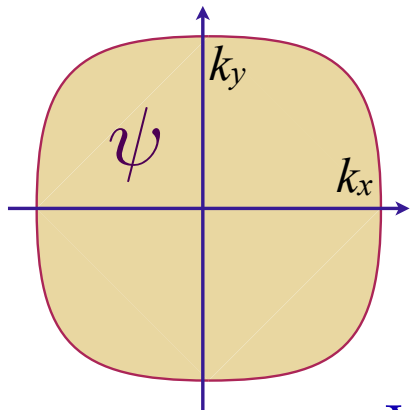


$$+s [\phi(\mathbf{r})]^2$$
$$+K [\nabla_{\mathbf{r}} \phi(\mathbf{r})]^2 + u [\phi(\mathbf{r})]^4$$

Fermi surface + critical boson with no spatial disorder

$$\mathcal{L}_\psi = \psi_{\mathbf{k}}^\dagger \left(\frac{\partial}{\partial \tau} + \varepsilon(\mathbf{k}) \right) \psi_{\mathbf{k}}$$

Type I: a critical boson ϕ
e.g. Ising ferromagnetism

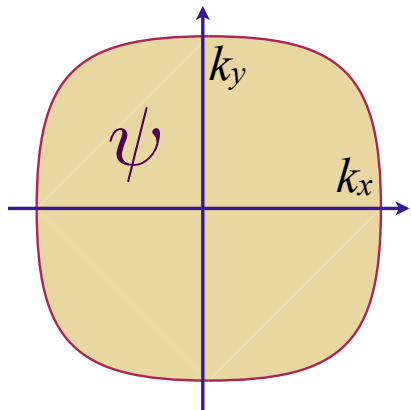


$$+s [\phi(\mathbf{r})]^2 \quad +g \psi^\dagger(\mathbf{r})\psi(\mathbf{r}) \phi(\mathbf{r})$$
$$+K [\nabla_{\mathbf{r}}\phi(\mathbf{r})]^2 + u [\phi(\mathbf{r})]^4$$

Yukawa coupling g between fermions and bosons

Fermi surface + critical boson with no spatial disorder

$$\mathcal{L}_\psi = \psi_{\mathbf{k}}^\dagger \left(\frac{\partial}{\partial \tau} + \varepsilon(\mathbf{k}) \right) \psi_{\mathbf{k}}$$



Type I: a critical boson ϕ
e.g. Ising ferromagnetism

$$+s [\phi(\mathbf{r})]^2 + K [\nabla_{\mathbf{r}} \phi(\mathbf{r})]^2 + u [\phi(\mathbf{r})]^4 + g \psi^\dagger(\mathbf{r}) \psi(\mathbf{r}) \phi(\mathbf{r})$$

Large N limit of:

$$\frac{g_{\alpha\beta\gamma}}{N} \psi_\alpha^\dagger(\mathbf{r}) \psi_\beta(\mathbf{r}) \phi_\gamma(\mathbf{r})$$

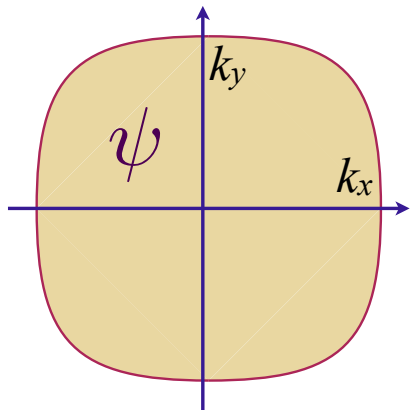
with $\alpha, \beta, \gamma = 1 \dots N$

and $g_{\alpha\beta\gamma}$ random in flavor space,
as in *Yukawa-SYK* models
of fermions and bosons

Fermi surface + critical boson with no spatial disorder

$$\mathcal{L}_\psi = \psi_{\mathbf{k}}^\dagger \left(\frac{\partial}{\partial \tau} + \varepsilon(\mathbf{k}) \right) \psi_{\mathbf{k}}$$

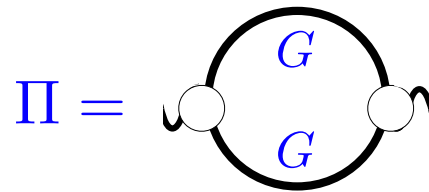
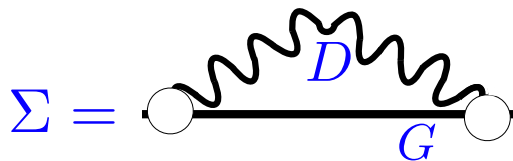
Type I: a critical boson ϕ
e.g. Ising ferromagnetism



$$+s [\phi(\mathbf{r})]^2$$

$$+g \psi^\dagger(\mathbf{r}) \psi(\mathbf{r}) \phi(\mathbf{r})$$

$$+K [\nabla_{\mathbf{r}} \phi(\mathbf{r})]^2 + u [\phi(\mathbf{r})]^4$$



Fermi surface + critical boson with no spatial disorder

SYK-type self-consistent equations

$$\Sigma(\tau, \mathbf{r}) = g^2 D(\tau, \mathbf{r}) G(\tau, \mathbf{r})$$

$$\Pi(\tau, \mathbf{r}) = -g^2 G(-\tau, -\mathbf{r}) G(\tau, \mathbf{r})$$

$$G(i\omega, \mathbf{k}) = \frac{1}{i\omega - \varepsilon(\mathbf{k}) + \mu - \Sigma(i\omega, \mathbf{k})},$$

$$D(i\Omega, \mathbf{q}) = \frac{1}{\Omega^2 + \mathbf{q}^2 + m_b^2 - \Pi(i\Omega, \mathbf{q})}.$$

Solution of Migdal-Eliashberg equations for electron (G)
and boson (D) Green's functions at small ω :

P.A. Lee (1989)

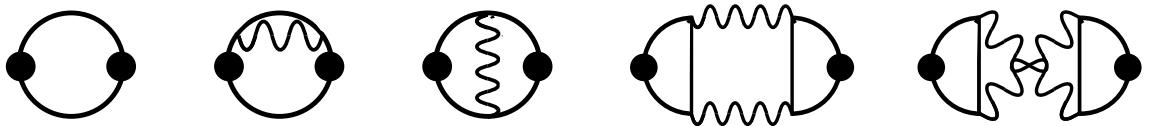
$$\Sigma(\hat{\mathbf{k}}, i\omega) \sim -i \text{sgn}(\omega) |\omega|^{2/3}, \quad G(\mathbf{k}, i\omega) = \frac{1}{i\omega - \varepsilon(\mathbf{k}) - \Sigma(\hat{\mathbf{k}}, i\omega)}, \quad D(\mathbf{q}, i\Omega) = \frac{1}{\Omega^2 + q^2 + \gamma |\Omega|/q}$$

$$\text{Entropy } S(T \rightarrow 0) \sim T^{2/3}$$

Sharp Fermi surface but no quasiparticles; Luttinger volume Fermi surface

Fermi surface + critical boson with no spatial disorder

Optical conductivity—Diagrams



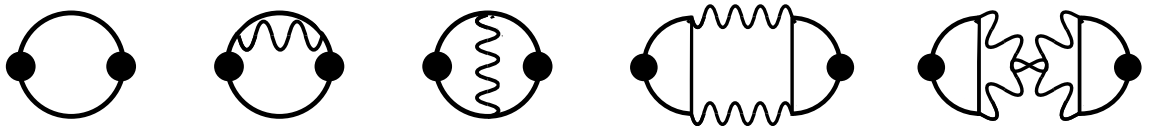
$$\text{Re} [\sigma(\omega)] = C |\omega|^{-2/3}$$

$$\rho(T) \sim T^{4/3}$$

Yong Baek Kim, A. Furusaki, Xiao-Gang Wen,
and P. A. Lee, PRB **50**, 17917 (1994).

Fermi surface + critical boson with no spatial disorder

Optical conductivity—Diagrams



$$\text{Re}[\sigma(\omega)] = C |\omega|^{-2/3}$$
$$\rho(T) \sim T^{4/3}$$

Yong Baek Kim, A. Furusaki, Xiao-Gang Wen,
and P. A. Lee, PRB **50**, 17917 (1994).

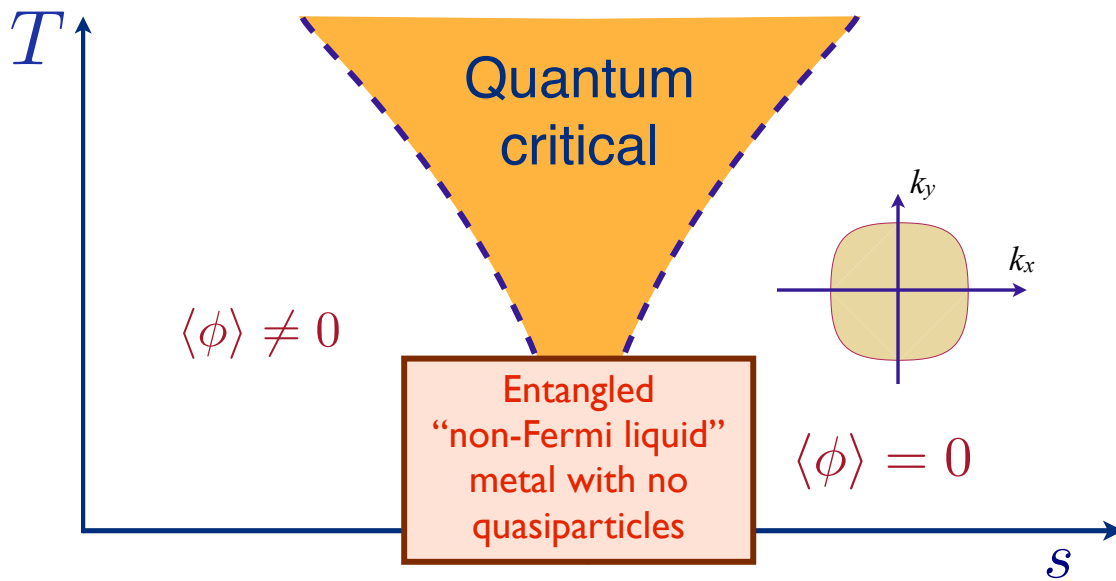
$$C = 0; \quad \sigma(\omega) = iD/(\omega - \omega_c) + \omega^0 + \dots$$

Haoyu Guo, Aavishkar Patel, Ilya Esterlis, S.S., PRB **106**, 115151 (2022);
Haoyu Guo, Davide Valentini, J. Schmalian, S.S., Aavishkar Patel, PRB **109**, 075162 (2024);
D.L. Maslov and A.V. Chubukov, Rep. Prog. Phys. **80**, 026503 (2017);
Zhengyan Darius Sh Dominic V. Else, Hart Goldman, T. Senthil, SciPost Phys. **14**, 113 (2023);
Haoyu Guo, arXiv: 2406.12967



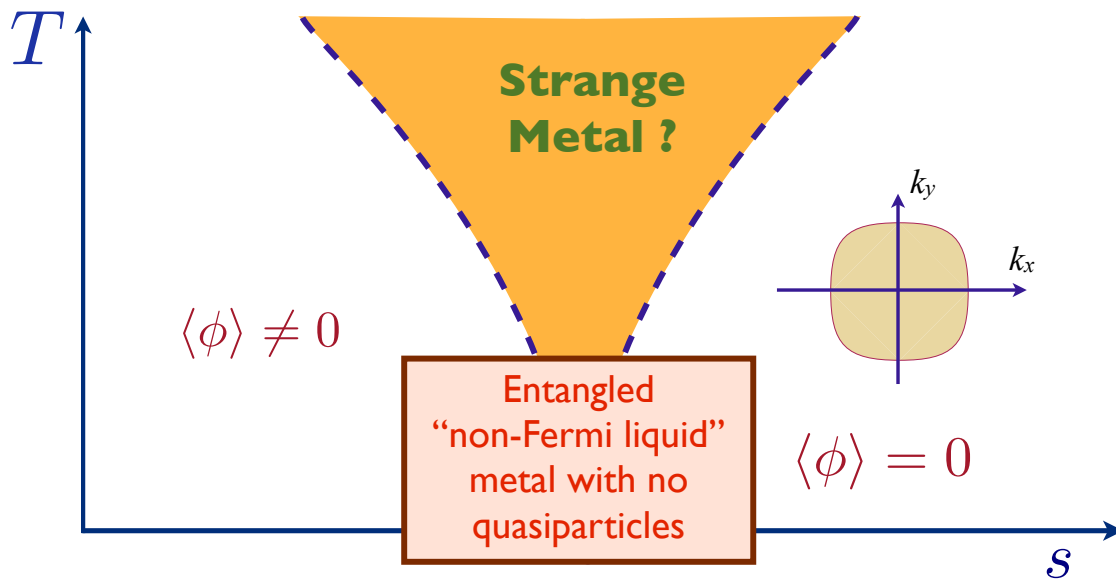
Fermi surface + critical boson with no spatial disorder

Type I, II, or III



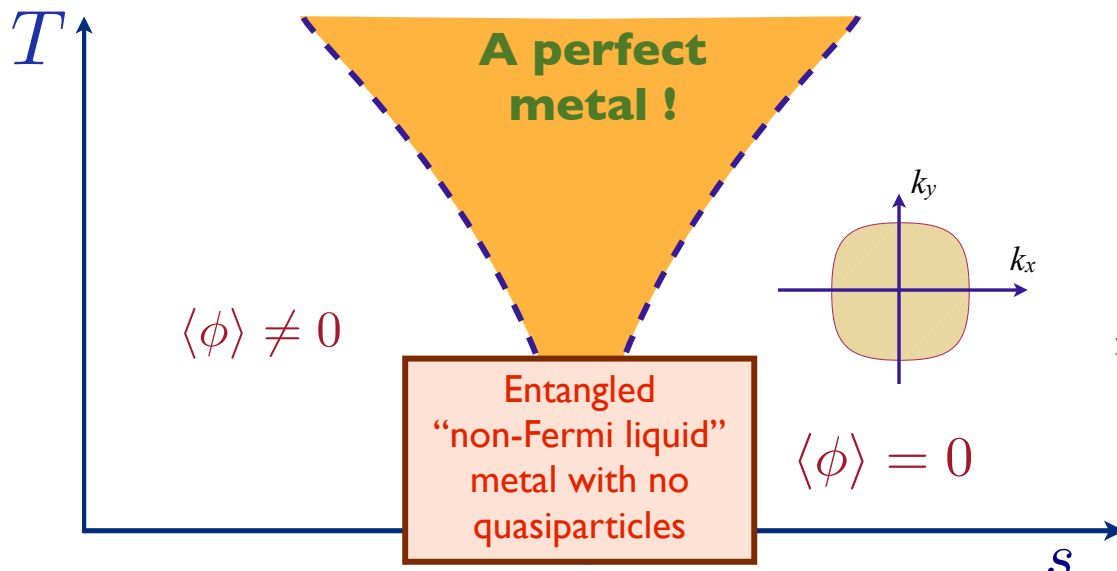
Fermi surface + critical boson with no spatial disorder

Type I, II, or III



Fermi surface + critical boson with no spatial disorder

Type I, II, or III



S.A. Hartnoll, P. K. Kovtun, M. Muller, and S.S., PRB **76**, 144502 (2007); S.A. Hartnoll, R. Mahajan, M. Punk, and S. S., PRB **89**, 155130 (2014); Aavishkar Patel and S.S., PRB **90**, 165146 (2014); Haoyu Guo, Aavishkar Patel, Ilya Esterlis, S.S., PRB **106**, 115151 (2022); Haoyu Guo, Davide Valentini, J. Schmalian, S.S., Aavishkar Patel, PRB **109**, 075162 (2024); D.L. Maslov and A.V. Chubukov, Rep. Prog. Phys. **80**, 026503 (2017); Zhengyan Darius Sh Dominic V. Else, Hart Goldman, T. Senthil, SciPost Phys. **14**, 113 (2023); Haoyu Guo, arXiv: 2406.12967

Extreme drag: the fermions ψ “drag” the bosons ϕ as they move, and so electrical current does not relax, even though strong ψ - ϕ scattering leads to absence of ψ quasiparticles.

Universal theory of strange metals:

**Quantum phase transitions
in inhomogeneous metals
described by the
two-dimensional Yukawa-SYK model**

Theory applies for types I, II, III, with only minor differences.



Ilya Esterlis
Wisconsin



Haoyu Guo
Cornell



Aavishkar Patel
Flatiron



Chenyuan Li
Harvard → Rice



Davide Valentinis
KIT



Joerg Schmalian
KIT



Peter Lunts
Harvard

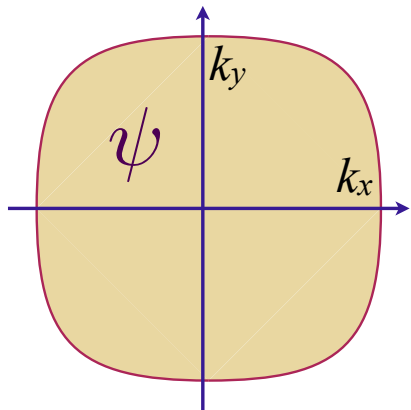
Aavishkar A. Patel, Haoyu Guo, Ilya Esterlis, S. S., *Science* **381**, 790 (2023)

Aavishkar A. Patel, Peter Lunts, S.S., *PNAS* **121**, e2402052121 (2024)

Chenyuan Li, Aavishkar A. Patel, Haoyu Guo, Davide Valentinis, Jorg Schmalian, S.S., Ilya Esterlis, arXiv:2406.07608

Fermi surface + critical boson with no spatial disorder

$$\mathcal{L}_\psi = \psi_{\mathbf{k}}^\dagger \left(\frac{\partial}{\partial \tau} + \varepsilon(\mathbf{k}) \right) \psi_{\mathbf{k}}$$



Type I, II, III: A critical boson ϕ

e.g. Ising ferromagnetism,
spin-density wave order,

Higgs boson for Fermi-volume changing transition

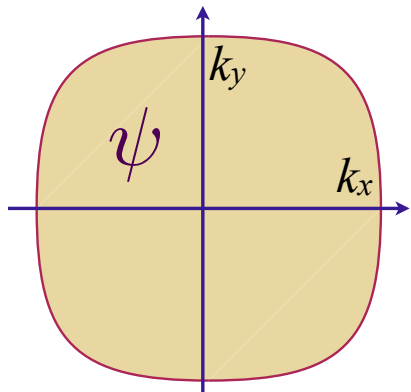
$$+s [\phi(\mathbf{r})]^2$$

$$+g \psi^\dagger(\mathbf{r}) \psi(\mathbf{r}) \phi(\mathbf{r})$$

$$+K [\nabla_{\mathbf{r}} \phi(\mathbf{r})]^2 + u [\phi(\mathbf{r})]^4$$

Fermi surface + critical boson with potential disorder

$$\mathcal{L}_\psi = \psi_{\mathbf{k}}^\dagger \left(\frac{\partial}{\partial \tau} + \varepsilon(\mathbf{k}) \right) \psi_{\mathbf{k}}$$



Type I, II, III: A critical boson ϕ

e.g. Ising ferromagnetism,
spin-density wave order,

Higgs boson for Fermi-volume changing transition

$$+s [\phi(\mathbf{r})]^2$$

$$+g \psi^\dagger(\mathbf{r})\psi(\mathbf{r})\phi(\mathbf{r})$$

$$+K [\nabla_{\mathbf{r}}\phi(\mathbf{r})]^2 + u [\phi(\mathbf{r})]^4 + v(\mathbf{r})\psi^\dagger(\mathbf{r})\psi(\mathbf{r})$$

Spatially random potential $v(\mathbf{r})$ with $\overline{v(\mathbf{r})} = 0$, $\overline{v(\mathbf{r})v(\mathbf{r}')} = v^2\delta(\mathbf{r} - \mathbf{r}')$

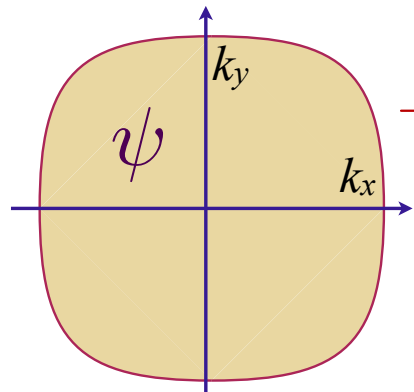
$v(\mathbf{r})$ leads to elastic scattering of ψ ;

localization of ψ only at long length scales, not relevant for experiments

Fermi surface + critical boson with potential and interaction disorder

$$\mathcal{L}_\psi = \psi_{\mathbf{k}}^\dagger \left(\frac{\partial}{\partial \tau} + \varepsilon(\mathbf{k}) \right) \psi_{\mathbf{k}}$$

Type I, II, III: A critical boson ϕ
e.g. Ising ferromagnetism,
 spin-density wave order,
 Higgs boson for Fermi-volume changing transition



$$+ [s + \delta s(\mathbf{r})] [\phi(\mathbf{r})]^2 + +g \psi^\dagger(\mathbf{r}) \psi(\mathbf{r}) \phi(\mathbf{r})$$

$$+ K [\nabla_{\mathbf{r}} \phi(\mathbf{r})]^2 + u [\phi(\mathbf{r})]^4 + v(\mathbf{r}) \psi^\dagger(\mathbf{r}) \psi(\mathbf{r})$$

Spatially random potential $v(\mathbf{r})$ with $\overline{v(\mathbf{r})} = 0$, $\overline{v(\mathbf{r})v(\mathbf{r}')} = v^2 \delta(\mathbf{r} - \mathbf{r}')$

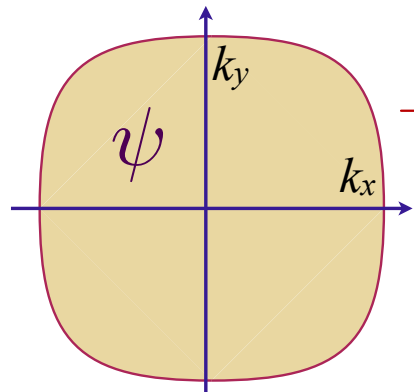
Spatially random mass $\delta s(\mathbf{r})$ with $\overline{\delta s(\mathbf{r})} = 0$, $\overline{\delta s(\mathbf{r})\delta s(\mathbf{r}')} = \delta s^2 \delta(\mathbf{r} - \mathbf{r}')$

$\delta s(\mathbf{r})$ creates inhomogeneity in the position of QCP (Harris disorder):
 Very important and should be accounted for first.

Fermi surface + critical boson with potential and interaction disorder

$$\mathcal{L}_\psi = \psi_{\mathbf{k}}^\dagger \left(\frac{\partial}{\partial \tau} + \varepsilon(\mathbf{k}) \right) \psi_{\mathbf{k}}$$

Type I, II, III: A critical boson ϕ
e.g. Ising ferromagnetism,
 spin-density wave order,
 Higgs boson for Fermi-volume changing transition



$$+ [s + \delta s(\mathbf{r})] [\phi(\mathbf{r})]^2 + \quad + g \psi^\dagger(\mathbf{r}) \psi(\mathbf{r}) \phi(\mathbf{r})$$

$$+ K [\nabla_{\mathbf{r}} \phi(\mathbf{r})]^2 + u [\phi(\mathbf{r})]^4 + v(\mathbf{r}) \psi^\dagger(\mathbf{r}) \psi(\mathbf{r})$$

Aavishkar A. Patel, Haoyu Guo, Ilya Esterlis, S. Sachdev, *Science* **381**, 790 (2023)

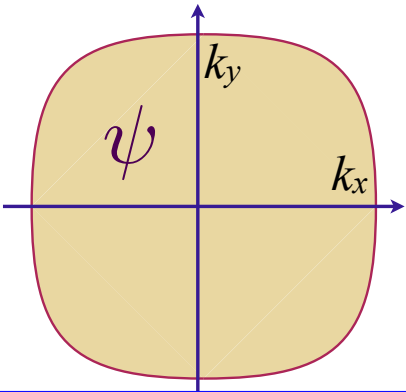
Spatially random potential $v(\mathbf{r})$ with $\overline{v(\mathbf{r})} = 0$, $\overline{v(\mathbf{r})v(\mathbf{r}')}$ = $v^2 \delta(\mathbf{r} - \mathbf{r}')$

Spatially random mass $\delta s(\mathbf{r})$ with $\overline{\delta s(\mathbf{r})} = 0$, $\overline{\delta s(\mathbf{r})\delta s(\mathbf{r}')}$ = $\delta s^2 \delta(\mathbf{r} - \mathbf{r}')$

$\delta s(\mathbf{r})$ creates inhomogeneity in the position of QCP (Harris disorder):
 Rescale $\phi(\mathbf{r})$ to obtain a theory with $\delta s(\mathbf{r}) = 0$.

2d-YSYK model: Fermi surface + critical boson with interaction disorder

$$\mathcal{L}_\psi = \psi_{\mathbf{k}}^\dagger \left(\frac{\partial}{\partial \tau} + \varepsilon(\mathbf{k}) \right) \psi_{\mathbf{k}}$$



Type I, II, III: A critical boson ϕ

e.g. Ising ferromagnetism,
spin-density wave order,

Higgs boson for Fermi-volume changing transition

$$+s [\phi(\mathbf{r})]^2 + [g + g'(\mathbf{r})] \psi^\dagger(\mathbf{r}) \psi(\mathbf{r}) \phi(\mathbf{r})$$

$$+K [\nabla_{\mathbf{r}} \phi(\mathbf{r})]^2 + u [\phi(\mathbf{r})]^4 + v(\mathbf{r}) \psi^\dagger(\mathbf{r}) \psi(\mathbf{r})$$

E. E. Aldape, T. Cookmeyer, A. A. Patel, and E. Altman, *PRB* **105**, 235111 (2022)
Aavishkar A. Patel, Haoyu Guo, Ilya Esterlis, S. Sachdev, *Science* **381**, 790 (2023)

Spatially random potential $v(\mathbf{r})$ with $\overline{v(\mathbf{r})} = 0$, $\overline{v(\mathbf{r})v(\mathbf{r}')}$ = $v^2 \delta(\mathbf{r} - \mathbf{r}')$

Spatially random Yukawa coupling $g'(\mathbf{r})$ with $\overline{g'(\mathbf{r})} = 0$, $\overline{g'(\mathbf{r})g'(\mathbf{r}')}$ = $g'^2 \delta(\mathbf{r} - \mathbf{r}')$

$g'(\mathbf{r})$ creates inhomogeneity in the position of QCP (Harris disorder):
the two-dimensional Yukawa-Sachdev-Ye-Kitaev model.

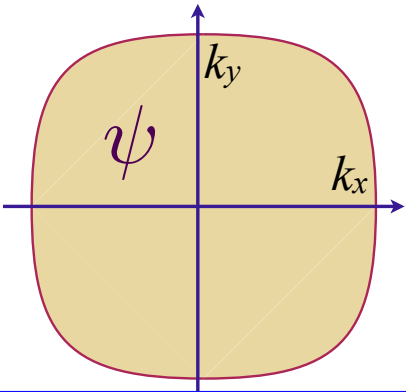
2d-YSYK model: Fermi surface + critical boson with interaction disorder

$$\mathcal{L}_\psi = \psi_{\mathbf{k}}^\dagger \left(\frac{\partial}{\partial \tau} + \varepsilon(\mathbf{k}) \right) \psi_{\mathbf{k}}$$

Type I, II, III: A critical boson ϕ

e.g. Ising ferromagnetism,
spin-density wave order,

Higgs boson for Fermi-volume changing transition



$$+s [\phi(\mathbf{r})]^2 + [g + g'(\mathbf{r})] \psi^\dagger(\mathbf{r}) \psi(\mathbf{r}) \phi(\mathbf{r})$$

$$+K [\nabla_{\mathbf{r}} \phi(\mathbf{r})]^2 + u [\phi(\mathbf{r})]^4 + v(\mathbf{r}) \psi^\dagger(\mathbf{r}) \psi(\mathbf{r})$$

Aavishkar A. Patel, Haoyu Guo, Ilya Esterlis, S. Sachdev, *Science* **381**, 790 (2023)

Spatially random potential $v(\mathbf{r})$ with $\overline{v(\mathbf{r})} = 0$, $\overline{v(\mathbf{r})v(\mathbf{r}')}$ = $v^2\delta(\mathbf{r} - \mathbf{r}')$

Spatially random Yukawa coupling $g'(\mathbf{r})$ with $\overline{g'(\mathbf{r})} = 0$, $\overline{g'(\mathbf{r})g'(\mathbf{r}')}$ = $g'^2\delta(\mathbf{r} - \mathbf{r}')$

Analyze 2d-YSYK model in a self-averaging manner as in the SYK model.

Should be applicable as long as eigenmodes of $\phi(\mathbf{r})$ are extended.

2d-YSYK model: Fermi surface + critical boson with interaction disorder

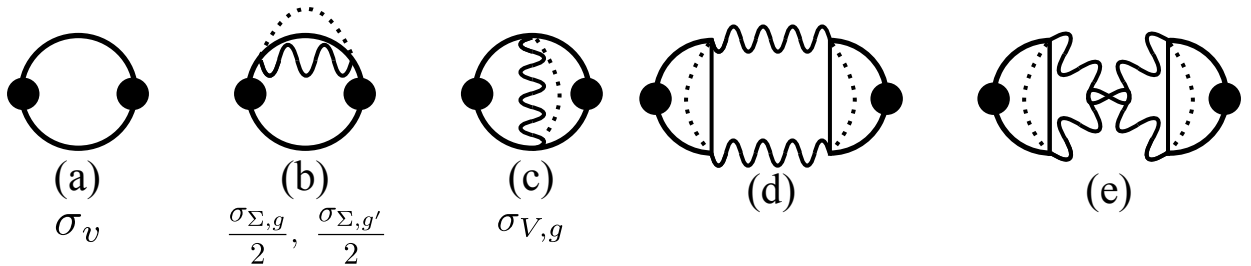
SYK-type self-consistent equations

$$\Sigma(\tau, \mathbf{r}) = g^2 D(\tau, \mathbf{r}) G(\tau, \mathbf{r}) + v^2 G(\tau, \mathbf{r}) \delta^2(\mathbf{r}) + g'^2 G(\tau, \mathbf{r}) D(\tau, \mathbf{r}) \delta^2(\mathbf{r}),$$

$$\Pi(\tau, \mathbf{r}) = -g^2 G(-\tau, -\mathbf{r}) G(\tau, \mathbf{r}) - g'^2 G(-\tau, \mathbf{r}) G(\tau, \mathbf{r}) \delta^2(\mathbf{r}),$$

$$G(i\omega, \mathbf{k}) = \frac{1}{i\omega - \varepsilon(\mathbf{k}) + \mu - \Sigma(i\omega, \mathbf{k})},$$

$$D(i\Omega, \mathbf{q}) = \frac{1}{\Omega^2 + \mathbf{q}^2 + m_b^2 - \Pi(i\Omega, \mathbf{q})}.$$



+ all ladders and bubbles.....

2d-YSYK model: Fermi surface + critical boson with interaction disorder

Electron Green's function:
$$G(\omega) \sim \frac{1}{\omega \frac{m^*(\omega)}{m} - \varepsilon(\mathbf{k}) + i \left(\frac{1}{\tau_e} + \frac{1}{\tau_{\text{in}}(\omega)} \right) \text{sgn}(\omega)}$$

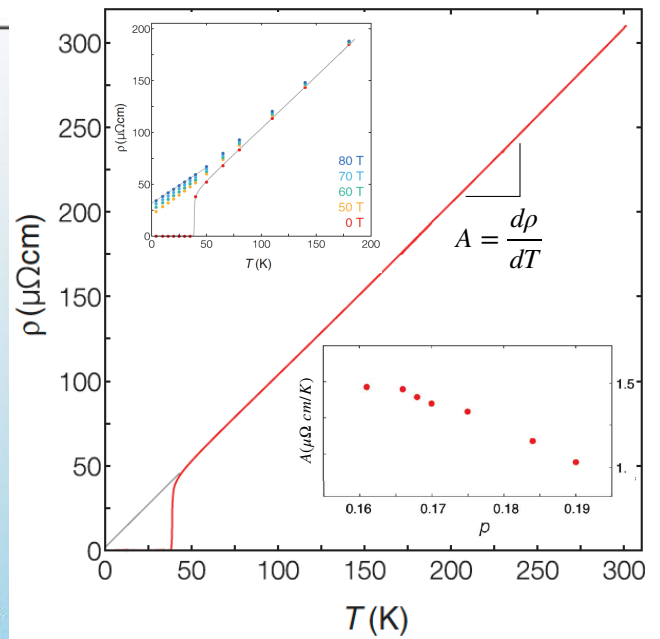
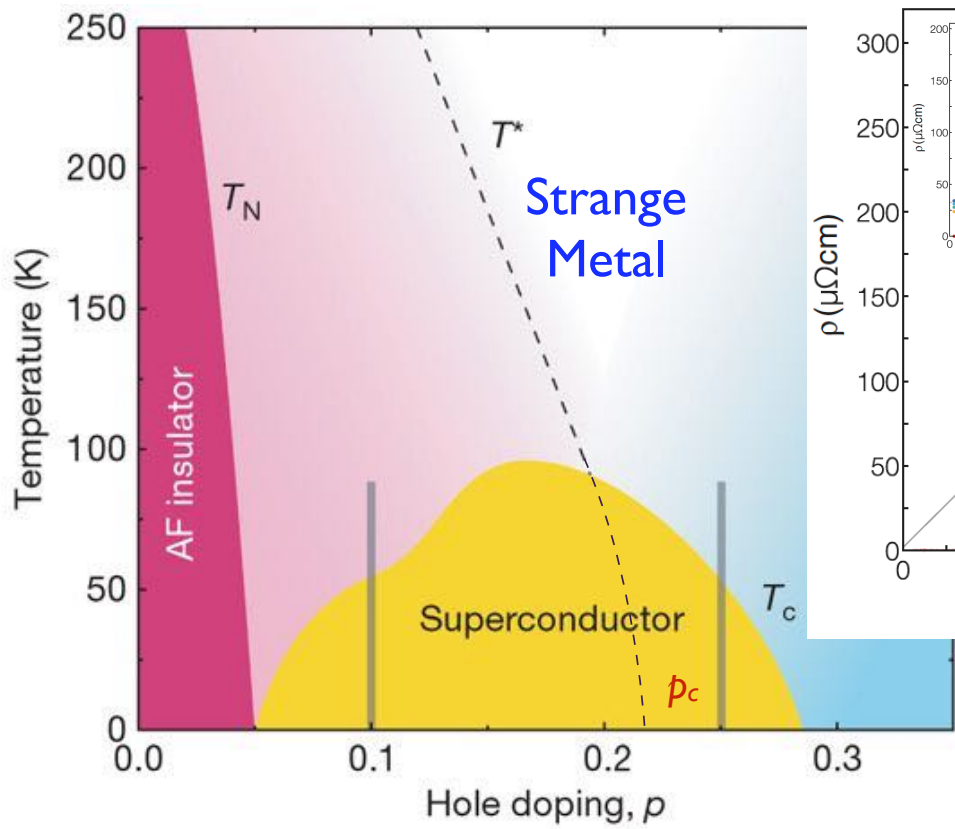
$$\frac{1}{\tau_e} \sim v^2 \quad ; \quad \frac{1}{\tau_{\text{in}}(\omega)} \sim \left(\frac{g^2}{v^2} + g'^2 \right) |\omega| \quad ; \quad \frac{m^*(\omega)}{m} \sim \frac{2}{\pi} \left(\frac{g^2}{v^2} + g'^2 \right) \ln(\Lambda/\omega)$$

Conductivity:
$$\sigma(\omega) \sim \frac{1}{\frac{1}{\tau_{\text{trans}}(\omega)} - i\omega \frac{m_{\text{trans}}^*(\omega)}{m}}$$

$$\frac{1}{\tau_{\text{trans}}(\omega)} \sim v^2 + g'^2 |\omega| \quad ; \quad \frac{m_{\text{trans}}^*(\omega)}{m} \sim \frac{2g'^2}{\pi} \ln(\Lambda/\omega)$$

E. E. Aldape, T. Cookmeyer, A. A. Patel, and E. Altman, PRB **105**, 235111 (2022)
Aavishkar A. Patel, Haoyu Guo, Ilya Esterlis, S. Sachdev, Science **381**, 790 (2023)

Residual resistivity is determined by v^2 ; Linear-in- T resistivity determined by g'^2 ;
Transport insensitive to g ; Marginal Fermi liquid self energy and $T \ln(1/T)$ specific heat.

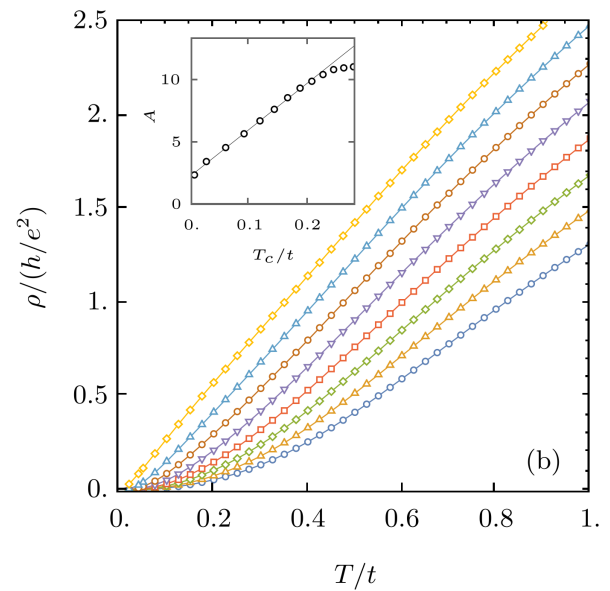
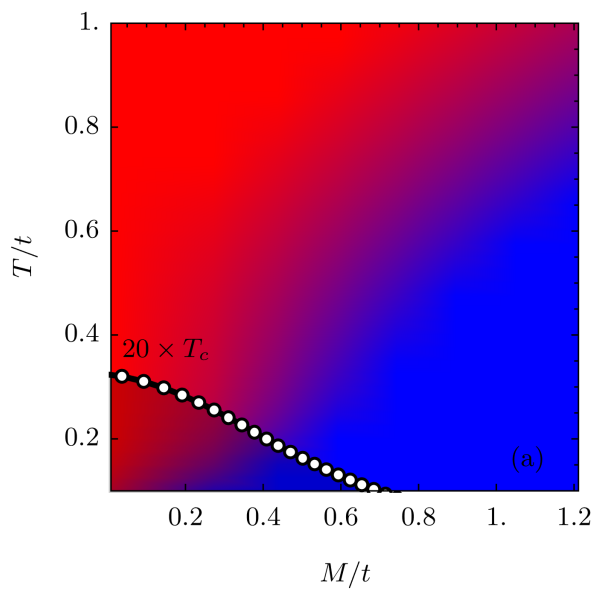


LSCO: Giraldo-Gallo et al. 2018

Strange metal and superconductor in the two-dimensional Yukawa-Sachdev-Ye-Kitaev model

$g = 0$

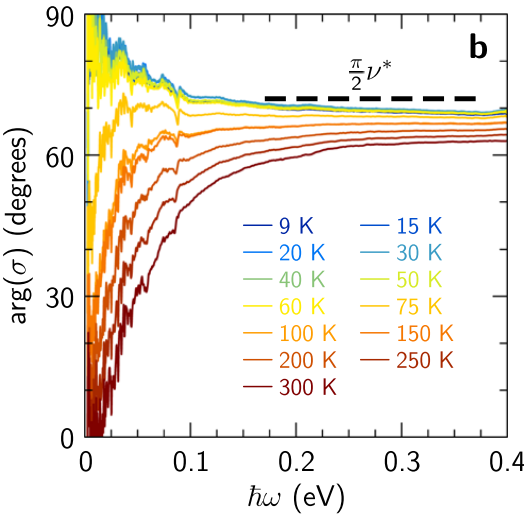
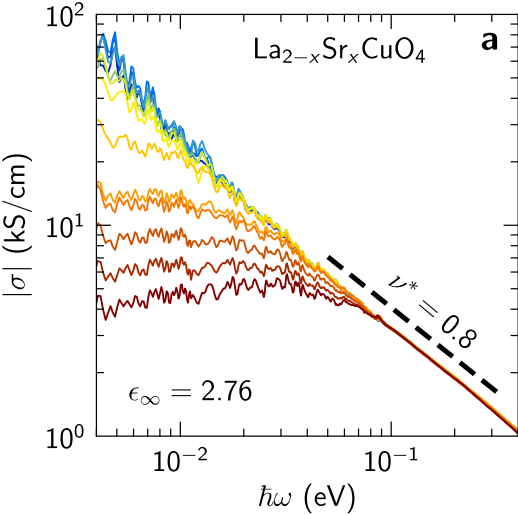
Chenyuan Li, Aavishkar A. Patel, Haoyu Guo, Davide Valentini, Jorg Schmalian, S.S., Ilya Esterlis, arXiv:2406.07608



Reconciling scaling of the optical conductivity of cuprate superconductors with Planckian resistivity and specific heat

B. Michon, C. Berthod, C. W. Rischau, A. Ataei, L. Chen, S. Komiya, S. Ono, L. Taillefer, D. van der Marel, A. Georges
Nature Communications **14**, Article number: 3033 (2023)

$$\sigma(\omega) = i \frac{e^2 K / (\hbar d_c)}{\hbar \omega \frac{m^*(\omega)}{m} + i \frac{\hbar}{\tau(\omega)}}$$



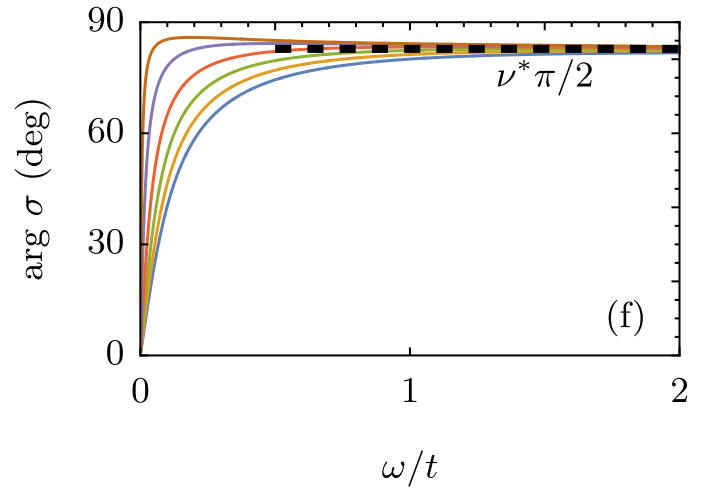
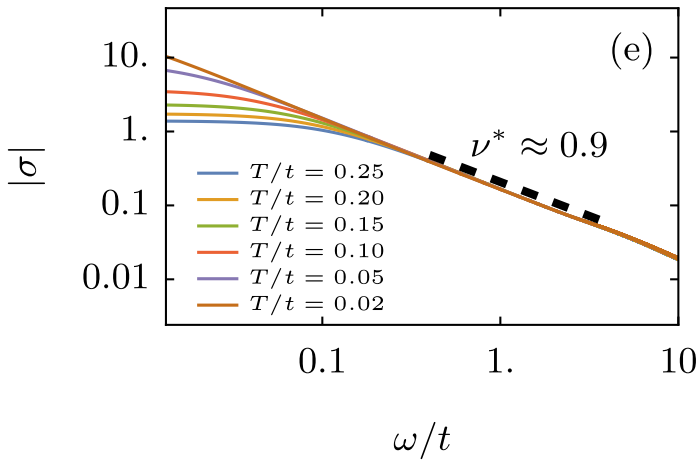
$\text{La}_{2-x}\text{Sr}_x\text{CuO}_4$
 $p = 0.24$
 $T_c = 19 \text{ K}$

Strange metal and superconductor in the two-dimensional Yukawa-Sachdev-Ye-Kitaev model

$g = 0$

Chenyuan Li, Aavishkar A. Patel, Haoyu Guo, Davide Valentini, Jorg Schmalian, S.S., Ilya Esterlis, arXiv:2406.07608

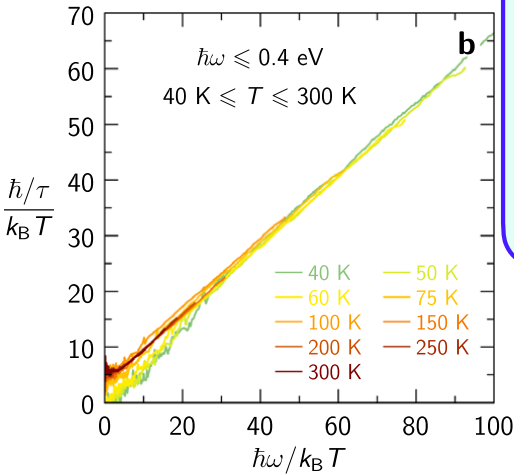
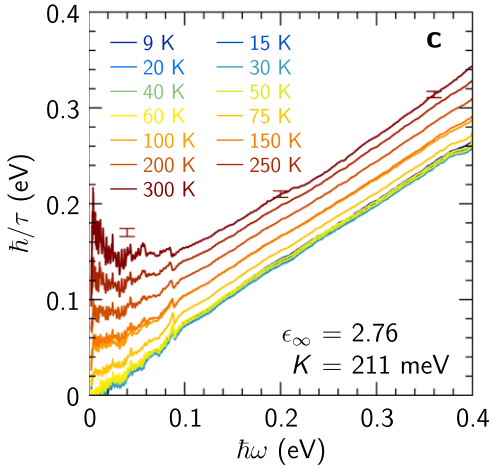
$$\sigma(\omega) = i \frac{e^2 K / (\hbar d_c)}{\hbar \omega \frac{m^*(\omega)}{m} + i \frac{\hbar}{\tau(\omega)}}$$



Reconciling scaling of the optical conductivity of cuprate superconductors with Planckian resistivity and specific heat

B. Michon, C. Berthod, C. W. Rischau, A. Ataei, L. Chen, S. Komiya, S. Ono, L. Taillefer, D. van der Marel, A. Georges
Nature Communications **14**, Article number: 3033 (2023)

$$\sigma(\omega) = i \frac{e^2 K / (\hbar d_c)}{\hbar \omega \frac{m^*(\omega)}{m} + i \frac{\hbar}{\tau(\omega)}}$$



Planckian dynamics!

$$\tau(\omega) = \frac{\hbar}{k_B T} F\left(\frac{\hbar\omega}{k_B T}\right)$$
 and entropy

$$S(T \rightarrow 0) \sim T \ln(1/T).$$

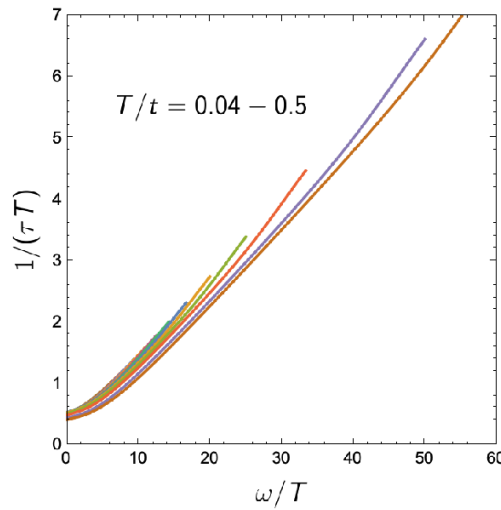
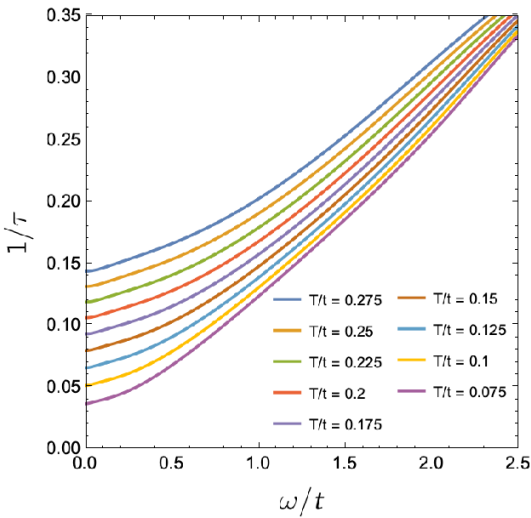
$\text{La}_{2-x}\text{Sr}_x\text{CuO}_4$
 $p = 0.24$
 $T_c = 19 \text{ K}$

Strange metal and superconductor in the two-dimensional Yukawa-Sachdev-Ye-Kitaev model

$g = 0$

Chenyuan Li, Aavishkar A. Patel, Haoyu Guo, Davide Valentini, Jorg Schmalian, S.S., Ilya Esterlis, arXiv:2406.07608

$$\sigma(\omega) = i \frac{e^2 K / (\hbar d_c)}{\hbar \omega \frac{m^*(\omega)}{m} + i \frac{\hbar}{\tau(\omega)}}$$



Planckian dynamics!

$$\tau(\omega) = \frac{\hbar}{k_B T} F\left(\frac{\hbar \omega}{k_B T}\right)$$

and entropy

$S(T \rightarrow 0) \sim T \ln(1/T)$
in 2d-YSYK model
(unlike zero temperature
entropy in SYK model).

Universal theory of strange metals:

**Quantum phase transitions
in inhomogeneous metals
described by the
two-dimensional Yukawa-SYK model**

Theory applies for types I, II, III, with only minor differences.

Universal theory of strange metals:

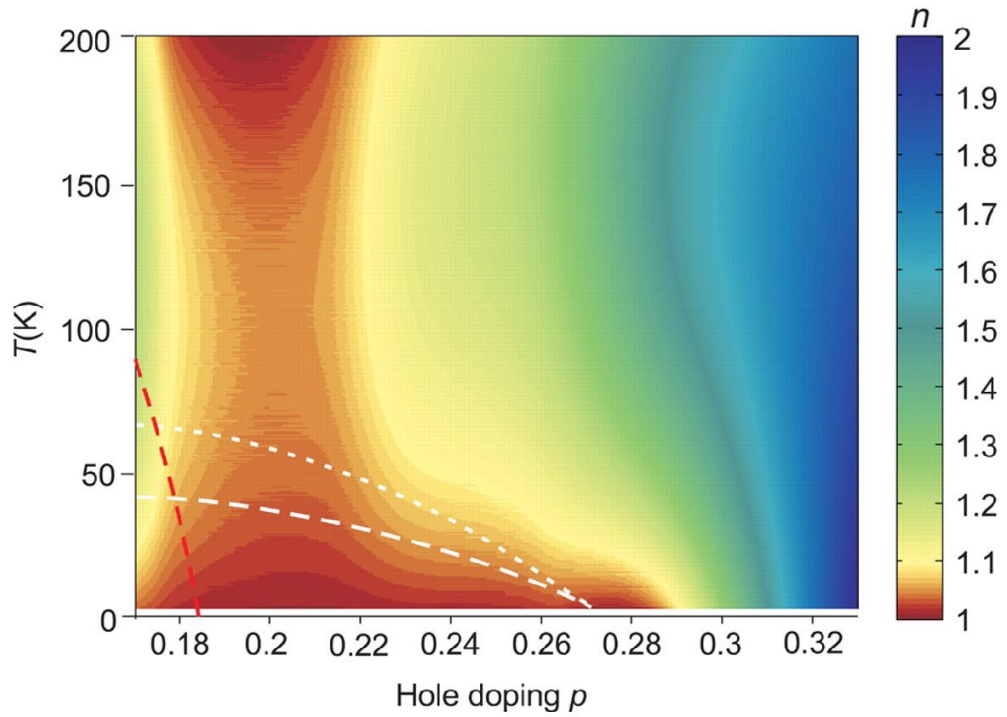
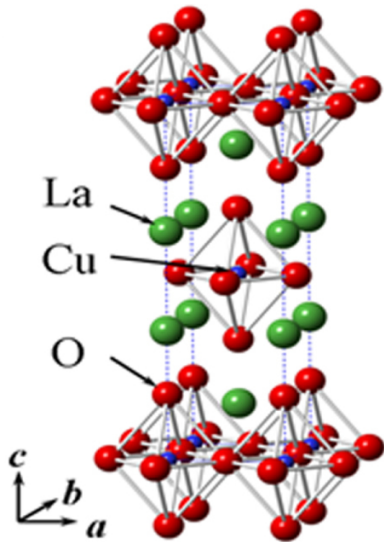
Quantum phase transitions
in inhomogeneous metals
described by the
two-dimensional Yukawa-SYK model

Boson localization and the "foot"

Anomalous Criticality in the Electrical Resistivity of $\text{La}_{2-x}\text{Sr}_x\text{CuO}_4$

R. A. Cooper,¹ Y. Wang,¹ B. Vignolle,² O. J. Lipscombe,¹ S. M. Hayden,¹ Y. Tanabe,³ T. Adachi,³ Y. Koike,³ M. Nohara,^{4*} H. Takagi,⁴ Cyril Proust,² N. E. Hussey^{1†}

SCIENCE VOL 323 603 2009



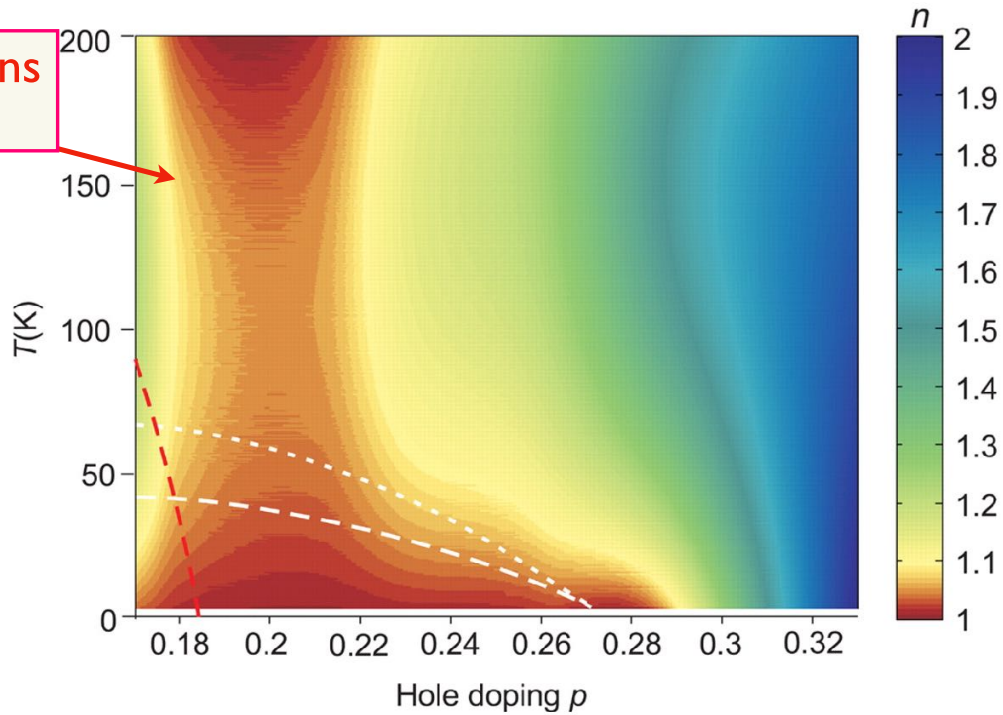
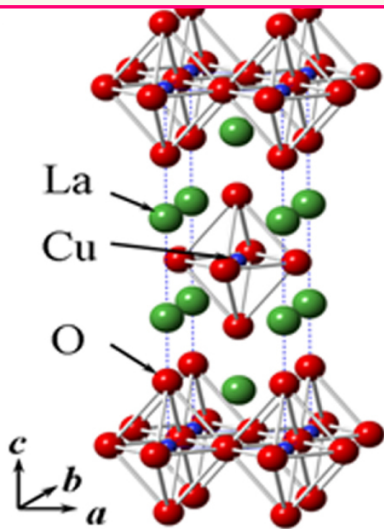
Anomalous Criticality in the Electrical Resistivity of $\text{La}_{2-x}\text{Sr}_x\text{CuO}_4$

R. A. Cooper,¹ Y. Wang,¹ B. Vignolle,² O. J. Lipscombe,¹ S. M. Hayden,¹ Y. Tanabe,³ T. Adachi,³ Y. Koike,³ M. Nohara,^{4*} H. Takagi,⁴ Cyril Proust,² N. E. Hussey^{1†}

SCIENCE VOL 323 603 2009

Aavishkar A. Patel, Peter Lunts, S.S., *PNAS* **121**, e2402052121 (2024)

Extended bosons and fermions in “fan”



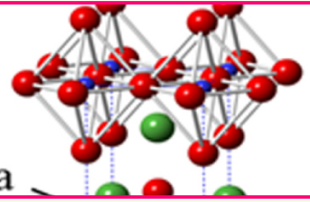
Anomalous Criticality in the Electrical Resistivity of $\text{La}_{2-x}\text{Sr}_x\text{CuO}_4$

R. A. Cooper,¹ Y. Wang,¹ B. Vignolle,² O. J. Lipscombe,¹ S. M. Hayden,¹ Y. Tanabe,³ T. Adachi,³ Y. Koike,³ M. Nohara,^{4*} H. Takagi,⁴ Cyril Proust,² N. E. Hussey^{1†}

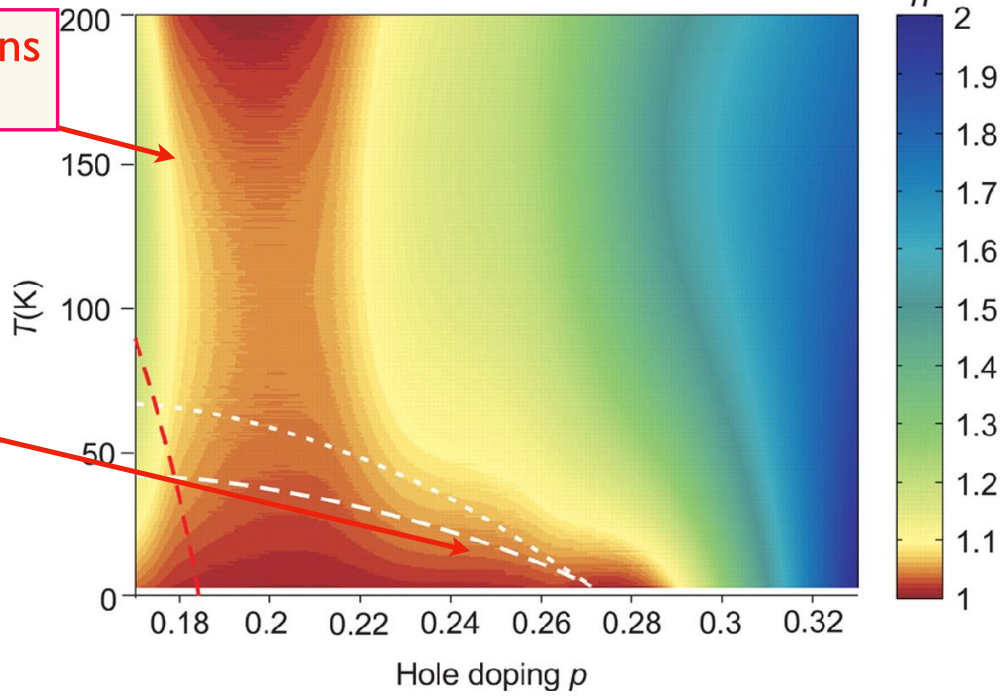
Aavishkar A. Patel, Peter Lunts, S.S., *PNAS* **121**, e2402052121 (2024)

SCIENCE VOL 323 603 2009

Extended bosons and fermions in "fan"



Localized overdamped bosons, but extended fermions in "foot"



The Sachdev-Ye-Kitaev model of many-particle entanglement:

- 🎧 No quasiparticles: yields a metal in which current is carried not by individual electrons, but by an entangled “quantum soup”.
- 🎧 Dual to low-energy theory of charged black holes in 3+1 dimensions

Quantum phase transitions of qubits

- 🎧 Described by a conformal field theory in 2+1 dimensions

Quantum phase transitions of metals

- 🎧 Breakdown of fermionic quasiparticles, but transport is that of a perfect metal.

Quantum phase transitions in inhomogeneous metals described by the 2d-YSYK model

- 🎧 Universal theory of strange metals, good agreement with transport and optical data. The “foot” in phase diagram is associated with boson localization.